University of Glasgow | Institute of Infection, Immunity & Inflammation

Using Metabolomic Analyses to Study Mode of Action of and Resistance to Eflornithine in *Trypanosoma brucei*

Isabel May Vincent BSc (Hons)

Submitted in fulfilment of the requirements for the degree of Doctor of Philosophy.

School of Life Sciences

College of Medical, Veterinary and Life Sciences

University of Glasgow

September 2011

Abstract

Human African trypanosomiasis (HAT) is a disease that is in desperate need of new pharmacological agents active against the causative parasite, the flagellated protozoan *Trypanosoma brucei*.

In this thesis, new metabolomics techniques have been developed to study pathways in response to drug action with the aim of defining the mode of action of current and future drugs. Eflornithine, a polyamine pathway inhibitor, was used as a proof of principle, revealing both expected changes that correlate well with the literature and unexpected changes that lead to pathways and metabolites not previously described in bloodstream form trypanosomes. One metabolite not previously described in trypanosomes is acetylornithine, whose levels correlate well with ornithine and whose production comes directly from ornithine transported from the medium. Nifurtimox and the nifurtimox-eflornithine combination therapy were assayed for changes to their metabolomes revealing changes in nifurtimox treatment that included alterations to sugar and purine levels. The combination therapy had reduced changes to some metabolites compared to each drug in isolation suggesting reasons for the combination's lack of synergy. Isotopically labelled metabolites were also of use in determining flux through the pathways identified as being affected by drug perturbation. These techniques, along with other biochemical techniques, were used to show arginase activity is absent in bloodstream form trypanosomes and that ornithine is not made from arginine when ornithine is present in the medium. Arginine can, however, be used to produce ornithine through an arginase-independent mechanism when exogenous ornithine is lacking. Evidence is also provided that parts of the pentose phosphate pathway, not thought to be active in bloodstream form trypanosomes, may still be active in *in vitro* grown cells.

A mechanism of resistance to eflornithine involving the deletion of an amino acid transporter that is able to transport eflornithine is also described. It is hoped that simple PCR-based tests for this resistance mechanism will be of use in resistant foci in prescribing appropriate drugs to HAT patients.

Contents

List of Tables

List of Figures

Acknowledgement

No man, or woman, is an island. People form networks, with links between them. These links can be the ideas they have shared, advice they have given and time that they have spent ensuring one is never alone in pursuit of scientific discovery. For me, Mike Barrett has been a formidable hub of information and ideas, but has also been as supportive a mentor as one could ever hope for. His knowledge of cricket, wine and Captain Sensible are also exemplary.

Charles Ebikeme is another person deserving particular mention for being ready to pour criticism onto my work at every step of my training. This was much needed criticism, and it is wonderful to know that he is still there to provide advice for me after he has moved to pastures new – even outwith the research community.

Thank you also to members of Team Barrett past and present, in particular to Darren Creek and Pui Ee Wong, to Richard Burchmore and to my friends. A special mention to Jonathan Hounsome, who took me for coffee breaks when a breath of air, and an ear to bend, was exactly what was needed.

Author’s Declaration

I declare that, except where explicit reference is made to the contribution of others, this dissertation is the result of my own work and has not been submitted for any other degree at The University of Glasgow or any other institution.

Signature _____

Printed name __Isabel Vincent_____

Abbreviations

1,3BPGA: 1,3-bisphosphoglycerate

3-PGA: 3-phosphoglycerate

AA: amino acid

AAT: amino acid transporter

AL: argininosuccinate lyase

Ala: alanine

AMP: adenosine monophosphate

ANOVA: analysis of variance

Arg: arginine

ArgE: N-acetylornithine deacetylase

Arg I: arginase 1

Arg II: arginase 2

AS: argininosuccinate synthetase

Asn: asparagine

Asp: aspartate

ATP: adenosine triphosphate

BARP: brucei alanine rich protein

BLAST: basic local alignment search tool

BSA: bovine serum albumin

C: cytochrome *c*

cAMP: cyclic adenosine monophosphate

CBSS: Carter's balanced saline solution (25 mM HEPES, 120 mM NaCl, 5.4 mM KCl, 0.55 mM $CaCl_2$, 0.4 mM $MgSO_4$, 1 mM Na_2HPO_4, 12 mM D-glucose, pH 7.4)

CCA: cisaconitate

CDP: cytidine diphosphate

Ci: curie

cm: centimetre

coA: coenzyme A

CPS: carbamoyl phosphate synthase

CSF: cerebrospinal fluid

Cys: Cysteine

DEPC: Diethylpyrocarbonate

DFMO: difluoromethylornithine

DFMOR: difluoromethylornithine resistant cell line

DHAP: dihydroxyacetone phosphate

DMSO: dimethylsulphoxide

DNA: deoxyribonucleioc acid

dTDP: deoxy thymidine diphosphate

EC: enzyme commission

EDTA: ethylenediaminetetra acetic acid

EP: a form of procyclin

Epi: epimastigote form

ESI: electrospray ionisation

F-6-P: fructose 6-phosphate

FAD: flavin adenine dinucleotide

FBP: fructose 1,6-bisphosphate

FCS: foetal calf serum

FDA: Food and Drug Administration

FHc: fumarase

FIC: fractional inhibitory combination

FT-ICR: fourier transform ion cyclotron resonance

FT-ICR-MS: fourier transform ion cyclotron resonance mass spectrometry

FWHM: full width at half maximum

g: gram

G-3-P: glyceraldehyde 3-phosphate

G-6-P: glucose 6-phosphate

GC: gas chromatography

GC-MS: gas chromatography mass spectrometry

Gln: glutamine

Glu: glutamate

Gly: glycine

Gly-3-P: glycerol 3-phosphate

GSH: glutathione

GPEET: a form of procyclin

GUI: graphical user interface

HAPT: high affinity pentamidine transporter

HAT: human African trypanosomiasis

HILIC: hydrophilic interaction chromatography

His: histidine

HMDB: human metabolite database

HMI-9: Hirumi medium 9

HPLC: high pressure liquid chromatography

IC_{50}: inhibitory concentration for 50 % growth reduction

ICR: Institute for Cancer Research

IDEOM: identification of metabolites

IgG: Immunoglobulin G

KEGG: Kyoto Encyclopedia of Genes and Genomes

Keq: equilibrium constant

kg: kilogram

Km: Michaelis constant

L: litre

LAPT: low affinity pentamidine transporter

LC: liquid chromatography

LC-MS: liquid chromatography mass spectrometry

LdAAP3: *Leishmania donovani* amino acid permease 3

Leu: leucine

LiAc: lithium acetate

Lys: lysine

Meta: metacyclic form

M+H: protonated mass

µl: microlitre

µM: micromolar

mCi: milicurie

mg: milligram

mM: milimolar

mmol: milimole

mm: milimetre

min(s): minute(s)

MOA: mode of action

mRNA: messenger RNA

MRPA: multidrug resistance protein A

m/z: mass over charge

NAGS: N-acetyl glutamate synthetase

NCBI: National Center for Biotechnology information

ND: not detected

ng: nanogram

NL: not labelled

nl: nanolitre

NADH: nicotinamide adenine dinucleotide

NADPH: nicotinamide adenine dinucleotide phosphate

NECT: nifurtimox-eflornithine combination therapy

NIST: National Institute of Standards and Technology

nM: nanometre

nmol: nanomole

NMR: nuclear magnetic resonance

NTR: nitroreductase

OA: 2-oxoacid

ODC: ornithine decarboxylase

OTC: ornithine transcarbamoylase

P1: aminopurine transporter 1

P2: aminopurine transporter 2

PAD: protein associated with differentiation

PC: procyclic form

PCA: principle components analysis

PCR: polymerase chain reaction

PEG: polyethylene glycol

PEP: phospho*enol*pyruvate

PEST: proline, glutamate, serine, threonine

Phe: phenylalanine

Pi: inorganic phosphate

PPi: inorganic pyrophosphate

PPM: parts per million

Pro: proline

P^{RRN}: ribosomal RNA promoter

PV: proventricular form

R: resistant

RCF: relative centrifugal force

RNA: ribonucleic acid

RNAi: ribonucleic acid interference

RSD: relative standard deviation

RT: retention time

SAM: S-adenosyl methionine

SDM-79: semi-defined medium 79

SDS: sodium dodocyl sulphate

s.e.m: standard error of the mean

Ser: serine

SIF: stumpy induction factor

siRNA: small interfering ribonucleic acid

SIT: sterile insect technique

SL: slender form

ST: Stumpy form

SucCoA: succinyl-CoA

TbAAT: *Trypanosoma brucei* amino acid transporter

TbAT1: *Trypanosoma brucei* adenosine transporter 1

TCA: tricarboxylic acid

TcAAAP411: *Trypanosoma cruzi* amino acid arginine permease 411

TE: tris-Cl ethylenediaminetetra acetic acid

Thr: threonine

TSH: trypanothione

Tyr: tyrosine

UMP: uracil monophosphate

UQ: ubiquinone pool

US: United States

Val: valine

Vmax: maximum velocity

VSG: variable surface glycoprotein

WHO: World Health Organisation

WT: wildtype

ZIC-HILIC: zwitterionic hydrophilic interaction chromatography

1. Introduction

Human African trypanosomiasis is a neglected disease with a paucity of useful drugs and resistance evident to many of those in use. For the drugs in use, the modes of action are largely unknown. This project was conceived with the aim of developing metabolomic technologies to analyse the mode of action and mechanism of resistance to trypanocidal chemotherapeutic agents.

1.1 Protozoan parasites

Protozoan parasites are responsible for many lethal and debilitating diseases worldwide. In the West, toxoplasmosis is the cause of around 40 % of first trimester miscarriages (Abdel-Hameed and Hassanein, 2004). *Trypanosoma cruzi*, the causative agent of Chagas disease, currently affects 10 million people in the Americas (Barfield *et al.*, 2011). In South America, the Middle East and India Leishmaniasis affects 13 million people at any one time (Kato *et al.*, 2010). Malaria is infamously linked with the statistic of "one child dies every 30 seconds" and the fight against malaria is one of the top priorities of the WHO and the Bill and Melinda Gates Foundation. These parasites are all protozoa (single-celled eukaryotes) and, with the exception of toxoplasma, are all transmitted by biting insects.

Trypanosomes are single-celled flagellated extracellular protozoa that reside in the nutrient-rich fluids of their host and can be found on all continents (Hamilton *et al.*, 2007). Plants, animals and humans can all be infected with trypanosomes, with biting insects acting as a vector for transmission between hosts. Mechanical transfer may also occur through sexual intercourse (Rocha *et al.*, 2004) or through blood sucking bats and insects (Vincent Alibu, University of Aberdeen, personal communication), but such cases are rare and species dependent.

1.2 Human African Trypanosomiasis

1.2.1 Causative species

Human African trypanosomiasis (HAT), also known as sleeping sickness, a name too benign for the disease it causes, is caused by a single species of protozoan parasite - *Trypanosoma brucei*. Disease progression can vary dramatically depending on the geographical location, leading Hoare (1973) to postulate that there were two human-infective sub-species of *Trypanosoma brucei* parasite: *T. b. rhodesiense* and *T. b. gambiense*. More recent genetic analyses have shown that taxonomy of *T. brucei* is actually much more complicated than Hoare's model suggested : *T. b. rhodesiense* is now regarded as a host-range variant of *T. b. brucei* (a sub-species not able to infect humans) (Gibson, 2002;Balmer *et al.*, 2011), with the added presence of a serum resistance protein, which allows *T. b. rhodesiense* to survive in human serum where *T. b. brucei* cannot.

T. b. gambiense variants are now classed into two groups. Group one is less diverse and displays low virulence in rodents (Inoue *et al.*, 1998) and group two is more genetically diverse, able to infect rodents and shows biological and genetic similarities to *T. b. brucei* (MacLeod et al., 2001).

T. b. gambiense causes 90 % of all infections and is found in West and Central sub-Saharan Africa. *T. b. rhodesiense* causes the remaining 10 % of infections in East sub-Saharan Africa (Simarro *et al.*, 2008). The tsetse fly (*Glossina spp.*) vectors for these two sub-species of *T. brucei* are physically separated by the mountains along the Rift Valley, which cause lower temperatures not conducive to insect survival and therefore prevent the two sub-species from mixing. The only country where the two sub-species of *T. brucei* co-exist is Uganda, where there still remains a spatial separation between the sub-species (Fig 1-1), mainly due to the different climatic and vegetative conditions required by the two species (Berrang-Ford *et al.*, 2010).

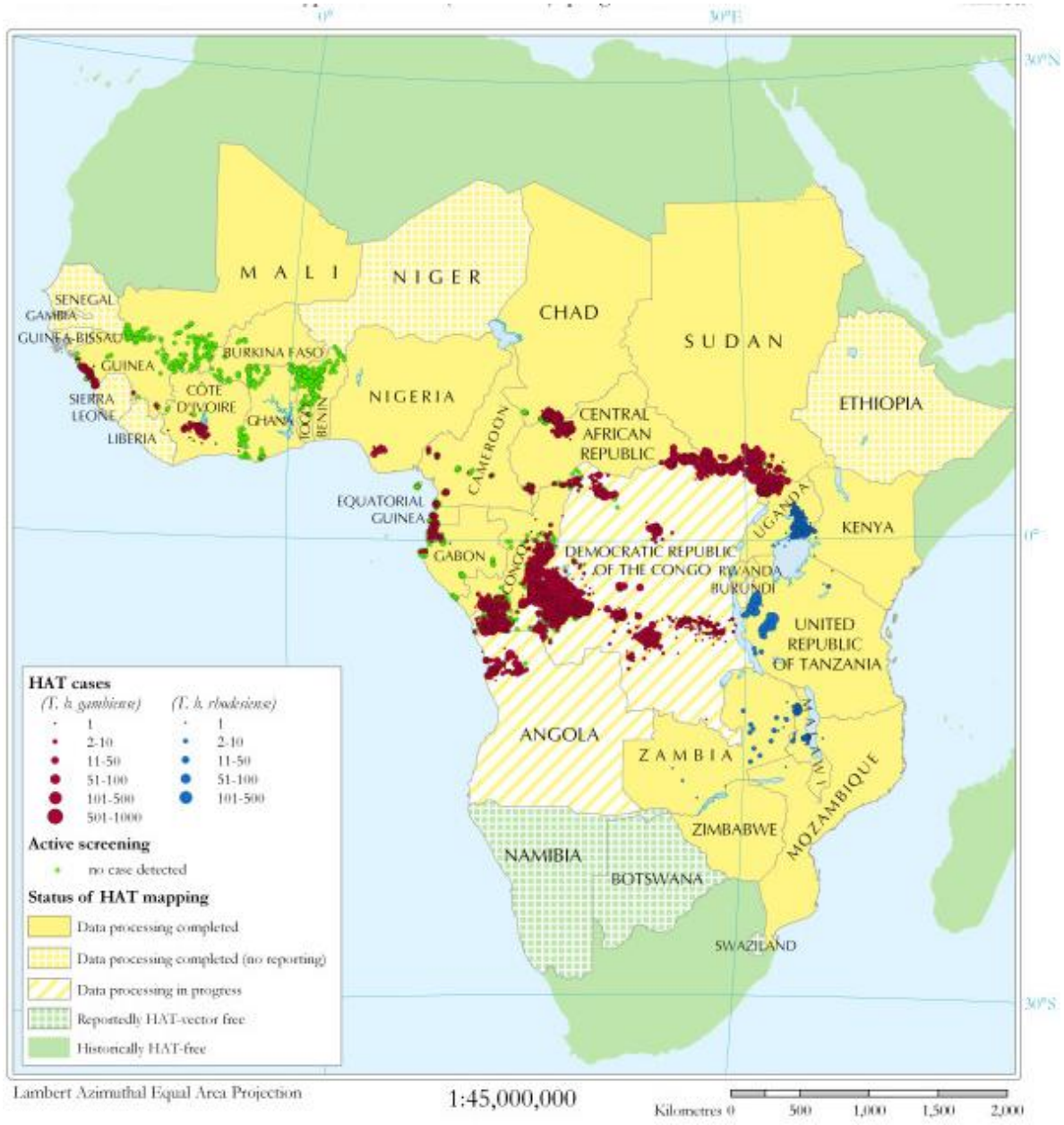

Figure 1-1. The distribution of human African trypanosomiasis. Red spots show the location of *T. b. gambiense,* blue spots show *T. b. rhodesiense*. From (Berrang-Ford *et al.*, 2010).

In 2006 it was estimated that 50,000-70,000 people were infected with HAT (World Health Organisation, 2006), although true figures are often difficult to come by due to under-reporting. For example, during an epidemic of *T. b. rhodesiense* sleeping sickness in Uganda between 1988 and 1990, it was estimated that with every death from HAT, twelve cases went undetected (Odiit et al., 2005). The most up to date figures from the World Heath Organisation put the number of people infected at fewer than 10, 000.

1.2.2 Stages of HAT

There are two stages of HAT, defined by the location of the parasites within the host. The first stage is characterised by parasite presence in the blood and lymph, but not the cerebral spinal fluid (CSF) of the host. Symptoms of the first stage of HAT can include swelling of the face, fever, loss of appetite, chancre, headaches and rashes, but not all of these symptoms need be present.

The second stage of HAT occurs when parasites enter the CSF and then the brain and is when patients will usually present at a clinic. The symptoms of this more serious stage are confusion, personality changes, altered sleep-wake patterns, difficulty in walking and coma. If untreated, HAT is 100 % fatal. It is difficult to design new compounds to counter this most commonly presenting stage mainly because the blood-brain barrier evolved as a very tight border control between the body and the delicate tissue of the brain. It is notoriously difficult to design trypanocides (or indeed any compounds) that can cross the blood-brain barrier and as a result there are only two licensed compounds active in the latter stages of the disease; melarsoprol and eflornithine.

1.2.3 History of control

During the mid 20th century there was a huge effort to eradicate HAT and the disease was largely brought under control (Barrett, 2006). Unfortunately, due to huge political restructuring over much of sub-Saharan Africa, successful control programmes broke down and HAT saw a re-emergence (Barrett, 1999). At the end of colonial rule the feeling was that HAT had been all but eradicated and a culture of complacency was born. After a massive resurgence in the late 1990s (Barrett, 1999) control efforts were again stepped up and the situation is again coming under control (Simarro *et al.*, 2011). The risk now is that control programmes will lose funding as governments see the disease as no longer posing an immediate critical problem. HAT is becoming closer to elimination and with a concerted effort could still be eradicated if regular screening is maintained, drugs are made available, drug resistance is combated and vector control programmes are not de-prioritised.

1.3 The *T. brucei* life cycle

Compared to many parasites, trypanosomes have a relatively simple life cycle. They must, however, be able to survive in several vastly differing environments from the blood, lymph and cerebrospinal fluid of the mammalian host to the gut and salivary glands of the tsetse fly vectors (Fig 1-2).

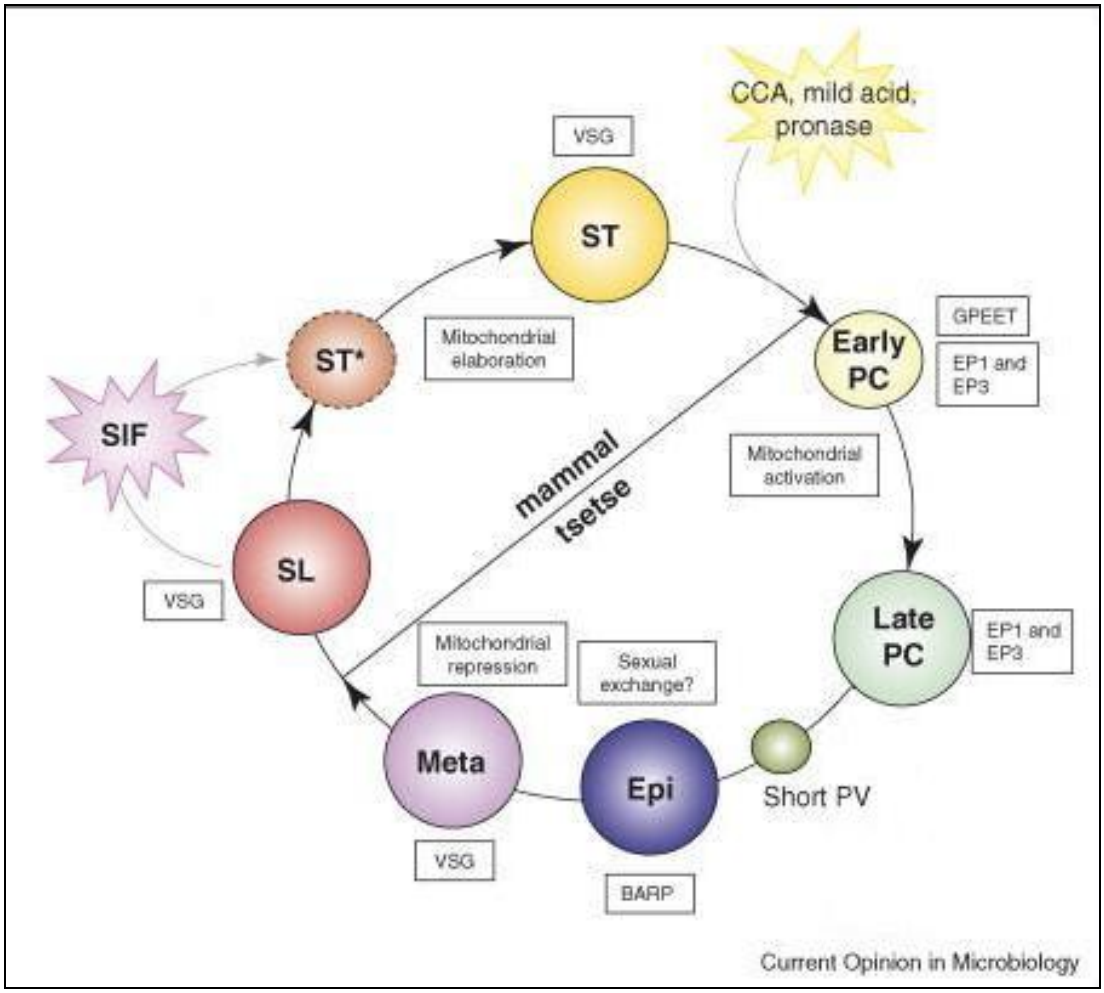

Figure 1-2. The Lifecycle of *Trypanosoma brucei*. The parasites develop through two mammalian stages and three insect stages in the tsetse fly vector. ST: stumpy form, SL: slender form, SIF: stumpy induction factor, PC: procyclic form, Epi: epimastigote form, Meta: metacyclic form, CCA: cisaconitate, GPEET: a type of procyclin, EP: a type of procyclin, PV: proventricular forms, BARP: brucei alanine rich protein, VSG: variable surface glycoprotein. From Fenn and Matthews (2007).

Starting with the bite of an infected mammal by a tsetse fly, stumpy forms of the parasite are taken up with the vector's blood meal. Differentiation from variable surface glycoprotein (VSG)-expressing bloodstream forms to procyclin-expressing insect forms, known as procyclic stages, takes place after pH and temperature triggers are activated. Citrate or cisaconitate (CCA) in the tsetse

midgut also appears to act as a trigger for stumpy to procyclic differentiation (Brun and Schonenberger, 1981;Czichos et al., 1986). Upon reaching the tsetse gut, parasite development and maturation takes 20-30 days (Aksoy *et al.*, 2003). Procyclic stages can be cultured in rich medium in the laboratory and so are well studied in comparison to the later epimastigote and metacyclic insect stages. Procyclic trypanosomes express a surface coat of GPEET and EP procyclin, with GPEET down regulated in later stages of development (Vassella *et al.*, 2004). After multiplication in the midgut of the tsetse fly, the cells migrate towards the salivary glands dividing asymmetrically on the way to produce the long, slender and the short epimastigote forms (Van Den *et al.*, 1999). Short epimastigotes attach to the salivary gland and are thought to undergo sexual genetic exchange. A new surface coat of brucei alanine rich protein (BARP) is expressed here (Urwyler *et al.*, 2007) and differentiation to the infective metacyclic forms takes place along with the acquisition of the VSG coat for evasion of the mammalian immune system.

Within the bloodstream of the mammalian host there are two distinct stages: slender and stumpy. Differentiation from the long, slender, rapidly dividing bloodstream forms to less active, stumpy forms appears to work via a quorum-sensing type mechanism where a soluble factor released by the slender trypanosomes builds up and promotes cell cycle arrest (Vassella *et al.*, 1997;Reuner *et al.*, 1997). This soluble factor has been named stumpy induction factor (SIF) although it has, as yet, eluded numerous efforts at identification. There is some evidence from factors that mimic SIF's action that the cAMP pathway is involved in SIF induction of differentiation (Vassella *et al.*, 1997; Laxman *et al.*, 2006), but this will not be conclusive until SIF is identified. A collaboration between the Barrett group at the University of Glasgow and the Matthews group at the University of Edinburgh is attempting to characterise the metabolome of trypanosomes throughout the lifecycle, which may identify this elusive factor.

Stumpy, bloodstream forms of *T. brucei* do not divide, which is a crucial characteristic for limiting parasitaemia within the host. Cell cycle arrest also seems to be important for the subsequent differentiation to procyclic forms when taken into a tsetse vector. Slender and intermediate forms cannot proceed to procyclic forms within the mammalian host, probably because they are

outwith the G1/G0 stage of growth (Matthews and Gull, 1994;Ziegelbauer *et al.*, 1990). Stumpy forms are primed to differentiate to procyclic forms upon uptake into the insect vector. This priming appears to involve production of a group of carboxylate transporters deemed PADs (Proteins Associated with Differentiation) (Dean *et al.*, 2009). These transporters are sequestered in the flagellar pocket of the trypanosome ready for transfer to the surface when citrate and CCA promote differentiation to procyclic forms (Dean *et al.*, 2009).

1.4 Trypanosome biology

Trypanosomes are model organisms, in which many novel processes have first been discovered, including RNA (ribonucleic acid) editing, trans-splicing, glycosylphosphatidylinositol membrane anchoring and polycistronic transcription of protein-coding eukaryotic genes (Field and Carrington, 2009). RNA interference is possible in trypanosomes, allowing the analysis of the effects of reduced or elimated expression of individual genes in an inducible system. Trypanosomes can also be cloned *in vitro* making them a popular choice for genetic and metabolic studies too.

African trypanosomes have a number of unusual features, which can make chemotherapy difficult and are described in detail below.

1.4.1 Gene expression regulation

Eukaryotic gene expression is usually controlled at the transcript level, producing less mRNA for a particular gene leading to reduced protein production. In trypanosomes, this method is not possible because genes are transcribed as multi-gene cistrons into pre-mRNA. These cistrons are often tens of genes long (Imboden *et al.,* 1987;Daniels *et al.,* 2010) meaning that the genes cannot be individually regulated at this level. Further evidence that expression is not regulated at the transcriptional level comes from an analysis of the level of the polycistronic transcript produced, which shows very little variation across the genome (Daniels *et al.,* 2010).

Gene regulation may occur when the cistrons are cut into individual genes or when the monocistronic pre-mRNAs are capped with a spliced leader sequence and polyadenylated to produce the final, functional mRNA (Huang and van der Ploeg, 1991). Another level of regulation may occur through mRNA degradation, which, contrary to most eukaryotes, occurs via two pathways attacking different ends of the transcript (Schwede *et al.*, 2009).

1.4.2 Variable surface glycoproteins

One of the most interesting aspects of the trypanosome is how they manage to survive extracellularly while avoiding clearance by the host immune system. The main reason trypanosomes are able to stay one step ahead of their host's defences lies in the fact that trypanosomes are covered in a thick VSG coat that they are able to shed and swap between generations. The coat is made of around 10^7 identical molecules with a conserved core structure of glycosylphosphatidylinositol anchored in the cell membrane and an exposed proteinacious antigen (Cross, 1975) (Fig 1-3). Only the exposed antigen of the VSG is capable of change and is able to do so via a repertoire of thousands of silent VSG genes and gene fragments that can be moved to one of several telomeric expression sites (Horn and Barry, 2005). There may be several million trypanosomes within a host at one time, all of which will be expressing the same VSG copy. The immune system will recognise this VSG and will launch an adaptive immune attack. Trypanosomes do not appear to recognise when they are under attack from the immune system (trypanosomes in the absence of an immune system act in the same way (Doyle *et al.*, 1980)), but a number of trypanosomes within the several million will exchange their expressed VSGs and as the trypanosomes with the first copy are killed, those with the second copies are able to clonally expand. This leads to a characteristic cyclic parasitaemia with an associated periodic fever and is useful in the diagnosis of HAT.

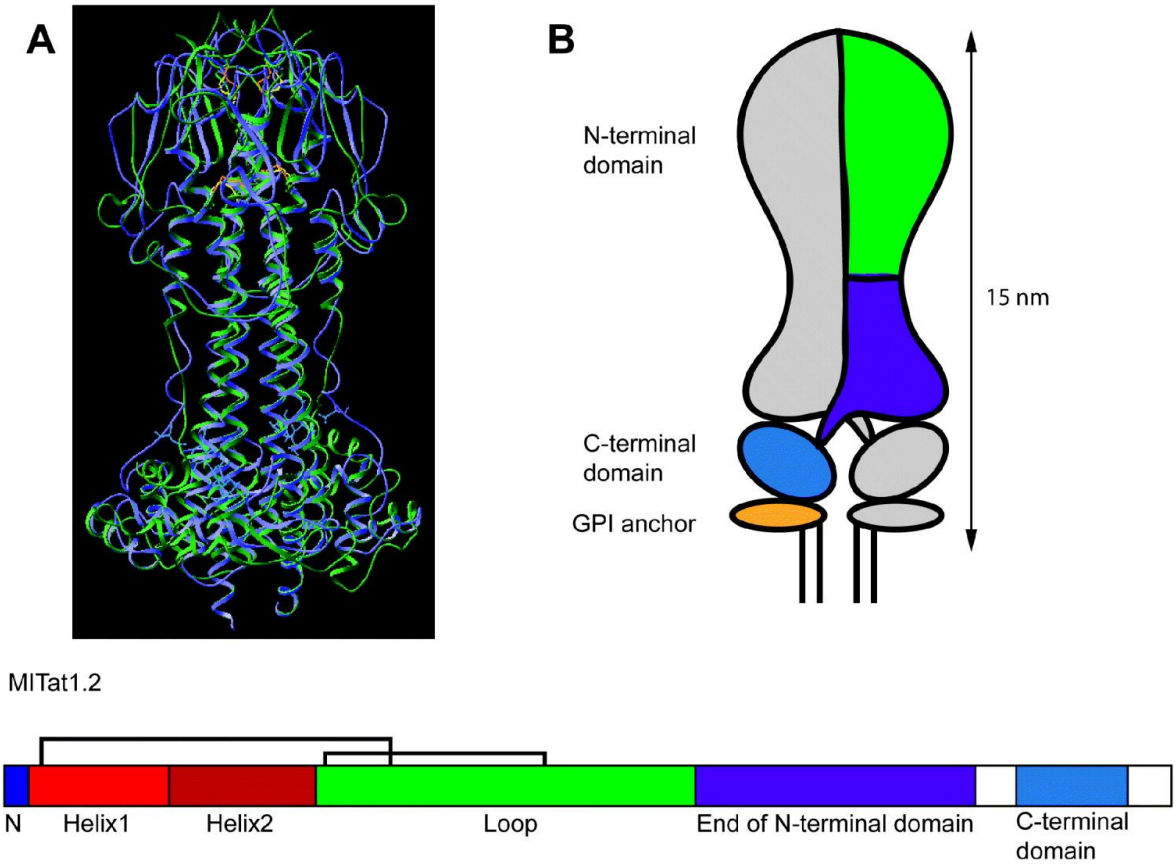

Figure 1-3. The structure of variable surface glycoprotein. A: the superimposed structures of the N-terminal domains of two VSGs (MITat1.2 and ILTat1.24) to show the highly conserved structure. B: The dimeric structure of a VSG. One monomer is depicted in grey, the other in colours that correspond to regions of the primary structure below. From Schwede and Carrington (2010).

The shedding of VSG is also problematic as it means that when antibodies are produced and adhere to the trypanosome's coat the molecule can be shed and the trypanosome can avoid destruction. Shedding affects the innate immune system in a similar way when complement binds in an attempt to construct its lysis machinery that would normally bind and make holes in the trypanosomes' cell membranes. The thickness of the coat and the presence of proteases is also problematic to complement-mediated lysis (Jokiranta *et al.*, 1995). The thickness of the coat prevents access to the membrane and the proteases degrade proteinaceous immune machinery.

1.4.3 Organelles

T. brucei have many peculiarities in their organelles, which has led them to be considered as a very old species and are evident in the eukaryotic lineage (as *Trypanosoma gray* in the blood of crocodiles) from around 480 million years ago

(Teixeira *et al.*, 2009). Whereas most eukaryotic cells have many small mitochondria, trypanosomes contain one large, spindle-shaped mitochondrion that spans the entire length of the cell joining the flagellum via the basal body. This mitochondrion contains its own DNA (deoxyribonucleic acid), as do other eukaryotic mitochondria, but unlike other eukaryotes the mitochondrial DNA is in a large complex with many copies of the same genome. This DNA complex is termed the kinetoplast. The kinetoplastid DNA is organised into around 5, 000 interlinking minicircles and around 25 maxicircles (Chen *et al.*, 1995). The maxicircles have been known to encode the usual mitochondrial and ribosomal proteins for many years, but the minicircles eluded explanation for a long time. Now we know that the maxicircles' RNA transcripts are extensively edited before becoming functional and the minicircles provide guide RNAs to allow the editing (a series of uridine additions and deletions) to proceed (Benne et al., 1986;Feagin et al., 1988;Blum et al., 1990; van der et al., 1991).

There is an extensive electron transport chain in the procyclic trypanosome's mitochondrion, which is essential to provide the majority of energy production (Bochud-Allemann and Schneider, 2002;Coustou *et al.*, 2003). Conversely, bloodstream form trypanosomes do not express cytochromes and lack many of the tri-carboxylic acid cycle intermediates required for oxidative phosphorylation (Clayton and Michels, 1996;Tielens and van Hellemond, 1998) and therefore require glycolysis to produce ATP (adenosine triphosphate).

Glycolysis within the kinetoplastida occurs within a specialised organelle termed the glycosome. Bearing many similarities in structure, origin and replication to peroxisomes, glycosomes encompass the first seven enzymes of the glycolytic pathway bound by a single phospholipid bilayer (Opperdoesand Borst, 1977) (Fig 1-4). In fact, 90 % of all the protein content of a glycosome comprises glycolytic enzymes (Michels *et al.*, 2006).

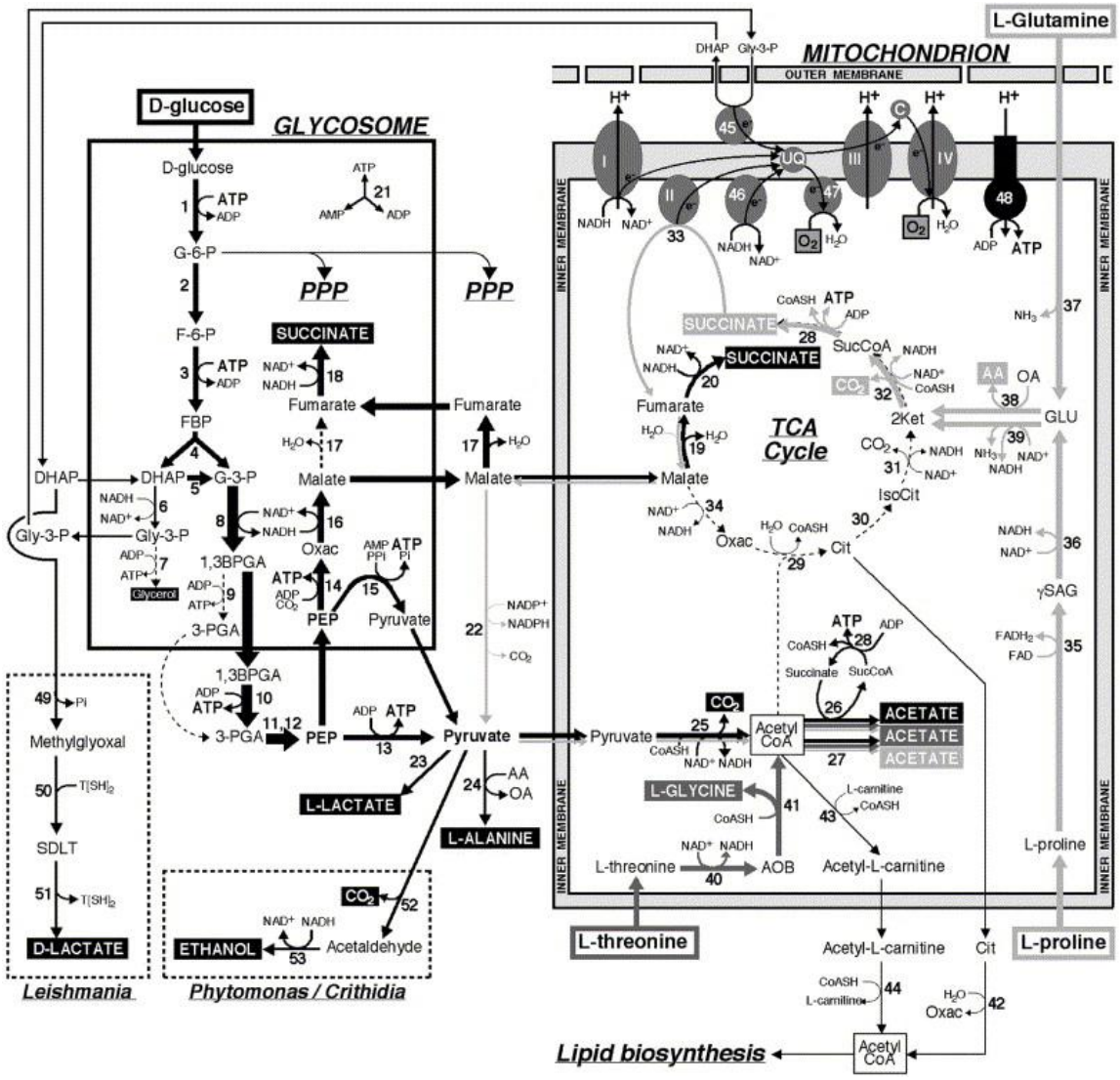

Figure 1-4. Energy generation in procyclic form trypanosomes. Light grey arrows highlight the pathways utilised when glucose is the energy source, dark grey when proline or threonine are used. Excreted end products are represented with white text on a black background. Abbreviations: AA, amino acid; 1,3BPGA, 1,3-bisphosphoglycerate; C, cytochrome *c*; CoASH, coenzyme A; DHAP, dihydroxyacetone phosphate; F-6-P, fructose 6-phosphate; FBP, fructose 1,6-bisphosphate; G-3-P, glyceraldehyde 3-phosphate; G-6-P, glucose 6-phosphate; Gly-3-P, glycerol 3-phosphate; OA, 2-oxoacid; PEP, phospho*enol*pyruvate; 3-PGA, 3-phosphoglycerate; Pi, inorganic phosphate; PPi, inorganic pyrophosphate; SucCoA, succinyl-CoA; UQ, ubiquinone pool. Enzymes are: 1, hexokinase: 2, glucose-6-phosphate isomerase; 3, phosphofructokinase; 4, aldolase; 5, triosephosphate isomerase; 6, glycerol-3-phosphate dehydrogenase; 7, glycerol kinase; 8, glyceraldehyde-3-phosphate dehydrogenase; 9, glycosomal phosphoglycerate kinase; 10, cytosolic phosphoglycerate kinase; 11, phosphoglycerate mutase; 12, enolase; 13, pyruvate kinase; 14, phospho*enol*pyruvate carboxykinase; 15, pyruvate phosphate dikinase; 16, glycosomal malate dehydrogenase; 17, cytosolic (and glycosomal) fumarase (FHc); 18, glycosomal NADH-dependent fumarate reductase; 19, mitochondrial fumarase (FHm); 20, mitochondrial NADH-dependent fumarate reductase; 21, glycosomal adenylate kinase; 22, malic enzyme; 23, unknown enzyme; 24, alanine aminotransferase; 25, pyruvate dehydrogenase complex; 26, acetate:succinate CoA-transferase; 27, unknown enzyme; 28, succinyl-CoA synthetase; 29, FAD-dependent glycerol-3-phosphate dehydrogenase; 30, rotenone-insensitive NADH dehydrogenase; 31, alternative oxidase; 32, F_0F_1-ATP synthase; I, II, III and IV, complexes of the respiratory chain. (Bringaud *et al.,* 2006).

The net production of ATP within the bloodstream form *T. brucei* glycosome is zero. All usable ATP from glycolysis is therefore produced by pyruvate kinase (enzyme 13 in Fig 1-4) in the cytosol. Sequestration of the glycolytic enzymes within the glycosome has been shown to be essential (Bakker *et al.*, 2000;Guerra-Giraldez *et al.*, 2002;Furuya *et al.*, 2002). Glycolysis in other organisms has negative feedback loops from glucose 6-phosphate or trehalose 6-phosphate on hexokinase and phosphofructokinase to prevent the autocatalytic pathway from losing control (Haanstra *et al.,* 2008). *T. brucei* has no such feedback and glycolysis is instead regulated by compartmentalisation allowing ATP levels to be controlled (Haanstra *et al.,* 2008). Without this compartmentalisation, ATP produced by the latter stages of the pathway would be accessible to the early stages causing a turbo explosion within the pathway leading to death by accumulation of toxic intermediates (Haanstra *et al.,* 2008). Flux balance analysis of glycolysis within the trypanosome highlights the rate of glucose transport to be the main regulator of glycolysis, and blocking glucose transport invokes an anti-homeostatic response, increasing the effects of the inhibition (Haanstra *et al.*, 2011). Both of these studies used computer models of glycolysis to build hypotheses with regards to regulation and control, which can then be tested biochemically. They highlight the use of modelling within drug discovery and in gaining a greater overall understanding of metabolism.

1.4.4 Biochemistry

Biochemically, trypanosomes evolved to maximise host energy exploitation and therefore rely on their insect and vertebrate hosts for the biosynthetic metabolic components such as purines, fatty acids, and sterols (Fairlamb, 1989). The parasites retain the capacity to induce many pathways but maintain a stream-lined metabolism in periods of nutritional abundance (Fig 1-5), utilising an extensive transporter repertoire over the entire trypanosome surface and endocytosis in the flagellar pocket to salvage nutrients. When the *T. b. brucei* genome was published there were estimated to be nearly 400 transporters, 38 of which were apparent amino acid transporters (although these figures are refined as more information is garnered about the transporter repertoire) (Berriman *et al.,* 2005). This is a significant proportion (more than 4 %) of the 9, 000

predicted genes, demonstrating how important salvage is to these parasites (Berriman *et al.*, 2005).

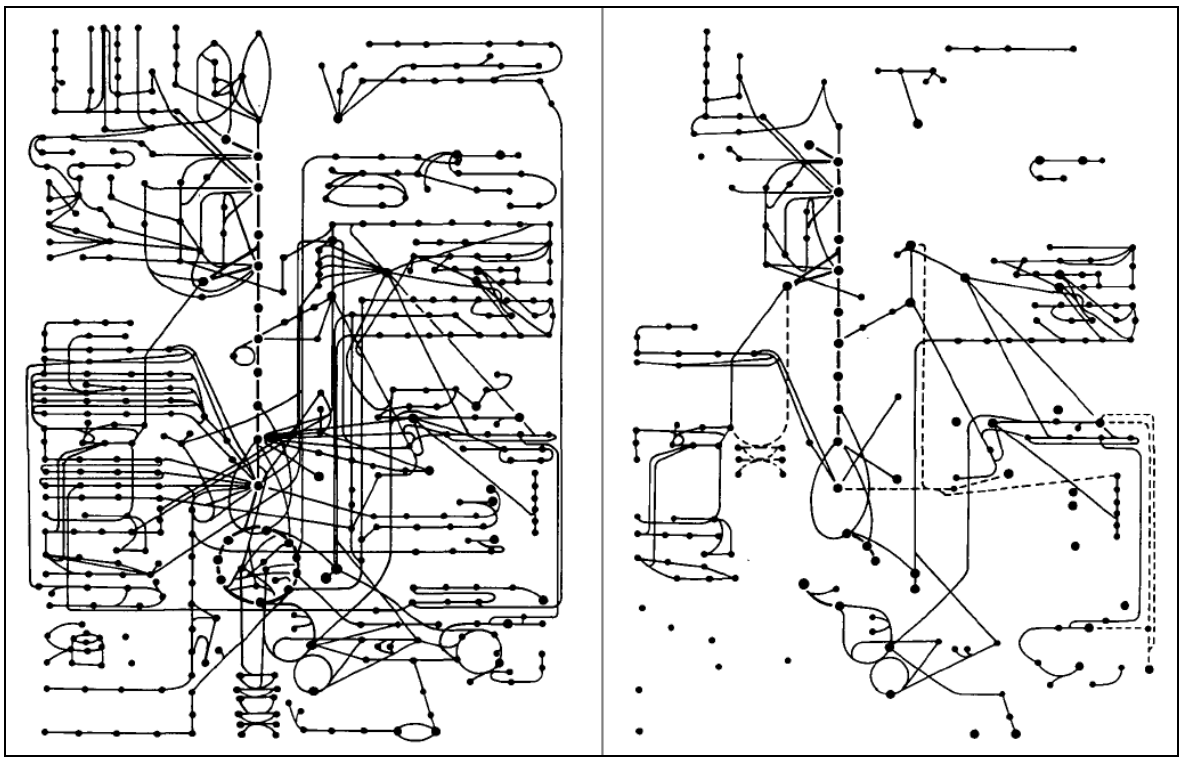

Figure 1-5. Metabolism within the trypanosome (right panel) is streamlined compared to a typical mammalian cell (left panel). Dots represent metabolites and lines represent biochemical transformations. From (Fairlamb, 1989)

Figure 1-5 depicts the greatly increased complexity and number of metabolites in the generalised mammalian metabolome as compared to the trypanosome metabolome (Fairlamb, 1989;Nerima *et al.*, 2010).

The flagellar pocket is a small invagination in the plasma membrane of the trypanosome, at the root of the flagellum. The flagellar pocket serves as the only site of exocytosis and endocytosis (Field and Carrington, 2009) and is the origin of cell division in the parasite (Hammarton, 2007).

The bloodstream is very rich in glucose as well as amino acids and other small molecules, allowing the trypanosome to use glucose as its main energy source. When the trypanosome is within the tsetse fly vector, however, glucose is scarce and proline (and to a lesser extent threonine) is used as a source of energy (Bringaud *et al.*, 2006). This clearly requires extensive re-modelling of the trypanosome metabolome upon differentiation from bloodstream to insect

stages of the parasite, which in turn means that many genes and proteins will not be in use in some stages of the parasite's lifecycle.

Another interesting aspect of trypanosome biochemistry is the production of trypanothione, a thiol unique to trypanosomatids. Trypanothione is produced upon the conjugation of two glutathione molecules with a spermidine group (Fig 1-6). This thiol is more efficient than glutathione as it can form intramolecular disulphide bonds more rapidly than glutathione (Olin-Sandoval *et al.,* 2010). Trypanothione has been the subject of much research in the hope that its essentiality (Li *et al.*, 1996; Huynh *et al.*, 2003;Comini *et al.*, 2004) will allow selective drugs to be designed that abrogate its production. Indeed, the only trypanocide in use with a known mode of action is thought to abrogate the production of this unique thiol (Fairlamb *et al.*,1987).

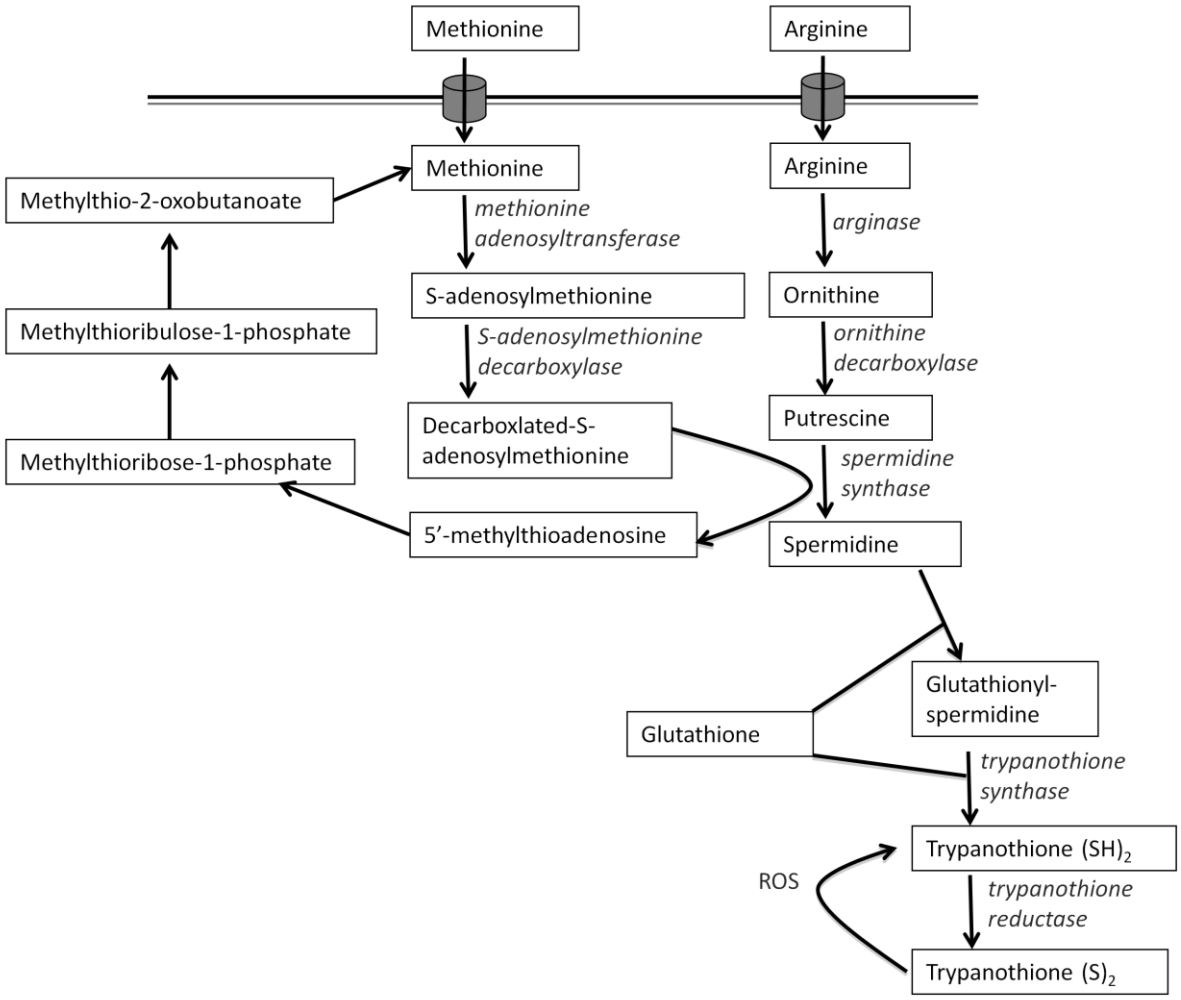

Figure 1-6. The polyamine pathway. L-arginine and L-methionine are transported across the plasma membrane (represented by double line) into the cell. Metabolites are in boxes. Enzymes are in italics. ROS; Reactive oxygen species.

It should be noted that although the arginase enzyme (EC: 3.5.3.1) has been annotated in many of the trypanosome databases, the identification is not robust and the possibility has been raised (Bakker *et al.*, 2010) that the annotated gene does not encode arginase in trypanosomes.

1.5 Control strategies

A multifaceted control strategy is possible in the fight against HAT. As *T. b. rhodesiense* (and possibly *T. b. gambiense* (Ezeani et al., 2008)) is zoonotic, animal reservoirs must be reduced where possible. Livestock may be treated with trypanocides and infected wild animals may be slaughtered. Financial problems, however, in many of the affected countries limit the drugs available to treat infected animals. The availability of new compounds to treat animals is also a limiting factor. Human trypanocides are not used in animals (with the exception of suramin in *T. evansi* (Muhammad *et al.*, 2007)) to reduce the risk of resistance building through over-use.

1.5.1 Tsetse control

During the 1980s the future of the tsetse fly looked uncertain. It was internationally recognised that reduction in tsetse numbers would have a hugely positive impact in reducing the number of infected individuals, and as a result, a large control programme was initiated across a 330, 000 km^2 area of Malawi, Mozambique, Zambia, Zimbabwe and Somalia (Jordan, 1985). Various strategies including aerial spraying, ground spraying, odour-baited traps and pyrethroid-treated cattle were used with much celebrated success. In the 1990s, however, European spending priorities changed and the onus fell on the local farmers to treat their cattle and to communities to maintain traps. This led to the development of smaller treatment foci, which are far less effective due to the mobile nature of tsetse populations (Torr *et al.*, 2005). The main problems associated with tsetse control are therefore political, although there is some work that can be done by the scientific community.

The sterile insect technique (SIT) has been the focus of much research of late due to its potential in the control of plasmodium carrying mosquitoes. SIT has been used successfully to eliminate *Glossina austeni* in Zanzibar (Vreysen *et al.*, 2000), but was very costly and the longer-term benefits are unclear as the vector moves back into the treated area. Methods used to produce sterile insects include irradiating them before release (Franz and Robinson, 2011). Cheaper,

and more effective SITs may be developed, such as the use of viruses specific to the tsetse fly (Lietze *et al.*, 2011), but are not available at present.

1.5.2 Vaccines

When variable surface glycoproteins (VSGs) were discovered in 1969 (Vickerman and Luckins, 1969) to be the trypanosome's main protection against the host immune system, researchers were excited to finally have an exposed epitope that they could purify and use to develop a vaccine. Indeed, early research suggested that the VSG repertoire was limited to no more than a dozen VSGs (Le Ray *et al.*, 1978;Barry *et al.*, 1979;Esser *et al.*, 1982;Crowe *et al.*, 1983). Attempts were made to vaccinate using irradiated metacyclic trypanosomes, which resulted in promising early results (Esser *et al.*, 1982). However, when it was subsequently discovered that the mosaic nature of expressed VSGs means that the repertoire is virtually limitless (McCulloch and Horn, 2009), exposed antigen vaccination programmes fell out of favour.

Trypanosomes require a highly developed cytoskeleton, integral to motility, flexibility and mechanical stability. As a consequence, ß-tubulin and actin are highly expressed and have been used as vaccine candidates, producing some positive results (Lubega *et al.*, 2002;Li *et al.*, 2007;Li *et al.*, 2009), although negative controls also offered some protection suggesting that the initially positive results are actually a result of a general immune system boost at a non-specific level.

Transmission blocking vaccines have been used successfully in experimental tests for malaria (Outchkourov *et al.*, 2008), leishmania (Saraiva *et al.*, 2006) and babesiosis(Willadsen *et al.*, 1995;de la Fuente *et al.*, 1998) and may be possible in trypanosomiasis too. Transmission blocking vaccines can follow a number of strategies. Interruption of the development of the parasites to the insect infective stage within the human body is one target. Similarly, development of the parasite within the midgut of the insect vector can be abrogated (as is the case with malaria and leishmania vaccine trials). Insect fecundity is also a target, taking advantage of the tsetse fly's requirement for albumin to provide osmoregulation during storage of the blood meal (Nogge and Giannetti, 1980). Antibodies against the insect mid-gut can also have devastating effects on the

vector population as was shown with babesiosis (Willadsen *et al.*, 1995;de la Fuente *et al.*, 1998). These methods hold their own controversies as they are often unspecific to the disease the arthropod vector is carrying.

In different cattle species, infected with *T. congolense*, there is a significant disparity in the disease progression, enabling animals to be labelled as trypanosusceptible and trypanotolerant. It appears that the main difference between the trypanosusceptble and the trypanotolerant cattle is that the latter are able to mount an anti-congopain IgG, an immunoglobulin produced by white blood cells of the adaptive immune response. Congopain is a cathepsin-L like cysteine protease in *T. congolense* trypanosomes and is under investigation as a vaccine candidate for cattle (Boulange *et al.*, 2011). Humans however, do not show the same spectrum of disease susceptibility as cattle and some researchers defined the cause of this discrepancy to be due to suppression of the immune system during human trypanosome infection (Murray *et al.*, 1974;Murray *et al.*, 1974;Askonas *et al.*, 1979;Clayton *et al.*, 1979). More recently, it has been reported that in addition to immune suppression there is a significant reduction in several B cell responses (Radwanska *et al.*, 2008). This destruction appears to be very rapid and permanent, explaining why the large majority of vaccines trialed up until now have shown promising initial results, but no long-term memory. This is a worry, not just for the future of trypanosome vaccination research, but also for vaccination programmes against the many other infections in the trypanosome-exposed population. A permanent destruction of B-cells, leading to a lack of herd immunity can vitiate a whole vaccination programme (e.g. for human immunodeficiency virus, schistosomiasis or malaria) so it may be beneficial to these programmes to invest in anti-trypanosome therapies before commencing vaccine trials.

1.5.3 Chemotherapy

There are only four drugs licensed for the treatment of HAT: pentamidine, suramin, melarsoprol and eflornithine (Fig 1-7). Although many of the drugs have been around for decades, we only know how one of these compounds, eflornithine, exerts its actions.

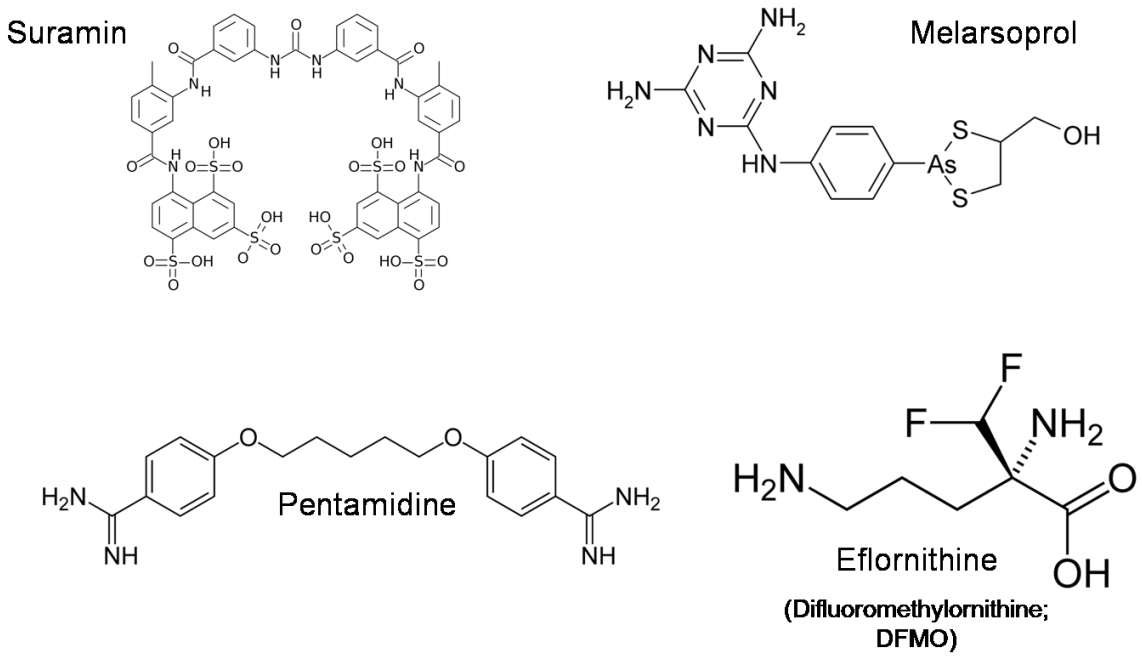

Figure 1-7. The four drugs licensed for use against HAT. Suramin and pentamidine are used in the early stages of infection. Melarsoprol and eflornithine in stage two of the disease when the CSF has been invaded.

1.5.3.1 Pentamidine

Pentamidine is a diamidine effective against stage one *T. b. gambiense* infections. It has been available since the early 1940s and has previously been heavily used as a prophylactic as well as a curative agent (Bacchi, 1993). The action of pentamidine appears to be multifactorial possibly due to the drug binding to DNA in regions of the minor groove rich in adenine and thymine (Moreno *et al.*, 2010). Pentamidine isethionate is currently given for free by Sanofi-Aventis to the WHO and distributed by Médecins Sans Frontières. Four milligrams per kilogram are given daily or on alternate days by intramuscular injection for 7-10 days (Sands *et al.*, 1985). Pentamidine is concentrated within trypanosomes principally via the P2 aminopurine permease (Lanteri *et al.*, 2004). High affinity and low affinity pentamidine transporters (HAPT and LAPT) also contribute to uptake (De Koning, 2001).

An analogue of pentamidine containing a furan ring has been developed and was, until recently, in clinical trials for use against *Pneumocystis jiroveci carinii* pneumonia, advanced immunodeficiency syndrome and malaria in addition to HAT (Lanteri *et al.*, 2004). It is administered as a pro-drug, DB289, and can be given orally, which is a major advantage for use in less developmentally advanced countries. The active compound of DB289, DB75 (2,5-bis-4-

amidinophenylfuran), is also fluorescent due to its furan and benzene ring conjugation systems and has been seen to localise to the mitochondrion in yeast cells (Lanteri *et al.,* 2004) along with other DNA containing organelles in the trypanosome (Mathis *et al.*, 2006). The usability of DB75 on trypanosomes may be limited however, as the mechanism of uptake is via the P2 transporter (Lanteri *et al.,* 2006) and so it is likely that the resistance mechanism will be the same as that for pentamidine (see section 1.6). DB289 was shown to be successful in phase III clinical trials as an oral drug against stage one HAT. During extended phase I trials, however, using a 14 day instead of the 10 day dose used in the phase III trials, serious toxic side effects were exposed and the drug has now been removed from clinical consideration (Paine *et al.*, 2010).

1.5.3.2 Suramin

Suramin is a polysulphonated naphthalene derivative (Barrett *et al.,* 2007) discovered by Oskar Dressel and Richard Kothe at Bayer in 1916 (Haberkorn *et al.*, 2001) and has been used to treat "surra", caused by *T. evansi,* in camels for many years (Zhou *et al.*, 2004). The large, negatively-charged polyanion appears to inhibit many positively-charged enzymes unspecifically, so it is difficult to conclude which may be the determinant of drug action (Pepin and Milord, 1994;Wang, 1995). Suramin (along with other naphthalene dyes) is selectively concentrated by trypanosomes through either receptor-mediated endocytosis when conjugated with low-density lipoproteins (Vansterkenburg *et al.,* 1993) or some other mechanism (Pal *et al.*, 2002). Suramin can be administered in stage one cases of *T. b. gambiense* and *rhodesiense* infection by five slow intravenous injections every 3-7 days for 28 days (Barrett *et al.,* 2007). There has, however, been some treatment failure in *T. b. gambiense*, so suramin has been reserved for preferential use against *T. b. rhodesiense*, where pentamidine is ineffective.

1.5.3.3 Melarsoprol

Only melarsoprol and eflornithine are effective in the latter stages of the disease when the parasites have invaded the brain and CSF due to difficulties in other compounds in crossing the blood-brain barrier. Melarsoprol, a melaminophenyl arsenical, was first synthesised in 1949 and its action is based on the severely toxic arsenic moiety. The severely toxic nature of this drug

results in the death of around 5 % of recipients treated (in HAT (Blum *et al.*, 2001) and leukaemia patients (Soignet *et al.*, 1999)), via a reactive arsenical encephalopathy. It is not known how melarsoprol kills trypanosomes, but it is known to form stable adducts with thiols, particularly with dihydrotrypanothione to form MelT (Fairlamb *et al.*, 1989). MelT then acts as a competitive inhibitor of trypanothione reductase, an essential enzyme that protects from oxidative stress (Bacchi, 1993). Adducts are also formed with lipoic acid (Barrett *et al.*, 2007) and glycolysis is targeted via fructose 6-phosphate 2-kinase (Bacchi, 1993). Actions on glycolysis do not appear to be the main mode of action of melarsoprol however, and the effects on this pathway are minimal (Bacchi, 1993). It is likely that there are more modes of action for melarsoprol.

Melarsoprol is distributed in glass vials and usually administered intravenously in glass syringes as the solvent (ethylene glycol) is known to dissolve plastic-ware. The recommended course is 10 days long with daily injections of 2.2 mg/kg (Brun *et al.*, 2010). Melarsoprol is the only drug effective against late stage *T. b. rhodesiense* infections.

1.5.3.4 Eflornithine

Due to the unacceptable toxicity of melarsoprol, eflornithine (DL-α-Difluoromethylornithine; DFMO) has been recommended by the WHO as the first line treatment in areas where *T. b. gambiense* is prevalent (Chappuis *et al.*, 2005;Balasegaram *et al.*, 2006;Priotto *et al.*, 2008). Eflornithine, manufactured by Sanofi-Aventis, is the only drug with a well understood mode of action. It was originally developed in the 1970s as an antineoplastic agent (Janne *et al.*, 1981;Heby *et al.*, 2007) and is a suicide inhibitor of ornithine decarboxylase (ODC) in the polyamine pathway (Fig 1-5). ODC exists in trypanosomes as a homodimer and is dependent of pyridoxal 5'-phosphate for its structural integrity (Grishin *et al.*,1999). ODC is irreversibly inhibited by the formation of adducts with eflornithine in the active site of the enzyme (Poulin *et al.*, 1992). In mice these adducts form at residues lysine 69 and cysteine 360, forming a Schiff base to pyridoxal 5'-phosphate (Poulin *et al.*, 1992). In the trypanosome enzyme, eflornithine also forms a schiff base with pyridoxal 5'-phosphate and covalently binds to cysteine 360 (Grishin *et al.*,1999).

Eflornithine is only active against *T. b. gambiense* forms of HAT possibly due to a reduced rate of ODC turnover in this sub-species (Iten *et al.*, 1997). The rate of turnover of ODC may be influenced by differences in the C-terminal peptides of the enzymes, as *T. b. gambiense* has been shown to lack a 36 amino acid region rich in proline, glutamate, aspartate, serine and threonine (PEST) when compared to the mouse orthologue (Phillips *et al.,* 1987), which has a much faster turnover rate. These PEST regions appear to be indicators of enzyme instability (Ghoda *et al.*, 1992).

Eflornithine treatment is difficult to administer in the field as it has poor bio-availability when given orally and therefore must be administered by intravenous infusion. Eflornithine's high IC_{50} (inhibitory concentration for 50 % growth reduction) (225 μM (Phillips and Wang, 1987) or 100 μM (Bellofatto *et al.,* 1987) *in vitro* for procyclic stages) and low half life of around three hours, also dictate that large quantities of the drug are required (nearly 4 kg for a 50 kg patient (Brun *et al.*, 2010)) for the treatment regime of 56 infusions over 14 days. It is logistically difficult to deliver and to administer the large quantities of drug required to the rural areas where patients are often diagnosed leading to a continued reliance on melarsoprol in some places. This problem is also driving research into combination therapies that might reduce the amount of drug required.

ODC inhibition by eflornithine leads to an increase in levels of ornithine, S-adenosyl methionine and decarboxylated S-adenosyl methionine, and a decrease in putrescine, spermidine and trypanothione after 48 hours (Fairlamb *et al.,* 1987). Bacchi *et al.* (1983) also recorded a decrease in putrescine and spermidine and an increase in dc-SAM, but also noted an increase in spermine. This is interesting as spermine is not thought to be synthesised or utilised in *T. brucei* and may even be toxic to the cells (Merkel *et al.*, 2007). Margaret Phillips's lab in Texas recorded polyamine levels by high performance liquid chromatography after the addition of eflornithine to bloodstream form cells *in vitro*. The group reported a depletion of putrescine and decreases (to 20-40 % of untreated levels) of spermidine, glutathionyl-spermidine, glutathione and trypanothione after three days, in agreement with the other studies (Xiao *et al.*, 2009). Decarboxylated S-adenosyl methionine levels increased around 40 % after

treatment with eflornithine as the previous studies showed, but S-adenosyl methionine levels were unchanged (Xiao *et al.,* 2009).

Bacchi *et al.* (1995) found that trypanosomes rapidly incorporate heavy methionine into S-adenosyl methionine, methylthioadenosine, S-adenosylhomocysteine, homocysteine, csytathione, cysteine and glutathione. When treated with eflornithine, these cells rapidly (within 30 minutes) accumulate S-adenosyl methionine but also accrue decarboxylated S-adenosyl methionine (Bacchi *et al.,* 1995), albeit at a slower rate.

Roles of spermidine include the formation of complexes with polynucleotides to alter their stability and transcription, the binding to membranes influencing stability and the enhancement of some enzyme catalysis (Li *et al.,* 1996). Spermidine conjugates with two molecules of glutathione to form trypanothione, a thiol unique to trypanosomatids (Heby *et al.,* 2007). The synthesis of polyamines is essential to parasite survival, since polyamines are important for G-S phase transition (Li *et al.,* 1996) and protection against oxidative stress (Steenkamp, 2002). The increase in S-adenosylmethionine levels causes aberrant methylation of proteins (Yarlett and Bacchi, 1988). Levels of all proteins including VSG decrease with eflornithine addition (Bitonti *et al.,* 1988;Heby *et al.,* 2007). The reduction in VSG exchange associated with the decrease in VSG expression may allow easier recognition by the host immune system (Bitonti *et al.,* 1988). Parasites treated with eflornithine are not actually killed by the drug directly, but are forced to differentiate to the non-replicative stumpy forms (Barrett *et al.,* 2007). These stumpy forms of the parasite are auxotrophic for polyamines (Barrett *et al.,* 2007) and are killed by the host immune system.

1.5.3.5 Nifurtimox-eflornithine combination therapy

Nifurtimox is a 5-nitrofuran pro-drug that has been used for more than 40 years to treat Chagas disease (American trypanosomiasis). To be active, the drug must undergo nitroreduction. In trypanosomes this nitroreduction is undertaken by NADH-dependent type I nitroreductases that are rare in eukaryotic cells (Wilkinson *et al.,* 2008).

An eflornithine-nifurtimox combination therapy (NECT) has been gaining momentum as an alternative to eflornithine monotherapy in recent years (Priotto *et al.*, 2009;Opigo and Woodrow, 2009). It has been suggested that eflornithine and nifurtimox work in synergy with one another, thus allowing lower doses of each drug to be prescribed. This postulated synergy is thought to be due to the reduction in polyamine levels (and consequently reduced trypanothione) during eflornithine treatment being insufficient to deal with the oxidative stress attributed to nifurtimox. That oxidative stress may be caused by nifurtimox is a matter of debate. It was observed that trypanosome extracts produced superoxide anions and nitro anion free radicals upon treatment with nifurtimox (Docampo and Stoppani, 1979;Docampo *et al.*, 1981), but there is little evidence that the same results occur *in vivo*. N-acetylcysteine can antagonise oxidative stress via interactions with free radicals produced by nifurtimox (Enanga *et al.*, 2003). When administered at 0.5 mM with nifurtimox on *in vitro* bloodstream form cells, N-acetylcysteine provided a mild protective effect (IC_{50} of 12.72 μM, compared to 3.37 μM without N-acetylcysteine) (Enanga *et al.*, 2003). However, the over-expression of trypanothione reductase (which would be expected to counteract any induced oxidative stress) confers no difference in susceptibility to nifurtimox over wildtype controls (Kelly *et al.*, 1993). Given the current evidence, no conclusions can be made on the mode of action of nifurtimox although recent evidence implicates an open chain nitrile that attcks macromolecules such as DNA and protein (Hall *et al.*, 2011).

The administration of the combination therapy compared to eflornithine monotherapy is much easier to implement. Nifurtimox can be given orally (three times a day for 10 days) and the eflornithine infusions are reduced in frequency to 14 over seven days. Logistically, drugs are easier to transport due to the lower quantities required and the reduction in refrigeration costs (the cost is reduced from €107 to €39 per patient (Yun *et al.*, 2010)). There are fewer infections at the site of infusion due to the reduced frequency of infusion and fewer side effects overall (Priotto *et al.*, 2009). It will be interesting to determine how this combination works biochemically after noting its effectiveness in the field.

1.6 Drug resistance

As with all monotherapies, resistance to each of the drugs used in isolation is a growing worry. A treatment failure has been defined as a resurgence of parasitaemia within 18 months (or 24 months in some studies) post treatment. It is difficult to note treatment failures due to the difficulties patients face in travelling to treatment centres, in most cases making patient monitoring very hard to implement. Treatment failures have been noted to all the drugs in the field (Barrett *et al.*, 2011), but determination as to the cause of the treatment failure is difficult and could be due to a number of factors including re-infection and non-compliance with the treatment regimes. Resistance to all the drugs in use has, however, been selected in the laboratory (Phillips and Wang, 1987;Scott et al., 1996;Scott et al., 1997; Bridges et al., 2007) allowing the study of the potential mechanisms of resistance, although these may not hold relevance in the field as life cycles are not completed and culture conditions are optimised *in vitro*.

Resistance to stage one drugs is unlikely to be detected in the field as it will be assumed that treatment failures at stage one will have resulted from a mis-diagnosis of a stage two infection and will therefore be re-treated as stage two.

There are multiple ways to confer resistance to a drug including a reduction in drug uptake, an increase in drug efflux, the loss of pro-drug activation, an increased production of the target enzyme, metabolism of drug, alterations to the drug target and increased ability to bypass the inhibited drug target (Borst and Ouellette, 1995). Two of these resistance mechanisms are transporter-based and transporters have been implicated in resistance to two of the drugs in use against HAT as discussed below.

Resistance to melarsoprol is a worry as it is the only drug available against late stage *T. b. rhodesiense* infections and treatment failures in some *T. b. gambiense* areas have already reached levels of 30 % (Legros *et al.*, 1999;Brun *et al.*, 2001;Stanghellini and Josenando, 2001). Parasites selected for resistance in the laboratory (Carter and Fairlamb, 1993;Barrett and Fairlamb, 1999;Maser *et al.*, 1999;Stewart *et al.*, 2005) have lost the P2 transporter, and several relapse

patients yielded parasite isolates deficient in P2 transport (Maser *et al.*, 1999;Matovu *et al.*, 2001;Stewart *et al.*, 2005). This is in contrast to the perceived fitness cost of losing the P2 transporter (Berger *et al.*, 1995;Bray *et al.*, 2003).

Loss of transporters can confer some resistance, but the gain or increased expression of a transporter that serves as an efflux mechanism for a drug can also lead to resistance, as has been seen in the case of Multidrug Resistance Protein A (MRPA). A homologue of this transporter protein (PGPA) was originally identified in leishmania as being responsible for resistance to arsenite or antimony drugs. PGPA and MRPA transport metal-thiol conjugates out of the cell and overexpression of MRPA can lead to 10 fold resistance of *T. b. brucei* to melarsoprol *in vitro* (Shahi *et al.,* 2002). Conversely, RNAi of MRPA in resistant isolates can increase sensitivity to melarsoprol (Alibu *et al.*, 2006).

During selection of pentamidine resistance *in vitro* the P2 and HAPT (and possibly LAPT) (Fig 1-8) transporters are usually lost in order, conferring increasing levels of resistance. Development of high levels of resistance appears to come with severe cost to parasite fitness (Berger *et al.*, 1995;Bridges *et al.*, 2007), which appears to be linked to loss of HAPT (Bridges *et al.,* 2007), thus restricting the chances of resistance developing in the field. Increased expression of MRPA does not provide a decreased sensitivity to pentamidine (Shahi *et al.,* 2002).

Visceral and cutaneous leishmaniasis is also occasionally treated with pentamidine and some resistance to this drug is emerging in *Leishmania donovani* (Sundar, 2001) and *L. mexicana* (Basselin *et al.,* 2002). These resistance mechanisms have been studied and in *L. mexicana* appear to involve diminished uptake of the drug into the mitochondrion associated with decreased mitochondrial membrane potential (Basselin *et al.,* 2002) and are not the same as the resistance mechanisms studied in trypanosomes so far.

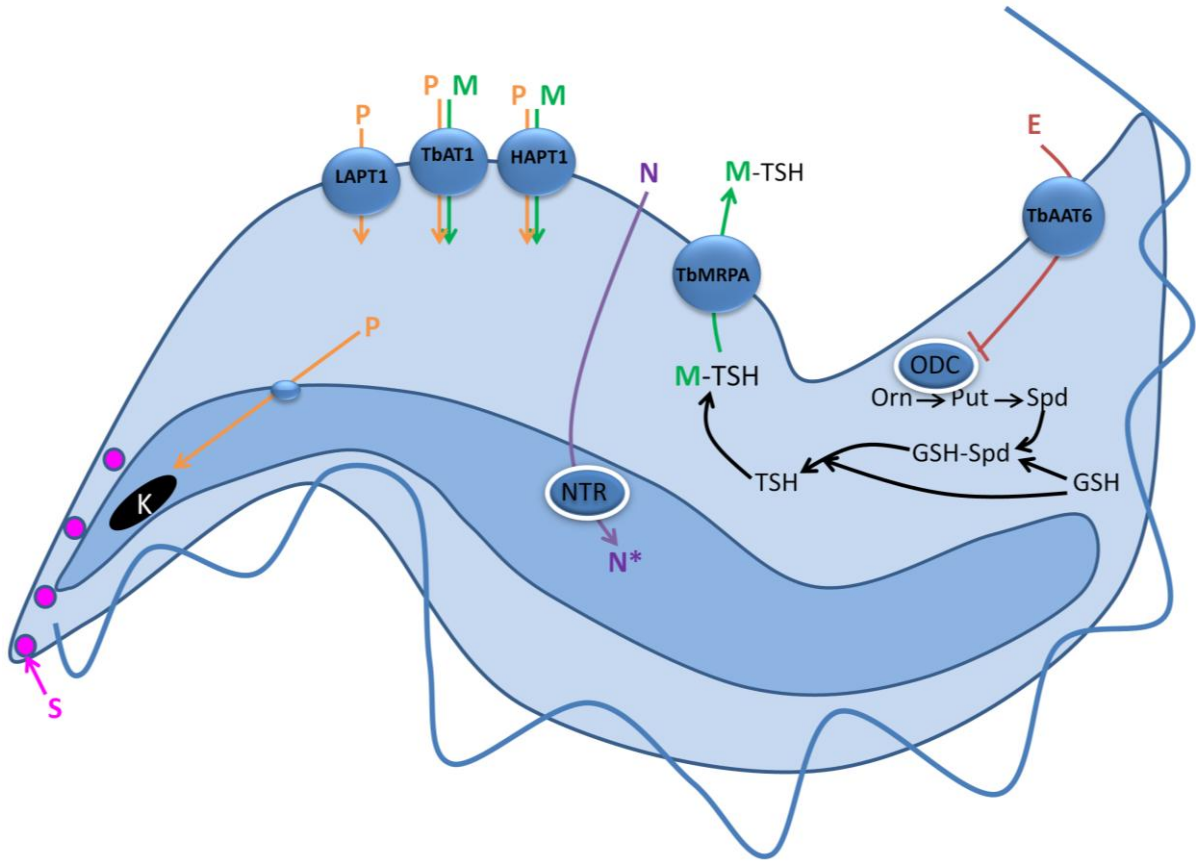

Figure 1-8. Routes of uptake for each of the currently used trypanocidal drugs. P (orange) = pentamidine, M (green) = melarsoprol, N (purple) = nifurtimox, E (red) = eflornithine, S (magenta) = suramin. Also, where known, cellular targets are marked, including ornithine decarboxylase (ODC) for eflornithine and the nitroreductase (NTR) that metabolises nifurtimox into its active form (N*). Pentamidine binds to kinetoplast DNA (K). Resistance to eflornithine relates to loss of TbAAT6. Resistance to melarsoprol (or its active metabolite melarsen oxide) relates to loss of the TbAT1 (P2) and HAPT1 transporters. Alternatively up-regulation of TbMRPA and can cause resistance when melarsen oxide-trypanothione conjugates are pumped from the cell. Pentamidine resistance also relates to loss of TbAT1 and HAPT1 transporters. Suramin enters by receptor mediated endocytosis at the flagellar pocket and resistance may relate to changes in the endocytic pathway. Nifurtimox resistance can come around when the nitroreductase activity involved in its activation is diminished.

Resistance to suramin was reported in the 1950s and resulted in its replacement with pentamidine as the recommended drug for early stage *T. b. gambiense* trypanosomiasis, although suramin is still used for *T. b. rhodesiense* HAT (Barrett *et al.*, 2007). The mechanisms for suramin resistance may involve changes to receptor-mediated endocytosis of the drug (David Horn, unpublished observations).

Resistance to eflornithine has not been officially reported in the field to date, although numerous anecdotal reports from physicians in the field suggest that treatment failures are a real and increasing threat to eflornithine's use (Matovu, 2011).

1.7 Transporters

1.7.1 Roles for membrane transporters

The lipid bilayer surrounding the trypanosome is permeable only to small lipophilic compounds. Larger compounds or lipophobic compounds must therefore gain entry via endocytosis or through transporter proteins. As noted earlier, trypanosomes have a high rate of endo and exocytosis within their flagellar pockets. The flagellar pocket also contains an aggregation of transporters, required for the uptake of many essential nutrients (Field and Carrington, 2009).

Trypanosomes are exposed to ever-changing environments during their life cycle through insect and vertebrate hosts and as such have a varying repertoire of transporters on their surfaces (Besteiro *et al.*, 2005;Berriman *et al.*, 2005). These can serve both as a means to pick up essential nutrients and as environmental sensors (Holsbeeks *et al.*, 2004). Putative transporters in trypanosomes can be identified by sequence or structural similarity with known transporters in other organisms. In addition, some genes encoding transporters in *Leishmania spp.* have been shown to have a conserved location (synteny) in trypanosomes (Jackson, 2007).

As trypanosomes have such a reliance on nutrient uptake, much effort has been invested into transport research in the hope that essential transporters can be discovered and chemically blocked leading to new chemotherapies.

Purine transport in particular has received much attention as one of the purine transporters (P2) carries melarsoprol and diamidines as well as purines (De Koning *et al.*, 2004). A recognition motif that allows compounds to enter the transporter has been identified and it was hoped that this motif may be grafted onto other compounds to target drugs to the trypanosome's interior (Barrett and Fairlamb, 1999;De Koning and Jarvis, 1999).

Glucose transport has also been a topic of trypanosomatid research as glycolysis is essential for bloodstream form trypanosomes. *T. brucei* express two glucose transporters, one, low affinity transporter in the bloodstream stage and one,

higher affinity transporter in the insect stages (Hasne and Barrett, 2000). A problem that arises when attempting to block glucose uptakes in bloodstream form is that blood glucose levels are in the milimolar range meaning that competitive inhibitors would be extremely difficult to administer (Hasne and Barrett, 2000).

The transport of many amino acids has also been studied. L-proline transport in procyclic forms was found to be inhibited by L-alanine and L-cysteine (L'Hostis *et al.*, 1993), L-methionine uptake was inhibited by D/L-homocysteine, L-leucine, L-phenylalanine and L-tryptophan (Hasne and Barrett, 2000) and L-glutamine and L-cysteine were shown to share a transporter (Marciano *et al.*, 2009). The apparent high level of redundancy in amino acid transporters suggests that blocking these would not cause detriment to the cells.

1.7.2 Transporter-mediated drug uptake

The transport mechanisms have been putatively identified for suramin (Vansterkenburg *et al.*, 1993), although these mechanisms have been much debated and it is now widely believed that suramin gains trypanosome entry via endocytosis (Barrett and Gilbert, 2006). Robust evidence exists for the role of the P2 transporter in pentamidine and melarsoprol uptake and HAPT and LAPT in pentamidine uptake (De Koning, 2001). HAPT may also play a role in melarsoprol uptake as has been eluded to in cross resistance studies where selection of high levels of pentamidine resistance due to loss of HAPT are also more resistant to cymelarsen (a melaminophenyl arsenical similar to melarsoprol) than loss of P2 alone (Teka *et al.*, 2011).

Eflornithine has been shown to be accumulated in *Neurospora crassa* by a permease for basic amino acids encoded by the *pmb* gene (Davis *et al.*, 1994), and in procyclic form trypanosomes transport of eflornithine is saturable (Phillips and Wang, 1987) apparently following Michaelis-Menten kinetics. However, Bitonti *et al.* (1986) claimed that eflornithine transport is unsaturated at 10 mM in bloodstream form *T. b. brucei* and concluded that the drug enters by passive diffusion. This study did however, reveal a temperature sensitivity of eflornithine uptake in *T. b. brucei* and mammalian cells and a partial uptake

inhibition by salicylhydroxamic acid, both of which suggest an active transport mechanism (Bitonti *et al.,* 1986).

Since eflornithine is an amino acid, structurally similar to the basic amino acids arginine and lysine (Fig 1-9), it is possible that there is a shared uptake mechanism.

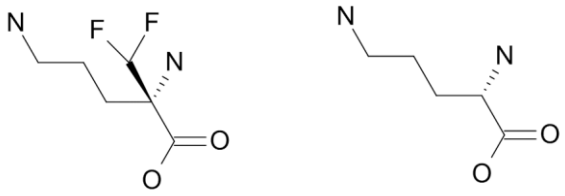

Figure 1-9. Eflornithine (left), a basic amino acid, is a modification of ornithine (right).

Using Andrew Jackson's classification system (Jackson, 2007), there are 48 predicted amino transporters in *T. b. brucei*. This differs from the genome project prediction of 38 (Berriman *et al.,* 2005), due to different prediction methods. These 48 transporters are divided into 17 groups based on sequence similarity, evolutionary relationships and synteny (Fig 1-10) (Jackson, 2007). None of these 17 groups contain a transporter annotated as being a transporter for basic amino acids, indeed the amino acid transporters are poorly annotated in general and most have not been functionally studied.

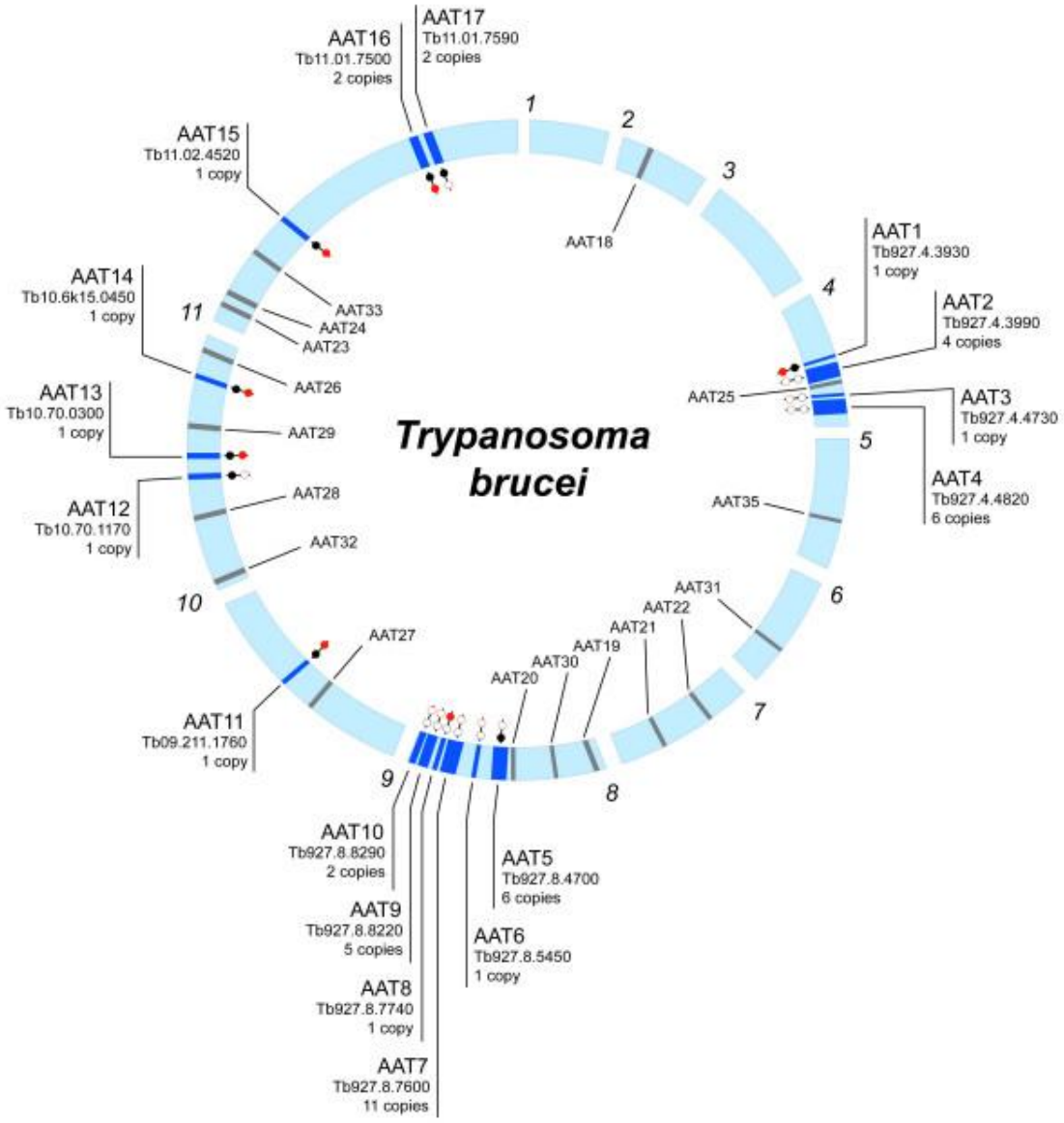

Figure 1-10. Amino acid transporters in *T. brucei.* There are 17 groups of amino acid transporters depicted here on the 11 chromosomes. There is a high concentration of transporters on chromosomes 4, 8, 10 and 11. AAT: amino acid transporter. From Jackson (2007).

1.8 Metabolomics

Defined as the analysis of all the small molecules (Mr<1200) within a cell, metabolomics is a rapidly growing branch of the –omic technologies (Griffin, 2006;Oldiges *et al.*, 2007). Measurements of the levels of substrates, products and cofactors of enzymatic reactions can be used as indicators of deeper-lying biological alterations at the genomic, transcriptomic or proteomic level.

There are a number of methods one can utilise to obtain information about metabolites within a cell. Nuclear magnetic resonance (NMR) can be used for targeted analyses as it is much more facile to quantify metabolites using a single internal standard, requires minimal separation and is non-destructive (Beckonert *et al.*, 2007). It is, however, far less sensitive than other techniques and provides a much reduced coverage of the metabolome. Raman spectroscopy detects vibrations or rotations in metabolites as they are excited by a laser, but as with NMR spectroscopy, Ramen spectroscopy does not provide a large coverage of the metabolome. The alternative to NMR and Ramen spectroscopies lies in mass spectrometry.

1.8.1 Mass spectrometry

Mass spectrometry is a method that measures the mass of a metabolite by creating charged species at the ion source, which are separated on mass and detected by the completion of an electronic circuit that produces a signal in the detector (Fig 1-11).

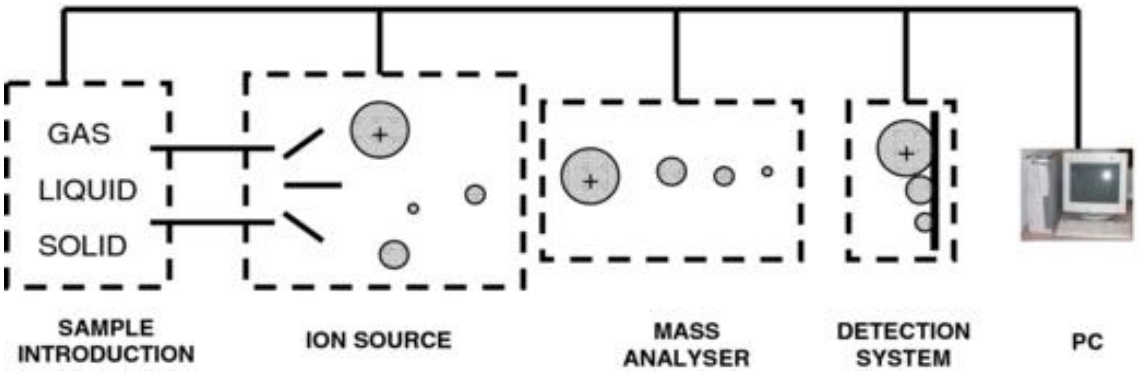

Figure 1-11. A generalised mass spectrometer from Dunn (2008). The sample is usually introduced in solvent from a chromatographic column into the ESI source. It is then ionised and the mass is analysed by filtering or by time of movement along a plane or around a pole. The detected masses are recorded in mass spectra files, usually with the time dimension from the chromatography column mapped for each mass detected against the intensity of the signal.

1.8.1.1 Chromatography

When analysing a complex metabolite sample it is usual to conduct some separation of the metabolites using chromatography columns reducing the complexity of the sample and reducing ion suppression effects. Metabolites travel along a column as either a gas (gas chromatography, GC) or a liquid (liquid chromatography, LC) phase. GC-MS is frequently used for volatile substances such as explosives, flavours and fragrances, although other, less volatile compounds may have to be derivatised before they can be run as a gas (Dorman *et al.,* 2010). The GC columns use phase partitioning to separate the mobile gas phase from a liquid phase on the inner surface of the column (Dorman *et al.,* 2010). Liquid chromatography is used for less volatile metabolites and is often considered more useful for metabolomics as metabolites have no requirement for derivatisation and sampling can therefore be more high-throughput.

There are several LC-MS columns used to separate metabolite samples. Lipophilic metabolites can be separated well by reverse-phase LC, but polar metabolites are not retained on these columns. HILIC (hydrophilic interaction chromatography) columns are therefore more frequently used for separating metabolite samples (Cubbon *et al.,* 2010). These columns use a stationary aqueous layer (such as water) and a mobile phase (such as acetonitrile) to separate metabolites based on both their polarity (more polar metabolites will

be retained for longer on the aqueous layer) and degree of salvation (Cubbon *et al.*, 2010).

1.8.1.2 Ionisation

There are many types of ionisation used in mass spectrometry, with electrospray ionisation (ESI) being most commonly coupled to LC-MS. ESI works via the production of a large voltage potential that creates a charge on the metabolites in solvent pushed through an ultra fine needle (Careri and Mangia, 2011). Charged solvent droplets exit the needle and, as solvent evaporates, the charge density in the droplet increases until the electrostatic repulsion between ions overcomes surface tension, and the droplet breaks up. Ultimately, charged solute ions are transferred to the gas phase and enter the ion path of the mass spectrometer, where they can be manipulated by electrodes for mass analysis and detection.

ESI can operate in two polarities (or modes), which means that a greater range of metabolites can be detected compared to techniques that operate in just one polarity. For example, some metabolites, such as amines are more stable in a protonated state and are therefore more easily detected by positive ionisation, whereas very acidic ions such as phosphates are more stable in a deprotonated form so are detected in negative mode (Watson, 2010).

ESI has a tendency to create multiply-charged ions (Careri and Mangia, 2011), which must be dealt with in the data processing stages of analysis. ESI also has a capability to fragment metabolites, which can be cumbersome during data analysis, but can also be very useful when providing structural information that can aid metabolite identification.

1.8.1.3 Mass analysers

Mass analysers measure the mass of a metabolite by detecting the time the metabolite takes to travel a certain distance (time of flight spectroscopy), how the metabolite oscillates in a magnetic field (Fourier transform ion cyclotron resonance mass spectroscopy (FT-ICR)), how the metabolite travels around a

central electropole in an orbit (Orbitrap), or sieves metabolites based on their charge and mass (Quadrupole) (Dunn, 2008).

1.8.1.4 Species detection

The detector in the mass spectrometer creates an electronic signal when a charge or an electrical current is detected as a charged species hits or passes by. This signal is often very small so signal amplification is common in detectors.

1.8.2 Applications

As metabolomic techniques develop the number of studies that involve an element of mass spectrometry or aim to improve methods and data processing are also increasing at a profound rate. Researchers will use the parts of the technologies that are useful to them allowing different areas of metabolomics to evolve independently of one another. For this reason, different areas have their own softwares that are more frequently in use. The terms in use can also differ between different niches of research. Some of the terms are described below (Dunn, 2008).

1.8.2.1 Metabolic fingerprinting – a snapshot of a metabolome aimed at sorting samples into groups rather than gaining high resolution metabolic data.

1.8.2.2 Metabolic Footprinting – the extracellular metabolome of an organism. (also known as the secretome) can be taken non-invasively.

1.8.2.3 Metabolomic Profiling - an untargeted look at as many metabolites within the organism of interest as possible. Multiple extraction methods will be used to gain as global an overview as possible. Relative intensities of each of the metabolite will be measured, but no real quantification is attempted.

1.8.2.4 Metabolite flux analysis – the rate at which carbon flows though a pathway. This can be measured using radio-labelled metabolites in a time course assay and can be useful in determining choke points within a pathway.

1.8.2.5 Choke points – a critical enzyme in a pathway where metabolites do not have an alternative route to synthesise the products of the reaction.

1.8.2.6 Metabonomics – a term that was at first used synonymously with metabolomics, but now refers to quantitative changes to a metabolome in response to pathophysiological or genetic stimuli.

1.8.2.7 Biomarker studies - much effort is currently being invested into technologies aimed at the detection of biomarkers of disease in blood or urine of diseased humans or animal models. If biomarkers are discovered, these could potentially have a huge impact in the development of new diagnostic tests for diseases such as cancer, diabetes or heart disease.

A major advantage of metabolomics over the other –omics technologies is that there are far fewer metabolites (around 3, 000 in the human metabolome (Kell, 2006)) than genes (around 32, 000 in the human genome) or proteins (at least one per gene) and so the data set is often much more manageable (provided only the cell metabolites are detected with minimal contaminants and background ions). Metabolomics can also be a much cheaper method of analysis

because sample preparation is not as difficult and labour intensive as in proteomics, as gel separations and trypsin digests are not required. Transcriptomics requires the use of costly chips specific to the organism under investigation, which are not required in metabolomics. Variability in metabolite signal intensities does, however, often necessitate additional machine runs.

High-throughput analyses can be performed with metabolomic technologies because metabolites are much more generic between organisms than proteins, RNA transcripts or genes (Kell *et al.*, 2005). For example, the metabolite glucose has the same structure in every organism, whereas the gene coding for hexokinase may have subtle sequence differences even within a species, and the protein may have additional post translational modifications even within a clonal population of cells.

1.8.2.8 Mode of action studies

Drug discovery is a very expensive process and the licensing of a drug is much easier if more is known about the compound's mode of action. Whereas drug discovery used to be led by the active compound, with definition of the mode of action coming later, new research is much more often drawn from the discovery of a good metabolic target.

Metabolomics can be an extremely useful technique when looking at a drug's effect on the small metabolites within a cell population. From a complex metabolome, a drug's mode of action may be inferred, allowing easier licensing and bringing down the cost of drug discovery.

There are two approaches that metabolomic-based mode of action studies generally take. In the first, a metabolic fingerprint of the changes the drug induces in the metabolome is taken and compared using multivariate statistical analysis to drugs with known modes of action (Yi *et al.,* 2007). The second takes a more detailed look at the individual metabolite abundance changes after drug introduction (Le Roch *et al.*, 2008). This approach provides much more information on the mode of action of a drug, allows new modes of action to be defined and allows the prediction of off-target effects. In addition to determining the modes of action of drugs on pathogens, it would be possible to

predict any side effects on human cells and tissues. This would be hugely beneficial to reduce the amount of animal testing required for new compounds if side effects can be recognised before animal trials begin. It would also potentially reduce the cost of developing new compounds and speed up the time it takes for a compound to reach the market.

If the pathways that a drug acts upon are known, then synergistic compounds can be sought and resistance mechanisms might be predicted.

Once a potential target has been identified, then further analyses can be undertaken to dissect the exact mode of action. For example, if the potential target is an enzyme, then the enzyme may be knocked down by RNA interference and the phenotype, drug IC_{50} and metabolomes of the drug treated and the knocked down target cells can be compared.

Jess Allen and colleagues at the University of Wales took metabolic fingerprints of *Saccharomyces cerevisiae* in response to antifungal drugs and analysed them by discriminant function and hierarchical cluster analyses (Allen *et al.*, 2004). When compared to drugs of known action, new compounds could be discriminated into classes of predicted mode of action (Allen *et al.*, 2004). Principal component analysis was used in a similar way to evaluate the mode of action of berberine on *Staphylococcus aureus* (Fig 1-12) (Yi *et al.*, 2007).

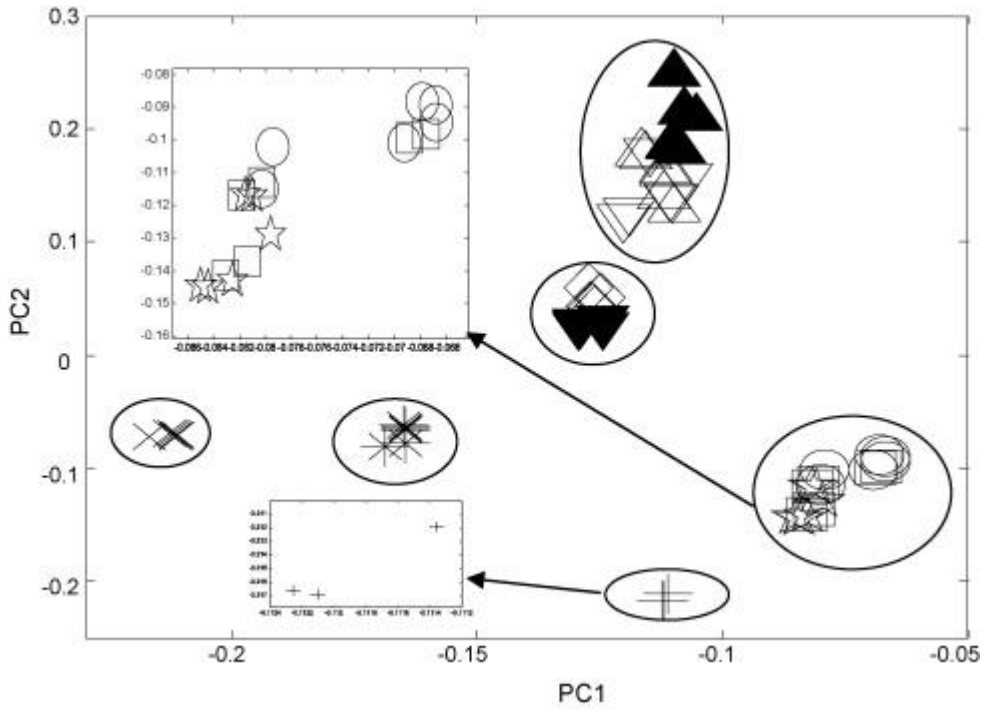

Figure 1-12. A principal components analysis of modes of action in anti-*Staphylococcus aureus* drugs. A mathematical transformation produces a single point on the graph for each mass spectrum. The different symbols indicate mass spectra for different pharmacological compounds. Clustering of different symbols is an indication of a similar metabolic profile between those compounds and therefore a similar mode of action. Taken from Yi *et al.* (2007).

These methods could have some use in putative drug classification if large comparison sets are available. However, many of the clusters are close together and would be largely influenced by small deviations in the data due to experimental error for example. These methods are also unable to determine the targets of the drugs, so target identification would always need to be undertaken alongside multivariate data analyses. Another drawback with the two approaches using pattern recognition is that drugs with novel modes of action cannot be classified.

A more sensitive method of pattern recognition has been developed using artificial neural network analysis with NMR (Aranibar *et al.*, 2001). This machine learning-based method uses a training set of metabolite profiles from herbicide-treated *Zea mays* to build a decision tree that can classify the profiles of other herbicide-treated *Z. mays* plants (Aranibar *et al.*, 2001). This method is similar to the previous two methods in that it is based on classification with spectra

from treatments with compounds with known modes of action, but machine learning can often reveal the individual metabolites responsible for classification. Aranibar's method used NMR spectra however, and was not of high enough sensitivity to define the metabolites important in the decision tree (Aranibar *et al.*, 2001). The authors also point out the sampling procedures need to be highly reproducible for this method to be of use (Aranibar *et al.*, 2001).

Untargeted metabolome studies to look at the mode of action of a drug are very rare although some targeted analyses have started to emerge. In 2008 Karine Le Roch and colleagues used heavy labelled phoshphocholine precursors to look at the effects of a bisthiazolium compound, T4, on phosphocholine biosynthesis in *Plasmodium falciparum* (Le Roch *et al.*, 2008). The group found a decrease in phosphocholine synthesis from choline and ethanolamine after treatment with T4 (Le Roch *et al.*, 2008).

In one untargeted metabolomics approach, FT-ICR-MS was used to analyse the modes of action of four toxins on the daphnid metabolome (Taylor *et al.*, 2010). The number of features in this study is large and the results very clearly highlight relevant pathways (such as effects on fatty acid metabolism after treatment with propranolol (a beta blocker) and disruption of amino sugar metabolism with fenvalerate (a pyrethroid insecticide) treatment (Taylor *et al.*, 2010) affected by the toxins. Data reduction has, however, been inefficient leading to an increased potential for false positive metabolite identifications. Data reduction is major part of analysing metabolomics data and is something that the metabolomics community are focussing resources on at present.

Where the genomics and proteomics communities have repositories that collect experimental data from the community (e.g. GenBank for genomics and UniProt for proteomics), the metabolomics community have been a step behind in the production of similar database. Since the release of the Human Metabolome Database (HMDB) however, researchers are beginning to appreciate the benefits of having a large, pooled reference dataset. There are difficulties in producing repositories based on experimental data for metabolomics as techniques are so widely variable: column retention times will differ depending on the column and the solvents used and ionisation and fragmentation techniques will change the mass and the mass:charge ratio of the metabolite. The Wishart group at the

University of Alberta have gone to extensive lengths to produce reference metabolomes for human cerebrospinal fluid (Wishart *et al.*, 2008) and human serum (Psychogios *et al.*, 2011), running multiple metabolomics platforms on clinical samples and conducting thorough literature searches to produce a searchable metabolite databank that includes quantitation of metabolites across various disease states. Another notable advancement in recent years is the improvement in compound databases such as KEGG, PubChem, ChemSpider, MassBank and Metlin. These databases are extremely useful in the identification of metabolites as well as raising awareness of the number of isomers a particular metabolite may have.

1.8.2.9 Biomarker discovery

There has been a recent surge in metabolomics papers attempting the discovery of biomarkers to various diseases and toxicities. In general, these studies endeavour to compare the metabolites of a sample of disease tissue or the biofluid of an infected patient to healthy controls (Mamas *et al.*, 2011).

Biomarkers are already routinely used to diagnose non-infectious diseases such as neuroblastoma (catecholamines (Monsaingeon *et al.*, 2003)), diabetes (insulin) and prostate cancer (sarcosine (Sreekumar *et al.*, 2009)) and there have been recent attempts to diagnose infectious diseases as well. One group analysed the serum and plasma of people in an *Onchocerca volvulus* endemic foci and discovered 14 biomarkers that were able to distinguish between infected and non-infected individuals (Denery *et al.*, 2010). This experiment was flawed, however in that there was not enough power behind many of the analyses and training sets used for the machine learning were also part of the test sample set, which forces the fit of the data to the model. The metabolic responses of mice to *T. b. brucei* infections have also been elucidated (Wang *et al.,* 2008) using NMR. This study pin-pointed many changes in the blood and urine of the infected mice as compared to the same mice pre-infection, including an increase in lactate, which may be due to an upregulation of glycolysis (Wang *et al.,* 2008). This increase in lactate was confirmed by another study that analysed the effects of co-infections of two *T. b. brucei* strains (Li *et al.*, 2011).

1.8.2.10 Computational models

As more and more quantitative metabolite information is created, efforts are increasingly being made to mathematically model the data to understand metabolism at a system-based level. It is the eventual aim to integrate genomic, transcriptomic and proteomic data with metabolomic information to form a "silicon cell", which can be virtually perturbed generating an output that would be similar to a live cell's response. The rates of enzyme activity are key to these models and have already been used to build models of parts of trypanosome metabolism. A kinetic model of glycolysis uses ordinary differential equations to describe glucose uptake and metabolism to pyruvate and highlights the importance of compartmentation within these systems (Bakker *et al.*, 1997;Bakker *et al.*, 2000). This model has helped to identify which enzymes within the pathway, would, when blocked, induce the greatest effects on glycolysis and would therefore be the most effective drugs. Enzymes within a pathway that consume just one substrate or produce just one product are known as choke points and these enzymes have been shown in *P. falciparum* to be better drug targets than other enzymes (Yeh *et al.*, 2004). MetExplore, a web server designed to automatically build connections between metabolites creating an *ab initio* network reconstruction, has been developed by Cottret *et al.* at the Institut National de Recherche Agronomique (Cottret *et al.*, 2010). Experimental data may be uploaded into MetExplore and information, such as how the relative levels of metabolites change after perturbation with a drug, can be mapped in the context of the whole metabolic network for the organism in question (Cottret *et al.*, 2010).

Ab initio models such as MetExplore are very useful, but could be even more useful once the community is able to record more quantitative measurements of the metabolites in the system. This would bolster the models and make more accurate predictions possible.

1.8.2.11 Quantitative metabolomics

A true quantification of metabolites is only really possible in a targeted analysis. Researchers have been developing methods to attempt a global quantification using universally heavy-labelled metabolites spiked into samples (Psychogios *et*

al., 2011;Wu *et al.*, 2005;Kiefer *et al.*, 2008). The ion suppression effects in these samples can be normalised by comparison to standards, but the data processing involved to deconvolute these data will be immense leading most people to pursue targeted analyses for quantification.

Once a target has been identified, a heavy-labelled version of the metabolite of interest can be spiked into the samples over a range of concentrations, creating a calibration curve against which the metabolite of interest can be measured.

1.8.2.12 Heavy metabolite tracking

Another use of heavy metabolites is to measure the flux of metabolites through pathways of interest. A metabolite with one or more heavy atoms is added to a population of cells, tissue or whole organism, samples are taken over a range of time points and the heavy atom or atoms are traced through the pathways, cells or tissues. This technique has been used to compare the metabolome of cancerous and non-cancerous human lung tissue (Fan *et al.*, 2009), finding a higher rate of glucose metabolism and anaplerotic pyruvate carboxylation in cancerous tissues.

In *P. falciparum,* Olszewski *et al.* used ^{13}C and/or ^{15}N-labelled glucose, aspartate and glutamine to analyse the tricarboxylic acid cycle and found that, contrary to biochemical textbooks, a branched structure was found, meaning that several enzymes must operate in the reverse direction (Olszewski *et al.*, 2010) within these parasites. This discovery was very surprising and has yet to be independently confirmed, but reveals the power of fluxomics in the metabolomic field.

1.8.3 Sample preparation

Sample preparation methods can vary enormously depending on the metabolites one is interested in detecting and the organisms under examination. Generally, a cellular sample for metabolic analysis is quenched in a solvent at extreme temperature (either hot or cold) to prevent further enzymatic processes. Cells are often washed and then lysed before cell debris is removed. Shin *et al.* (2010) evaluated sample preparation methods in the Gram negative bacterium

Saccharophagus degradans. They compared pure methanol, acetonitrile:water (1:1, v/v), acetonitrile:methanol:water (2:2:1) and water:isopropanol:methanol (2:2:5) for the metabolite intensity, total number of metabolites detected and the reproducibility of detected metabolites. They found that both acetonitrile:methanol:water and water:isopropanol:methanol performed well, but covered different ranges of metabolites. Similar studies have produced optimised extraction solvents for almost all cell populations and tissues including liver (Masson *et al.*, 2010), erythrocytes (Darghouth *et al.*, 2010), leishmania (t'Kindt *et al.*, 2010;Saunders *et al.*, 2010), adherent cell cultures (Danielsson *et al.*, 2010) and plants (Kim and Verpoorte, 2010). The literature on the extraction of the trypanosome metabolome is lacking so optimisation of extraction methods is a priority.

There have been efforts to standardise the techniques used for sample extraction and analysis within the metabolomics community (Jenkins *et al.*, 2004;Sansone *et al.*, 2007), but as each organism requires different treatment during the extraction method, and methods will vary depending on what metabolites a researcher is interested in and what mass spectrometry instrument is in use, these efforts have not yet proven successful and are often abandoned.

1.8.4 Computation in metabolomics

Perhaps the main reason that metabolomics is not as widely used as the other –omic technologies lies in the lack of reliable computational solutions for the deconvolution of the highly complex data. There are many programmes available, but of the ones that are freely available there is not one that accomplishes all the needs of the biologist without extensive training in computer languages. One of the biggest hurdles in deconvoluting the raw files from the mass spectrometer is in finding a way for the computer to recognise a peak relating to one mass eluting from the chromatography apparatus. Simple programmes can choose peaks that are of a certain abundance (such as the Xcalibur software), but these will miss the more subtle peaks that are robust but small. Other, more sophisticated programmes are able to recognise the shape of a peak and match this shape and the retention time of the peak across replicates

enabling a more robust mass identification and comparison between samples (Smith *et al.*, 2006).

Other issues in the software are in comparing samples and performing statistical analyses. If the programmes are too generous in their parameters then huge lists of metabolites are generated with a large proportion being false positives. Conversely, if the parameters are too strict then many of the smaller or more variable peaks will be lost. This is an issue that cannot be resolved without having an understanding of how reliable an individual user's data is and therefore cannot be automated and parameters must be user-defined.

Another big issue in the simplification of metabolomics data is the number of related peaks that are generated from one metabolite. Masses may be multiply-charged or fragmented or have isomers, isotopes or adducts, which all produce extra peaks relating to a parent metabolite. Reducing the data based on these features will be vital in producing a dataset that is able to be interpreted in a biological context. MzMatch is a new software that resolves many of these issues, by identifying and combining related peaks, but is also modular so that users can decide how robust they would like the filtering of their data to be (Scheltema *et al.*, 2011).

1.8.5 Trypanosome metabolism

There have been notably few metabolomics studies in trypanosomes so far. Studies have focussed on glycolysis(Visser and Opperdoes, 1980; Mackenzie *et al.*, 1983; Albert *et al.*, 2005;Haanstra *et al.*, 2008) and trypanothione synthesis (Fairlamb *et al.*, 1987;Shim and Fairlamb, 1988;Xiao *et al.*, 2009). These metabolites were recorded using either HPLC, NMR or classical biochemistry techniques. NMR has been used to quantify phosphorylated compounds in bloodstream and procyclic *T. brucei* (Moreno *et al.*, 2000) and to analyse the effects of enzyme deletions in procyclic *T. brucei* (Coustou *et al.*, 2005;Coustou *et al.*, 2008). These studies are, however, all targeted to the pathways of interest and so could miss many interesting metabolite changes.

The HILIC-Orbitrap mass spectrometry platform was previously used to analyse the changes that occur in the procyclic trypanosomes metabolism in an

untargeted way when they switch from a glucose (the carbon source in the *in vitro* growth medium SDM-79) to a proline (the carbon source available in the tsetse midgut) carbon source (Kamleh *et al.,* 2008). This study revealed a shift in proline metabolism resulting in many changes including higher levels of glutamate, glutathione and carboxypyrroline in the proline-grown cells (Kamleh *et al.,* 2008).

Trypanosomes may be the ideal organisms to study the applications of metabolomics as they have a minimal set of metabolites (Fairlamb, 2002;Breitling *et al.,* 2006) due to the parasitic nature of the organism's lifestyle i.e. they salvage many more metabolites from their host than other organisms. The bloodstream form of the parasite, for example, appears not to have a fully functional TCA cycle, whereas the insect stages do(Fairlamb, 2002;van Weelden *et al.*, 2005). This would suggest that some of the citric acid cycle intermediates are salvaged from the mammalian host, but are not salvaged in the insect vector. The bloodstream forms of the parasite therefore have to rely on substrate level phosphorylation (from glycolysis) for ATP production (Carter and Fairlamb, 1993;Besteiro *et al.*, 2005).

Trypanosomes are also relatively easy to grow *in vitro* in large numbers creating a large, clonal population on which metabolite extractions can be performed.

1.9 Metabolomics at the University of Glasgow

The Orbitrap mass spectrometer is a type of Fourier transform mass spectrometer that was developed by Alexander Makarov. The Orbitrap is much smaller than fourier transform ion cyclotron resonance (FT-ICR) mass spectrometers as it does not use electromagnets whereas FT-ICRs do. Instead, the Orbitrap uses an electric field to trap ions in separate kinetic energies orbiting around a central electrode (Makarov *et al.,* 2006). This mass spectrometer achieves an ultra high mass accuracy of two parts per million (ppm) using ubiquitous plasticising agents as internal calibrant masses. A resolution of over 100, 000 fwhm (full width at half maximum, a measurement of pulse duration) is achieved allowing spectra to be generated in the order of up to three per second (Makarov *et al.,* 2006). A high resolution mass spectrometer

permits non-isobaric metabolites to be distinguished between much more easily, allowing separation steps to be removed or reduced (Breitling *et al.*, 2006). Scheltema *et al.* (2008) showed that the advertised mass accuracy of the Orbitrap (2 ppm) can be improved to 0.21 ppm using internal background ions for additional calibration.

Generally it is thought that the use of buffers to help prevent cell damage needs to be limited as excess salt can clog the skimmer in the mass spectrometer (Mashego *et al.*, 2007) causing inefficient ionisation. Ion suppression can also occur, whereby molecules with a stronger potential to catch the charge (e.g. salts) are preferentially ionised, abrogating the potential for other molecules to become charged. Salt accumulation can also limit the amount of sample that can be analysed by HPLC (high performance liquid chromatography) (Theobald *et al.*, 1997) as can high protein concentrations.

To improve the confidence of identification of a metabolite, separation apparatus is often coupled to the mass spectrometer, which also has the advantage of minimising suppression effects by keeping metabolites separate as they enter the ionisation source. Chromatography columns are used that can separate on mass, charge or polarity. The ZIC-HILIC (hydrophilic interaction chromatography) uses acetonitrile and water to separate metabolites on the basis of their polarity. Less polar metabolites are washed through the column with the solvent phase, while more polar metabolites are retained for longer, so two masses with different hydrophobicities should be distinguishable by their retention time on the column.

MzMatch is a modular programme developed by Richard Scheltema and Andris Jankeviks. The pipeline used in this project (IDEOM) was automated and given a graphical user interface (GUI) by Darren Creek. The components of the software used in our analyses are summarised in figure 1-13.

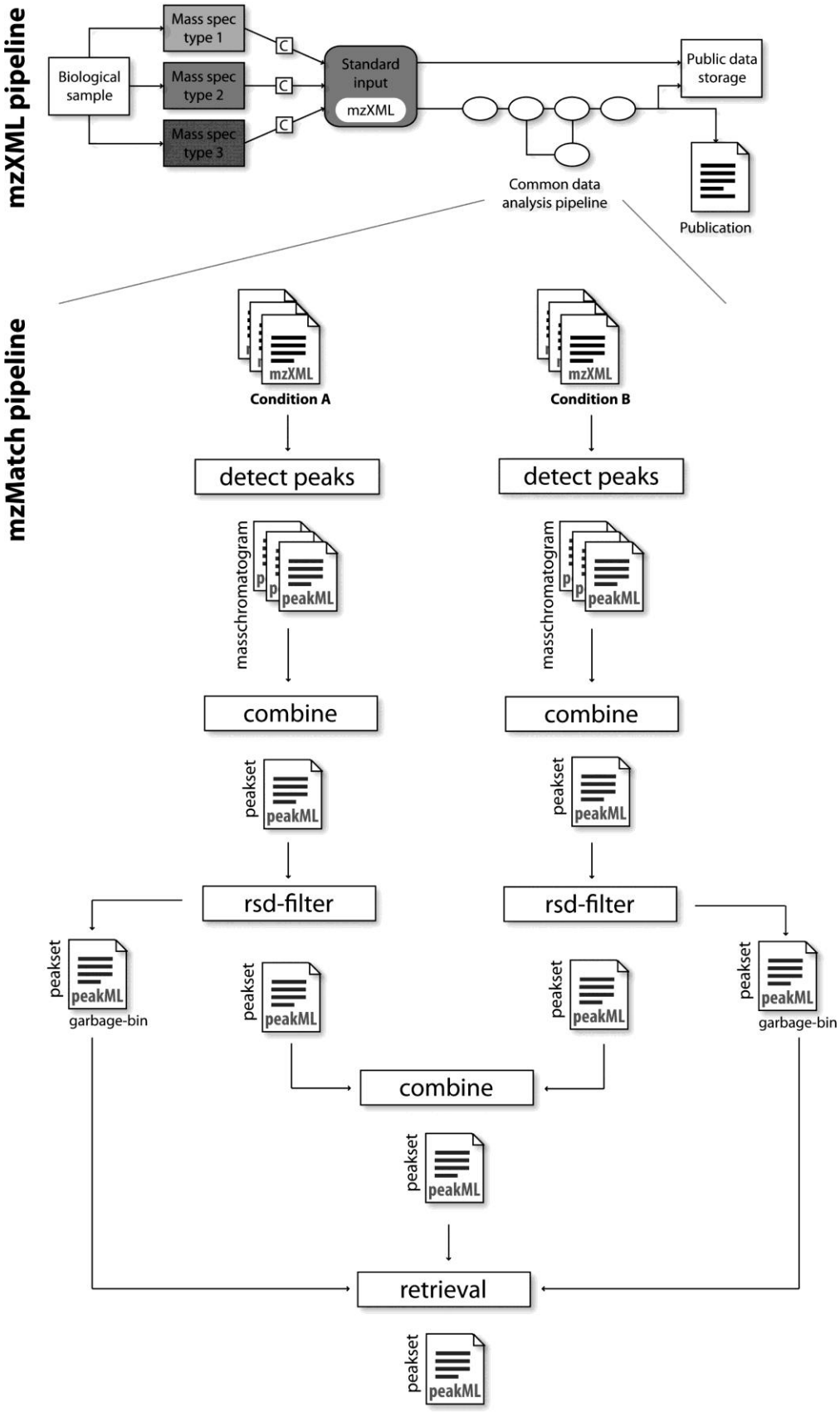

Figure 1-13. The metabolomics pipeline used at the University of Glasgow (Sheltema *et al.*, 2011). MzXML files are obtained by simple processing of the raw MS data. Peaks of metabolites eluting from the chromatography apparatus are the isolated and compared across replicates and samples. These are then filtered according to their relative standard deviation (rsd) and combined into one data set, which can be used to search metabolite databases allowing putative metabolite names to be assigned.

The accuracy of identification was improved by the development of a retention time predictor by Darren Creek. This algorithm predicts the time that a metabolite will exit our chromatography apparatus (the ZIC-HILIC column) for the metabolites which we do not have a standard for. Having retention times predicted aids enormously in the identification stage of the analysis and helps the computer distinguish between isomers more easily.

1.10 Aims

Human African trypanosomiasis is a disease that has neared elimination in the past. There is a paucity of drugs that are effective against either early or late stages of the disease. Those that are available are often dangerously toxic and are difficult to transport to and store in places of need. Resistance to the drugs in use also poses a problem for the future of the available compounds. The mechanisms of resistance to many of the drugs have been investigated, but the drug that is increasing in use most rapidly, eflornithine, has no predicted mechanism of resistance.

Metabolomics is a relatively new set of technologies that measure the presence and levels of small molecules within tissues or cell populations. There is a huge scope for useful applications of these new technologies.

The aims of this project were to:

1, Investigate the mechanism of resistance to eflornithine in order to combat it before it occurs in the field. A combination of classic biochemical and molecular techniques were used in addition to newer metabolomic techniques.

2, Analyse the mode of action of drugs on trypanosomes using eflornithine as a proof of principle.

3, Develop new metabolomic methodologies for the analysis of pathways in *T. brucei*. Quantification of specific metabolites and heavy metabolite tracking were used to analyse the flux of nitrogen through the bloodstream form polyamine pathway.

2. Methods

2.1 Trypanosome growth and resistance selection

2.1.1 Culturing cells

Bloodstream form trypanosomes were grown in HMI-9 (Biosera) (Hirumi *et al.*, 1977) supplemented with 10 % foetal calf serum (FCS, Biosera), incubated at 37˚C, 5 % CO_2. Procyclic form trypanosomes were grown in SDM-79 (Biosera) with 10 % FCS at 28˚C. Generally, growth was in 10 ml medium in 25 cm^2 Corning vented culture flasks (unvented for procyclic forms). A typical starting density of 10^4 cells per ml was used (counted by haemocytometer), and cells reached stationary phase after 2-3 days for bloodstream form or 5 days for procyclic forms. Cells were bulked up for metabolomics and uptake assays in 175 ml medium in 500 cm^2 Corning vented culture flasks.

Leishmania mexicana were cultured in Homem medium (Biosera) with 10 % FCS. Conditions were the same as for procyclic trypanosomes.

2.1.2 Selection of eflornithine resistance

Wildtype bloodstream form 427 cells were grown in 5 ml cultures in 25 cm^2 flasks as described above. The first drug concentration used on the wildtype cells was 10 μM. At each passage, three flasks were created; 1, drug-free. 2, drug concentration equal to previous passage. 3, two times the drug concentration from the previous passage. Cells were cloned out and stabilated at various stages of the selection process for later analyses.

2.1.3 Microscopy

Trypanosomes were centrifuged at 1, 250 RCF and resuspended at a high density before smearing onto a glass slide. Smears were air dried and stained in 10 % Giemsa (v/v in water) for 24 hours and destained for several washes in water. Cells were observed with 100 x magnification under oil immersion with a Zeiss Axioplan 2 microscope and Velocity software.

2.1.4 Cloning of trypanosomes

Clonal populations of cells were diluted to one parasite per ml medium and 200 μL medium was added to each well of a 96 well plate. If fewer than 30 % (calculated for a 96 well plate using a poisson distribution) of the wells contained live cells after 14 days then the populations were considered to be clonal.

2.1.5 Creating stabilates

Stabilates were created from clonal populations of cells by adding 15 % glycerol to confluent cells at approximately 5 x 10^5 cells/ml. These were then wrapped in cotton wool and frozen at -80ºC before transferring to liquid nitrogen for long-term storage.

2.1.6 Alamar Blue assay

The alamar Blue assay developed by Raz *et al*. (1997) for bloodstream form trypanosomes was used. Bloodstream form parasites were diluted to a concentration of 4 x 10^4 cells per ml. The drug under test was diluted in medium to twice the maximum desired concentration. 200 μL of drug in medium was added to the first two wells in the first column of a 96 well plate. 100 μL of medium was added to the remaining wells on the plate in the top four rows. The drug was serially diluted from left to right and top to bottom along the 96 well plate, leaving the last two wells drug free. 100 μL of 4 x 10^4 cells per ml parasites were added to each well.

Plates were incubated for 48 hours at 37˚C, 5 % CO_2 then 20 μL Resazurin dye (Sigma) at 0.49 μM was added to each well. Plates were incubated for a further 24 hours then read on a fluorimeter (emission 530, excitation 595) (FLUOstar Optima, BMG Labtech).

For isobologram analyses, alamar Blue assays were conducted for one drug in the presence of three different concentrations (IC_{50}, 2 x IC_{50} and 0.5 x IC_{50}) of another drug.

2.1.7 Mouse work

All mouse work was conducted by Dr. Pui Ee Wong, University of Glasgow.

Cells from culture were prepared for inoculation into adult female ICR (Institute of Cancer Research) mice by washing twice in CBSS (Carter's Buffered Salt Solution). They were re-suspended to a density of 5 x 10^5/ml and 0.2 ml (1 x 10^5) cells were injected intraperitontoneally into the mouse.

Blood straws were defrosted into 0.2 ml CBSS and 0.2 ml of the resulting suspension was injected into the peritoneum.

Mice were exsanguinated with 100 international units of heparin sodium per 1 ml of blood. Trypanosomes were purified on a PSG (Na_2HPO_4 (57 mM), NaH_2PO_4 (3.9 mM), NaCl (44 mM), glucose (61 mM)) resin column.

2.2 Metabolomics

2.2.1 Metabolite extraction

Mass spectrometry was undertaken by Darren Creek (University of Glasgow) or Muhammed Anas Kamleh (University of Strathclyde). Metabolite extraction methods were adapted from *Leishmania spp* extraction techniques developed by groups in Melbourne, Australia (Saunders *et al.,* 2010) and Antwerp, Belgium (t'Kindt *et al.,* 2010).

Cells were grown in 500 ml Corning flasks to a maximum volume of 175 ml in HMI-9. Cultures were kept in log phase growth (below 1 x 10^6/ml). At the time of harvest, 4 x 10^7 cells were rapidly cooled to 4 ˚C by submersion of the flask in a dry ice-ethanol bath, and kept at 4 ˚C for all subsequent steps. The cold cell culture was centrifuged at 1, 250 RCF for 10 minutes and the supernatant completely removed. Cell lysis and protein denaturation was achieved by addition of 200 µL of 4 ºC chloroform:methanol:water (ratio 1:3:1) plus internal standards (theophylline, 5-fluorouridine, Cl-phenyl cAMP, N-methyl glucamine, canavanine and piperazine, all at 1 µM), followed by vigorous mixing for 1 hour at 4 ºC.

Extract mixtures were centrifuged for two minutes at 16, 000 RCF, 4˚C. The supernatant was collected, frozen and stored at -80˚C until further analysis.

2.2.2 Mass Spectrometry

Samples were analysed on an Exactive Orbitrap mass spectrometer (Thermo Fisher) in both positive and negative modes (rapid switching), coupled to HPLC with a ZIC-HILIC column. The apparatus was operated by either Muhammed Anas Kamleh (University of Strathclyde) or Darren Creek (University of Glasgow). Exactive data was acquired at 25,000 resolution, with spray voltages +4.5kV and -2.6kV, capillary temperature 275 ˚C, sheath gas 20 units, auxillary gas 15 units and sweep gas 1 unit. Minor adjustments were made to the published (Kamleh *et al.*, 2008) HPLC mobile phase gradient as follows: Solvent A is 0.1 % formic acid in water, and solvent B is 0.1 % formic acid in acetonitrile, 80 % B (0 min), 50 % B (12 min), 50 % B (26 min), 20 % B (28 min), 20 % B (36 min), 80 % B (37 min), 80 % B (47 min).

2.2.3 Metabolomics data processing

2.2.3.1 Untargeted metabolomics

Peaks of metabolite signals eluting from the chromatography apparatus were identified and relative quantitation was undertaken using mzMatch software developed by Richard Scheltema (University of Groningen) and Andris Jankevics (University of Glasgow) (Scheltema *et al.*, 2011). An Excel-based macro system (IDEOM – IDEntification Of Metabolites) developed by Darren Creek (University of Glasgow, in press) was used to identify metabolites, merge related peaks and compare relative intensities of metabolites between sample sets. A retention time error of 5 % was allowed for retention times for which standards have been run and 35 % was allowed for calculated retention times.

Raw files from the Orbitrap mass spectrometer were converted to mzXML using msconvert and metabolite peaks were picked using xcms (Smith *et al.*, 2006). Data was filtered and reduced using mzMatch (Scheltema *et al.*, 2011) with a rsd filter of one, an intensity filter of 10, 000 and a minimum number of detections of two.

2.2.3.2 Targeted metabolomics

To analyse specific pathways, Xcalibur software (Thermo Scientific) was used to create a processing file with user-specified masses and retention times and run it through a sample list picking out all the metabolite relative intensities, using the Quan Browser, within a set of samples.

Accuracy of metabolite identification was improved for targeted and untargeted analyses using retention times. These were either identified using standards and calibrated using an internal standard mix or calculated using an algorithm developed by Darren Creek.

2.2.4 Radiolabel tracking

Amino acids were obtained with ^{15}N incorporation from Cambridge Isotope Laboratories (L-threonine (98 % enrichment, one incorporation, alpha-N, cat:NLM-742-0), L-glutamine (98 % enrichment, one incorporation, alpha-N, cat: NLM-1016-0), L-aspartic acid (98 % enrichment, one incorporation, alpha-N, NLM-718-0), L-arginine (98 % enrichment, four incorporations, allo-N, cat: NLM-396-0), L-ornithine (98 % enrichment, two incorporations, allo-N, cat: NLM-3610-0), L-lysine (95 - 99% enrichment, one incorporation, alpha-N, cat: NLM-143-0)) or Sigma Aldrich (L-proline (98 % enrichment, one incorporation, alpha-N, cat: 608998), L-glutamate (98 % enrichment, one incorporation, alpha-N, cat: 332143)).

Cells were grown in 500 ml Corning flasks to a maximum volume of 175 ml in HMI-9. Cultures were kept in log phase growth (below 2 x 10^6/ml). At the time of harvest, cells were centrifuged at 1, 250 RCF for 10 minutes and the supernatant completely removed and resuspended in CBSS. Cells were split into aliquots of 4 x 10^7 cells. Labelled and unlabelled amino acid was added at 1 mM. Cell extracts were prepared as method 2.2.1.

2.3 Molecular Biology

2.3.1 Gene searches

Nucleotide sequences for genes were located either via text searches for the gene names in GeneDB (www.genedb.org) or TriTrypDB (tritrypdb.org). For proteins that were not annotated, amino acid sequences for bacterial or protozoan microorganisms were taken from NCBI databases (www.ncbi.nlm.nih.gov) and a BLAST (Basic Local Alignment Search Tool) search of these against the parasite genomes was performed in GeneDB or TriTrypDB.

2.3.2 PCR

Generally, genomic DNA was denatured at 94˚C for two minutes, followed by 30 cycles of 94˚C for 15 seconds, annealing for 15 seconds (variable annealing temperatures between 50 and 65˚C) and extension at 72˚C for 30 seconds/500 bases. A final elongation of 7 minutes was used. GoTaq polymerase (Promega) was used for low fidelity PCRs and KOD Hot Start polymerase (Novagen) for high fidelity reactions according to manufacturer's instructions. Mg^{2+} was used at 1.5 mM and dNTPs at 200 µM.

Approximately 10 ng of DNA in water was used in each reaction along with 100 ng of each primer (Table 2-1).

For PCR from blood cultures of trypanosomes, blood was spotted on to FTA® cards (Whatman) and washed four times with FTA® purification reagent (200 µL for five 2 mm discs, cut with a hole punch), then three times with TE buffer (10 mM Tris-Cl, pH 7.5. 1 mM EDTA) (200 µL). Generally, one disc was used in each PCR reaction.

Primer	Sequence	Gene
AAT1 forward	ATATGGATCCGCGATTTCTCACGAGCCTACG	Tb927.4.3930
AAT1 reverse	ACATCTCGAGTACGACACCTCACCACCAAAA	Tb927.4.3930
AAT2 forward	ATATGGATCCACATTCTTTACGAAGGTGAGT	Tb927.4.3990
AAT2 reverse	ACATCTCGAGGATCACAATGACAAAATACAC	Tb927.4.3990
AAT3 forward	GGAGAAGCACAAAAGCCCGA	Tb927.4.4730
AAT3 reverse	GATGAAGAGTGCGGGGAATA	Tb927.4.4730

AAT4 forward	ATATGGATCCGCTAATGAGGGAGAAGGGGAA	Tb927.4.4840/4820/4860/4830
AAT4 reverse	ACATCTCGAGGTGCCGAAGAGGTGAATGCCC	Tb927.4.4840/4820/4860/4830
AAT5 forward	ATATGGATCCACCGCGCGGTGGTGCCCTTCC	Tb927.8.4710
AAT5 reverse	ACATCTCGAGTTCACATGACAAAGATAAGCG	Tb927.8.4710
AAT6 forward	CCAATCGCGTGTTGATACGT	Tb927.8.5450
AAT6 reverse	GCGGCACACCACAGCTCGGA	Tb927.8.5450
AAT7 forward	ATATGGATCCGTGAGTCTATTTATGGCAACT	Tb927.8.7600/7680
AAT7 reverse	ACATCTCGAGGCATGAGTGCACTACAATGGC	Tb927.8.7600/7680
AAT8 forward	ACGGGTGAACCGTTCGTTAG	Tb927.8.7740/Tb927.4.4730
AAT8 reverse	GATTTGCGTAGGGGTCGTAA	Tb927.8.7740/Tb927.4.4730
AAT9 forward	ATATGGATCCTGATGTGGTAAAGGAAGTGAA	Tb927.8.8220
AAT9 reverse	ACATCTCGAGATAGCCAAGATAATCACCAAC	Tb927.8.8220
AAT10 forward	ATATGGATCCTCGTGTCTAAATGGGCTTCCG	Tb927.8.8290/8300
AAT10 reverse	ACATCTCGAGCTTTGGGATGAAGAGACCCAA	Tb927.8.8290/8300
AAT11 forward	ATATGGATCCTGCATGCATTAGTGGTGGTTA	Tb09.211.1760
AAT11 reverse	ACATCTCGAGCCTCCAGGGATCTGGATGAAG	Tb09.211.1760
AAT12 forward	AAGGGGAACGCTTTAGTGGT	Tb10.70.1170
AAT12 reverse	TCTGCAAACAGTGATGAGGC	Tb10.70.1170
AAT13 forward	ATATGGATCCAAACAGATCAATTCCCTGCGC	Tb10.70.0300
AAT13 reverse	ACATCTCGAGACATAATTTGGCAACGAGCCC	Tb10.70.0300
AAT14 forward	ATATGGATCCGTAAACGTCGGGCTGTGATTG	Tb10.6k15.0450
AAT14 reverse	ACATCTCGAGAATTTCGCACAATGTCACCAC	Tb10.6k15.0450
AAT15 forward	TCGAACGCTGCCTTCTTAAT	Tb11.02.4520
AAT15 reverse	CCTTCTCGTATGCTTGCTCC	Tb11.02.4520
AAT16 forward	ATATAAGCTTCCTCACTTACTGCGCATATTG	Tb11.01.7500/7520
AAT16 reverse	ACATGGATCCGAGGGTATACTTCAATTAGGT	Tb11.01.7500/7520
AAT17 forward	ATATGGATCCTTTTCCCTGCATATCCTGTCA	Tb11.01.7590
AAT17 reverse	ACATCTCGAGGAACCTGGCACAGCTGCGCTT	Tb11.01.7590
ODC forward	ATGACCACCAAATCAACCCC	Tb11.01.5300
ODC reverse	TTATGATTTTTGACTTTTCAACTC	Tb11.01.5300
Tb-44_forwards	CCTATGCTATGTTCACGCTG	Tb927.8.5460
Tb-44_reverse	GCAGAACCCATCAGTAATGC	Tb927.8.5460
Tb927.8.5410_F	TGGACAGCTGAGGCACATAG	Tb927.8.5410
Tb927.8.5410_R	ACGCCTTAGTTCCTTGAGCA	Tb927.8.5410
Tb927.8.5420_F	TCCTCGGTATAAGCCGATTG	Tb927.8.5420
Tb927.8.5420_R	TCAACTGTTGGGTTTCCACA	Tb927.8.5420
Tb927.8.5430_F	ATGGGCAACAACGGAAGTAG	Tb927.8.5430
Tb927.8.5430_R	GTTGTGATACCGGGACAACC	Tb927.8.5430
Tb927.8.5480_F	CAGCAACTGAGATGAAGGCA	Tb927.8.5480
Tb927.8.5480_R	CGCGTCAAACTTCTTGAACA	Tb927.8.5480
Tb927.8.5490_R	AAAACGAGAGCCAACTCGAA	Tb927.8.5490
Tb927.8.5490_R	GTCAGCAAGCGCAGTGATTA	Tb927.8.5490
TbAAT6 RNAi forward	GATCGGGCCCGGTACCAAATTTATTTTCGGGCCACC	Tb927.8.5450
TbAAT6 RNAi	GATCTCTAGAGGATCCGTCTTCTGATTGCATCC	Tb927.8.5450

reverse	GGT	

Table 2-1. Primers used for PCRs and for the production of expression and RNA interference constructs.

2.3.3 Constructs for RNAi, gene knock outs and overexpression

The pRPa^{iSL} (RNAi (Alsford and Horn, 2008)), pGL1688 (knock out, a gift from Jeremy Mottram) and pHD676 (overexpression (Biebinger *et al.*, 1997)) constructs were created by PCR of a gene fragment (400 bases chosen using RNAit (http://trypanofan.path.cam.ac.uk/software/RNAit.html) for RNAi, gene flanking regions for knock out vectors and the whole gene for overexpression vectors). PCR products were created using the KOD high fidelity polymerase and treated with Taq polymerase to create a T overhang. These DNA fragments were ligated into the pGEM-T vector (Promega) using the instructions included in the kit. 2 µl of plasmid was added to 50 µl chemically competent DH5α *Escherichia coli* cells and left for 30 minutes on ice. Cells were heat shocked for 45 seconds at 42˚C then put on ice for two minutes. 1 ml of Luria broth was added and the cells were left to recover for one hour at 37˚C. 200 µl of cells were plated out onto an Luria broth agar plate with 50 µg/ml ampicillin. Colonies positive for the plasmid (by PCR) extracted from overnight cultures in Luria broth using a miniprep kit (Qiagen) and digested for ligation to the final construct using one unit of the digestion enzyme as specified in the literature (Biebinger *et al.*, 1997;Alsford and Horn, 2008;).

2.3.4 Southern blot and hybridisation

Southern blots were performed according to standard procedures (Sambrook and Russell, 2001).

5-10 µg DNA was digested with *Eco RI* (Promega) and ran on a 0.7 % agarose gel with 8 µL SYBR Safe stain (10,000 x Invitrogen) in 100 ml. The gel was blotted using a hybond-N membrane (Amersham) and probed with Easytides ^{32}P-ATP (Perkin Elmer) incorporated into the gene of interest using the Stratagene Prime-it kit with random primers used on ß-actin, ornithine decarboxylase and TbAAT6 containing DNA fragments extracted from plasmids.

2.3.5 Transfection of Trypanosomes

2 x 10^7 of bloodstream form cells (LaCount *et al.*, 2000) were attained from cultures of no more than 1 x 10^6 cells/ml. These cells were centrifuged at 2,500 RCF for 10 minutes and re-suspended in 100 µl T cell buffer (Lonza). 10 µg of linearised plasmid was added and cells were transferred to 0.4 cm gap transfection cuvettes. Cells were electroporated using programme X-001 on an Lonza Nucleofector II and then added to HMI-9 with 10 % FCS. After a recovery period of 24 hours, appropriate selection drugs were added (hygromycin (15 µg/ml), neomycin (15 µg/ml), phleomycin (0.5 µg/ml) or puromycin (0.2 µg/ml)). These cells were cloned out and stabilated.

The same protocol was used for 29-13 procyclic trypanosomes, but with 5 x 10^7 of no more than 5 x 10^6/ml cells.

2.3.6 RNAi in trypanosomes

2Ti bloodstream form cells (Alsford and Horn, 2008) were used to create the RNAi cell line with the pRPa^{iSL} construct. Cells were grown in tetracycline-free medium and induced with 1 µg/ml tetracycline. The pRPa^{iSL} plasmid (Alsford and Horn, 2008) (modified for use in 29-13 cells by Dr. Jane Munday, University of Glasgow) was also used to transfect 29-13 procyclic trypanosomes, which were inducible in the same way as the bloodstream form cells.

2.3.7 Northern blot

Northern blots were performed according to standard procedures (Sambrook and Russell, 2001). Certified RNA-free equipment was used and equipment was sprayed with RNaseZap (Ambion) or treated with DEPC water.

20 µg RNA was extracted using Trizol reagent (Invitrogen), run on a formaldehyde (16 %), Na_2HPO_4 (18 mM), NaH_2PO_4 (2 mM), agarose (1 %) gel, blotted using a hybond-N membrane (Amersham) and probed with Easytides ^{32}P-ATP (Perkin Elmer) incorporated into the gene of interest using the Stratagene Prime-it kit.

2.3.8 Tritiated amino acid uptake – cell preparation

Radiolabelled amino acids were obtained from Sigma Aldrich (L-arginine (2,3-^{3}H, specific activity: 60 Ci/mmol, concentration: 0.95 mCi/mL)), Moravec Biochemicals (L-proline (2,3,4,5-^{3}H, specific activity: 71.3 Ci/mmol, concentration: 5.0 mCi/ml), L-eflornithine (specific activity: 1.6 Ci/mmol concentration: 1 mCi/ml), D-ribose (1-^{3}H, specific activity: 14.3Ci/mmol, concentration: 1 mCi/ ml)) or American Radiolabeled Chemicals L-ornithine (4,5-^{3}H, specific activity: 40 Ci/ mmol, concentration: 1 mCi/ ml).

2.3.8.1 Trypanosoma brucei brucei

Mid-log phase cells were cultured to attain sufficient cell densities to permit use of more than 2 x 10^{7} cells per reaction. Cells were centrifuged at 1, 250 RCF for 10 minutes and re-suspended in CBSS buffer. Cells were centrifuged again at 1, 250 RCF and re-suspended to approximately 2 x 10^{8}/ml in CBSS buffer. Cells were counted, using a haemocytometer, and stored on ice until ready to use.

2.3.8.2 Leishmania mexicana

Leishmania mexicana were harvested at logarithmic stage of growth (between 5 x 10^{5} and 2 x 10^{7} cells per ml) and treated in the same way as *T. b. brucei*.

2.3.9 Tritiated amino acid uptake – rapid oil/stop protocol

A rapid oil/stop spin protocol, previously described by Carter & Fairlamb (1993), was used to determine uptake of radiolabelled compounds. 100 µl of oil (1-Bromodo-decane, density: 1.066 g/cm^{3} (50 % mineral oil was used for *Leishmania*)) (Aldrich) and 100 µl radiolabelled compound in CBSS buffer was added to 0.5 ml Eppendorf tubes. These were centrifuged briefly to remove bubbles.

Cells were added to the tubes at room temperature and centrifuged through the oil at 16, 000 RCF for one minute to stop the reaction after a specified length of time.

Cells were centrifuged for one minute at 16, 000 RCF in a centrifuge (Biofuge). The resulting cell pellet was flash frozen in liquid nitrogen and the base of the tube containing the pellet was cut into 200 µl of 2 % SDS in scintillation vials and left for 30 minutes. Three ml of scintillation fluid was added to each vial and these were left overnight at room temperature. A control with 200 µl SDS, 10 µl radiolabelled compound and three ml scintillation fluid (Optiphase 'hisafe' 2; PerkinElmer) was included to work out the counts per minute of the radiolabel.

Counts per minute were read on a 1450 microbeta liquid scintillation counter (Perkin Elmer) and normalised between samples for the cell density. This was then converted to moles of compound uptake per 10^7 cells. Michaelis-Menton kinetic analyses were performed using Graphpad Prism 5.

2.3.10 Arginase assay

A QuantiChrom Arginase assay kit (BioAssay Systems) was used to spectrophotometrically measure the amount of urea produced in the conversion of arginine to ornithine. *L. mexicana* and *T. brucei* cells were used at 1 x 10^8 per sample. Controls with no arginine and with no cells and a standard with 1 mM urea were used to calculate final urea production values. Urea levels were read on a spectrophotometer (Dynex) at a wavelength of 450 nM.

2.4 Computational Analyses

2.4.1 Heat maps

Heat maps were created in Microsoft Excel. Using conditional formatting on a three colour scale with a minimum of blue set at 0.2 (ratio of 0 time point divided by comparison time point), yellow set at 1 and the maximal red set at a five.

2.4.2 Metabolite identification

Metabolites were identified from the mass and retention time information output of mzMatch using IDEOM, a software developed by Darren Creek at the

University of Glasgow (unpublished). Pathways were compared to the Metacyc and KEGG trypanosome metabolite databases.

2.4.3 Statistics

Graphs and Student's *t*-test values were created in Microsoft Excel. ANOVAs were performed in Graphpad Prism 5.

2.4.4 Cladogram construction

Cladograms were constructed using the CLC genomics workbench software alignment and tree building tools. A neighbour joining algorithm was used and the tree was bootstrapped 1, 000 times.

2.4.5 Sequence Alignments

Sequence alignments were created from amino acid sequences sourced through the NCBI database (www.ncbi.nlm.nih.gov) in CLC workbench. A gap open cost of 10 and a gap extension cost of one were used.

3. Resistance to eflornithine

3.1 Introduction

There are numerous drawbacks with the drugs currently available for the treatment of HAT. Side effects such as rashes (melarsoprol, suramin, eflornithine and pentamidine), renal problems (melarsoprol, eflornithine and pentamidine), encephalopathy (melarsoprol) and pain (melarsoprol, eflornithine and suramin) are often severe and can cause patients to deviate from recommended treatment regimes. Failure to complete the full treatment course can result in treatment failure and can expose parasites to sub-lethal levels of drug, that may result in the selection of drug resistance. Drug resistant parasites can also be selected through prophylactic use or from using sub-lethal levels of drug (which may be a problem if drugs are shared amongst communities with inadequate funding – a less prominent problem for HAT where drugs are distributed through dedicated health centres).

Resistance can be difficult to detect. Currently relapse rates in the field are not systematically recorded. If a patient does relapse, it may not be clear whether they were re-infected or if the treatment failed for some reason. It has been shown that eflornithine in mice is not efficient at crossing the blood-brain barrier (Levin *et al.*, 1983) and so levels of the drug may be sub-lethal in the brain and may therefore help to select resistant parasites (Sanderson *et al.*, 2008). In humans, however, there seems to be more uptake into the brain (Burri and Brun, 2003) and suramin has been shown to increase the concentration of eflornithine crossing the barrier in mice (Jennings, 1993;Sanderson *et al.*, 2008). In humans it has been suggested that a transporter carriers eflornithine over the blood-brain barrier (O'Kane *et al.*, 2006) creating CSF:plasma ratios of between 0.1 and 0.9 (Barrett *et al.*, 2007).

Eflornithine is administered intravenously as a racemate in saline solution (Barrett *et al.*, 2007). Patients must spend at least 14 days in hospital to receive a total of 56 infusions (Barrett *et al.*, 2007). This extended hospital stay is clearly very costly to the family of the patient and the large drug volumes are difficult to transport to the places where they are required. These two big issues

with eflornithine treatment mean that many people with the disease die unnecessarily either because they cannot travel to a clinic and spend large amounts of time away from their families and livelihoods or because the drugs cannot be transported close enough to them. Efforts to reduce the amount of drug required (and therefore reduce transport issues) have resulted in nifurtimox-eflornithine combination therapy (NECT). However, this therapy does still require a 10 day stay in hospital. Greater efforts to reduce the quantities of drugs required would be beneficial.

Eflornithine targets ornithine decarboxylase (ODC) in trypanosomes (Bacchi *et al.*, 1983;Phillips *et al.*, 1987), and this was shown to cause diminished polyamine biosynthesis (Bacchi *et al.,* 1983) and reduced production of the trypanosome-specific redox-active metabolite trypanothione (Fairlamb *et al.,* 1987). Accumulation of S-adenosyl methionine, measured by HPLC, has been reported in eflornithine-treated cells, which might perturb cellular methylation reactions (Yarlett and Bacchi, 1988) although more recent data, obtained through the use of RNA interference to reduce expression of ODC, increased levels of decarboxylated S-adenosyl methionine, but not of its precursor, S-adenosyl methionine (Xiao *et al.,* 2009).

How eflornithine enters trypanosomes is a subject of debate. An early report measuring the uptake of ^{14}C-eflornithine in bloodstream form trypanosomes and in hepatoma human cells showed that eflornithine uptake was not saturable, generating the hypothesis that eflornithine enters trypanosomes by passive diffusion (Bitonti *et al.,* 1986). However, studies on eflornithine resistant procyclic trypanosomes showed reduced accumulation of ^{14}C-eflornithine (Phillips and Wang, 1987) and uptake of eflornithine was saturable (at 0.01 nmol per 10^7 cells) in the resistant line, which is typical of a transporter. Bellofatto *et al* (1987) also found uptake of eflornithine in procyclic cells to be temperature dependent and thus likely to be transporter mediated. Indeed as a zwitterionic, charged amino acid, eflornithine would not be expected to diffuse across membranes and transport-mediated uptake is a more likely route of entry, perhaps via one of the numerous amino acid transporters that are encoded in the trypanosome genome.

In *T. brucei,* loss of transport has been shown to be a key determinant in resistance to melaminophenylarsenicals (Carter and Fairlamb, 1993) and diamidine drugs (Barrett and Fairlamb, 1999; Matovu *et al.,* 2001;Stewart *et al.*, 2005). It would be interesting to determine whether loss of transport is also a factor in resistance to eflornithine.

The mechanisms of drug resistance are often discovered after resistance has been detected in the field. It is an arms race where biologists are often caught on the back foot. Given the increased use of eflornithine, alone or in combination with nifurtimox, a better understanding of the risk of resistance is critical. Such an understanding may help limit its spread and allow the development of diagnostic tools. Fluorescence-based tests are available to predict the loss of the P2 transporter and therefore resistance to melarsoprol (Stewart *et al.,* 2005). Genetic tests would be of less use to determine the status of the P2 transporter as different, often complex, genetic mutations are seen in different isolates (Stewart *et al.,* 2010).

As described above, eflornithine is now preferentially used in combination with nifurtimox. It was predicted that nifurtimox and eflornithine would work synergistically with one another as nifurtimox was shown to induce oxidative stress in cell extracts (Docampo and Stoppani, 1979;Docampo and Moreno, 1984;Viode et al., 1999) and eflornithine reduces the thiol pool which would otherwise deal with this stress (Fairlamb *et al.,* 1987). This synergism has not, however, been formally shown. If resistance to eflornithine is easily selected then it may be that the use of the combination therapy is under threat. In this chapter, I describe work revealing a molecular mechanism for resistance to eflornithine.

3.2 Results

3.2.1 Selection of eflornithine resistant bloodstream form T. b. brucei.

Although there has been anecdotal evidence of eflornithine treatment failures in the field (Enock Matovu, unpublished data), resistant samples have not, as yet, been isolated. To investigate mechanisms of eflornithine resistance, parasites were selected *in vitro* from a wildtype bloodstream form *T. b. brucei* strain 427 by growth in increasing concentrations of eflornithine. *T. b. brucei* was used as it is a tractable, non-human infective sub-species, which has a much better annotated genome sequence than *T. b. gambiense* (although there is some concern that *T. b. brucei* is genetically more similar to *T. b. rhodesiense* (see section 1.2 of this thesis), and *T. b. rhodesiense* is insensitive to eflornithine).

It took two months (24 passages) to attain a line demonstrating forty fold less sensitivity to drug, based on the IC_{50} value of eflornithine in the drug sensitive parent strain (Fig 3-1A). No altered growth phenotype was observed (data not shown). Two independent cell lines (DFMOR1 and DFMOR2) were generated in this way. The IC_{50} levels were also recorded by alamar Blue assay at various stages during the selection process to measure the levels of resistance. This is also shown in figure 3-1. It should be noted that eflornithine is thought to act in a cytostatic way (Bitonti *et al.,* 1986), so IC_{50} levels should be taken as a relative measure of the resistance, rather than the absolute amount of drug required to kill the cells. In an *in vivo* assay, where there is a healthy immune system, it is likely that the IC_{50} will be lower.

The resistant lines also grew in female ICR mice and exhibited resistance to both the minimum curative dose of 2 % w/v and a higher dose of 5 % w/v eflornithine whilst mice infected with wildtype cells were cured with the lower 2 % w/v dose. Resistant cells remained susceptible to pentamidine (4 mg/kg, four daily doses) (Fig 3-1B), as was also seen *in vitro* (Table 3-1). This demonstrates that the *in vitro* selected mechanism for resistance is also operative *in vivo*.

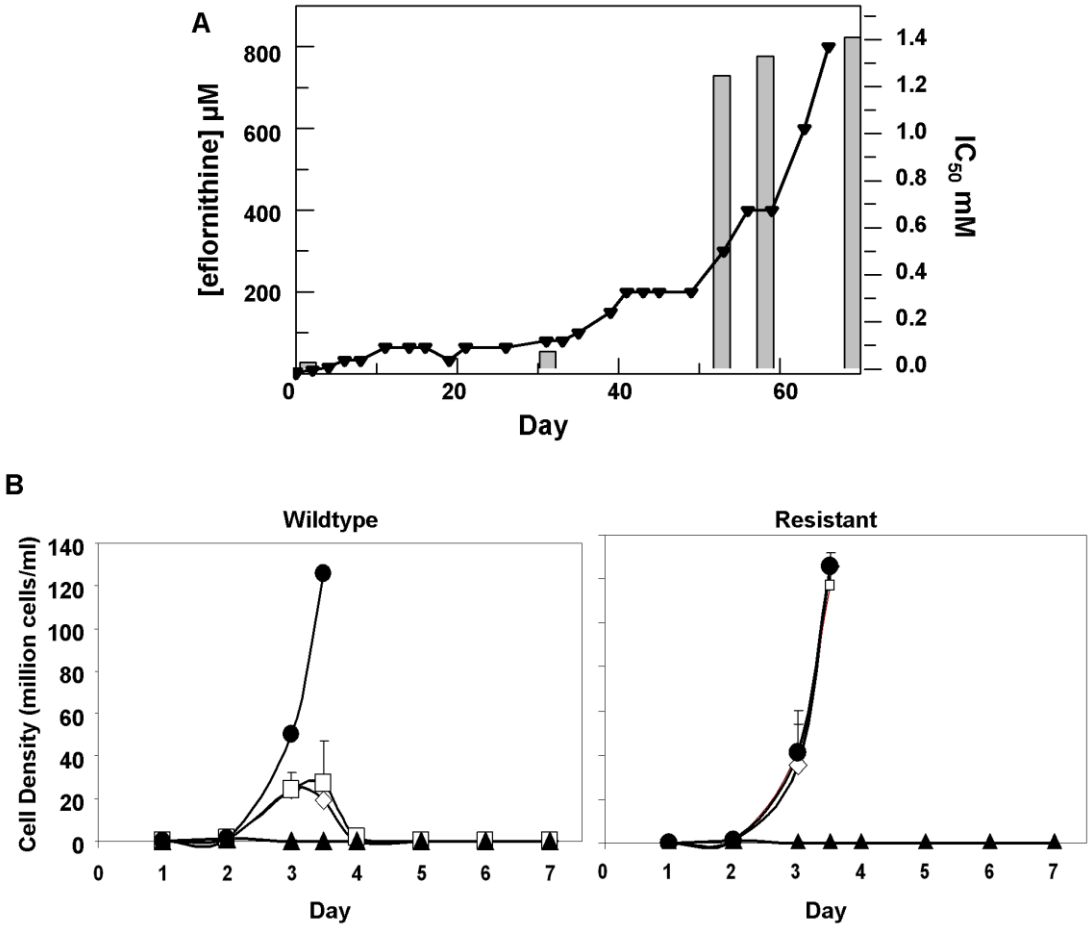

Figure 3-1 Eflornithine resistance in *T. b. brucei. (A)*, Selection of eflornithine resistance in *T. b. brucei*. Black triangles and left hand y-axis show the eflornithine concentration in which the parasites grew. Bars and the right hand y-axis show milimolar IC_{50} values at various stages of the selection process. One clone out of two is shown. *(B)*, Treatment of mice infected with wildtype or eflornithine resistant (DFMOR1) parasites. Closed circles; untreated, open diamonds; 2 % eflornithine, open squares; 5 % eflornithine, closed triangles; pentamidine (4 mg/kg).

An alamar blue assay was used on the wildtype and DFMOR1 lines to determine whether there was cross-resistance with other trypanocides (Table 3-1). This would indicate a shared mode of entry, mode of action or drug efflux mechanism. There was no cross-resistance with other currently used trypanocides, although there was a significant increase in sensitivity to pentamidine.

Trypanocide	Wildtype IC_{50} (nM)	Resistant IC_{50} (nM)	Average R:WT
Suramin (n = 3)	4.6 ± 0.7	4.4 ± 0.4	0.99
Melarsen Oxide (n = 2)	4.3	2.4	0.67
Cymelarsan (n = 2)	6.3	3.7	0.73
Nifurtimox (n = 5)	2, 940 ± 600	2, 880 ± 300	1.09
Pentamidine (n = 5)	0.43 ± 0.1	0.1 ± 0.04	0.27*
Eflornithine (n = 5)	22, 000 ± 3, 000	906, 000 ± 192, 000	41.46*

Table 3-1 IC_{50} values for known trypanocides on wildtype and eflornithine resistant cell lines. Number of replicates are in parentheses, numbers represent mean ± s.e.m where appropriate. * indicates significance at a p = 0.05 level from a paired *t*-test.

3.2.2 Analysis of resistant lines

Initial metabolomics experiments were undertaken before a full protocol optimisation was completed. As a result, the intensities of some of the metabolites (notably the more water-soluble metabolites) may be reduced, but the relative intensities between the two groups remain valid. Briefly, the wildtype and DFMOR1 cells were grown to a density of 1-2 x 10^6/ml. These cells were concentrated by centrifugation (1, 250 RCF) to 1 x 10^9/ml. 2 x 10^8 cells suspended in HMI-9 were quenched in 800 µl 80ºC ethanol and the supernatant after centrifugation (at 16, 000 RCF) was flash frozen in liquid nitrogen.

Samples were run on the Orbitrap at the University of Strathclyde, Glasgow by Dr. Muhammed Anas Kamleh.

Significant differences between the untargeted metabolite profiles of wildtype and resistant cells were not apparent using multivariate statistical analysis (Appendix 8.1), nor were changes seen in any of the identified polyamine pathway metabolites. It was previously shown in eflornithine resistant procyclic stages of the parasite that an increased uptake of putrescine can relieve the blockage of ODC caused by eflornithine (Bacchi *et al.*, 1993). An increase in putrescine was not observed in our analyses, however, so it seems that increased putrescine uptake is not required for resistance in bloodstream forms of the

parasite. There was a slight, although not significant, decrease in ornithine levels in the resistant cell line (Fig 3-2).

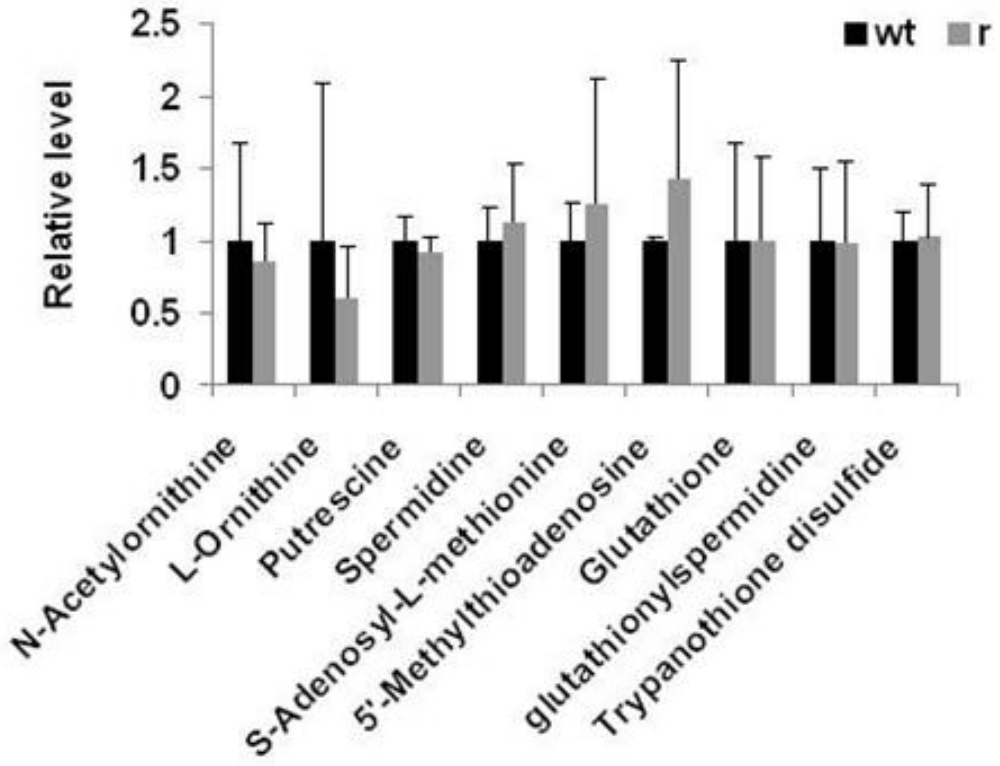

Figure 3-2 Metabolomic analysis of eflornithine resistance. Relative abundance of polyamine metabolites in wildtype (WT) and eflornithine resistant (R) cell extracts. Error bars show standard deviation.

This reduction in ornithine in the resistant cell line could be explained by reduced ornithine uptake. This was investigated with tritiated ornithine at a concentration of 10 μM over a 30 minute time period using ribose uptake as a control (Fig 3-3).

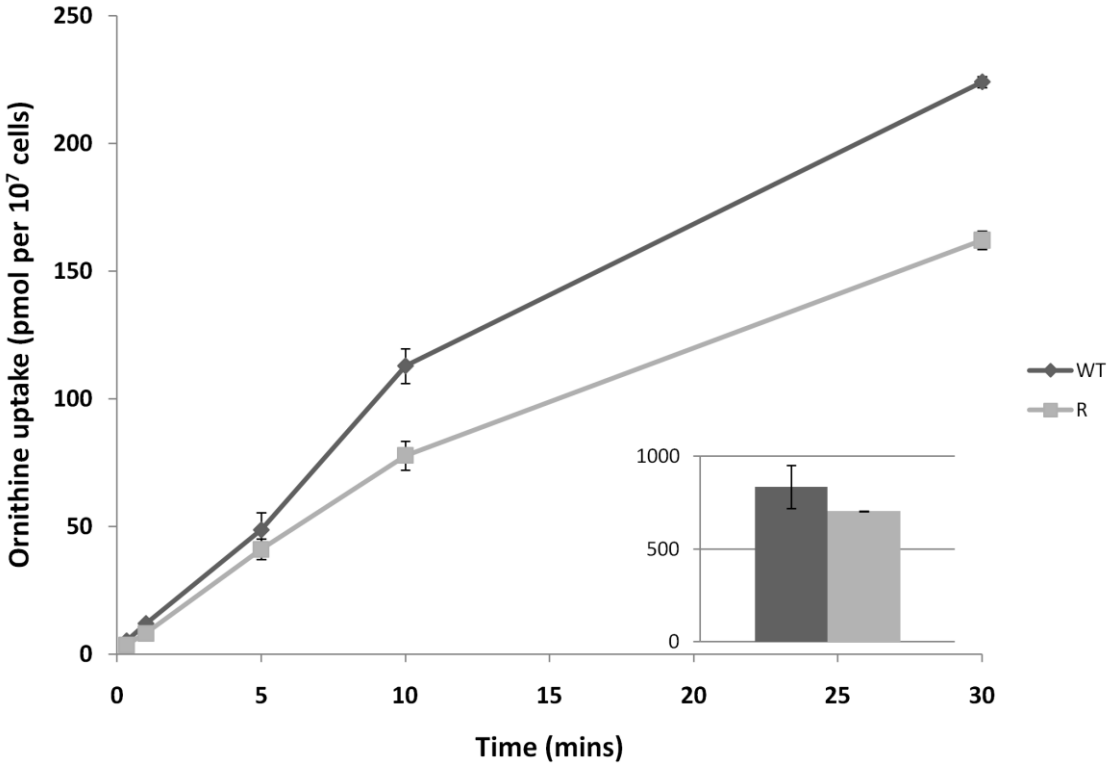

Figure 3-3. The uptake of ornithine into wildtype and DFMOR1 cell lines. Tritiated ornithine was used to determine whether ornithine uptake was lost in the resistant cell line. Ribose uptake (inset) was monitored as a control (30 minute time point shown). Data shown is one of four replicates. P = 0.318 from a 2 tailed *t*-test comparing 0 and 30 minute time points.

The reduced levels of ornithine in the resistant cells do not appear to be a consequence of reduced uptake (the difference in uptake seen in figure 3-3 is not reproducible or significant, especially when normalised to the difference in ribose uptake). It is therefore likely that the reduction in ornithine is due to a metabolic mechanism such as increased flux through ornithine decarboxylase. This could be analysed further by tracking the metabolism of isotopically-labelled ornithine through wildtype and the resistant cell lines, but was not followed up as part of this work. This was because in a targeted analysis of eflornithine (m/z = 183.0940, RT = 19.72 minutes) accumulation using mass spectrometry, it was evident that eflornithine levels were greatly reduced in resistant cells compared to wildtype (Fig 3-4). This result indicated that exclusion of drug from the resistant line (DFMOR1) rather than changes to metabolism were responsible for loss of sensitivity.

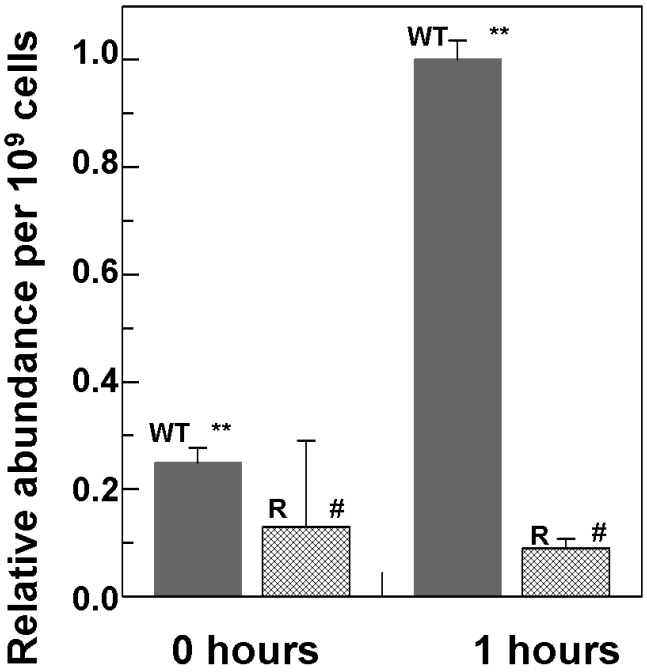

Figure 3-4, The uptake of eflornithine (m/z = 183.0940, RT = 19.72) into wildtype and DFMOR1 cell lines. Wildtype (filled bars) show an increased accumulation of eflornithine compared to resistant cells (hatched bars) over one hour. Stars indicate a significant difference at a p=0.01 level between WT at time 0 and WT after 60 minutes. A hash indicates that R at time 0 and R after 60 minutes show no significant difference at a p=0.05 level.

There are no known isomers of eflornithine and since the retention time detected is very similar to the predicted retention time from the empirical formula of eflornithine (-0.2 % error) we can be extremely confident that the detected peak represents eflornithine.

The slight change in sensitivity to pentamidine observed in DFMOR1 was also investigated using metabolomics. A time course experiment (0, 1 and 2 hours) with 40 nM (ten times the IC_{50}) pentamidine was conducted, but no significant differences in levels of any metabolites were observed apart from reduced ornithine levels in all resistant samples (data not shown) as seen in the comparison of wildtype and resistant cell lines. This indicates that visible changes to the metabolome are not seen within two hours of pentamidine treatment in wildtype or in resistant cells.

Eflornithine targets the enzyme ornithine decarboxylase. Alterations to the amino acid composition of proteins is often responsible for drug resistance as

variants with diminished ability to bind drug are selected (Farooq and Mahajan, 2004). To rule this out we amplified the ODC gene from the wildtype and the resistant cell line (DFMOR1 and DFMOR2) and found no differences in the sequence (Appendix 8.2).

3.2.3 Loss of eflornithine accumulation into resistant cells.

To determine quantitatively the relative transport rates of the drug in wildtype and resistant cells, ^{3}H-eflornithine was used to measure accumulation in each cell type. Eflornithine was used at a concentration of 20 μM. Threonine uptake was assayed as a control (as threonine is another amino acid, but is uncharged and likely therefore to use alternative transport mechanisms). A greater rate of eflornithine uptake was observed in the wildtype cell line compared to the resistant line (DFMOR1), with around five fold more drug taken into wildtype cells after 30 minutes (Fig 3-5). Levels of threonine uptake were the same in both cell lines.

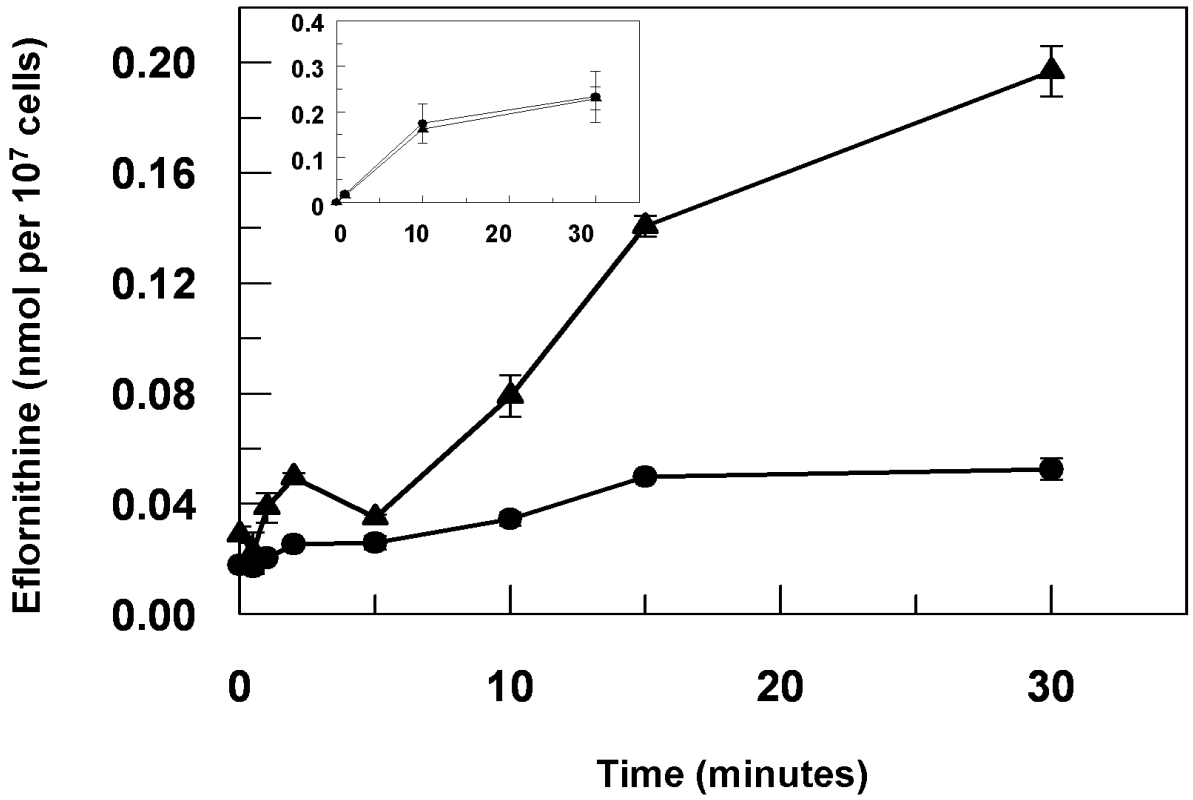

Figure 3-5. Quantitative uptake of eflornithine in wildtype and DFMOR1 cell lines. ^{3}H-eflornithine transported into wildtype (triangles) and resistant (circles) cells was measured over 30 minutes. Measurements are an average of four separate experiments, each with three internal replicates. Error bars are the standard error of the mean. Inset graph shows threonine uptake in the same cell lines. The y-axis shows nmol of threonine per 10^7 cells. The x-axis shows the time in minutes.

The transporter appears to be concentrative, as an internal concentration of 344 µM is measured (assuming a trypanosome cell volume of 0.58 µL per 10^7 cells (Opperdoes *et al.*, 1984)) compared to the external concentration of 20 µM. In procyclic cells the internal concentration measured by Bellofatto *et al.* was 47 µM after 70 minutes in 100 µM tritiated eflornithine (1987), which led them to conclude that eflornithine is not transported. Phillips and Wang measured 180 µM after 60 minutes in 54 µM (1987), also in procyclic cells, which led them to conclude that eflornithine is transported. Whether the transporter is active and concentrative within procyclic forms of the trypanosome is therefore inconclusive.

It might have been expected that ornithine and eflornithine share an uptake mechanism. In fact, we found no appreciable difference in ornithine uptake between the wildtype and the resistant cell lines (Fig 3-3) but we saw much

reduced eflornithine uptake in the resistant line (Fig 3-5). These observations lead to three possible hypotheses: 1, Eflornithine and ornithine do not share an uptake mechanism, 2, an eflornithine efflux mechanism has no effect on ornithine or 3, ornithine is able to use a wider variety or transporters than eflornithine and loss of one does not prevent ornithine entry into the cell.

To determine whether ornithine and eflornithine share an uptake mechanism ornithine uptake assays were performed in increasing competition with cold eflornithine (Fig 3-6) and cold ornithine as a control.

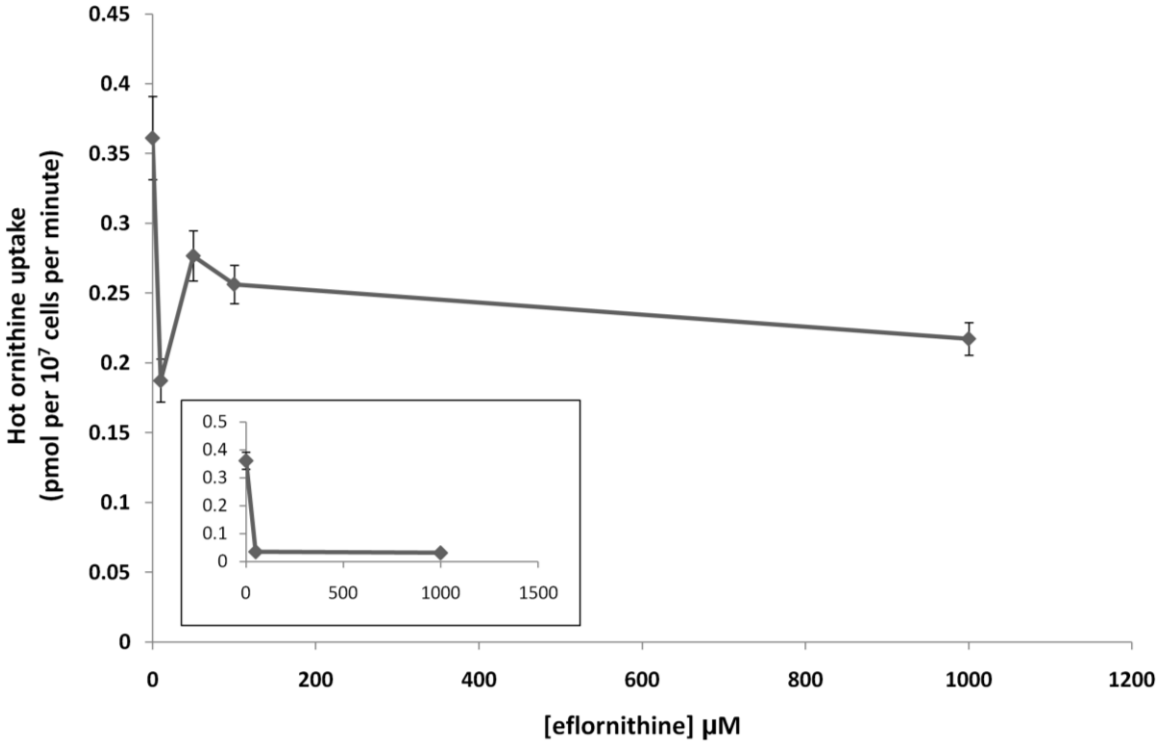

Figure 3-6. Eflornithine inhibition of ornithine uptake in wildype 427 bloodstream form cells. Increasing concentrations of cold eflornithine (x-axis) do not significantly inhibit the uptake of tritiated ornithine (y-axis). Inset: tritiated ornithine uptake (y-axis) can be inhibited by cold ornithine (x-axis).

Reciprocal experiments with ornithine inhibition of eflornithine uptake confirmed a lack of uptake cross inhibition (data not shown). Increasing concentrations of cold eflornithine have no effect on ornithine uptake suggesting either that ornithine is accumulated via multiple transporters, which can compensate for the inhibition of one transporter, or that the two amino acids do not share a transport mechanism.

Whether ornithine and eflornithine share a transporter or not remains to be concluded, but the data indicate a transporter phenotype for eflornithine resistance, as seen previously in selection of resistance to melamine-based arsenicals (Carter and Fairlamb, 1993) and diamidines (Barrett and Fairlamb, 1999; Stewart *et al.*, 2005; Lanteri *et al.*, 2006;Bridges et al., 2007). As eflornithine is an amino acid analogue (Fig 1-9), we hypothesised loss of an amino acid transporter. Several members of this amino acid transporter family were characterised by Charles Ebikeme (University of Glasgow). The TbAAT7 locus (which encodes at least nine amino acid transporters) was shown to transport threonine, glycine, cysteine, asparagine, alanine and serine, but none of the other 13 essential amino acids assayed (tyrosine was not assayed) (Ebikeme, 2008). With the exception of asparagine, which is a relatively poor substrate at this locus, all of these amino acids are neutral and have a small side chain of fewer than two carbon unit. The TbAAT5 locus was also investigated by RNAi and was shown not to transport proline (Ebikeme, 2008). It is not known which members of the amino acid permease superfamily transport lysine, arginine or ornithine, the closest amino acids to eflornithine based on structure and charge.

To test the theory that eflornithine resistance occurs due to loss of an amino acid permease, all members of the amino acid permease gene family (Fig 3-7) in the *T. brucei* genome (Jackson, 2007) were systematically amplified from both wildtype and each of the two independently selected resistant lines.

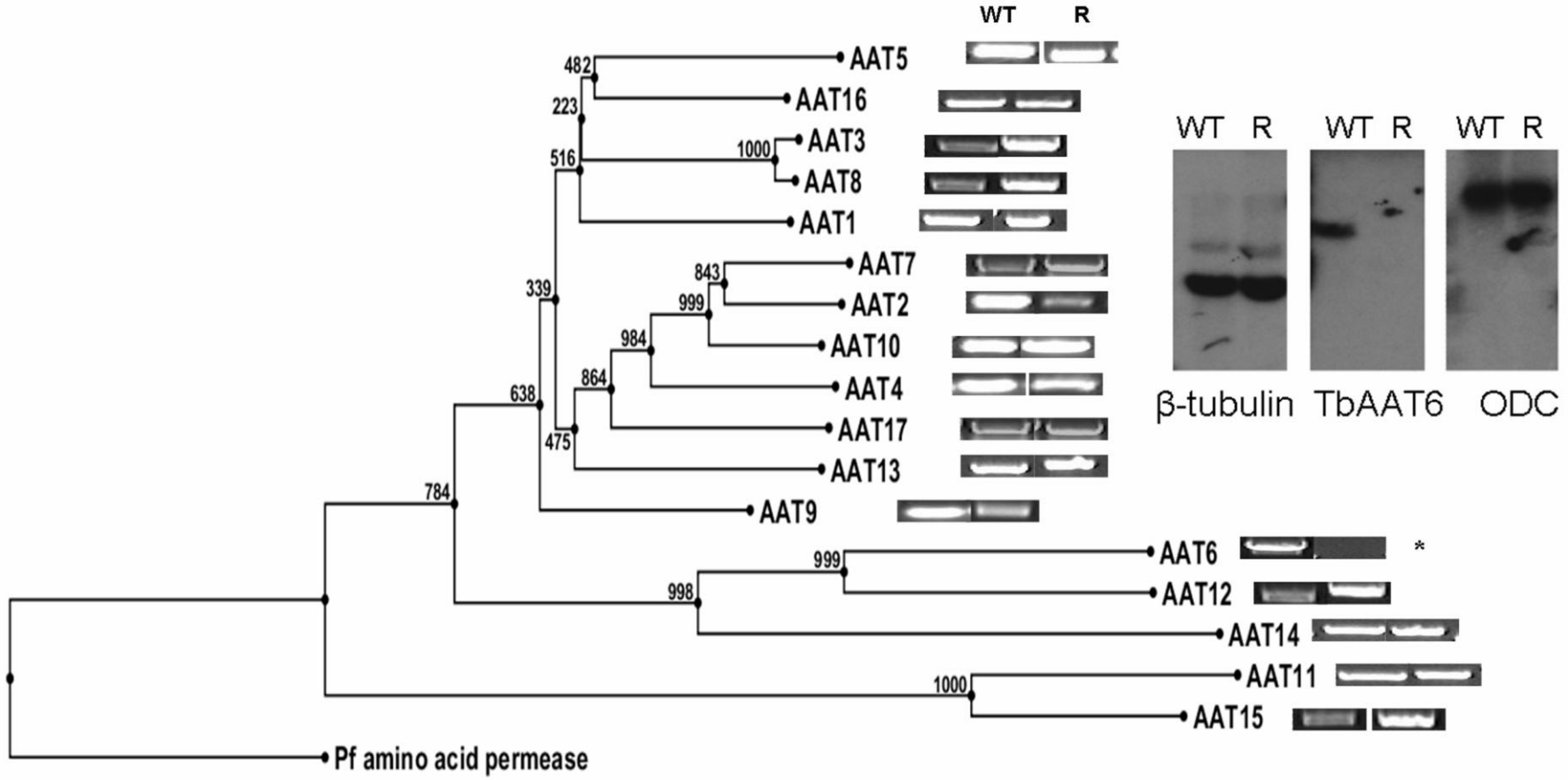

Figure 3-7 Cladogram of the amino acid transporters predicted to be in *T. b. brucei* and genomic status in wildtype and DFMOR1 lines. Amplification of wildtype and resistant cell PCR products of 17 amino acid transporters from the wildtype and resistant cell lines shows *TbAAT6* to be absent. Inset: Southern blotting showed the loss of *TbAAT6* in resistant, but not wildtype cells. *ODC* (ornithine decarboxylase) and *β-tubulin* remained unchanged. Branch length corresponds to the average rate of substitutions. Numbers on branches show bootstrap values out of 1000.

In each of the independently selected lines only one single copy amino acid transporter gene, *TbAAT6* (Tb927.8.5450), was shown to be absent (Fig 3-7). Southern blot analysis confirmed this and also demonstrated that there were no alterations in ODC copy number.

TbAAT6 appears to be an orphan within the amino acid transporter family; it has no homologue in leishmania or *T. cruzi* and where other amino acid transporters appear in clusters on their chromosomes, many with tandem repeats, TbAAT6 stands alone (Jackson, 2007). This is an advantage for molecular characterisation as it means that expression can be inhibited by RNA interference with less risk of unintentional knockdown of other genes with similar sequences. The identification of TbAAT6 also provides the possibility of expression in a heterologous system for further analysis of function.

PCR analysis indicated a deletion of TbAAT6, and surrounding genes, from both resistant lines (DFMOR1 and DFMOR2) (Fig 3-8a). This result indicated the possibility that the *TbAAT6* gene could play a role in eflornithine's entry into *T. brucei* and that its loss was responsible for drug resistance. The gene was amplifiable at day 34 of the selection process, but by day 50 was no longer amplifiable (Fig 3-8b), this correlates with the loss of sensitivity to eflornithine between days 34 and 50.

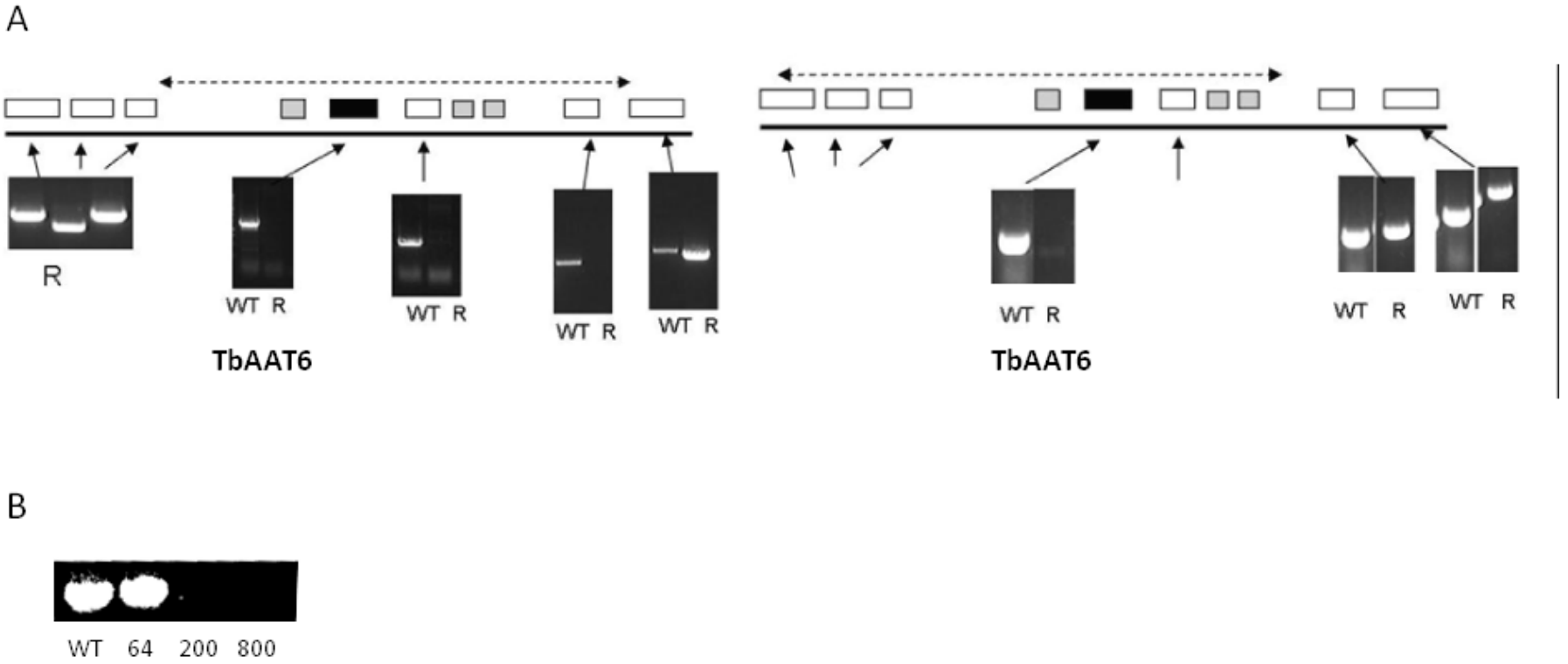

Figure 3-8. PCR analysis of the region of chromosome 8 housing the single copy *TbAAT6* (black box) in *T.b. brucei*. (A) Chromosome 8. DFMOR1 shown on the left, DFMOR2 shown on the right. An area of DNA is missing in both strains including *TbAAT6*. The exact boundary of the missing area is unknown (represented by the dotted line). Genes are (left to right) Tb927.8.5410 (hypothetical), Tb927.8.5420 (hypothetical), Tb927.8.5430 (hypothetical), Tb927.8.5440 (*Tb-24*, a flagellar calcium-binding protein), Tb927.8.5450 (*TbAAT6*), Tb927.8.5460 (*Tb-44* a flagellar calcium-binding protein), Tb927.8.5465 (*Tb-24*, a flagellar calcium-binding protein), Tb927.8.5470 (*Tb-17* a flagellar calcium-binding protein), Tb927.8.5480 (hypothetical), Tb927.8.5490 (hypothetical). Not all of these genes were amplified as *Tb17*, *Tb24* and *Tb44* are repetitive throughout the genome. Not all of the genes in DFMOR2 were amplified. (B) Status of TbAAT6 during the selection of resistance. The gene is present when cells are grown in 64 µM (day 34 of the selection process) eflornithine, but is lost when they are grown in 200 µM (day 50 of selection).

As eflornithine is less effective in *T. b. rhodesiense* parasites, the status of the rhodesiense gene was checked by PCR on DNA isolated from the field (a kind gift of Craig Duffy, University of Glasgow) and the gene was found to be present and of a similar size to the *T. b. brucei* gene. The sequence of this gene was not analysed, however, as the genome of *T. b. rhodesiense* is not published.

Patients from the field who have been shown to be refractory to eflornithine treatment, or who have shown a resurgence of parasitaemia after eflornithine treatment, may routinely have a blood sample spotted on to an FTA® card. FTA® cards lyse cells, denature proteins and protect nucleic acids. Cards are washed to remove contaminating red blood cells and any parasite DNA can be amplified. Blood spots from eflornithine-relapse and eflornithine-cured patients were obtained from Omugo, Uganda courtesy of Enock Matovu, (Makerere University). Several attempts to amplify TbAAT6 or phospholipase C (as a positive control) were made using PCR and nested PCR without success. The parasitaemia within the samples was not recorded, but was thought to be very low, which may explain why parasites could not be detected even with the positive control.

3.2.4 Functional confirmation of a role for TbAAT6 in eflornithine resistance.

To confirm a role for TbAAT6 in eflornithine resistance we used RNA interference (Alsford and Horn, 2008) to ablate its expression in *T. b. brucei*. The pRPa^{iSL} vector was used which integrates into a ribosomal spacer locus of the trypanosome DNA in the 2Ti cell line, completing a hygromycin resistance marker to achieve efficient integration rates and reproducible siRNA transcript levels. The vector contains a stem-loop system to create the double stranded RNA. This is thought to be more efficient than using opposing T7 promoters as intermolecular RNA interactions are more likely than intramolecular interactions (Alsford and Horn, 2008).

The gene sequence to be used in the vector was chosen using the RNAit programme (http://trypanofan.path.cam.ac.uk/software/RNAit.html) using the

same 400 bases for each section of the stem-loop vector. Positive transfections were selected using hygromycin.

Five cloned lines were selected and were induced with tetracycline for six days before commencing the alamar blue assay to determine the IC_{50} for eflornithine. The induced lines showed no growth defect over seven days (data not shown). All five of the *TbAAT6*^{RNAi} mutants became resistant to eflornithine to an extent similar to the lines selected for resistance to the drug (40 x resistance factor) (Fig 3-9A). These cells did not become resistant to DB75, used as a control (data not shown). Attempts to confirm knock down of TbAAT6 by northern analysis were unsuccessful, even with ß-actin controls.

Attempts were made to create a TbAAT6 null mutant line, but removal of the second allele of the gene was not achieved. This is unexpected as selection of resistance was very fast, implying that the gene would not be difficult to remove. It is therefore likely that other changes are required to enable the loss of TbAAT6. The line with just one allele of TbAAT6 was analysed in an alamar blue assay and was surprisingly found to be more sensitive to eflornithine than the wildtype parent line (IC_{50} 10.7 ± 3.2 µM c.f. 47.5 ± 6.5 µM for wildtype (results are mean ± s.e.m, n = 4)). This may be due to a compensatory mechanism within the heterozygote line such as increased expression of the one allele, but has not been confirmed.

A procyclic RNAi line for TbAAT6 was also created using the same construct as the bloodstream form, with a slight modification to remove the partial hygromycin resistance marker and replacing it with a full hygromycin resistance gene. This 29-13 derived line (Jane Munday, University of Glasgow) showed no growth defect over nine days when induced with tetracycline, but as neither induced or non-induced cells were sensitive to eflornithine (in an alamar blue assay with eflornithine concentrations up to 20 mM, data not shown), a resistance phenotype could not be determined. It is of note that the Horn group at the London School of Hygiene and Tropical Medicine reported a growth defect in RNAi ablation of TbAAT6 expression in procyclic cells during a large scale RNAi library screen, but that this defect was not reproduced in a targeted RNAi assay for TbAAT6 (David Horn, personal communication).

Next, we expressed the *TbAAT6* gene in the eflornithine resistant trypanosomes using vector pHD676 (Biebinger *et al.*, 1997). This vector also integrates into the ribosomal spacer regions of the trypanosome DNA and constitutively expresses TbAAT6 using a P_{RRN} promoter (a ribosomal RNA promoter) (Biebinger *et al.*, 1997). Cloned cells in which the gene was re-expressed re-gained levels of eflornithine sensitivity similar to wildtype (Fig 3-9B).

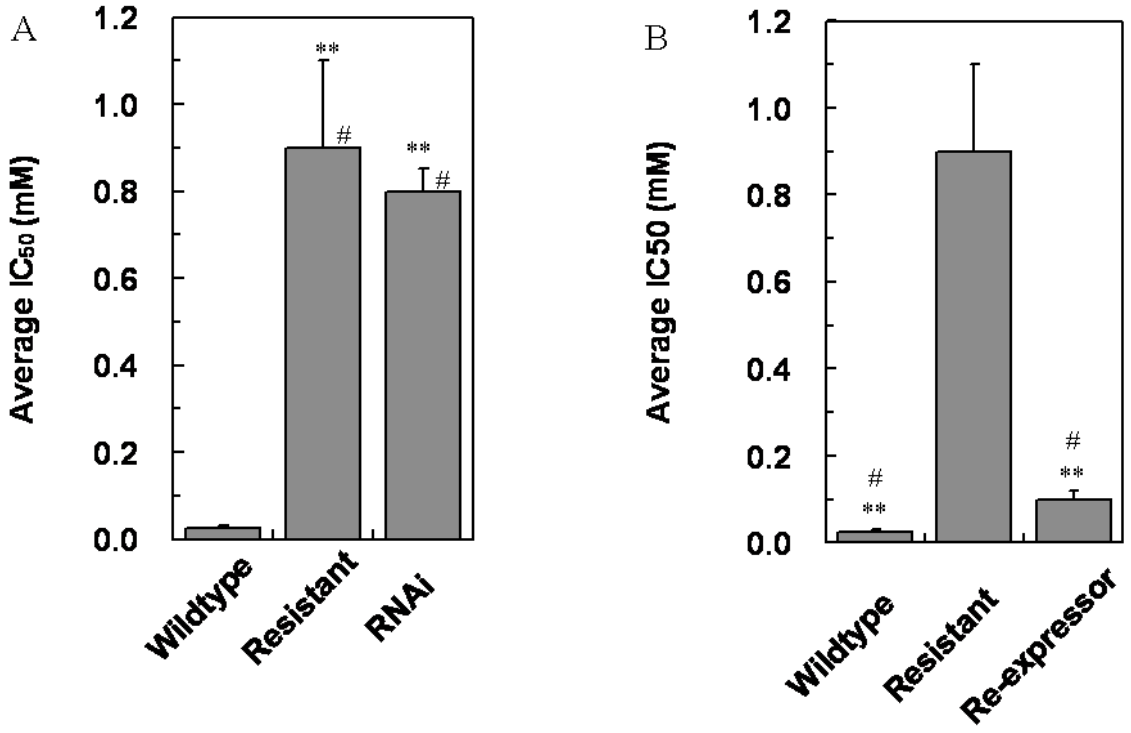

Figure 3-9 RNAi and re-expression of TbAAT6. (A) RNAi was induced for 12 days and the IC_{50} value to eflornithine measured. Stars indicate significant difference at a p = 0.05 level compared to wildtype, whereas a hash indicates that RNAi (773 ± 53 µM) and resistant lines (886 ± 200 µM) show no significant difference. (B) Re-expression of TbAAT6, IC_{50} values for eflornithine of the wildtype parent line (24.6 ± 5.8 µM), the resistant line (886 ± 200 µM) and the resistant line constitutively re-expressing TbAAT6 (111 ± 18 µM). Stars indicate a significant difference at a p = 0.05 level compared to resistant, whereas a hash indicates that wildtype and re-expressor show no significant difference. IC_{50} measurements were at least n = 5.

Loss of expression of TbAAT6 is therefore both necessary and sufficient to confer resistance to eflornithine and its re-expression in defective lines is capable of restoring sensitivity, regardless of other changes to the cell.

To analyse further the natural substrate of TbAAT6, a heterologous expression system without endogenous eflornithine uptake was sought. Leishmania were

found to transport eflornithine (Fig 3-10), so were eliminated as a potential expression system.

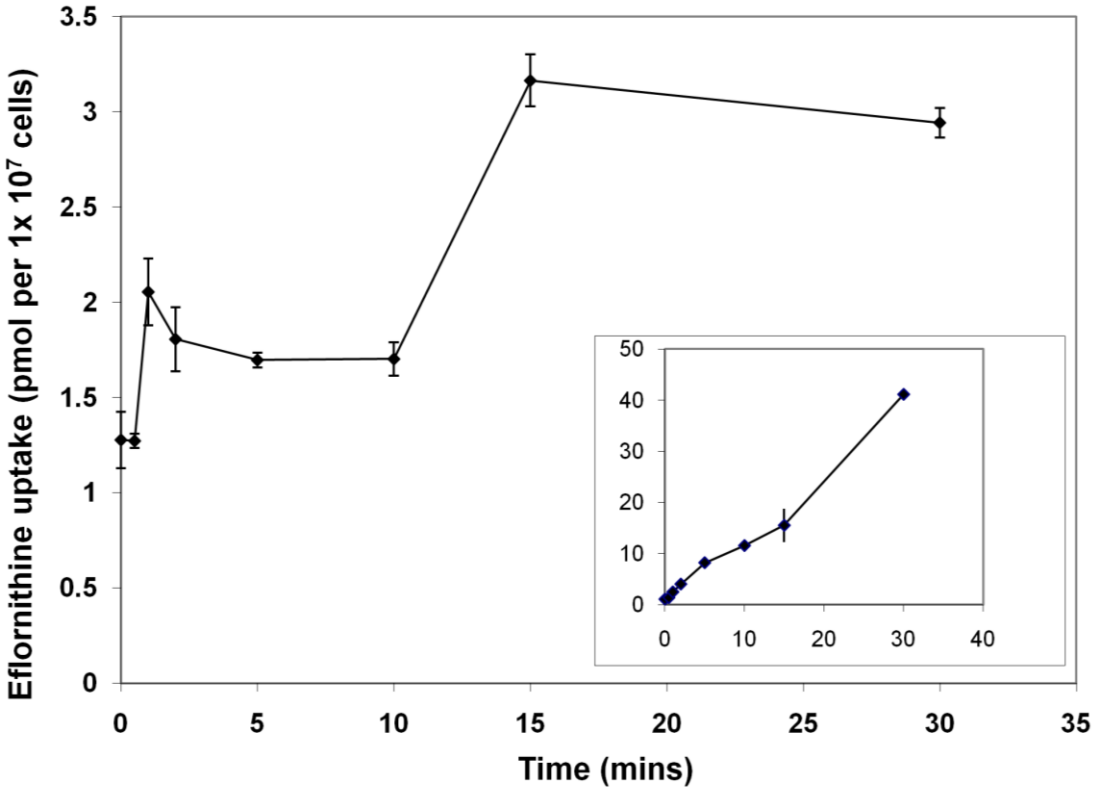

Figure 3-10. Eflornithine uptake in *L. mexicana.* The increase in eflornithine signal from 1.25 to 3 pmol per minute is indicative of uptake in *Leishmania spp*. Proline uptake (inset) was used as a control.

3.2.5 Further studies of TbAAT6

Eflornithine is a chiral amino acid with L- and D- enantiomers. In the field, eflornithine is administered as a racemate and we know that both the L- and D-enantiomers are able to interact with trypanosome ornithine decarboxylase (Margaret Phillips, personal communication). The L-enantiomer does, however exhibit 20 fold more potency on the human ODC (Qu *et al.,* 2003). We do not know, however, whether both enantiomers of eflornithine are able to enter the trypanosomes and knowing whether this is the case or not could have implications for drug formulations in the field.

To determine the stereospecificity of TbAAT6, alamar blue assays were used to establish the IC_{50} values of each enantiomer of eflornithine (Fig 3-11).

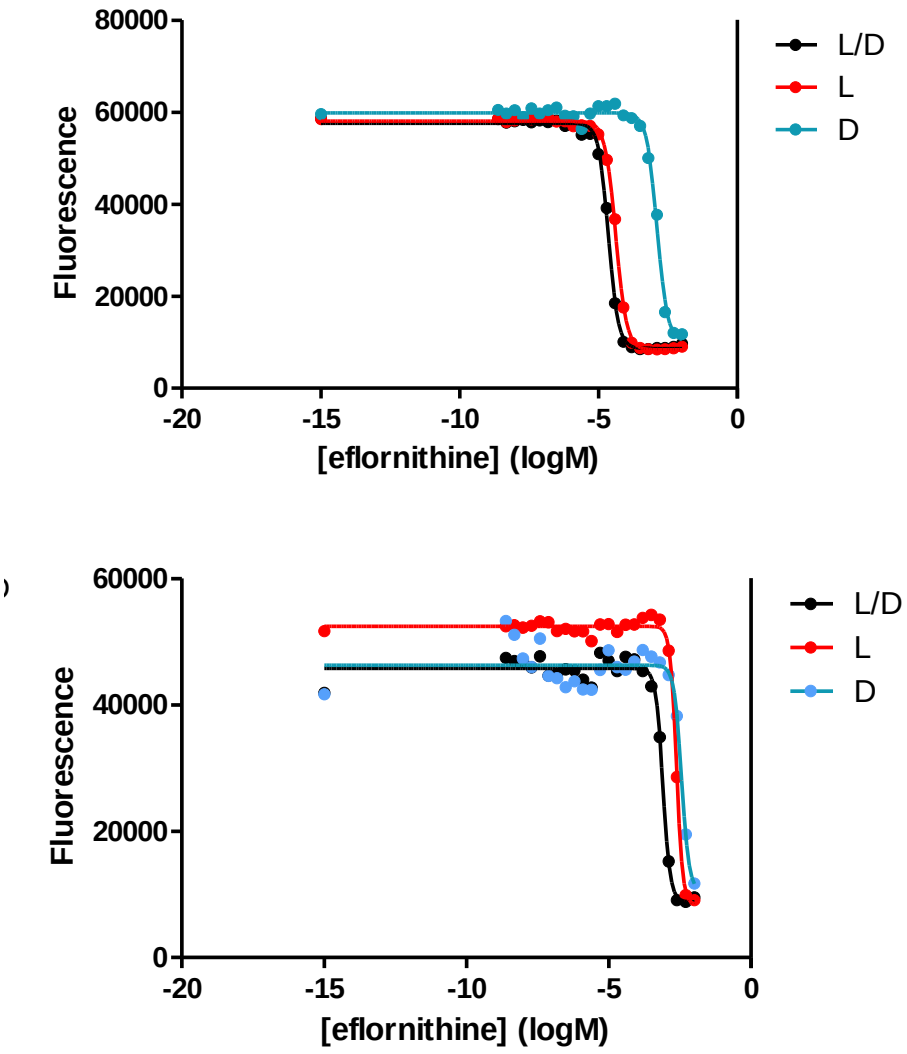

Figure 3-11. Alamar blue assays on different enantiomers of eflornithine. The IC_{50} values for wildtype cells (top graph) were; L-eflornithine (42 µM), D-eflornithine (1277 µM), D/L-eflornithine (23 µM). The IC_{50} values for resistant cells (bottom graph) were; L-eflornithine (2400 µM), D-eflornithine (3600 µM), D/L-eflornithine (800 µM). Points from an average of two experiments is shown with line of best fit.

The L-enantiomer of eflornithine has a similar IC_{50} value to the L/D mixture used as the final drug in wildtype cells. The D-enantiomer has an IC_{50} value more similar to the resistant cell lines where uptake of the drug is not observed. As both isoforms are able to bind to ornithine decarboxylase, this suggests that D-eflornithine is not internalised by TbAAT6. The L-enantiomer of eflornithine was not more efficacious than the D/L racemate of eflornithine. It is not known what the ratio of L to D eflornithine is in the racemate. It is possible that there is a high ratio of L-eflornithine already within the racemic eflornithine.

3.3 Discussion

Note; parts of the work in this chapter have now been published (Vincent *et al.*, 2010) (Appendix 8-3).

3.3.1 Selection of resistance

In the absence of useful eflornithine refractory field isolates of trypanosomes, resistance was selected by increasing concentrations of drug. Resistance was fast to select for and the resistance gene, TbAAT6 appeared to be lost at a selection pressure of 200 μM eflornithine, after 40 days of selection.

There was no cross-resistance with other known trypanocides, not unexpected now we know that the resistance is due to loss of an eflornithine transporter. The structures of the other trypanocides are very dissimilar to eflornithine and are therefore unlikely to share a transport mechanism.

There was an increased sensitivity to pentamidine upon selection of eflornithine resistance. This is unlikely to be related to a transport mechanism for pentamidine as pentamidine uptake is well characterised and a role for TbAAT6 in uptake is highly unlikely. It is therefore likely that there are other changes in the resistant cells apart from the loss of the transporter and the surrounding genes. This theory is supported by the slight increase in resistance seen when cells are grown in 64 μM eflornithine (Fig 3-1).

The metabolomes of the resistant and wildtype cells were compared and the only difference was in ornithine levels, with around 40 % less in the resistant cells. Not all metabolites within the cells are detectable, however, in the metabolomic methods used, so changes may still occur in levels of metabolites that weren't detected. Other changes that could have occurred include greater expression of ornithine decarboxylase or another enzyme or post-translational modifications that alter the function of ODC or of other proteins.

3.3.2 Uptake of eflornithine

Selection of eflornithine resistance results in reduced eflornithine uptake into the trypanosome. The loss of TbAAT6 either by gene deletion as observed in the selected drug resistance lines, or by RNAi is sufficient to render trypanosomes over 40 fold less sensitive to eflornithine than wildtype cells. Furthermore, ectopic expression of *TbAAT6* in trypanosomes that have deleted the gene is sufficient to restore wildtype levels of eflornithine sensitivity confirming that loss of *TbAAT6* alone is necessary and sufficient to generate resistance.

The fact that TbAAT6 was lost so easily is very interesting. In Leishmania, genes can be amplified easily by the creation of a circular amplicon. These are created by homologous recombination at tandem repeats around the area of interest (Grondin *et al.*, 1996;Leprohon *et al.*, 2009). It is not known, however, if trypanosomes are able to amplify genes in the same way or if genes can be deleted by homologous recombination in this way. It is notable, however, that the amplification of circular replicons is frequently seen in Leishmania, but not *T. brucei* selected for drug resistance. As there is a high degree of repetition around TbAAT6, it is possible that this will aid recombination to remove the transporter, but this is yet to be proven as a mechanism of gene deletion. It is interesting that the entire TbAAT6 gene has been deleted, whereas smaller mutations may also result in loss of function. Both point mutations and whole genes losses have been seen in TbAT1 (Stewart *et al.*, 2010).

It has been shown that there is redundancy in the trypanosome amino acid transporter repertoire. This redundancy allows amino acid transporters to be lost without affecting the nutrients available to the cell and loss of transporters is not uncommon (e.g. (Lanteri *et al.*, 2006)). It is still unclear, however, why the trypanosome would delete TbAAT6 at the genomic level rather than reduce its expression. It may be a function of the transcription of trypanosome mRNA being polycistronic, meaning that regulation at the transcriptional level is not possible. However the transporter regulation occurs, its plasticity allows quick adaptation to different environments.

We have, as yet, been unable to assign a physiological function to TbAAT6 in African trypanosomes. Ornithine transport, which would be expected to share a

route of entry with its difluormethylated derivative, was not reduced significantly in the eflornithine resistant line. Ornithine was not able to inhibit uptake of eflornithine, providing further evidence that the two amino acids do not share a mechanism of uptake.

TbAAT6 is one of a large family of related genes described in the kinetoplastida belong to the amino acid transporter 1 superfamily. Only a few other members of the family have been functionally characterised. These include an arginine transporter in *Leishmania donovani* (Shaked-Mishan *et al.,* 2006), an arginine transporter in *T. cruzi* (Canepa *et al.*, 2004) and polyamine transporters in *L. major* (Hasne and Ullman, 2005) and *T. cruzi* (Hasne *et al.*, 2010). The TbAAT6 gene is not syntenic with genes in *Leishmania spp.* or *T. cruzi*. Furthermore, the evolution of the AAT family (Jackson, 2007) makes it impossible, currently, to define specific functionality to any of these transporters, based on homology alone.

We also provide evidence that L, but not D-eflornithine enters the trypanosome via TbAAT6. As both enantiomers are known to inhibit ODC in humans (Qu *et al.*, 2003) and trypanosomes (Margaret Phillips, personal communication) and eflornithine is not thought to need any processing or activation then the higher IC_{50} value for D-eflornithine compared to L-eflornithine suggests that D-eflornithine cannot be taken into the cell through TbAAT6. It is possible to separate the enantiomers of eflornithine (Jansson-Lofmark *et al.*, 2010), but the process of separation is very costly and inefficient. If the costs and efficiency can be optimised, however, then the cost at the field level would be very significantly reduced. The transportation, saline and administration costs would be significantly depreciated, which may make research into enantiomer separation a very worthwhile research avenue to pursue. However, in our *in vitro* assay racemic eflornithine is as effective as L-eflornithine, suggesting that the ratio of D to L is already low.

3.3.3 Implications for the field

Since eflornithine has only recently been implemented as first line treatment for stage two HAT, formal published reports of clinical resistance have not yet appeared, although unpublished data (Enock Matovu (Makerere University),

personal communication) points to a substantial increase in eflornithine treatment failures in Northern Uganda. Nifurtimox resistance has been selected *in vitro* and has been shown to be cross resistant with another emerging trypanocide, fexinidazole, currently in clinical trials (Torrelle *et al.,* 2010). Given nifurtimox's lack of efficiency (Janssens and De Muynck, 1977), eflornithine resistance alone is likely to lead to large numbers of treatment failures from the combination. If the loss of *TbAAT6* is involved in resistance in the field, then it will be possible to implement a simple PCR-based test for resistance, allowing for more suitable treatments to be administered. Tests conducted so far with blood samples on FTA® cards were not successful. It is thought that this is due to very low levels of parasitaemia on the cards, so efficient methods of extracting DNA from the field samples will be required. Methods of concentrating trypanosomes in blood are continually improving to aid in HAT diagnosis (Buscher *et al.*, 2009) and can also be used to detect resistance phenotypes by PCR. Fluorescence-based tests are unlikely to be developed for use in the same way as for melarsoprol resistance (Stewart *et al.,* 2005), as an amino acid transporter would be unlikely to import a large, charged fluorophore. It will be interesting to see if, now that the data on TbAAT6 is published, scientists in the field will start to report finding resistant parasites missing TbAAT6.

Given the ease with which trypanosomes become resistant, it is perhaps surprising that resistance has not been seen in the field more often. It is of course possible that the loss of TbAAT6 would be detrimental to the survival of the parasites within the insect vector and therefore the mechanism of resistance would not be transmissible through the parasite's life cycle. Preliminary results with RNAi in procyclic forms do not show a growth defect or resistance to eflornithine, but without confirmation of knockdown by northern blot or reverse transcriptase real time PCR, conclusions on the function of TbAAT6 in procyclic cells cannot be drawn. David Horn's group developed a high throughput RNAi screen for trypanosomes and indicated that TbAAT6 is essential in procyclic form trypanosomes, but not bloodstream forms (Alsford *et al.*, 2011). However, more targeted analyses of TbAAT6 counteract this data with evidence that TbAAT6 is not essential in procyclic forms (David Horn, personal communication).

Resistance to nifurtimox has been selected *in vitro* and cell lines were found to be cross resistant with other nitro-drugs including fexinidazole, a clinical trial candidate retaining their virulence and resistance in mice (Sokolova *et al.*, 2010). This highlights the need for combination therapies, and in particular, the need to provide combination therapies with drugs that work on different pathways. This also therefore highlights the need to understand the modes of action of all the drugs in use against HAT in order to design these combination therapies. Care must be taken, however, as resistance to one of the drugs within a combination therapy could mean that sub-lethal doses of monotherapy are inadvertently administered leading to the likely selection of multidrug resistant strains. Tests for the presence of resistant strains are therefore of paramount importance.

The evidence presented in this chapter conclusively demonstrates that TbAAT6, an L-eflornithine transporter from the amino acid permease family, is lost in *in vitro* derived, eflornithine resistant, cell lines. This has since been independently corroborated in two high-throughput RNAi screens (Baker *et al.*, 2011;Burkard *et al.*, 2010).

4. Determining Drug mode of action by metabolomics

4.1 Introduction

It is very rare for a new chemotherapeutic agent to be licensed without prior knowledge of its mode of action (MOA). In 2009, 19 drugs were approved by the FDA's centre for drug evaluation and Research in the US, only one of which had a wholly unknown MOA (Hughes, 2010). A knowledge of the MOA reduces the risk of toxicity and allows synergism and resistance to be predicted. Currently, the MOA of a drug is predicted using expensive and time-consuming enzyme-based assays.

Mode of action studies using metabolomic techniques are only just starting to be used (Aranibar *et al.*, 2001; Allen et al., 2004;Bando et al., 2010;Sun et al., 2011 and often involve clustering metabolic profiles from compounds with known MOAs without analysing the individual metabolites involved. This means that drugs with novel MOAs would not be detected, so new, unique compounds need another method for determining their MOA.

There have been a limited number of studies that look at the individual metabolites within an organism and the changes that are induced in these metabolites in response to drugs. One such study used a systems biology approach to combine proteomic, transcriptomic and metabolomic data in the analysis of methamphetamine-induced perturbations to *Drosophila* homeostasis (Sun *et al.*, 2011). Using GC-MS they observed decreased trehalose, a major blood sugar and antioxidant in insects, and using transcriptomics they also saw decreased aconitase (a regulator of antioxidant production and cell death) and alcohol dehydrogenase expression, which they attributed to increased oxidative stress caused by the drug (Sun *et al.*, 2011). Unfortunately, the metabolomics branch of this study focussed on sugars, so levels of glutathione and other metabolites known to be important in oxidative stress were not analysed.

Another study looked at the toxicity of hydrazine, a metabolite of many drugs including the antihypertensive agent, hydralyzine (Bando *et al.*, 2010). GC-MS was used to analyse the plasma and urine of rats treated with hydrazine, followed by principle components analysis (PCA) of the spectra. The loadings plots of the PCAs revealed the masses that were responsible for causing the highest degrees of separation between treated and untreated groups. Gas chromatography provides a highly reproducible separation, allowing masses to be matched to library entries for mass spectra of standards, providing an identification of the metabolites altered during hydrazine toxicity. The group recorded an increase in cysteine, glutamate, glycine (all glutathione precursors), ascorbate and oxoproline, due to the increase in oxidative stress as well as changes to the urea and tricarboxylic acid cycles (Bando *et al.*, 2010).

New lead compounds against HAT are rare and not seen as financially beneficial for most drugs companies. Knowing the MOA and potential side effects of a compound could bring down the cost of research by predicting side effects and toxicity before drugs reach clinical trials. If the cost of research can be brought down, then it is possible that the pharmaceutical industry will be persuaded to invest more in compound validation for this, and other deadly diseases. As trypanosomes are considered model organisms and have a relatively simple metabolome they could also be very useful for more general metabolomic MOA studies. This is especially true as trypanosome populations can be clonally expanded and can be grown to relatively large quantities.

There are five drugs in use against HAT (see section 1.5.3 of this thesis). Of these five, only eflornithine has a known MOA (Fig 4-1). Eflornithine inhibits ornithine decarboxylase only (Poulin *et al.*, 1992;Grishin *et al.*, 1999), making it ideal for use as a proof of principle for MOA action studies using metabolomics. In addition to the four licensed drugs, nifurtimox has been recommended by the World Health Organisation for use against late-stage disease in combination with eflornithine (Priotto *et al.*, 2009). The MOA for nifurtimox has, however, yet to be fully elucidated.

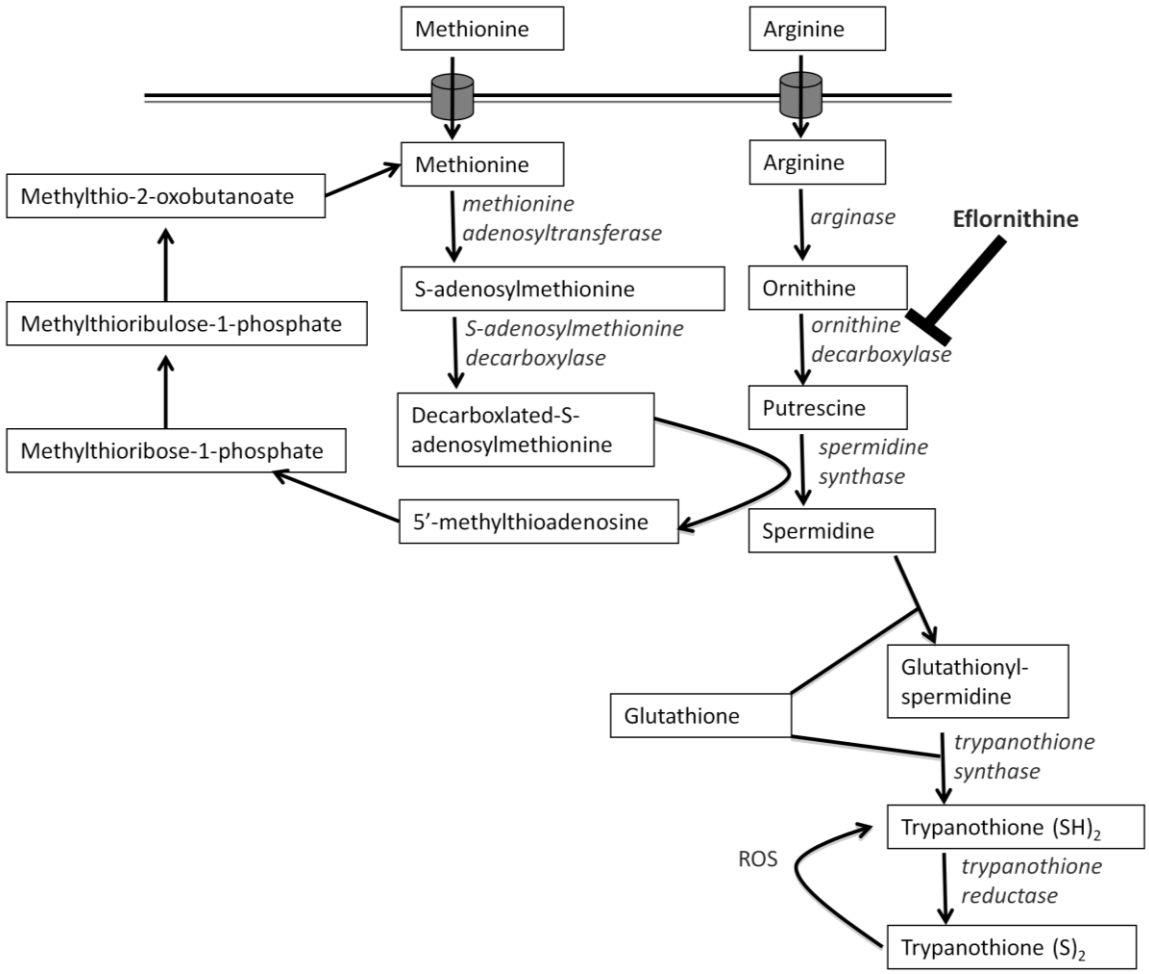

Figure 4-1. Eflornithine is an inhibitor of ornithine decarboxylase in the polyamine pathway. Enzymes are shown in italics, metabolites in boxes. The cell membrane is depicted by a double line and transporters as cylinders. The probable absence of arginase is discussed in chapter 5 of this thesis, although included here, representative of the classical pathway.

ODC inhibition (Fig 4-1) by eflornithine has been studied *in vivo* and was shown to lead to an increase in levels of ornithine, S-adenosyl methionine and decarboxylated S-adenosyl methionine, and a decrease in putrescine, spermidine and trypanothione after 48 hours (Bacchi et al., 1983; Fairlamb et al., 1987). *In vitro* studies by Margaret Phillips's lab in Texas used HPLC after the addition of eflornithine to bloodstream form cells to measure polyamine levels. The group reported a complete depletion of putrescine and decreases in spermidine, glutathionyl-spermidine, glutathione and trypanothione levels after three days, in agreement with the *in vivo* studies (Xiao *et al.*, 2009). The depletion in glutathione levels suggests that there is a feedback mechanism that controls the levels of glutathione when the polyamine levels are depleted as glutathione is not produced from ornithine. Decarboxylated S-adenosyl methionine levels

increased around 40 % after treatment with eflornithine as the previous studies showed, but S-adenosyl methionine levels were unchanged (Xiao *et al.,* 2009).

These targeted studies all focussed on metabolite levels in the polyamine pathway and therefore it would be interesting to conduct an untargeted assay on the alterations to the whole trypanosome metabolome on eflornithine addition.

The Bacchi study administered eflornithine in drinking water (after dehydration for 12 hours) with rats consuming an average of at 1.7 g/kg/12 hours and recorded serum levels of 10-70 μM (Bacchi *et al.,* 1983). The Fairlamb group also administered eflornithine in drinking water (after 12 hours of dehydration) and recorded an average of 560 μM after 12 hours, 400 μM after 36 hours and 1,340 μM eflornithine in rat blood plasma after 48 hours (Fairlamb *et al.,* 1987). The amount of eflornithine water consumed by the rats was not reported in the Fairlamb study so if higher levels were used then this would account for the difference in serum levels. Levels within the trypanosome did not appear to be higher than those in plasma (Fairlamb *et al.,* 1987). The *in vitro* study (Xiao *et al.,* 2009) administered eflornithine in medium at 12.5 μM (half the calculated IC_{50}).

It has been proposed in *T. cruzi* that nifurtimox induces oxidative stress (Maya *et al.*, 1997) and this may be a reason why the nifurtimox-eflornithine combination is thought to be synergistic. Recently, however, Boiani *et al.* (2010) have presented evidence against the oxidative stress theory in *T. cruzi*. The team used Ellman's method (Ellman (1959)) to measure the thiol content of the cells after nifurtimox treatment and found that thiols (all sulfhydryl groups) decrease significantly, but reactive oxygen species are not produced and redox cycling is not upregulated except at very high doses (Boiani *et al.,* 2010). The Wilkinson lab subsequently showed that nifurtimox is metabolised to an open chain metabolite firstly through reduction by a type 1 (oxygen insensitive) nitroreductase before dehydration of the furyl hydroxylamine and furan ring opening (Hall *et al.,* 2011). The group were only able to detect nifurtimox and the unsaturated open chain nitrile in their HPLC assay, suggesting that the intermediate, necessary steps are rapid. The open chain nitrile was saturated slowly at more than 24 hours. The open chain nitrile is likely to exert its effects

by binding to macromolecules rather than causing oxidative stress (Hall *et al.*, 2011).

In this study we aimed to go beyond clustering techniques and look at how the metabolism of the trypanosome is altered in real time in response to drugs. An untargeted approach was taken, allowing an unbiased analysis of perturbations. Cell lysates were separated on a ZIC-HILIC column coupled to an Orbitrap mass spectrometer and MS data was deconvoluted using mzMatch (Scheltema *et al.*, 2011) and IDEOM (Darren Creek, University of Glasgow) softwares for automated processing. Metabolites of interest were selected on the basis of altered abundance and were verified and compared using Thermo Xcalibur software.

4.2 Results

4.2.1 Eflornithine MOA

4.2.1.1 Experimental design

It has been reported that eflornithine is a cytostatic drug and a healthy immune system is required for cell clearance (Bitonti *et al.,* 1986). Rats treated with dexamethasone, an antibody production inhibitor, at the same time as eflornithine were less able to clear trypanosome infections than controls not treated with dexamethasone (Bitonti *et al.,* 1986). Nude (athymic) mice are cured of trypanosomes, but eventually succumb to relapse (Bitonti *et al.,* 1986). The MOA *in vitro* may therefore differ from the MOA *in vivo*. The IC_{50} is likely to be higher as the cells will not die at the concentrations required to turn them into stumpy forms and may still metabolise the resazurin dye used in the alamar blue assay. The *T. b. brucei* 427 bloodstream form line used in these assays is monomorphic, however, and is therefore unable to transform into stumpy forms of the parasite.

Eflornithine levels in blood reach 49.2 μM in children and 87.5 μM in adults (68.9 μM in CSF) (Milord *et al.,* 1993) during the standard treatment regime of 14 days, which is higher, although not much higher, than the IC_{50} *in vitro* of 35 μM (Fig 4-2). This is in line with the Bacchi level recorded in mice of between 10 and 70 μM, but not with the Fairlamb levels of 560 μM (Bacchi *et al.,* 1983; Fairlamb *et al.,* 1987).

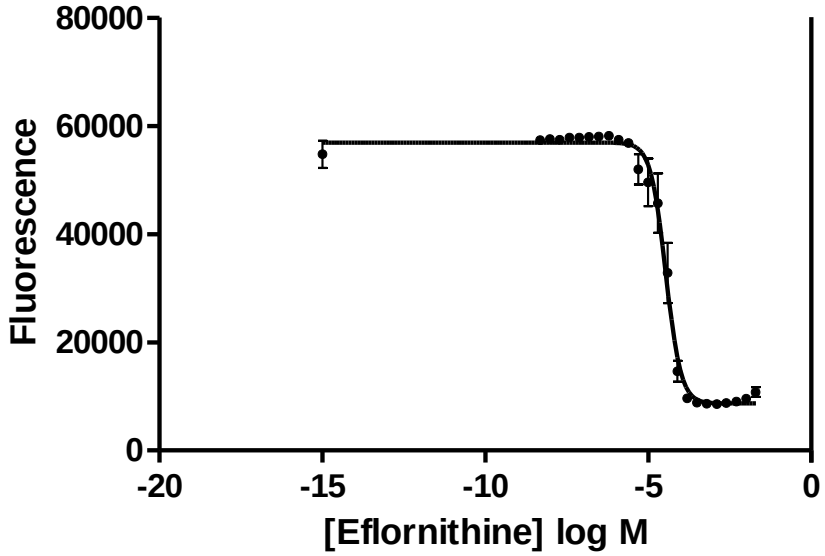

Figure 4-2. The IC_{50} value of eflornithine *in vitro* is 35 μM. An average of five experiments is shown. Error bars depict standard error of the mean.

Upon inspection of the cells in the alamar blue assay, it was found that the cells were still alive in many of the wells where the resazurin dye was not metabolised, although were dead at higher doses of the drug. Eflornithine was therefore acting cytostatically at 35 μM, and prevented the metabolism of the dye, but did not kill the cells at the IC_{50} dose.

Although the Fairlamb study found that eflornithine was not concentrated within the trypanosome (Fairlamb *et al.*, 1987), data from the previous chapter of this thesis clearly shows that eflornithine is transported into the trypanosome (Fig 3-5).

To determine the levels at which eflornithine is cytostatic and cytotoxic, time course assays were conducted with drug at various concentrations (Fig 4-3). Eflornithine was found to be cytostatic (cells remained at the same density before dying) even at 500 μM until around 55 hours in drug. There was no sign of stumpy formation, but as the 427 strain is monomorphic, this would not be expected.

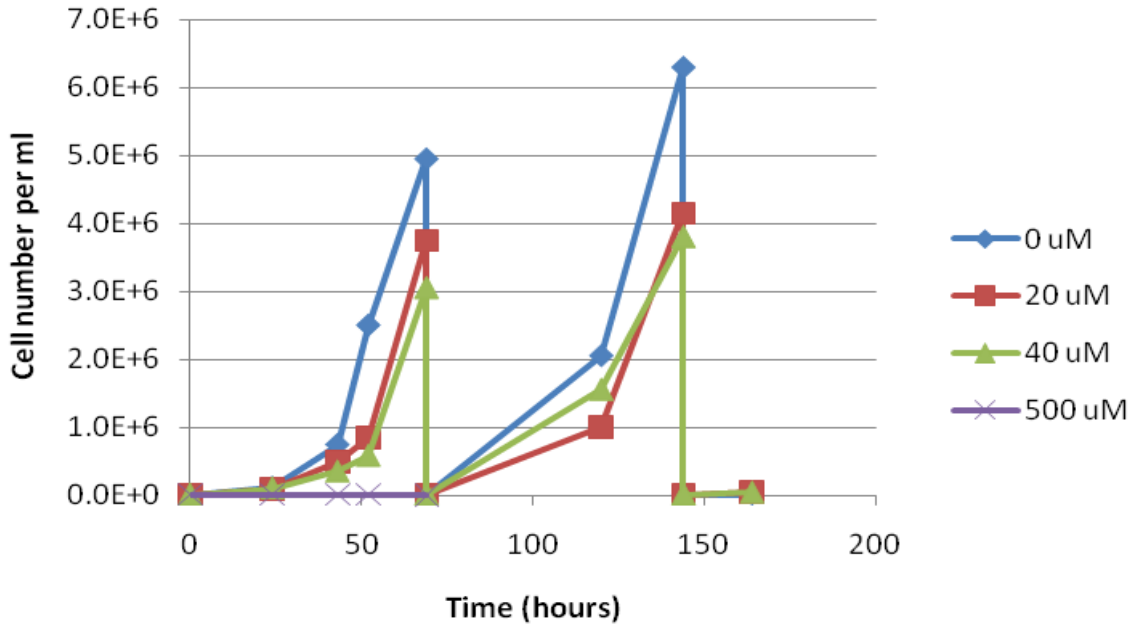

Figure 4-3. Eflornithine time course. A time course was conducted with various concentrations of eflornithine. Cells in 500 µM eflornithine do not die, until between 52 and 69 hours, but do not increase in number.

It was decided to conduct two experiments to determine eflornithine's MOA. In order to be able to detect the molecular target of the drug, levels below the IC_{50} (20 µM) were used so that the metabolites changing in direct response to the target inhibition could be assayed without the risk of masking with general toxicity-related effects. To detect how the cell died from the drug, higher levels of drug were also used at 500 µM (14 times the IC_{50} value).

Drug was added to the 427 bloodstream form wildtype cell line in growth medium so that cells were metabolising as normal apart from the perturbation by the drug.

For the sub-IC_{50} experiments early time points (0 and one hour) were taken to determine the target of eflornithine. Later time points were also taken (24, 48 and 72 hours) to determine later effects of the inhibition and to detect any off-target effects.

For the measurements of metabolites in dying cells more early time points were taken (at 0, 0.5, 1, 2 and 5 hours) to determine how quickly this higher dose of drug disseminates its effects through the metabolome. Later time points (24 and

48 hours) were taken as the cells were dying. Cells generally died at approximately 55 hours at this drug dose of 500 μM.

Cells were quenched in chloroform:methanol:water (1:3:1), run on the Orbitrap mass spectrometer and changes in metabolite abundance were analysed using our in-house software, mzMatch (Scheltema *et al.,* 2011) and IDEOM (Creek *et al*. in preparation for publication) (see method 2.2 of this thesis). Where there was more than one possible isomer for a metabolite mass the most likely metabolite (predicted from retention time on the column) is displayed.

4.2.1.2 Sub IC_{50} metabolome

The stringent filtering systems in the mzMatch and IDEOM software reduced the number of peaks in the spectra from several hundred thousand to 127 robust masses. The flexible parameters in IDEOM were standardised. A relative standard deviation allowance of one and an intensity filter of 10, 000 were chosen as filters to remove less robust peaks. The minimum number of detections across the replicates was set at two out of three replicates.

The majority of metabolite levels were unaltered over the time points taken indicating a high state of robustness within the trypanosome metabolome. Only ornithine (M+H: 133.0971, RT: 27.9 minutes) from the polyamine pathway metabolites (Table 4-1) was found to be highly increased over the time course (Fig 4-4). Putrescine (M+H: 89.1073, RT: 36.91 minutes) was the only metabolite to significantly decrease over time. Acetylated versions of ornithine and putrescine were also identified and these correlated highly with their non-acetylated counterparts. N-acetyl ornithine (M+H: 175.1077, RT: 15.3 minutes) showed the most striking correlation as shown in figure 4-4. Acetyl-putrescine (M+H: 131.1178, RT: 15.5 minutes) was seen in early samples (detected from more targeted analyses), but levels rapidly (after the 0 hour time point) fell below the level of detection (1, 000) from an average intensity of 41, 000 (peak height) before drug addition, correlating with the decrease in putrescine.

M/Z	Retention Time	Formula	Isomers	Name	Ratio compared to 0 hour time point			
					1	24	48	72
297.0898	9.5	$C_{11}H_{15}N_5O_3S$	2	Methylthio - adenosine	1.64	1.41	1.16	1.46
174.1117	26.9	$C_6H_{14}N_4O_2$	1	Arginine	1.02	0.91	1.02	0.98
130.1106	15.5	$C_6H_{14}N_2O$	2	Acetylputrescine	0	0	0	0
307.0841	14.5	$C_{10}H_{17}N_3O_6S$	3	Glutathione	2.20	2.69	1.48	1.00
132.0899	27.9	$C_5H_{12}N_2O_2$	3	Ornithine	1.97	5.04	6.31	4.89
149.0511	13.1	$C_5H_{11}NO_2S$	4	Methionine	1.01	0.90	1.02	0.99
174.1005	15.3	$C_7H_{14}N_2O_3$	4	Acetylornithine	2.59	6.22	7.53	5.01
88.09997	36.8	$C_4H_{12}N_2$	1	Putrescine	0.81	0.41	0.30	0.23
398.1376	34.1	$C_{15}H_{23}N_6O_5S$	1	S-Adenosyl-L-methionine	1.12	0.87	1.42	1.18
360.6447	29.8	$C_{27}H_{47}N_9O_{10}S_2$	1	Trypanothione disulfide	1.29	1.16	1.24	0.98
187.1686	35.2	$C_9H_{21}N_3O$	2	Acetylspermidine	0.75	0.57	1.20	0.62
182.0868	23.1	$C_6H_{12}F_2N_2O_2$	1	Eflornithine	3824	3928	4691	5563

Table 4-1. The metabolite levels of the polyamine pathway after treatment with eflornithine (peak height). Glutathionylspermidine, dc-S-adenosylmethionine, methylthioribose 1-phosphate, methylthioribulose 1-phosphate and methylthio 2-oxobutanoate could not be detected. The isomers column states how many metabolites the mass could represent predicted from database searches. Spermidine was not identified in this analysis as it eluted from the column very late (42 minutes) and as such the whole peak was not detected. 'M/Z' relates to the detected mass charge ratio (peak height) corrected for positive or negative ionisation.

Yarlett and Bacchi have previously shown that adenosylmethionine and decarboxylated adenosyl methionine levels are greatly increased (48 fold and 390 fold respectively over 36 hours) after eflornithine treatment (Yarlett and Bacchi, 1988). This increases the methylation index nearly 20 fold, causing aberrant methylation of proteins within the trypanosomes. Adenosylmethionine was not increased in our experiment and decarboxylated adenosylmethionine was not detected. The Yarlett experiment treated trypanosomes in rats with 4 % eflornithine in drinking water, but didn't record how much water the rats drank, so it is unknown whether the cells were exposed to a higher drug dose.

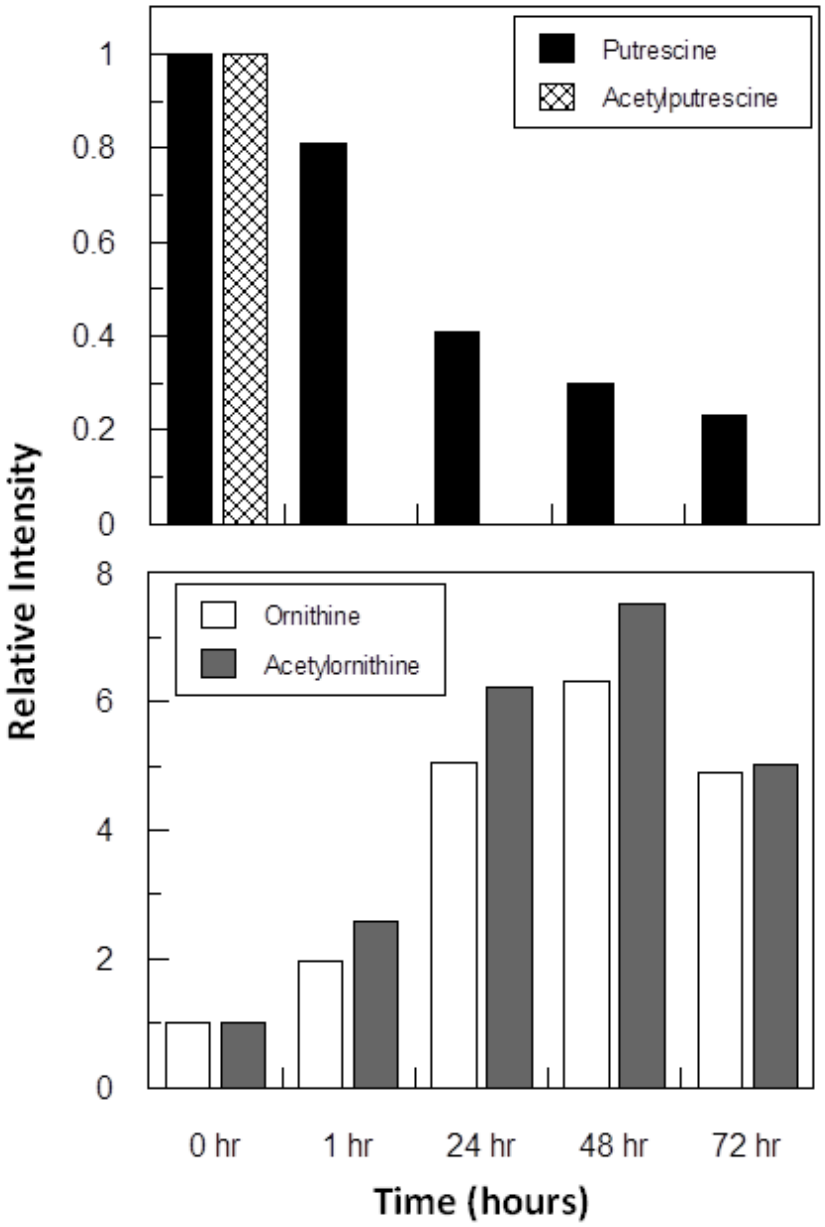

Figure 4-4. Ornithine, N-acetylornithine, putrescine and N-acetylputrescine levels upon the addition of eflornithine to wildtype cells in culture. Intensities (peak heights) are shown relative to the 0 hour time point level on the y-axis. A representative of three separate experiments is shown.

It is interesting to see a recovery in affected metabolite levels at the 72 hour time point (e.g. glutathione, ornithine, acetylornithine and trypanothione disulphide (Table 4-1)). The cells appear to be adapting to the non-lethal dose of drug, perhaps through increased expression of ODC or reduced transport of eflornithine through TbAAT6. Levels of eflornithine stay high at 72 hours (Fig 4-5), but this may be exogenous eflornithine that is carried over when the cells are quenched. The turnover rate of ODC is 18 hours in *T. b. gambiense* (Iten *et al.*, 1997). It therefore seems feasible that *T. b. brucei* are able to upregulate ODC

production within a 72 hour time scale. Ornithine decarboxylase protein regulation is noted for being complicated and levels are controlled at the level of transcription, translation, post translationally and through an inhibitor termed antizyme (Xiao *et al.*, 2009). Antizyme binds to the ODC monomer preventing homodimerisation of the ODC subunits (Pegg, 2006). The inhibitor is produced by a +1 frame shift during ODC translation. The mistranslated enzyme bound to ODC is degraded by the 26 S proteosome, but binds an antizyme inhibitor with a higher affinity. Transcription of the antizyme inhibitor is stimulated during cell growth, freeing antizyme from ODC. Antizyme translation is upregulated by polyamines (Pegg, 2006).

Isomers for each metabolite were identified using the IDEOM database, which incorporates information from KEGG, Lipidmaps, HMDB and Metacyc as well as metabolites manually added by our laboratory. There are three isomers for acetylornithine (Val-Gly, L-prolinylglycine, theanine), two for ornithine (diaminopentanoate and N4-acetyl-N4-hydroxy-1-aminopropane) and none for putrescine. Acetylputrescine had one isomer (aminocaproamide). Validation of the acetylornithine identification was conducted using isotopically labelled ornithine and is discussed further in section 5.3.3.5.

Standards were run for ornithine, putrescine, methylthioadenosine, glutathione, S-adenosyl methionine and trypanothione disulphide to verify the identification of the masses in our assay by retention time. These standards were run for each metabolomics assay conducted and identifications were made when the retention times were within 5 % of the standard.

The increase of ornithine and the decrease of putrescine after treatment of trypanosomes with eflornithine are in line with the published literature and predicted mode of action (Bacchi *et al.*, 1983;Fairlamb *et al.*, 1987;Xiao *et al.*, 2009) . Fairlamb *et al.* and Bacchi *et al.* also noted increases in S-adenosyl methionine, which are not replicated in our assay, and decarboxylated S-adenosyl methionine, which was also not detected in our assay. The decreases in spermidine and trypanothione observed by Fairlamb and Bacchi were also not seen in our data. The Phillips group reported decreases in glutathionyl-spermidine (a metabolite not detectable in our data) and glutathione and an increase in decarboxylated S-adenosyl methionine (in direct opposition to the

Fairlamb and Bacchi results) (Xiao *et al.*, 2009) there may be differences between the *in vitro* and *in vivo* data if there is a carry over of some metabolites from the rat blood or from the medium. HMI-9 used in our experiments and the Phillips experiment contains some blood serum, but at 10 %, carry-over of polyamine metabolites from this would be less than with rat blood. HMI-9 is not expected to contain any of the polyamine pathway metabolites except for the amino acids. The decrease in glutathione observed by Phillips was not seen in our data. Xiao *et al.* used a similar drug concentration (12.5 μM) as our experiment (20 μM) and was in the same *in vitro* medium, so it might have been expected that results would have been similar.

Glutathione would not be expected to be affected by an inhibition of ODC as its synthesis occurs in a different branch of the polyamine pathway (Fig 4-1). It may, however, be regulated via levels of another metabolite such as spermidine, which was decreased in the Phillips assay (Xiao *et al.*, 2009), but not in ours.

The Fairlamb group reported eflornithine serum levels of between 560 and 1,340 μM (Fairlamb *et al.*, 1987), which is much higher than the levels used in our assays so may be expected to exhibit more changes. The Bacchi group reported serum levels of 10 - 70 μM, which is in the same order of magnitude as our experiments. As these assays were both conducted *in vivo* however, any differences between the profiles may be due to the different growth conditions (Fairlamb *et al.*, 1987).

N-acetylornithine has not been seen in trypanosomes before. Differences in the retention times between ornithine (RT = 27.9 minutes) and acetylornithine (RT = 15.3 minutes) suggest that ornithine has not been acetylated in the ionisation process during mass spectrometry as the ionisation occurs after chromatographic separation. Also, we have shown in subsequent experiments that ornithine in CBSS buffer solution or in medium does not spontaneously convert to acetylornithine (see chapter 5, particularly figure 5-13). N-acetylornithine is highly correlated with ornithine implying that it is closely linked in the metabolic network, which indicates a direct metabolic link between the two metabolites. There is a metabolic pathway in some bacteria that is able to

convert glutamate to ornithine via acetylornithine. This is discussed further in chapter 5.

Acetylputrescine also appears to be a biologically relevant metabolite as it too has a significantly different retention time to putrescine. The metabolite has just one isomer, aminocaproamide, not thought to be a naturally occurring metabolite in trypanosomes. Acetylputrescine is used in the conversion of putrescine to aminobutanoate. There is no specific putrescine acetylase, but promiscuous acetyltransferases may be able to acetylate putrescine. There are at least 10 putative acetyltransferases annotated in TritrypDB (Tb427.01.4490, Tb427.05.2280, Tb427.07.2360, Tb427.07.2530, Tb427.08.3310, Tb427tmp.160.2010, Tb427.10.3150, Tb427.10.8310, Tb427.10.12830 and Tb427tmp.01.2886).

Other metabolites that exhibited large fold changes over the 72 hours are shown in figure 4-5.

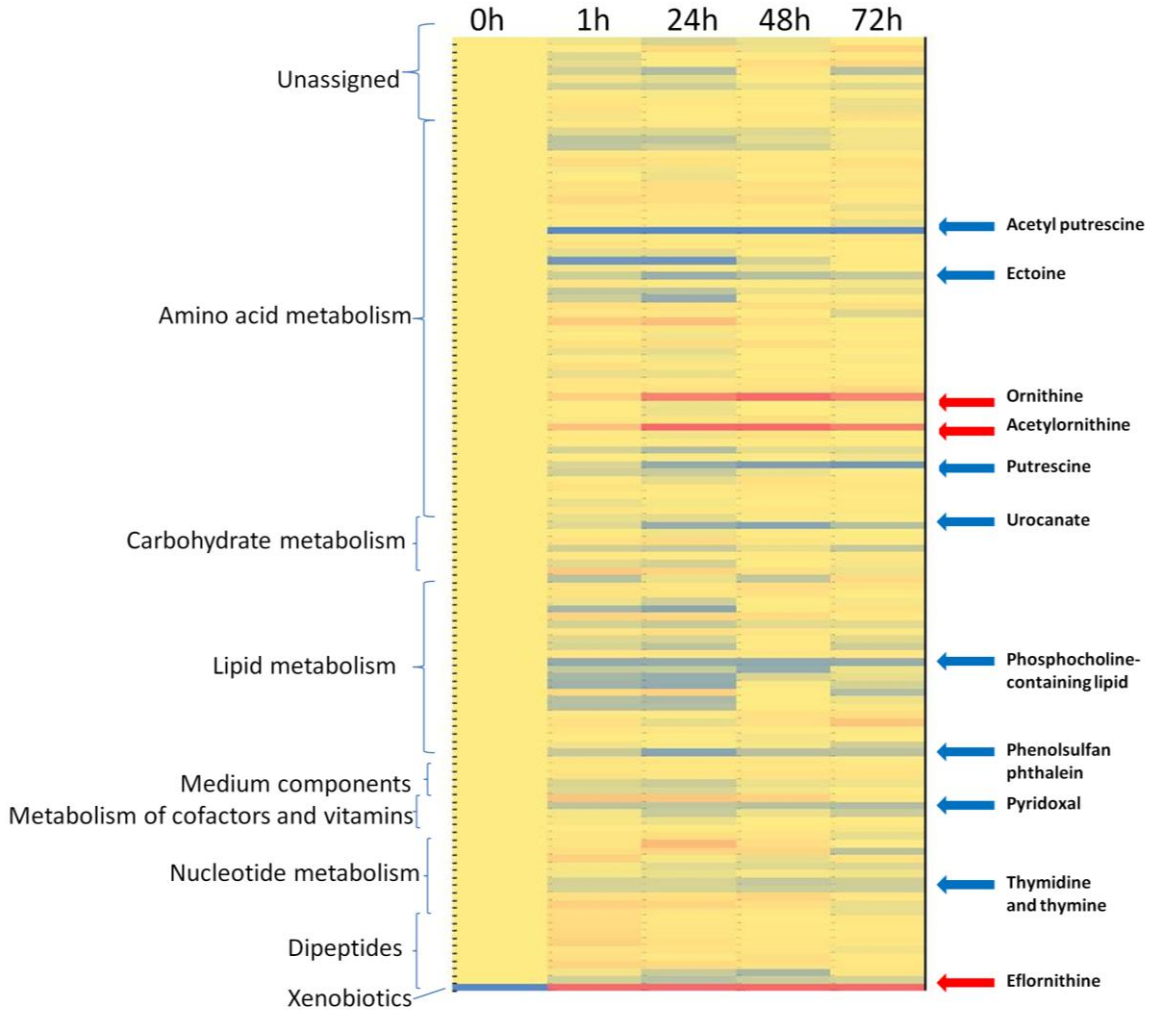

Figure 4-5. Heat map showing that the majority of metabolites are unchanged with the addition of low level eflornithine to wildtype cells. Yellow boxes show levels remaining the same. Red shows an increase and blue shows a decrease. Metabolites are classified down the left hand side. Red arrows highlight metabolites that consistently increase, blue highlights those consistently decreased over the time course.

The metabolites highlighted with blue and red arrows indicate those masses with small, but consistent increases or decreases respectively. Ectoine is a pyrimidine breakdown product and its reduced levels may relate to the reduced levels of thymidine and thymine seen. Why this group of metabolites, normally involved in DNA synthesis, should be reduced, however, is unclear, but it could be that trypanosomes are stopping DNA synthesis as the trypanostatic drug takes effect.

Urocanate (m/z: 139.0502, RT: 10.9 minutes) results from the loss of ammonia from histidine (m/z: 156.0767, RT: 25.0 minutes). As the retention times are not

similar, this loss is not thought to be a mass spectrometry artefact and may result from an enzymatic conversion through histidine-ammonia lyase. Levels of histidine are not significantly altered, but due to the high levels of amino acids in the medium (from 78 μM (tryptophan) to 4 mM (glutamine), histidine is at 271 μM), changes in levels of these metabolites can be masked. Urocanate can be used to create more glutamate or oxoglutarate. All but one of the enzymes for this pathway are present in *T. cruzi* (histidine ammonia lyase (Tc00.1047053506247.220), urocanate hydratase (Tc00.1047053504047.5) and imidazolone propionase (Tc00.1047053509137.30)), but absent in *T. brucei*. An increase in glutamate may be required to keep glutathione levels stable.

The phosphocholine-containing lipid shows reduced levels over the 72 hours (Fig 4-5), as do phenolsulfan phthalein (phenol red – a pH indicator in the medium) and pyridoxal (vitamin B6). These three changes appear to hold no obvious connections either to the polyamine pathway or to one another, so their alterations may be explained by biological variation and perhaps, were the experiment to be repeated, these changes would not persist.

Ornithine decarboxylase requires pyridoxal 5'-phosphate as a cofactor in the conversion of ornithine to putrescine (Jackson *et al.*, 2004). Pyridoxal 5' phosphate can be detected from the standard mix used to calibrate the masses from the Orbitrap mass spectrometer around six minutes after pyridoxal elutes. This standard mixture contains 1 μM pyridoxal 5'-phosphate, but the intensity detected is relatively low, suggesting that it is either not well ionised or not well detected. The pyridoxal seen (m/z: 168.0655, RT: 14.0 minutes) (Fig 4-5) may be due to an increased phosphorylation of pyridoxal to provide more pyridoxal 5'-phosphate for ornithine decarboxylase. It would be interesting to see how levels of pyridoxal kinase (Tb927.6.2740) are affected by incubation with eflornithine or to see if kinase inhibitors are synergistic with eflornithine.

4.2.1.3 The eflornithine toxicity metabolome

At 500 μM eflornithine, bloodstream form trypanosomes stop dividing over 48 hours in drug. This is reflected by many more changes to the metabolome (Appendix 8.4 and on included compact disc).

A targeted analysis of the polyamine pathway metabolites was undertaken using the Xcalibur Quan Browser from Thermo Scientific (Fig 4-6). Putrescine and spermidine decreased over the 48 hours in drug whereas ornithine and acetylornithine were seen to increase. Methythioadenosine increased over the first five hours in drug and then remained relatively level. This was not reported in previous studies. Trypanothione disulphide stayed level over the first five hours before decreasing slightly, but not significantly. The reported decrease in S-adenosylmethionine seen by Bacchi *et al.*, (1983) and Fairlamb *et al.* (1987) and or the increase as seen by Xiao *et al.* (2009) was not observed, with levels staying relatively stable. In the sub IC_{50} experiment only ornithine, putrescine and their acetylated counterparts were altered. Higher doses therefore show a greater cascade effect through the metabolome after ODC inhibition.

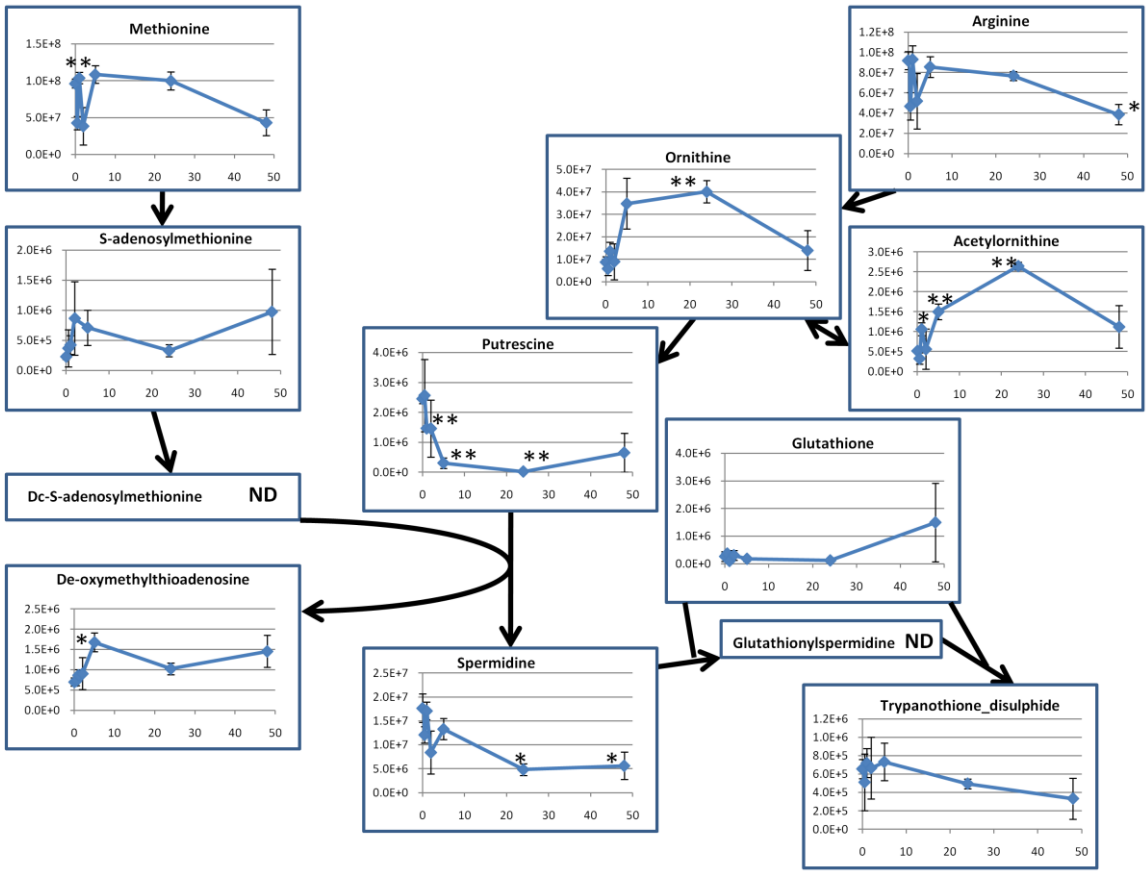

Figure 4-6. Polyamine metabolite changes in 500 µM eflornithine. X-axes indicate the time in hours since drug addition. Y-axes indicate the relative intensity (area under the curve) of each metabolite. ND: not detected. Methionine (M+H: 150.0581, RT: 11.9 minutes), S-adenosylmethionine (M+H: 399.1444, RT: 22.7 minutes), methylthioadenosine (M+H: 298.0968, RT: 7.82 minutes), arginine (M+H: 175.1190, RT: 25.3 minutes), ornithine (M+H: 133.0971, RT: 21.9 minutes), acetylornithine (M+H: 175.1077, RT: 17.12 minutes), putrescine (M+H: 89.1072, RT: 23.9 minutes), spermidine (M+H: 146.1652, RT: 41.8 minutes), glutathione (M+H: 308.0910, RT: 15.3 minutes) and trypanothione disulphide (M+H: 722.2960, RT: 22.7 minutes). * indicates a p-value less than 0.05 in a Student's paired *t*-test to the 0 time point, ** indicates a p-value less than 0.001. N = 3.

It was hypothesised that the first few hours in drug would show eflornithine-specific effects and the last two time points (24 and 48 hours) would show changes related to cell death, unspecific to eflornithine.

Five hundred and seventy masses were putatively identified using the mzMatch and IDEOM softwares. This is much more than the number detected in the sub IC_{50} experiments as the samples were all run at the same time in this experiment, whereas in the previous experiment they were not, producing differences in machine efficiency. Table 4-2 shows all of the metabolites that change significantly over three replicate experiments for the first five hours (from paired *t*-tests comparing 0 and five hours, $p<0.05$).

S-adenosylmethionine decarboxylase is thought to be stimulated by putrescine in humans and *T. cruzi* (Clyne et al., 2002) and weakly stimulated in *T. brucei* (Bitonti *et al.*, 1986) meaning the decrease in putrescine caused by the blockage of ornithine decarboxylase activity would be expected to cause an increase in S-adenosylmethionine and a decrease in decarboxylated-S-adenosylmethionine. As decarboxylated S-adenosylmethionine was not observed and S-adenosylmethionine levels were not significantly altered, conclusions on this theory could not be drawn.

M/Z	RT	Formula	Isomers	Name	Fold Change	p-value
416.2325	7.6	$C_{21}H_{37}O_6P$	1	1-octadecanoyl-sn-glycero-2,3-cyclic phosphate	3.20	0.011
222.0674	21.2	$C_7H_{14}N_2O_4S$	4	Cystathionine	2.75	0.011
297.0896	7.8	$C_{11}H_{15}N_5O_3S$	2	Methylthioadenosine	2.23	0.013
130.1107	13.3	$C_6H_{14}N_2O$	2	Acetylputrescine	0.37	0.017
568.2426	19.7	$C_{23}H_{36}N_8O_7S$	1	Arg-Cys-Gln-Tyr	4.31	0.017
801.5525	7.8	$C_{43}H_{80}NO_{10}P$	1	Phospho glycerol (17:0/20:4)	1.25	0.027
114.0793	13.9	$C_5H_{10}N_2O$	2	proline amide	1.61	0.029
402.0227	19.7	$C_{10}H_{16}N_2O_{11}P_2$	1	dTDP	1.30	0.030
163.0666	8.6	$C_6H_{13}NO_2S$	6	Methylmethionine	1.66	0.030
182.0867	19.7	$C_6H_{12}F_2N_2O_2$	1	Eflornithine	1.98	0.034
101.0476	22.7	$C_4H_7NO_2$	5	Azetidine 2-carboxylic acid	2.11	0.035
133.0739	11.6	$C_5H_{11}NO_3$	4	Hydroxyvaline	2.54	0.036
174.1004	16.2	$C_7H_{14}N_2O_3$	5	Acetylornithine	3.03	0.036
96.0209	15.5	$C_5H_4O_2$	3	Furfural	1.47	0.038
202.1317	8.3	$C_9H_{18}N_2O_3$	3	Leu-Ala	1.40	0.042

Table 4-2. Metabolites changing significantly over the first five hours in 500 μM eflornithine. Peptides are shaded blue and lipids yellow. 'M/Z' relates to the detected mass charge ratio (peak height) corrected for positive or negative ionisation. Fold change relates to the ratio of the five hour sample intensity compared to 0 hour intensity. P-values were calculated using a Student's *t*-test.

The important thiols within the trypanosome are thought to include trypanothione, cysteine, methionine, glutathionylspermidine, methylthioadenosine and ovothiol A (Steenkamp, 2002) (Fig 4-7). The precise role of ovothiol A as an antioxidant is not well understood, but is thought to be absent in bloodstream form trypanosomes (Ariyanayagam and Fairlamb, 2001).

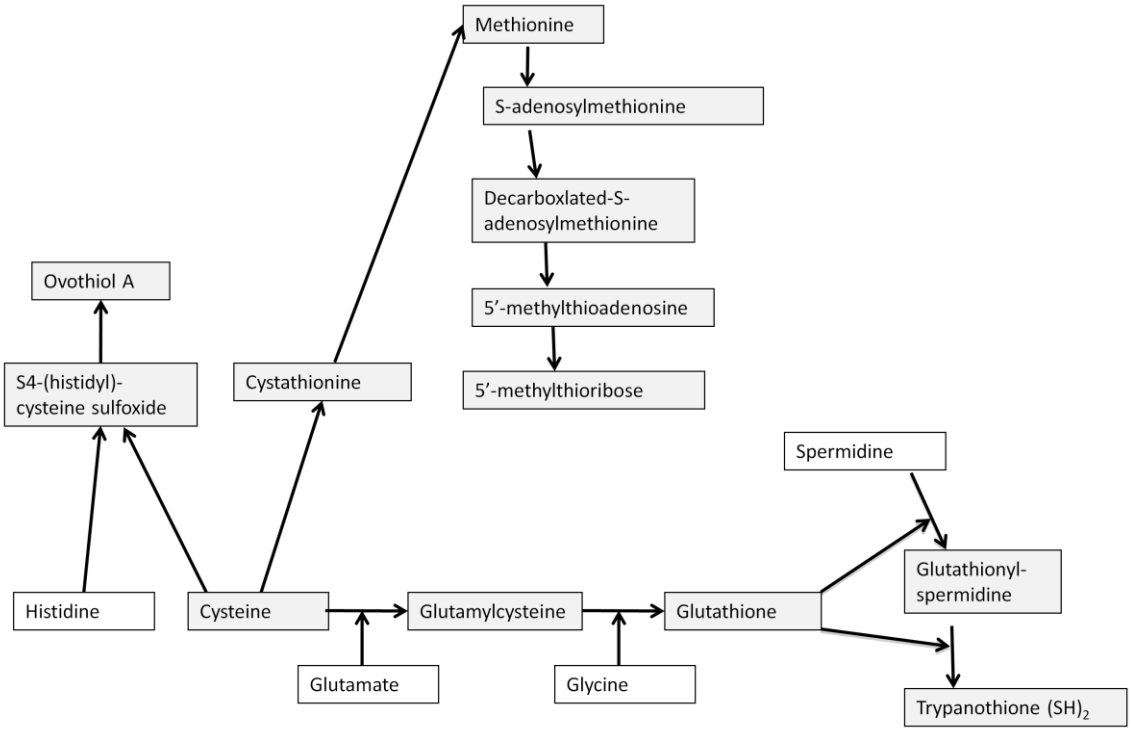

Figure 4-7. Thiols in *T. brucei*. Thiols are in shaded boxes. From KEGG and Vogt *et al.* (2001).

There is a general increase in thiols (cystathionine, methylthioadenosine and methyl-methionine) seen over the first five hours in toxic doses of eflornithine (ovothiol A could not be measured as several peaks with the same mass were seen and the one corresponding to ovothiol A could not be determined). This may be due to an attempt by the cells to combat the oxidative stress caused by a reduction in trypanothione and spermidine levels. Cystathionine is a stereoisomer of a threonine-cysteine dipeptide, but the retention time matches that of the cystathionine standard (0.1 % error) so the identification of cystathionine can be made with a high degree of confidence. Levels of cysteine decrease (although not significantly) over the five hours suggesting that cysteine may combine with ketobutyrate to form cystathionine, which may, in turn, be used to produce homocysteine and methionine. The enzymes in this pathway, cystathione gamma lyase (Tb427tmp.211.3330) and homocysteine S-methyltransferase (Tb927.1.1270), are present in *T. b. brucei*. Methionine levels do not increase, however, this may be due to high levels in the medium (200 μM) masking any changes within the cells. Homocysteine levels fall below the minimum peak intensity so cannot be analysed. S-adenosyl methionine and

methylthioadenosine were increased also, increasing the general thiol pool to counter any increased oxidative stress.

Ornithine, putrescine and spermidine were not picked out in this automatic processing either because the peak picking software (XCMS) missed a peak or because the relative standard deviation was higher than the filter allowed. These metabolites were therefore analysed manually (Fig 4-6).

The increases in hydroxyvaline, proline amide and the peptide levels may be indications of protein break down as cells die.

The lipids, shaded in yellow in table 4-2, both increase with eflornithine addition. Trypanosomes are able to synthesise all major phospholipids (Serricchio and Butikofer, 2011), unlike most other eukaryotes. Trypanosomes do also take up a lot of lipids from the host serum (Voorheis, 1980;Bowes *et al.*, 1993) and it is unclear whether the increase in these lipids is due to enhanced synthesis, uptake or indeed from the breakdown of trypanosome membranes.

Furfural is a sugar fragment and shares a retention time with glucose suggesting it is an ionisation artefact of glucose. Azetidine 2- carboxylic acid is also likely to be a fragment as it has no reported biological role except as a proline analogue in plants. It shares a retention time with adenosylmethionine and also shows the same pattern of perturbation (fold changes for one hour, two hours, five hours, 24 hours and 48 hours of 1.35, 2.11, 1.31 and 3.53 compared to 1.87, 2.99, 1.46 and 5.07 for adenosylmethionine) over the 48 hour assay, indicating that it is a fragment of adenosylmethionine.

Thymidine diphosphate is significantly altered after five hours in eflornithine, but doesn't show a large change in levels (just a 30 % increase). Thymine and thymidine were seen to show an opposite trend in sub IC_{50} levels of eflornithine, but were not seen to be altered at this drug level.

There were many more metabolites changing over the 48 hours. There were 45 significantly changing metabolites (*t*-test on 0 and 48 hour time point, significance taken as $p<0.05$) (Table 4-3).

M/Z	RT	Formula	Isomers	name	Fold change	p-value
324.1055	14.8	$C_{12}H_{20}O_{10}$	4	Fructose 1,2':2,3'-dianhydride	0.36	0.000
130.1107	13.3	$C_6H_{14}N_2O$	2	Acetylputrescine	0.21	0.001
146.0691	17.5	$C_5H_{10}N_2O_3$	6	Glutamine	0.64	0.003
155.0347	19.9	$C_3H_{10}NO_4P$	3	Aminopropan-2-ol O-phosphate	0.31	0.005
482.1712	17.5	$C_{18}H_{26}N_8O_6S$	1	Cys-Ser-His-His	0.32	0.005
309.1687	10.9	$C_{15}H_{23}N_3O_4$	2	Pro-Pro-Pro	0.44	0.006
176.0681	7.5	$C_7H_{12}O_5$	7	Propylmalate	9.67	0.007
147.0529	9.0	$C_5H_9NO_4$	14	hydroxyisopropyloxamate	0.40	0.009
117.0790	15.9	$C_5H_{11}NO_2$	16	Betaine	0.22	0.010
250.0904	15.8	$C_{18}H_{28}N_8O_7S$	1	Asn-Cys-Gln-His	0.17	0.012
129.0902	21.1	$C_5H_{11}N_3O$	3	piperazine-2-carboxamide	0.42	0.012
89.0476	15.6	$C_3H_7NO_2$	9	beta-Alanine	0.53	0.013
157.0349	15.7	$C_{10}H_{20}O_7P_2$	6	[PR] Geranyl pyrophosphte	0.46	0.014
466.1002	15.7	$C_{17}H_{19}N_6O_8P$	1	Adenylanthranilate	0.33	0.014
174.1117	21.1	$C_6H_{14}N_4O_2$	2	Arginine	0.42	0.014
165.0790	10.1	$C_9H_{11}NO_2$	7	Phenylalanine	0.35	0.016
133.0198	14.3	$C_4H_7NO_2S$	1	Thiazolidine-4-carboxylate	0.23	0.016
358.0840	17.5	$C_{14}H_{18}N_2O_7S$	1	Miraxanthin-I	0.62	0.016
100.0160	7.1	$C_4H_4O_3$	1	2-oxobut-3-enanoate	0.65	0.018
347.0630	20.3	$C_{10}H_{14}N_5O_7P$	7	3'-AMP	0.35	0.018
174.1003	11.0	$C_7H_{14}N_2O_3$	5	Ethylglutamine	0.46	0.018
257.1029	20.7	$C_8H_{20}NO_6P$	1	sn-glycero-3-Phosphocholine	0.31	0.022
405.1381	16.1	$C_{15}H_{23}N_3O_{10}$	1	Glu-Glu-Glu	0.35	0.024
147.0354	12.1	$C_5H_9NO_{2S}$	1	Thiomorpholine 3-carboxylate	0.24	0.024
150.0526	15.4	$C_5H_{10}O_5$	37	Xylulose	0.63	0.024
132.0535	17.9	$C_4H_8N_2O_3$	6	Asparagine	0.28	0.025
180.0632	15.5	$C_6H_{12}O_6$	57	Glucose	0.61	0.025
259.0455	23.3	$C_6H_{14}NO_8P$	8	Glucosamine 6-phosphate	0.25	0.026
131.0583	16.5	$C_5H_9NO_3$	14	Glutamate 5-semialdehyde	0.40	0.028
250.0702	8.1	$C_{20}H_{28}N_4O_7S_2$	1	Glu-Phe-Cys-Cys	0.25	0.028
805.5621	7.6	$C_{46}H_{80}NO_8P$	28	Phosphocholine (16:0/22:6)	0.50	0.030
147.0531	15.9	$C_5H_9NO_4$	14	Glutamate	0.40	0.031
260.1371	10.5	$C_{11}H_{20}N_2O_5$	4	Glu-Leu	0.59	0.033
154.0376	12.0	$C_6H_6N_2O_3$	2	Imidazol-5-yl-pyruvate	0.39	0.034
268.9702	16.1	$C_{12}H_{17}BrN_2O_{13}P_2$	1	uridine-5'-diphosphate bromoacetol	0.16	0.035
565.4470	10.0	$C_{30}H_{64}NO_6P$	4	Phosphocholine (10:2/12:2)	2.43	0.037
793.5615	7.7	$C_{45}H_{80}NO_8P$	28	Phosphocholine (15:0/22:5)	0.44	0.037
136.0370	13.6	$C_4H_8O_5$	3	Fatty acid trihydroxy (4:0)	0.32	0.037
244.0693	12.0	$C_9H_{12}N_2O_6$	2	Pseudouridine	0.37	0.037
246.1215	11.9	$C_{10}H_{18}N_2O_5$	6	Glu-Val	0.62	0.039
137.0477	5.9	$C_7H_7NO_2$	13	Anthranilate	2.61	0.039
285.3032	6.1	$C_{18}H_{39}NO$	1	deoxy-sphinganine	2.94	0.041
96.0209	15.5	$C_5H_4O_2$	3	Furfural	0.57	0.043
324.0356	23.2	$C_9H_{13}N_2O_9P$	4	Pseudouridine 5'-phosphate	0.16	0.043
755.5471	7.7	$C_{42}H_{78}NO_8P$	17	Phosphocholine (16:0/18:3)	0.38	0.045

Table 4-3. Metabolites significantly changed after 48 hours in 500 µM eflornithine. Significance was calculated in IDEOM using the Student's paired *t*-test. Peptides are shaded

blue and lipids yellow. 'M/Z' relates to the detected mass charge ratio (peak height) corrected for positive or negative ionisation. Fold change relates to the ratio of the 48 hour sample intensity compared to 0 hour intensity.

The fact that the majority of metabolites decrease at the 48 hour time point suggests that the cell membrane has been compromised. The cells were observed under the light microscope and appeared more convoluted than healthy cells, but were clearly still alive and moving. Bacchi *et al*. reported double nuclei and two undulating membranes in eflornithine treated cells (Bacchi *et al.*, 1983). The cells were fixed and Giemsa stained (Fig 4-8), but no differences in the cell architecture were obvious. The processing of the cells involves cooling them to 0 ºC in a dry ice–ethanol bath and two centrifugation steps (See methods section 2.2.1 of this thesis). These weakened cells are therefore potentially more leaky than cells that have not been compromised for so long in the drug. This is evident in the large amount of blue colouration at 48 hours in the heat map (Fig 4-9), relating to a decrease in the majority of metabolites.

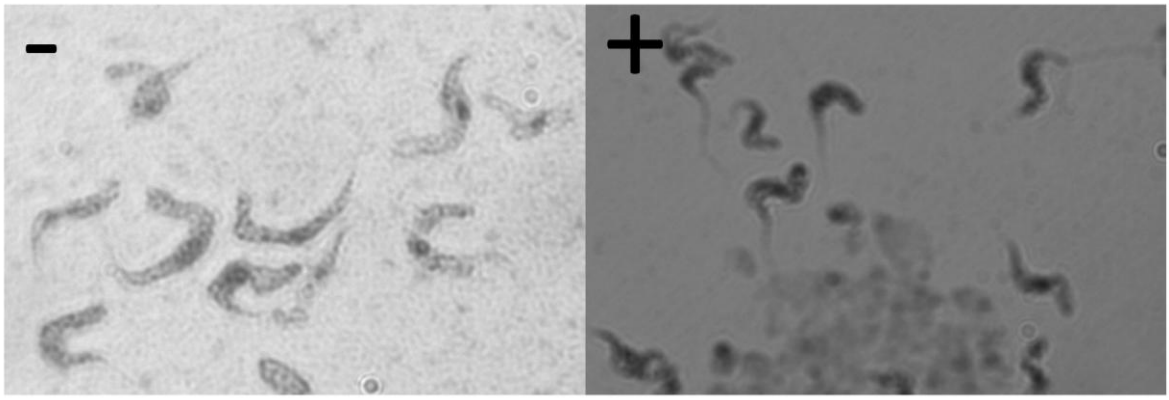

Figure 4-8. Cells at 48 hours with (+) and without (-) 500 μM eflornithine treatment. 100 x magnification under oil immersion.

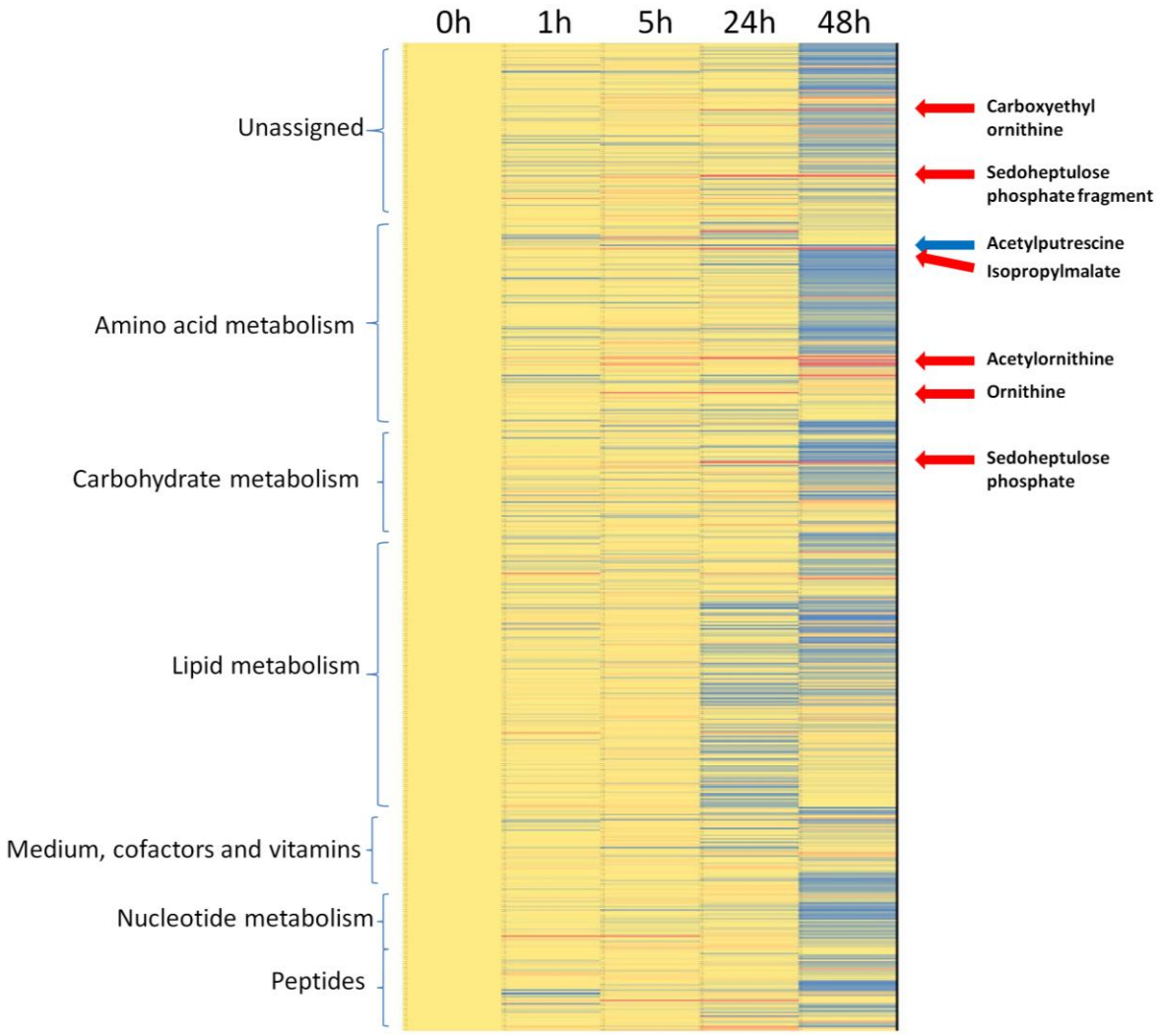

Figure 4-9. Heat map of cells in 500 μM eflornithine. Blue represents a decrease in metabolite intensity, red an increase and yellow represents unchanged levels. Metabolites are classified down the left hand side. Red arrows highlight metabolites that consistently increase, blue highlights those consistently decreased over the time course.

There are only two metabolites that significantly increase at the 48 hour time point. Propylmalate (the only isomers in our database, methylhydroxyglutarate and validone, have RT errors of 7.6 % and 47.7 % respectively, compared to 1.4 % for propylmalate) (Fig 4-10). Increases steadily over the 48 hours in eflornithine and anthranilate stays relatively stable and then increases at the 48 hour time point (Fig 4-11). An unsaturated phosphocholine and deoxy-sphinganine also increase, whereas saturated phosphocholines decrease. The unsaturation of lipids means that hydrogen atoms are being lost from the carbon chains. This may be due to attack by reactive oxygen species, which would remove a hydrogen atom from the chain. The increase in deoxysphinganine may be a reflection of the degradation of sphingophospholipds, key structural components

of the membrane (Serricchio and Butikofer, 2011). Free lipids generally decrease after 24 hours. This may indicate that the trypanosomes are using these free lipids in an attempt to maintain their cell membranes.

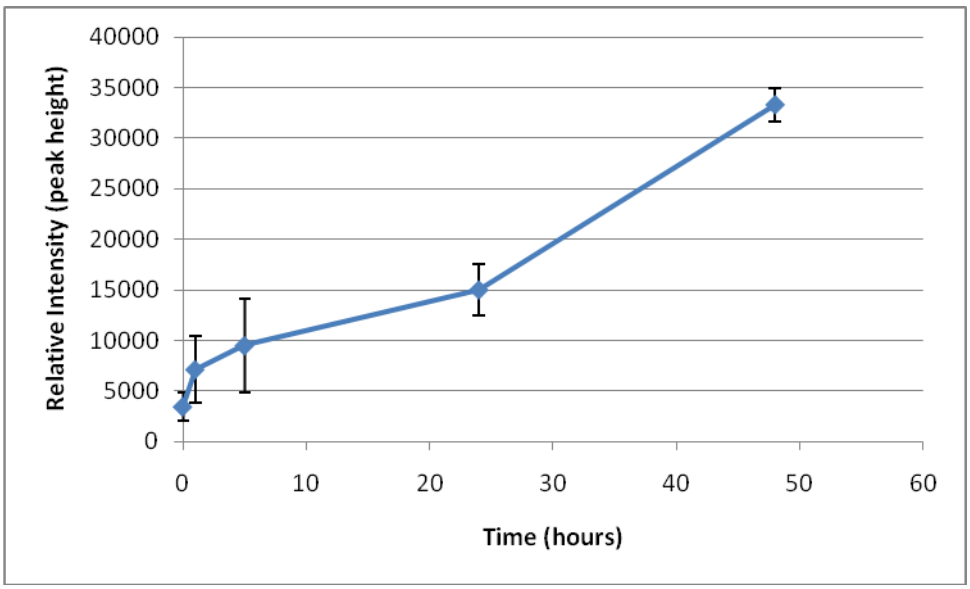

Figure 4-10. Propylmalate levels increase in eflornithine. Error bars shown standard error of the mean from three replicates.

Propylmalate has a retention time of 7.5 minutes, similar to the retention times of many of the phosphocholines, which are decreasing over the 48 hours. Propylmalate could therefore be a breakdown product of these lipids.

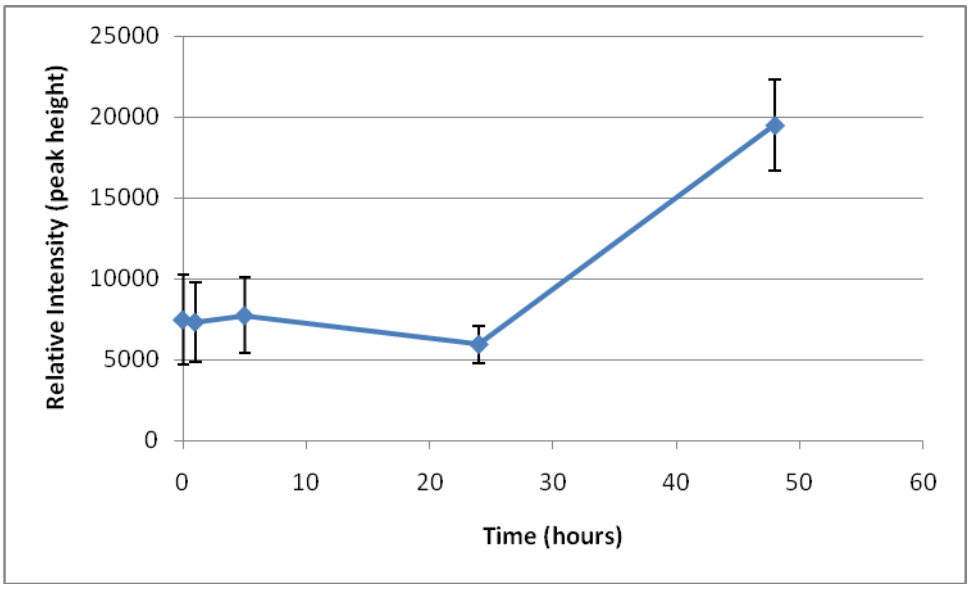

Figure 4-11. Anthranilate levels increase after 48 hours in eflornithine. Error bars show standard error of the mean from three replicates.

Anthranilate is a precursor to tryptophan biosynthesis (or a breakdown product in its degradation) and can be degraded in the tricarboxylic acid cycle in many organisms (Choi et al., 2011). It has many stereoisomers, but anthranilate is the most likely based on the retention time and genes present in *T. brucei*. Anthanilate is interestingly also thought to be a precursor in quinolone (a kynurenine) quorum signalling in *Pseudomonas aeroginosa*. Kynurenines have also been shown to modulate the host immune response, reducing inflammatory responses (De Ravin et al., 2010), although some kynurenines (but not anthranilate) were shown to be antimicrobial (Narui et al., 2009). The decrease in adenylanthranilate concurrent with the increase in anthanilate suggests that anthranilate is being released from the base, perhaps in order to form more ATP for energy. Why anthranilate should be conjugated to adenine is unclear. Kynurenines can also be converted to nicotinamide through conjugation to a ribonucleotide. It is possible therefore that adenylanthranilate may be related to nicotinamide synthesis. Nicotinamidase has been annotated in the *T. vivax* (TvY486_0901400) and *T. b. gambiense* (Tbg972.9.2100) genomes, but its syntenic partner (Tb427tmp.160.2600) is not annotated in the *T. b. brucei* genome (despite 100 % similarity at the amino acid level to the *T. b. gambiense* gene). Nicotinamide (m/z: 123.0553, RT: 7.9 minutes) and ribosylnicotinamide (m/z: 255.0973, RT: 14.0 minutes) are detected in the data set, but are not significantly altered until the decrease, with the majority of metabolites, at 48 hours.

An adenine-anthranilate conjugate has not been reported previously in the literature. More analysis of the role of anthranilate in eflornithine-treated cells would be useful, perhaps with the use of isotopically labelled tryptophan.

Interestingly, eflornithine levels in the cells did not increase significantly over the 48 hours although this is probably due to high levels of residual eflornithine from the medium masking any uptake.

Some metabolites were seen to increase, but not significantly due to the large levels of variation see in the biological data. Sedoheptulose (m/z: 210.0738, RT: 14.9 minutes), sedoheptulose phosphate (m/z: 290.0400, RT: 25.4 minutes) and

the water loss in-source fragment of sedoheptulose phosphate (m/z: 272.0296, RT: 25.4 minutes) showed the same trend (Fig 4-12).

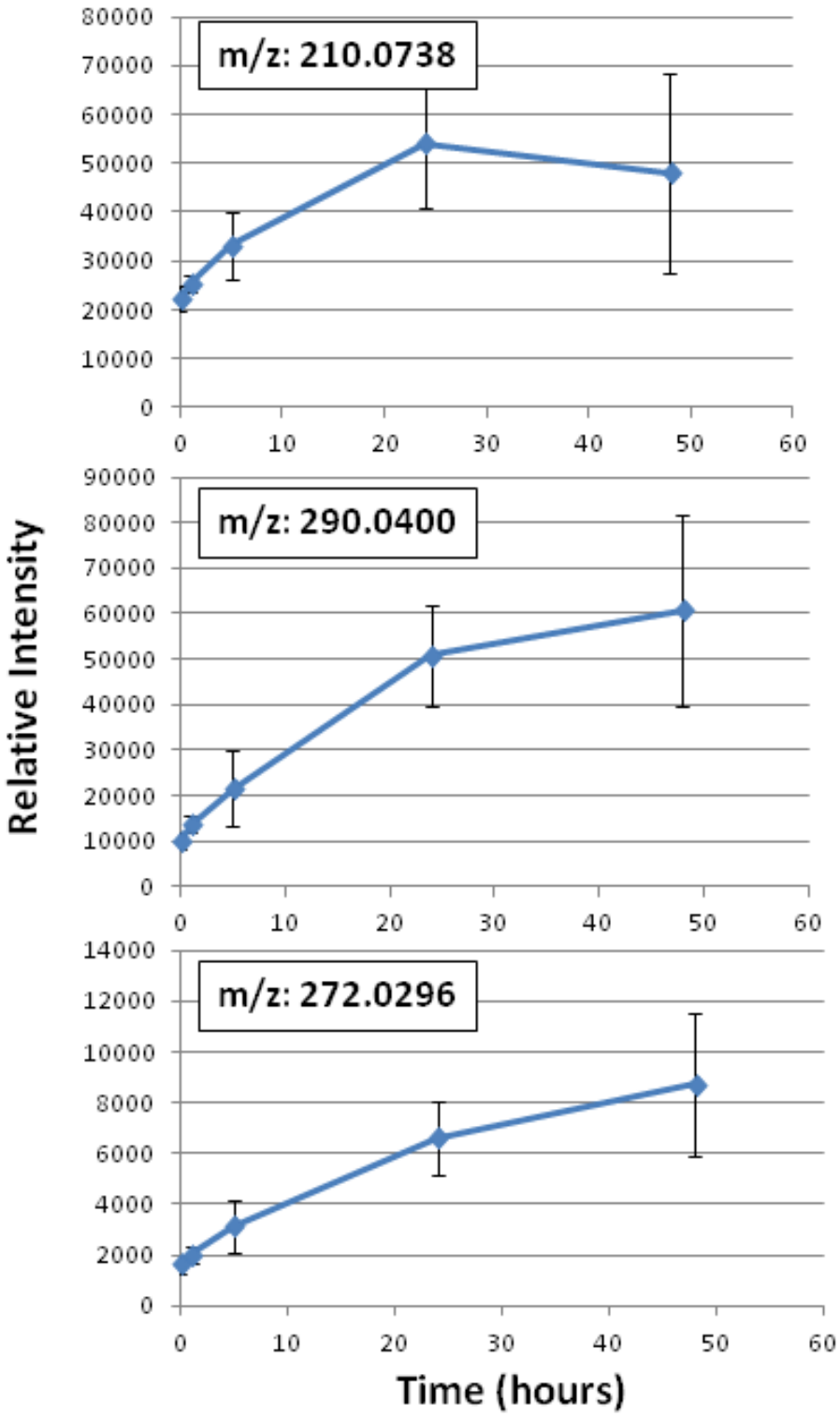

Figure 4-12. Sedoheptulose (top graph), sedoheptulose phosphate (middle graph) and the fragment of sedoheptulose phosphate increase with 500 µM eflornithine. X-axes show time in hours, Y-axes relative intensity (peak height). Error bars show standard error of the mean from three replicates.

Sedoheptulose phosphate is a seven carbon sugar of the pentose phosphate pathway formed, along with glyceraldehyde 3-phosphate, from ribose-5-phosphate and xylulose-5-phosphate through transketolase (Tb927.8.6170) action. Transketolase has, however, been shown not to have activity in bloodstream-form trypanosomes (Stoffel *et al.*, 2011).That being said, sedoheptulose 7-phosphate was evident in procyclic trypanosomes knocked out for transketolase, albeit at reduced levels, indicating an alternative source of the metabolite in these cells. Xyulose and ribose 5-phosphate levels are not altered over the time course to 48 hours, further suggesting an alternative source of sedoheptulose phosphate. The increase in sedoheptulose may also be indicative of stumpy formation if this is the mode of killing by eflornithine as was suggested by Alan Bitonti (Bitonti *et al.*, (1986).

Sedoheptulose phosphate can also be formed through transaldolase (Tb927.8.5600) from erythrose 4-phosphate and fructose 6-phosphate but it is unclear why the trypanosomes would do this in response to eflornithine exposure. Moreover, this reaction requires a supply of erythrose 4-phosphate, usually produced by the absent transketolase. Trypanosomes might, therefore, have another, as yet unidentified, source of erythrose 4-phosphate (erythrose 4-phosphate is not detected in this dataset, but erythrose (m/z: 119.0349, RT: 9.4 minutes) is (Appendix 8-4)). Of note also is that aldolase can fuse sugar phosphates to yield longer chain bisphosphates that could then be cleaved with a bisphosphatase. For example, erythrose 4-phosphate and dihydroxyacetone phosphate would yield sedoheptulose 1,7-bisphosphate that could then yield sedoheptulose 7-phosphate by sedoheptulose 1,7-bisphosphatase (Tb427.02.5800) (Clasquin *et al.*, 2011).

To ensure that the metabolites seen as altered from eflornithine treatment are specific to eflornithine or if they are implicated in a more generalised drug response. Another trypanocide, nifurtimox, was also analysed by metabolomics.

4.2.2 Nifurtimox and eflornithine synergy

The IC_{50} of nifurtimox was found to be 4 µM in bloodstream form *T. b. brucei* by alamar blue assay (Fig 4-13). Nifurtimox given orally (15 mg/kg) gives a maximum serum concentration of 2.6 µM (Gonzalez-Martin *et al.*, 1992) and it appears to be concentrated in the CSF of mice from 6 µM in perfused serum to 12 µM in the CSF (Jeganathan *et al.*, 2011) indicating that nifurtimox would be more useful for stage two HAT where parasites have invaded the brain.

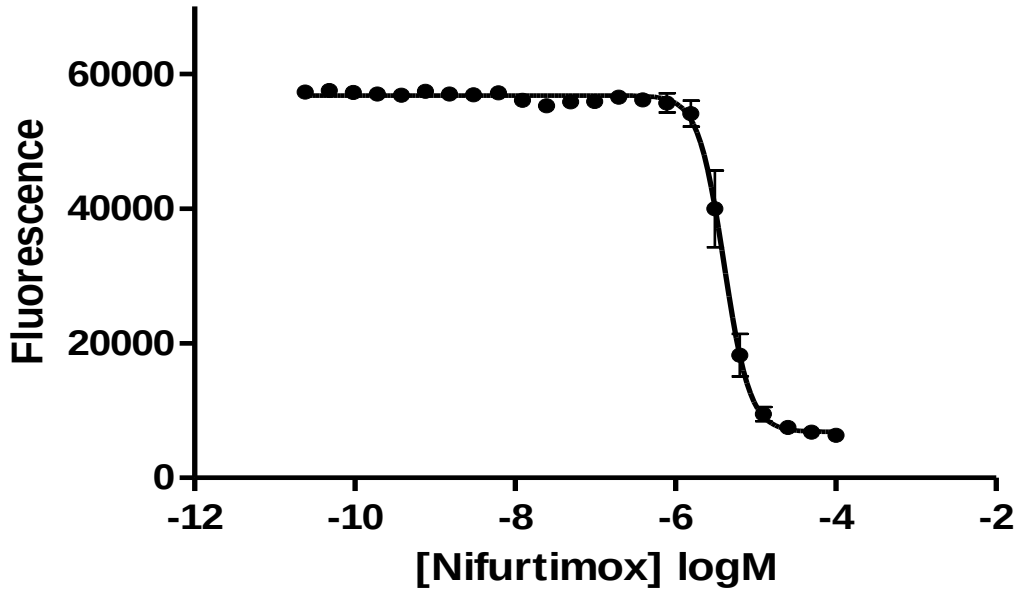

Figure 4-13. The IC_{50} value of nifurtimox in bloodstream form *T. b. brucei* is 4 µM. N = 4, error bars depict standard error of the mean.

As eflornithine use in the field is increasingly being superceded by a nifurtimox-eflornithine combination therapy, we wanted to see how the two drugs interact in trypanosomes.

Alamar blue assays were used to ascertain whether the two drugs were synergistic *in vitro*.

Interestingly, isobologram analyses (Fig 4-14) revealed that nifurtimox and eflornithine are not synergistic to one another's activity *in vitro*.

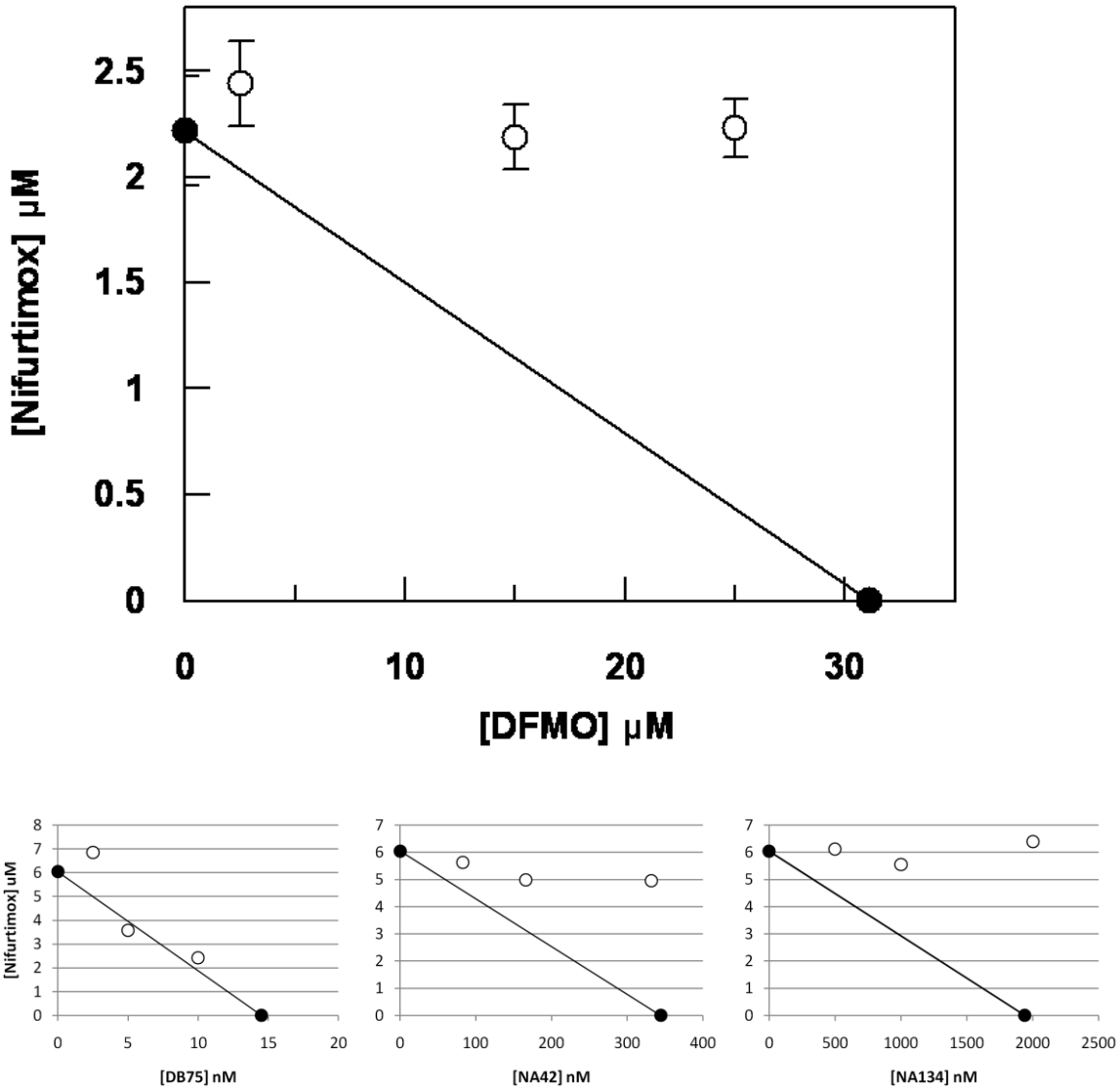

Figure 4-14. Isobologram analysis shows that nifurtimox and eflornithine (DFMO) are antagonistic *in vitro* (top graph). DB75 (bottom left) was additive, but NA42 (bottom middle) and NA134 (bottom right) were midly antagonistic. Y-axes show the nifurtimox concentration in µM. X-axes show the combination drug used in µM (DB75) or nM (NA42 and NA134). Black points show the IC_{50} of the drugs in isolation. White points show the drug combination IC_{50}s. N = at least 3.

The average fractional inhibitory concentration (FIC) is used as a measure of interaction between two drugs and is a sum of the IC_{50} of the drug acting in combination divided by the IC_{50} of the drug acting alone. An FIC of 1.5 was recorded for eflornithine and nifurtimox (n = 3), where a value ≥1.4 is taken as antagonistic (Snyder et al., 2007). This was interesting given the theory that eflornithine would deplete cellular trypanothione thus rendering the cells more susceptible to oxidative stress induced by nifurtimox. The fact that eflornithine is trypanostatic, rather than trypanocidal may explain why the two drugs are

antagonistic *in vitro* i.e. if nifurtimox requires dividing cells to exert its effects then eflornithine combination would be counteractive. It would be interesting to measure nitroreductase activity in eflornithine-treated cells to ascertain whether it is down-regulated or not. Isobologram analyses with other trypanostatic drugs (adenosine analogues NA42 and NA134 (Rodenko *et al.*, 2007)) found antagonism with the adenosine analogue NA42 (FIC: 1.4) and with NA134 (FIC: 1.6), but not with DB75 (FIC: 1.1) suggesting that the antagonism may be due to the static nature of eflornithine's mode of action, although other factors may also be involved.

4.2.3 Nifurtimox mode of action

To ascertain the nifurtimox concentrations suitable for a sub IC_{50} and a nifurtimox to death study, growth curves were conducted in various concentrations of nifurtimox (Fig 4-15).

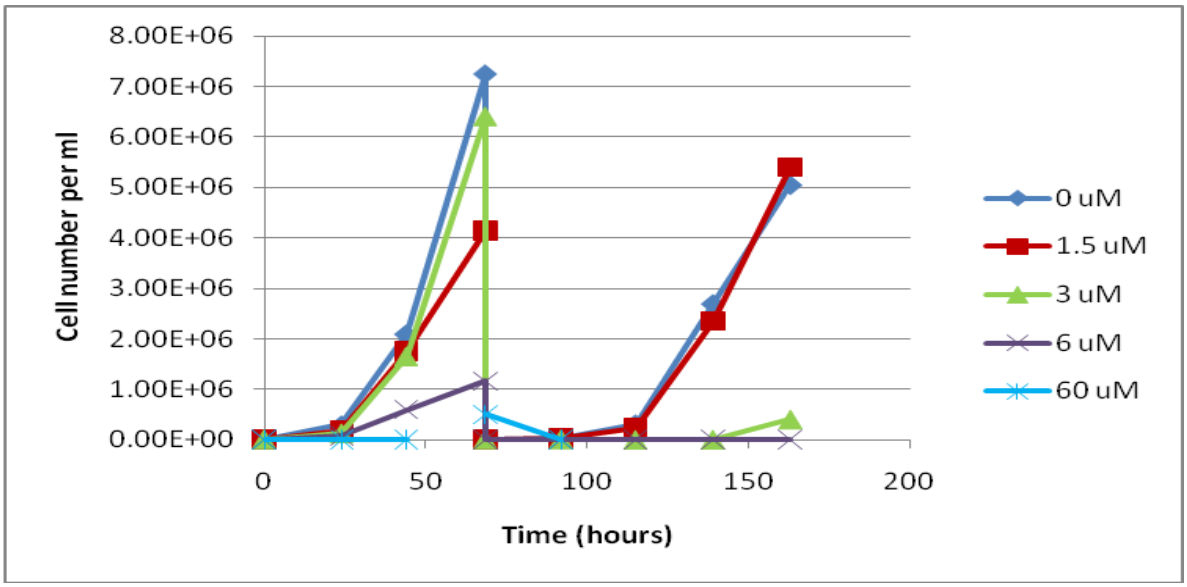

Figure 4-15. Growth curves of wildtype *T. b. brucei* in nifurtimox. Cells in 6 µM nifurtimox fail to survive after 55 hours. Cells cultured in 60 µM nifurtimox start to die at 5 hours (data not shown).

A level of 1.5 µM was chosen for the sub IC_{50} metabolome measurements as this was shown to be non lethal over 48 hours. 60 µM was used for toxicity experiments, but as the cells died at between 5 and 8 hours time points of 0, 1,

2 and five hours were taken. All metabolomics experiments were performed at least in triplicate.

4.2.3.1 Sub IC_{50} metabolome

After data reduction through the mzMatch and IDEOM softwares, 594 reproducible metabolites were identified. Polyamine pathway metabolites were largely unchanged in cells challenged with 1.5 μM nifurtimox (Fig 4-16). This data adds support to the specific changes seen with DFMO treatment. Thiol levels within the cells also remained largely unchanged (Table 4-4), although some fluctuations were seen. Ovothiol (unconfirmed identification, due to an absence of an ovothiol standard) levels increased the most, but the increase was not statistically significant (p-value 0.079 from *t*-test).

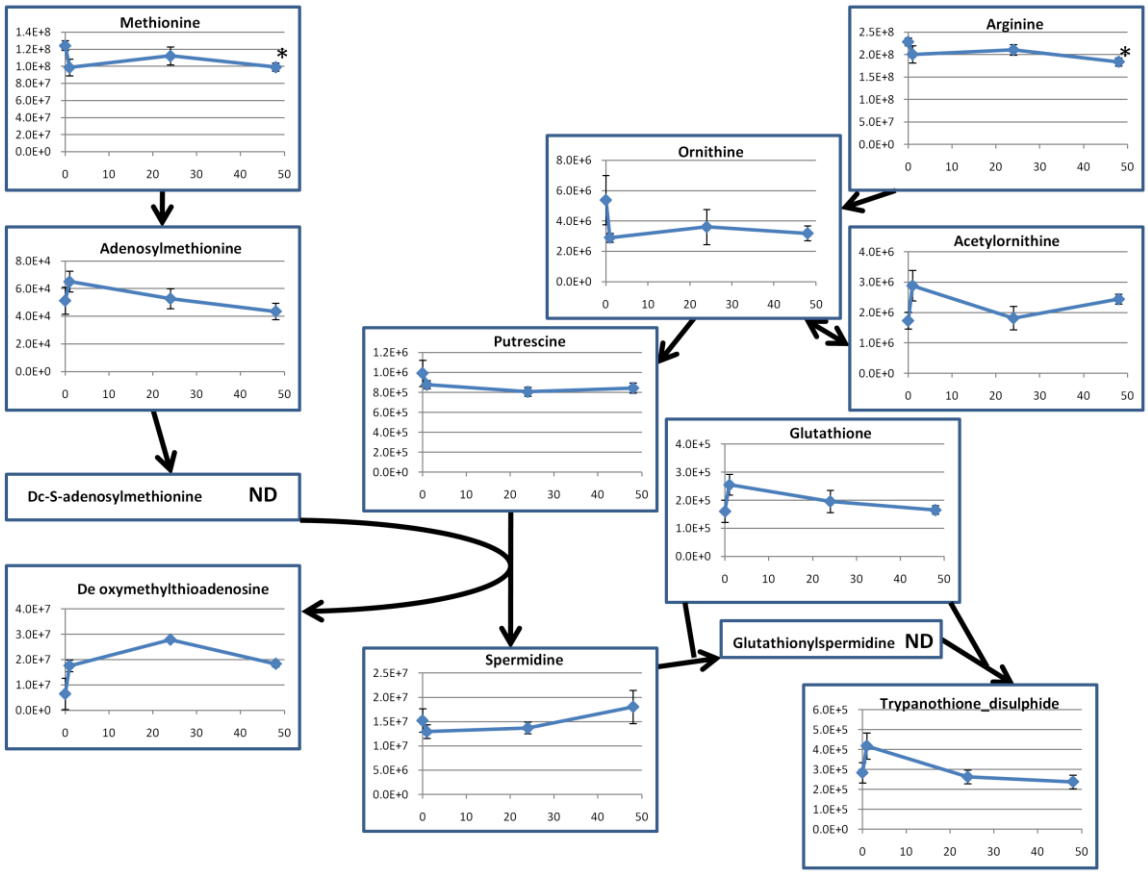

Figure 4-16. Polyamine metabolite changes in 1.5 µM nifurtimox. X-axes indicate the time in hours since drug addition. Y-axes indicate the relative intensity (area under the curve) of each metabolite. ND: not detected. Methionine (M+H: 150.0581, RT: 12.4 minutes), S-adenosylmethionine (M+H: 399.1444, RT: 26.7 minutes), methylthioadenosine (M+H: 298.0968, RT: 9.1 minutes), arginine (M+H: 175.1190, RT: 23.8 minutes), ornithine (M+H: 133.0971, RT: 24.0 minutes), acetylornithine (M+H: 175.1077, RT: 15.1 minutes), putrescine (M+H: 89.1072, RT: 29.6 minutes), spermidine (M+H: 146.1652, RT: 41.9 minutes), glutathione (M+H: 308.0910, RT: 19.6 minutes) and trypanothione disulphide (M+H: 722.2960, RT: 24.7 minutes). * indicates a p-value less than 0.05 in a Student's paired *t*-test to the 0 time point, ** indicates a p-value less than 0.001. N = 3.

Thiol	Time point			
	0	1	24	48
Methylthiobutanoate	1.00	0.81	0.60	0.86
Methylthioribose1phosphate	1.00	1.58	1.25	1.38
Homocysteinethiolactone	1.00	0.84	1.39	0.72
Cysteine	1.00	0.54	1.28	0.99
Ovothiol A	1.00	2.40	1.77	1.13

Table 4-4. Thiol levels in nifurtimox treated cells. Numbers show ratios (area under curve) compared to time 0. Methylthiobutanoate (M+H: 147.0122, RT: 6.0 minutes), methylthioribulose 1-phosphate (M+H: 259.0048, RT: 9.7 minutes), homocysteinethiolactone (M+H: 118.0320, RT: 13.25 minutes), cysteine (M+H: 122.0270, RT: 14.5 minutes) and ovothiol A (M+H: 202.0642, RT: 20.33 minutes). N = 3.

Metabolites found to be significantly altered ($p<0.05$ comparing 0 and 48 hour time points) in the *T. b. brucei* metabolome after challenge with nifurtimox are listed in Table 4-5.

M/Z	RT	Formula	Isomers	Name	Fold change	P-value
78.0139	8.4	C_2H_6OS	3	Mercaptoethanol	470	0.005
243.1219	15.5	$C_{10}H_{17}N_3O_4$	2	Ala-Gly-Pro	0.48	0.006
219.0855	19.7	$C_7H_{13}N_3O_5$	3	Gly-Gly-Ser	0.69	0.006
168.0899	7.5	$C_8H_{12}N_2O_2$	3	Cyclo(deltaAla-L-Val)	0.74	0.007
309.1323	15.3	$C_{14}H_{19}N_3O_5$	3	Ala-Gly-Tyr	0.81	0.007
243.1218	15.2	$C_{10}H_{17}N_3O_4$	2	Gln-Pro	0.38	0.008
446.2373	9.2	$C_{19}H_{34}N_4O_8$	8	Asp-Leu-Leu-Ser	0.65	0.009
222.0564	5.5	$C_8H_{14}O_5S$	1	Methylthio propylmalate	0.64	0.013
204.1110	15.2	$C_8H_{16}N_2O_4$	5	Val-Ser	0.57	0.020
289.1638	12.9	$C_{12}H_{23}N_3O_5$	5	Leu-Ala-Ser	0.72	0.022
281.2718	5.5	$C_{18}H_{35}NO$	1	Fatty acid (18:1)	1.35	0.023
523.1906	13.5	$C_{22}H_{29}N_5O_{10}$	2	Asp-Phe-Asp-Gln	0.62	0.024
358.1850	17.0	$C_{15}H_{26}N_4O_6$	3	Ala-Thr-Ala-Pro	0.75	0.031
129.5949	24.2	$C_{12}H_{25}N_3O_3$	2	Leu-Lys	0.79	0.033
254.1379	24.0	$C_{11}H_{18}N_4O_3$	2	Val-His	0.66	0.033
310.1165	14.4	$C_{14}H_{18}N_2O_6$	2	Glu-Tyr	0.81	0.033
181.0740	13.2	$C_9H_{11}NO_3$	5	Threo phenylserine	0.83	0.033
252.0857	16.7	$C_{10}H_{12}N_4O_4$	2	Ribosylpurine	1.47	0.037
188.1526	24.7	$C_9H_{20}N_2O_2$	2	N6,N6,N6-Trimethyl lysine	0.77	0.038
197.0798	15.1	$C_8H_{11}N_3O_3$	3	acetylhistidine	0.59	0.040
276.0959	16.3	$C_{10}H_{16}N_2O_7$	2	Glu-Glu	2.04	0.041
331.2106	10.9	$C_{15}H_{29}N_3O_5$	5	Leu-Leu-Ser	0.79	0.041
174.1118	23.8	$C_6H_{14}N_4O_2$	1	Arginine	0.84	0.042
231.1217	15.3	$C_9H_{17}N_3O_4$	3	Val-Asn	0.51	0.043
229.1061	16.7	$C_9H_{15}N_3O_4$	2	Asn-Pro	2.05	0.044
131.0946	11.6	$C_6H_{13}NO_2$	9	Leucine	0.88	0.045

Table 4-5. Metabolites significantly altered after treatment with sub IC_{50} levels of nifurtimox. Peptides are shaded blue and lipids yellow. 'M/Z' relates to the detected mass charge ratio (peak height) corrected for positive or negative ionisation. Fold change relates to the ratio of the 48 hour sample intensity compared to 0 hour intensity. P-values were calculated using a Student's *t*-test.

The metabolite with the smallest p-value was labelled as mercaptoethanol, but as mercaptoethanol is a stereoisomer of DMSO (dimethyl sulfoxide) and DMSO is used to dissolve the nifurtimox then the more likely metabolite is DMSO (even though the RT error for DMSO is 27.3 % from the calculated RT while for mercaptoethanol the RT error is 6.4 %).

Propylmalate was seen to increase in eflornithine toxicity studies, but methylthio propylmalate, a thiol derivative of propylmalate, is seen to decrease upon nifurtimox challenge. Methylthio propylmalate is not thought to be involved in any naturally occurring pathways (from KEGG). Propylmalate in the eflornithine study appeared to be a lipid fragment, methylthio propylmalate could equally be a lipid fragment (it elutes at the same time as a group of fatty acids and sphingolipids), although the thiol is not present in any of these lipids.

Ribosylpurine (32.4 % error form calculated RT (the deoxyinosine isomer has a RT error of 45.6 %)) was seen to increase 47 % after 48 hours in 1.5 µM nifurtimox. When the whole time course is taken into consideration however, the relatively minor increase is not very convincing (Fig 4-17).

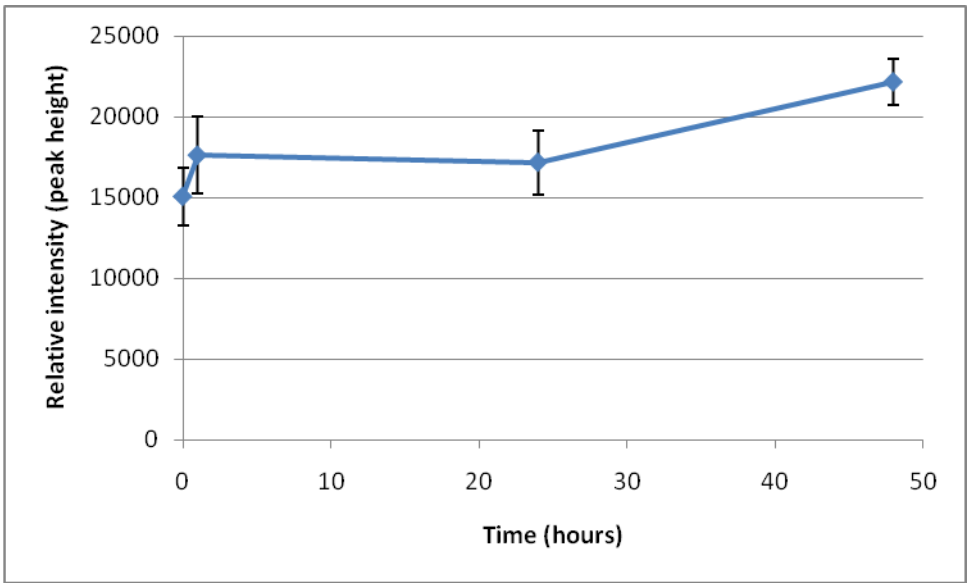

Figure 4-17. Ribosylpurine increases slightly after treatment with sub IC_{50} levels of nifurtimox. Error bars show standard error of the mean over three biological replicates.

All the peptides, amino acids and amino acid derivatives that had significant changes were decreased after 48 hours in nifurtimox except for the asparagine-proline and glutamate-glutamate dipeptides. The Asp-Pro peak is, however, in a very noisy region and it is likely that the processing software removed the peak for the 0 hour time points due to the large amount of noise. This dipeptide is therefore not significantly altered over the time course. The glutamate dipeptide only doubled after 48 hours after having fluctuated at the one and 24

hour time points. The inconsistent increases in this metabolite's levels are probably just due to biological variation.

The decreases in peptides may indicate a reduced uptake of peptides from the medium or a reduction in the breakdown of proteins, indicating that the cells are entering a more senescent state. However, the heat map (Fig 4-18) of metabolite levels shows a clear correlation between the one and 48 hour time points. In this assay, the one and 48 hour time points were extracted together as were the 0 and 24 hour time points. This trend indicates the paramount importance of extracting all metabolite samples on the same day at the same time and under the same conditions.

Overall, not many metabolites were altered after nifurtimox challenge as shown in the heat map although a lot of the map is blue, depicting a decrease. This may mean that the 0 hour samples have a greater concentration of metabolites in them due to experimental error.

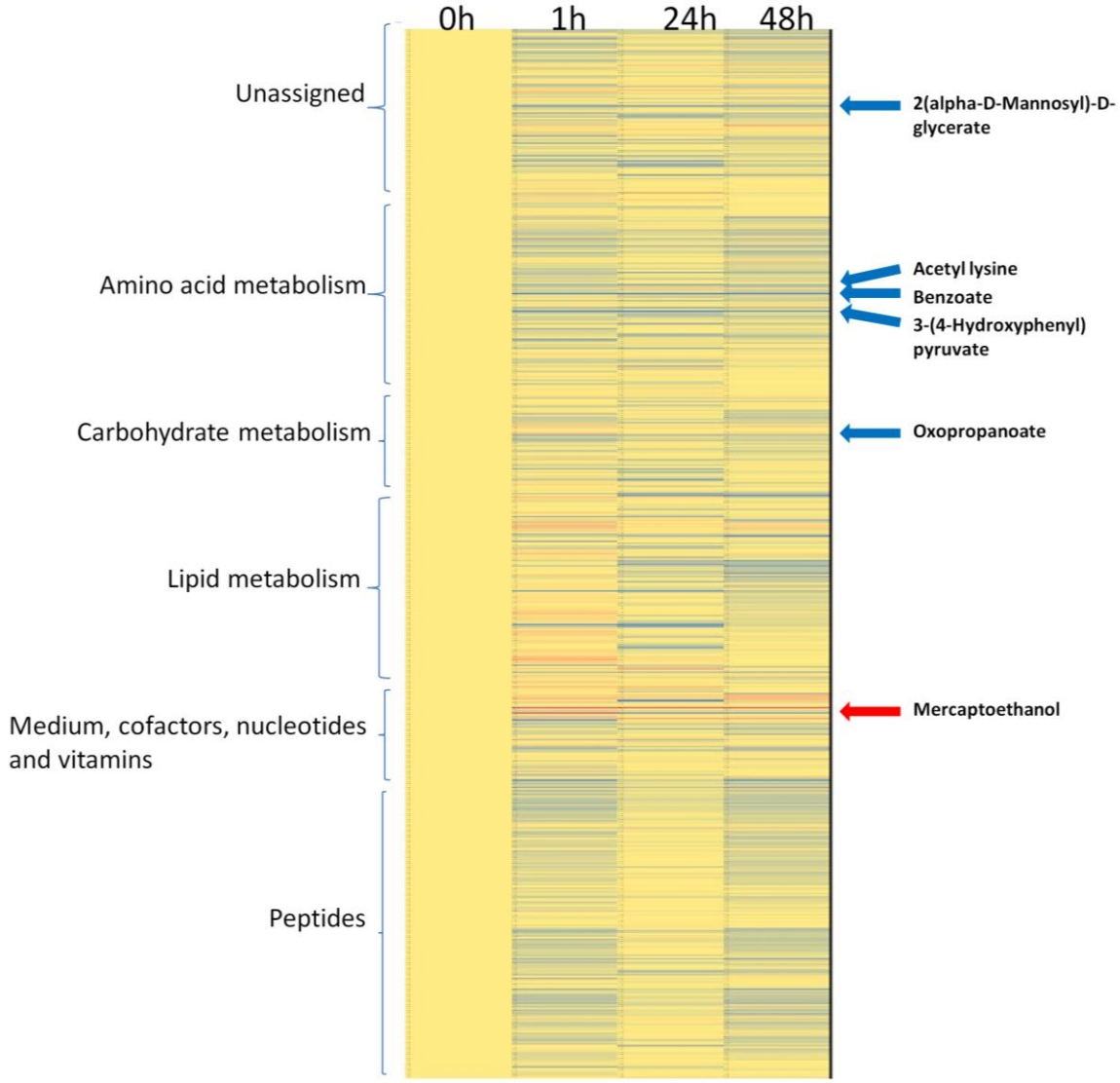

Figure 4-18. Heat map of metabolites altered after nifurtimox challenge at sub IC_{50}. Blue represents a decrease in metabolite intensity, red an increase and yellow represents unchanged levels. Metabolites are classified down the left hand side. The red arrows highlight metabolites that consistently increase, blue highlights those consistently decreased over the time course.

Arginine phosphate levels have previously been shown to increase in *T. cruzi* treated with 10 μM nifurtimox (Miranda *et al*. 2006), but in these samples the relative intensity remains stable (data not shown).

Analysis of nifurtimox levels in the cells showed that the drug levels decrease between 24 and 48 hours (Fig 4-19).

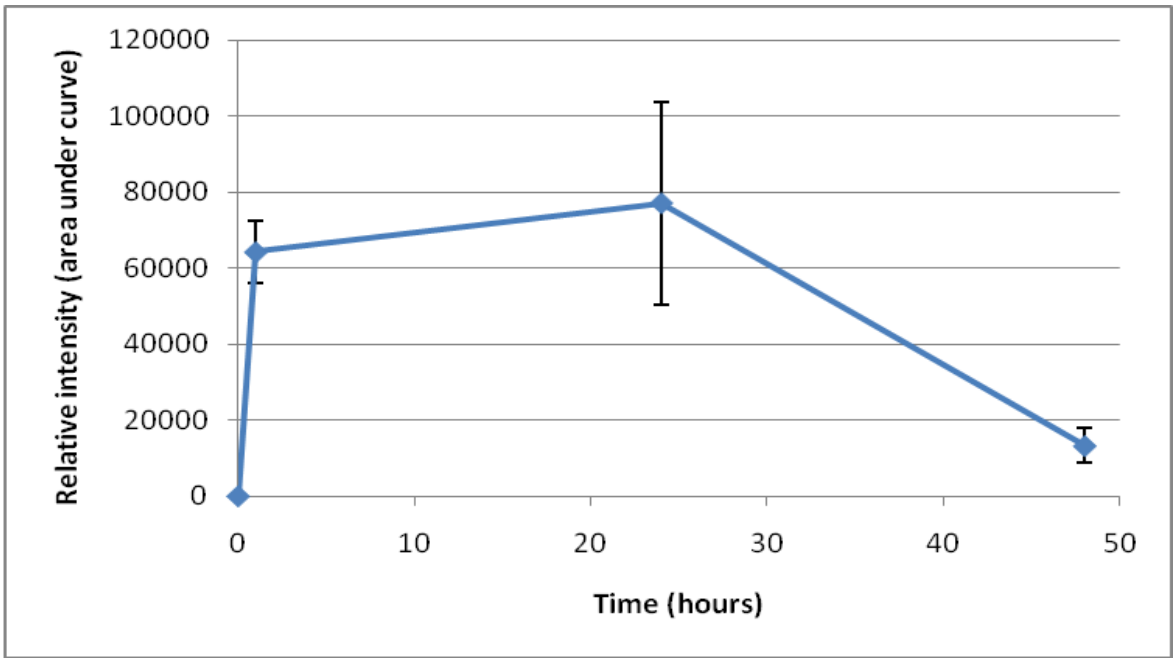

Figure 4-19. Nifurtimox levels in cells treated for 48 hours. Nifurtimox (M+H 288.0648, RT: 5.5 minutes) decreases between the 24 and the 48 hour time points. N = 3. Error bars show standard error of the mean.

Shane Wilkinson at the Queen Mary University of London showed that nifurtimox is reduced by type I nitroreductases to form a reactive open chain nitrile (Hall *et al.*, 2011). This decrease in the nifurtimox levels may therefore be due to nifurtimox's metabolism to this open chain nitrile. A targeted search for the nitrile metabolite revealed no peaks for the mass in positive mode (M+H: 256.0750), negative mode (M-H: 254.0606), positive mode with a sodium adduct (M+NaH: 278.0575) or negative mode with a sodium adduct (M-H+Na: 276.0431). Wilkinson's group postulated that the open chain nitrile may act as a Michael acceptor, attacking any carbon next to a ketone as a way of binding to macromolecules such as DNA and proteins. As the nitrile would be expected to be extremely reactive, it is unlikely that we would see it as a free metabolite and we therefore searched the data for any metabolite mass with an additional 256.0750 atomic mass units (the nitrile adduct).

The nitrile could not be detected as an adduct attached to any metabolites in our dataset. The mass spectrometry platform used scans for metabolites in a mass range of 70 - 1, 400 atomic mass units. The vast majority of macromolecules are outwith this range and therefore would not be detected. A proteomics assay on treated cells may reveal the metabolite attached to

proteins and larger peptides. A large number of peptides are detected in our datasets, however, none of these were discovered with a mass corresponding to their conjugation to the nitrile adduct. It is likely that the levels of the nitrile within the cells would be very low and this may be why no peaks could be detected. A higher dose of nifurtimox may reveal the presence of the nitrile.

4.2.3.2 Nifurtimox toxicity

A higher dose of eflornithine at 60 μM was used for toxicity experiments with samples collected after 0, 1, 2 and 5 hours in drug. After data reduction through the mzMatch and IDEOM softwares, 670 reproducible metabolites were identified (see included CD). Thirty metabolites showed a significant difference between the 0 and the 5 hour time point (Table 4-6).

Over a third of the metabolites with significantly altered intensities were lipids, although the changes were not consistently up or down. The phosphocholines were all decreased over the time course, however, which may indicate that the cells are using these to increase synthesis of the other lipids.

Purines (deoxyadenosine, AMP and GMP) are all increased whereas sugars and sugar phosphates (glucose 6-phosphate (two peaks probably representing different isomers as the retention times are different), succinate and deoxyribose (two peaks probably representing different isomers)) are decreased.

The increase in purines and in uracil may be a result of RNA and DNA degradation as the nifurtimox active metabolite is thought to bind to macromolecules (Hall *et al.,* 2011) and nucleic acid breakdown might be stimulated on modified DNA. Most of the peptides seen also increase, which may mean that nifurtimox also binds to proteins causing degradation. A targeted look for the nifurtimox metabolite (M+H: 258.0906) attached to macromolecules produced no hits with peptides, purines and pyrimidines. Since the Orbitrap only records masses up to 1,400, however, larger molecules with nifurtimox attached would not be detected.

Formyldihydrofolate is likely to result from the spontaneous oxidation of formylfolate. Formyl tetrahydrofolate has been shown to be important in

regulating purine levels in leishmania (Vickers *et al.*, 2009). However, the identity of this metabolite is not certain and the IDEOM software highlighted this mass as possibly relating to the phosphocholines, as a fragment.

M/Z	RT	Formula	Isomers	Name	Fold change	P-value
434.2432	4.8	$C_{21}H_{39}O_7P$	3	Lipophosphatidic acid (0:0/18:2)	1.36	0.002
112.0274	7.9	$C_4H_4N_2O_2$	1	Uracil	2.62	0.003
260.0298	17.4	$C_6H_{13}O_9P$	46	Glucose 6-phosphate	0.46	0.003
862.5579	4.4	$C_{45}H_{83}O_{13}P$	9	Phosphatidylinositol (18:0/18:0)	1.26	0.006
250.0987	16.6	$C_9H_{18}N_2O_4S$	1	Met-Thr	2.52	0.009
141.0192	19.7	$C_2H_8NO_4P$	2	Ethanolamine phosphate	0.44	0.011
507.3691	9.6	$C_{26}H_{54}NO_6P$	6	Phophocholine (18:1)	0.66	0.012
118.0268	6.6	$C_4H_6O_4$	7	Succinate	0.75	0.013
260.0297	18.1	$C_6H_{13}O_9P$	46	D-Glucose 6-phosphate	0.55	0.013
260.1373	15.2	$C_{11}H_{20}N_2O_5$	4	Glu-Leu	1.32	0.013
134.0578	7.8	$C_5H_{10}O_4$	6	Deoxyribose	0.42	0.014
266.1267	15.2	$C_{13}H_{18}N_2O_4$	1	Phe-Thr	2.56	0.014
273.2667	12.0	$C_{16}H_{35}NO_2$	1	Hexadecasphinganine	0.60	0.019
134.0579	7.6	$C_5H_{10}O_4$	6	Deoxyribose	0.41	0.019
479.3376	9.9	$C_{24}H_{50}NO_6P$	5	Phosphocholine (16:1)	0.49	0.020
213.044	22.6	$C_{13}H_{22}N_4O_8S_2$	2	Asp-Cys-Cys-Ser	0.49	0.021
251.1018	13.2	$C_{10}H_{13}N_5O_3$	4	Deoxyadenosine	4.11	0.021
602.5274	4.4	$C_{39}H_{70}O_4$	1	Glycerolipid (15:0/8:0)	1.22	0.023
701.5364	5.9	$C_{39}H_{76}NO_7P$	11	Phosphoethanolamine (16:0/18:1)	1.39	0.028
617.4785	4.8	$C_{34}H_{68}NO_6P$	1	sphingeninephosphate (16:0)	0.74	0.030
471.1503	10.1	$C_{20}H_{21}N_7O_7$	1	10-Formyldihydrofolate	0.73	0.030
465.322	10.1	$C_{23}H_{48}NO_6P$	3	Phosphocholine (15:1)	0.43	0.033
446.3393	5.0	$C_{28}H_{46}O_4$	22	Dehydroteasterone	11.32	0.035
699.5197	5.8	$C_{39}H_{74}NO_7P$	6	Phosphoethanolamine (16:1/18:1)	1.40	0.040
347.0631	17.8	$C_{10}H_{14}N_5O_7P$	7	AMP	3.61	0.041
774.5416	4.3	$C_{42}H_{79}O_{10}P$	9	Phosphoglycerol (18:1/18:1)	1.30	0.041
188.1161	17.5	$C_8H_{16}N_2O_3$	7	Val-Ala	2.35	0.041
363.0580	17.5	$C_{10}H_{14}N_5O_8P$	5	GMP	1.52	0.044
801.5518	7.9	$C_{43}H_{80}NO_{10}P$	1	Phosphoglycerol (17:0/20:4)	0.78	0.046
166.0057	39.3	$C_8H_{14}NO_9S_2$	1	Glucocapparin	0.88	0.048

Table 4-6. Significantly changing metabolites with 60 µM nifurtimox. Peptides are shaded blue and lipids yellow. 'M/Z' relates to the detected mass charge ratio (peak height) corrected for positive or negative ionisation. Fold change relates to the ratio of the five hour sample intensity compared to 0 hour intensity. P-values were calculated using a Student's *t*-test.

Dehydroxyteasterone is a hormone and would not be present in trypanosomes. Its levels increase steadily over the time course and the mass is likely to relate to nifurtimox, especially as the retention time is very similar to nifurtimox (RT:

5.4 minutes). However, the mass of dehydroxyteasterone (m/z 446.3393) minus the mass of the open chain nitrile (either saturated or unsaturated) or nifurtimox reveals no hits in the metabolite databases. The identity of this large, early eluting (and therefore non-polar) metabolite remains unknown for now, although fragmentation could be undertaken in the future to aid its identification. Metabolites of the polyamine pathway are not significantly altered over the nifurtimox time course (Fig 4-20) although there is a a slight increase in glutathione and decrease in trypanothione after 5 hours. Thiol levels are also not significantly altered (Table 4-7). The lack of changes in thiol and polyamine levels suggests that oxidative stress is not important in nifurtimox killing, although the redox state of the thiols was not measured so a definitive conclusion cannot be drawn.

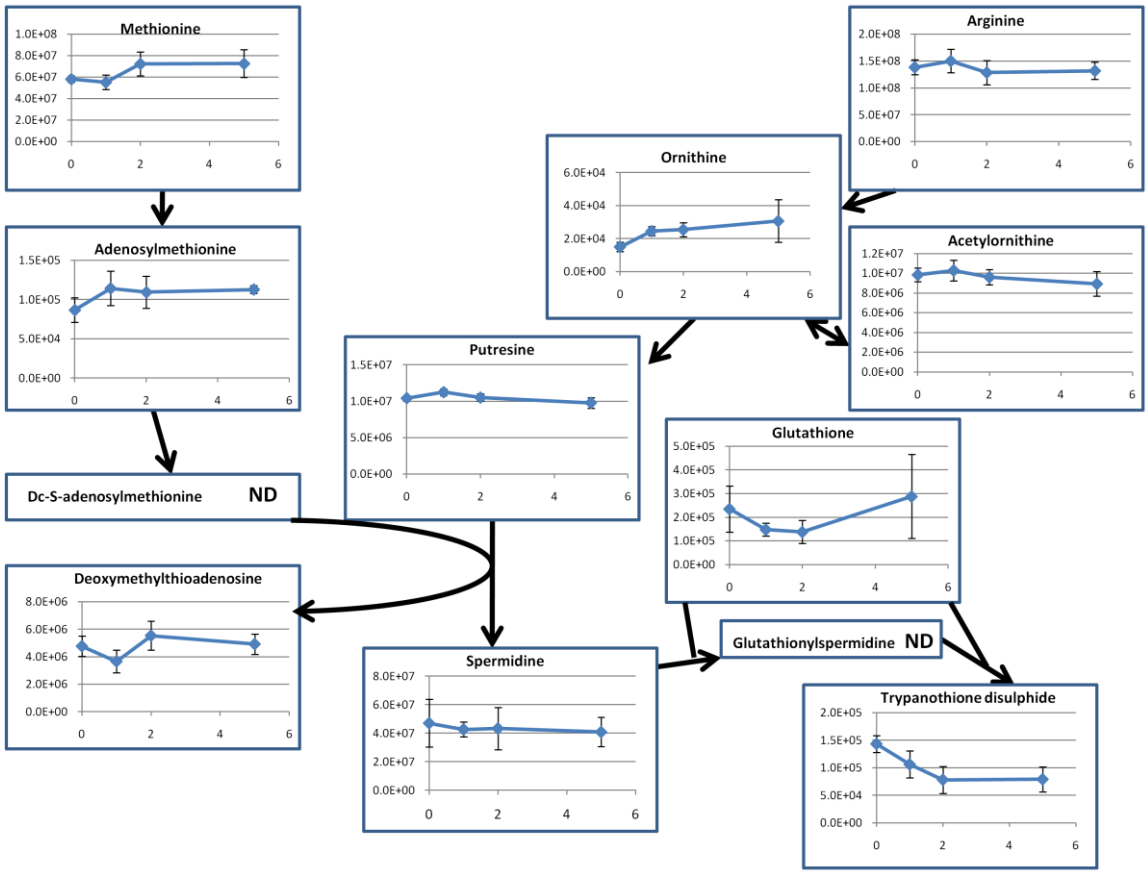

Figure 4-20. Polyamine metabolite changes in 60 µM nifurtimox. X-axes indicate the time in hours since drug addition. Y-axes indicate the relative intensity (area under the curve) of each metabolite. ND: not detected. Methionine (M+H: 150.0581, RT: 14.5 minutes), S-adenosylmethionine (M+H: 399.1444, RT: 32.6 minutes), methylthioadenosine (M+H: 298.0968, RT: 11.1 minutes), arginine (M+H: 175.1190, RT: 28.7 minutes), ornithine (M+H: 133.0971, RT: 28.8 minutes), acetylornithine (M+H: 175.1077, RT: 18.0 minutes), spermidine (M+H: 146.1652, RT: 33.9 minutes), glutathione (M+H: 308.0910, RT: 16.7 minutes) and trypanothione disulphide (M+H: 722.2960, RT: 29.9 minutes). No metabolites showed significance at a p = 0.0.5 level in a *t*-test comparing levels to the 0 hour time point. N = 3.

Thiol	Time Point			
	0	1	2	5
methylthiobutanoate	1.00	0.91	0.91	0.83
deoxymethylthioadenosine	1.00	0.77	1.16	1.03
cysteine	1.00	1.08	0.88	1.17
methionine	1.00	0.95	1.24	1.25
glutathione	1.00	0.63	0.59	1.22
trypanothione disulphide	1.00	0.74	0.55	0.55
adenosylmethionine	1.00	1.32	1.26	1.30

Table 4-7. Thiol levels in 60 µM nifurtimox treated cells. Numbers show ratios compared to time 0 (area under curve). Methylthiobutanoate (M+H: 147.0122, RT: 5.8 minutes), deoxymethylthioadenosine (M+H: 298.0968, RT: 11.1 minutes), cysteine (M+H: 122.0270, RT: 16.7 minutes), methionine (M+H: 150.0581, RT: 14.45 minutes), glutathione (M+H: 308.0910, RT: 16.6 minutes), trypanothione disulphide (M+H: 722.2960, RT: 29.8 and adenosylmethionine (M+H: 399.1444, RT: 32.7 minutes. Ovothiol A could not be detected. N = 3.

Reduction of nifurtimox to its reactive metabolite requires several steps (Fig 4-21) (Hall *et al.*, 2011).

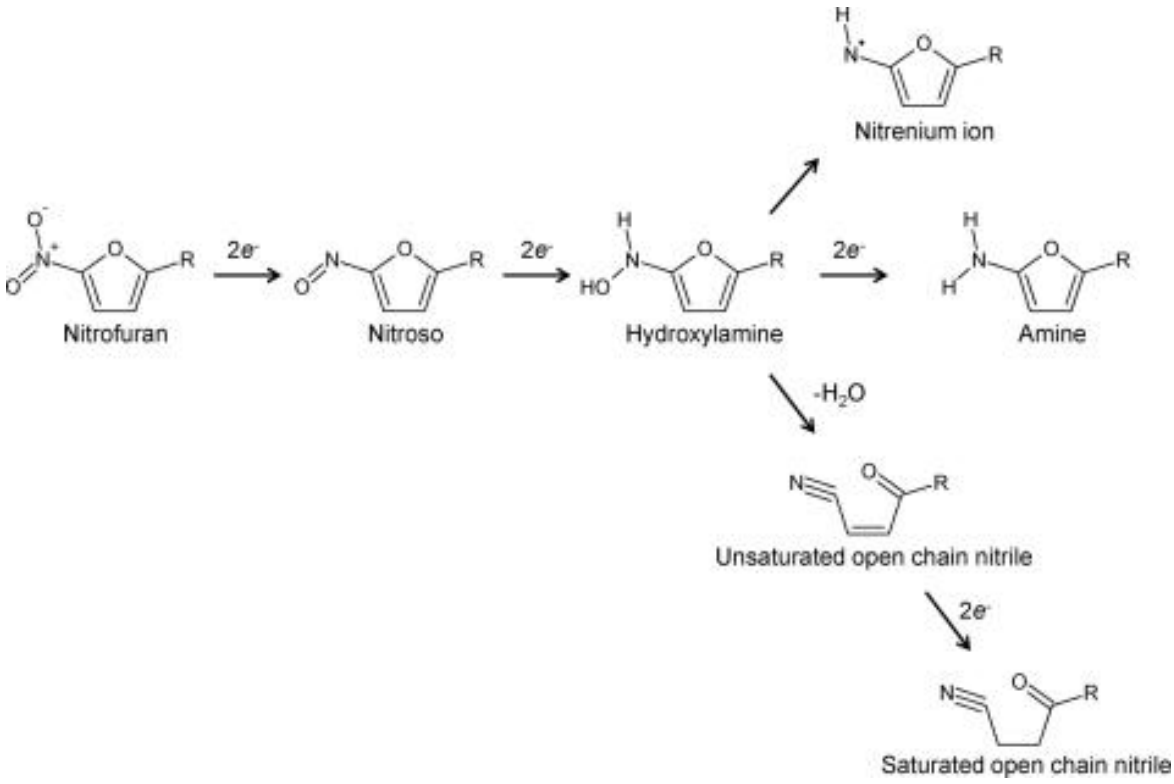

Figure 4-21. The reduction of nifurtimox (a nitrofuran) to its active compound, a saturated open chain nitrile. (From (Hall *et al.,* 2011))

A targeted search for the metabolites in the reduction of nifurtimox to its saturated open chain nitrile revealed just the start and end metabolites of the pathway, not the intermediates (Fig 4-22). This indicates that the reduction is rapid and intermediates in the pathway do not persist or persist at very low, undetectable levels.

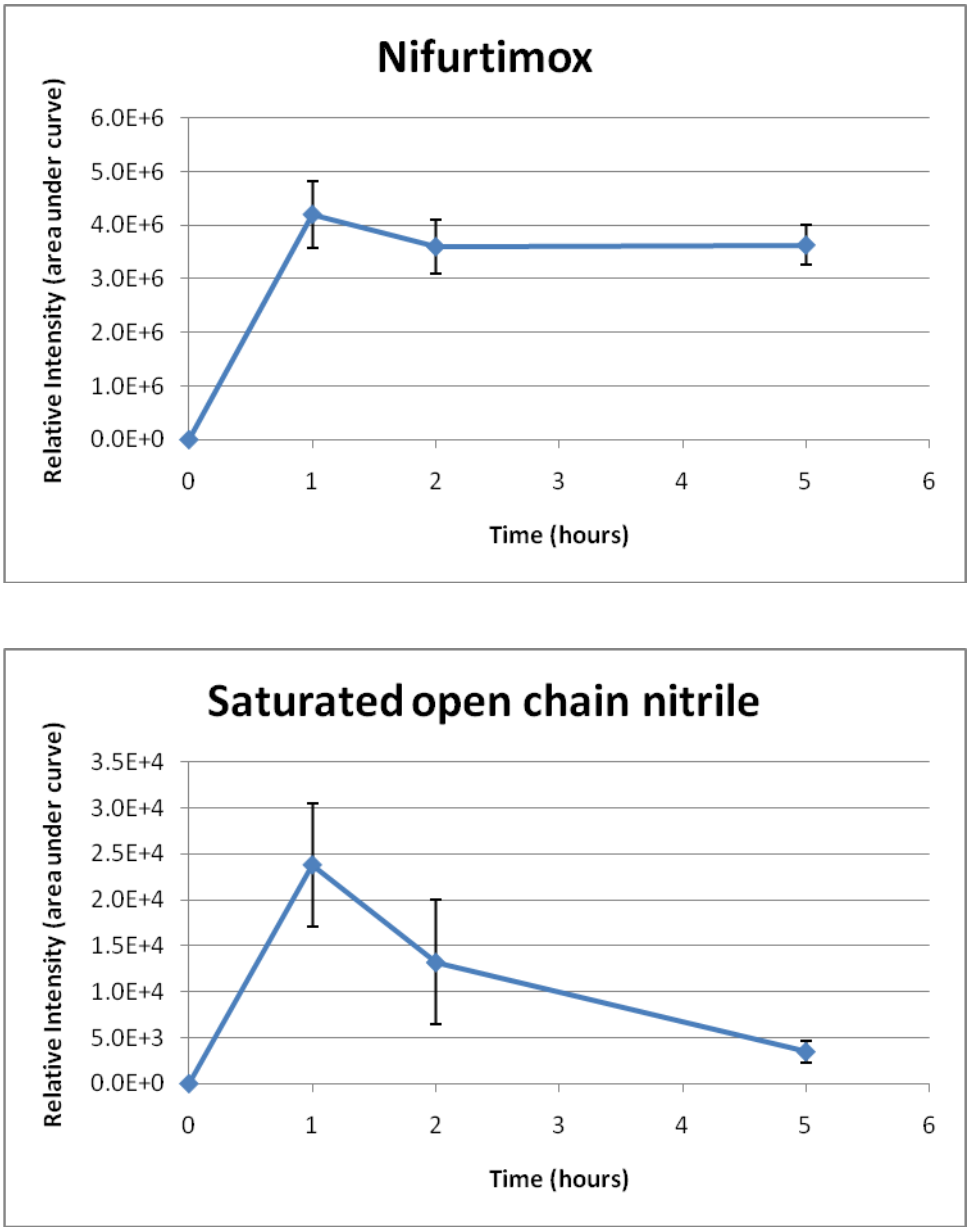

Figure 4-22. Nifurtimox reduction in *T. b. brucei.* Nifurtimox (M+H: 288.0648, RT: 5.4 minutes) is reduced, through a number of steps to an open chain nitrile (M+H: 258.0906, RT: 5.7 minutes). Neither metabolite is detected at the 0 time point (where no drug is added). N = 3.

The high levels of nifurtimox observed are probably related to exogenous nifurtimox levels, which are very high as cells are not washed after quenching, rather than internal nifurtimox. The saturated open chain nitrile levels

decreased after an initial peak at one hour. This is interesting as it means that the pool of the active metabolite is not maintained during the nifurtimox time course, even though the levels of nifurtimox are high. Either uptake of nifurtimox must be reduced or the processing to the active metabolite is down regulated. The uptake mechanism of nifurtimox is unknown, but the current data are consistent with passive diffusion (Delespaux and De Koning, 2007). The Wilkinson group only recorded the saturated nitrile after 24 hours of drug exposure, whereas our assay shows its appearance after just one hour. This difference may be due to different experimental conditions as the Wilkinson group measured activity in purified nitroreductase (Hall *et al.,* 2011), whereas whole cells were utilised for the study shown here.

4.2.4 NECT metabolome

The nifurtimox-eflornithine combination therapy is gaining momentum as a preferred treatment of late-stage *T. b. gambiense* HAT (Yun *et al.*, 2010). Synergism of the two drugs has not be proven, however, either *in vitro* or in the field.

As the nifurtimox-eflornithine combination therapy was shown to be antagonistic in our *in vitro* assay (as were other trypanostatic drugs in combination with nifurtimox (Fig 4-14)), we wanted to measure the metabolome of the combination therapy and compare it to the metabolomes of each drug in isolation. It was thought that the antagonism could be due to a decrease in nifurtimox reduction in non-dividing cells. The metabolome of NECT treated cells was therefore measured using drug levels that were toxic in the monotharapies (500 μM for eflornithine and 60 μM for nifurtimox) and the time points used in the nifurtimox toxicity assay (0, 1, 2 and 5 hours) (see included CD). A targeted look at nifurtimox reduction was conducted (Fig 4-23), but the reduction to the open chain nitrile was still achieved over the five hours.

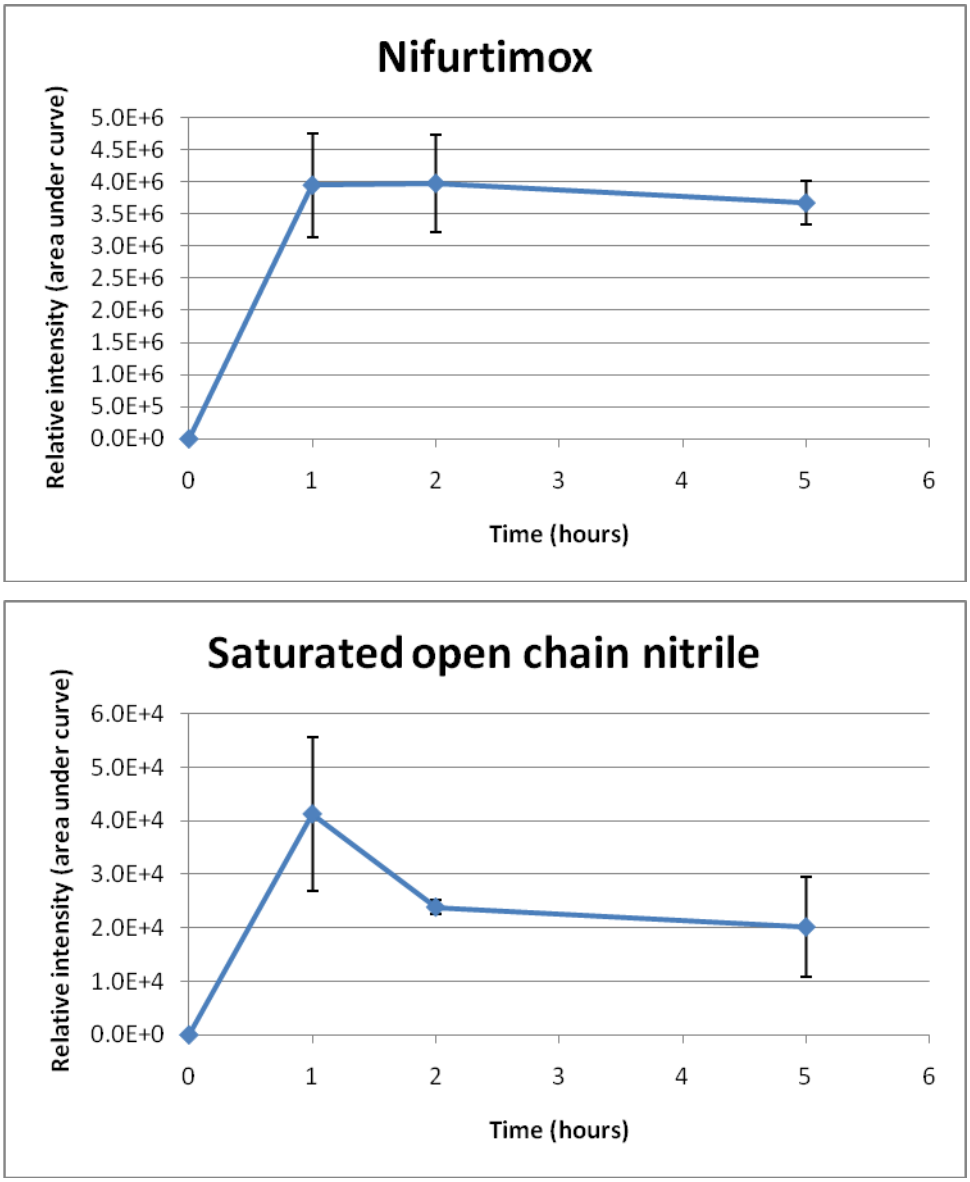

Figure 4-23. Nifurtimox reduction in *T. b. brucei* treated with a nifurtimox-eflornithine combination. Nifurtimox (M+H: 288.0648, RT: 5.4 minutes) is reduced, through a number of steps to an open chain nitrile (M+H: 258.0906, RT: 5.7 minutes). Neither metabolite is detected at the 0 time point (where no drug is added). N = 3.

The polyamine pathway metabolites were also analysed in the combination therapy using a targeted approach (Fig 4-24). Ornithine levels at one hour and trypanothione levels at five hours and putrescine levels showed significant differences at a level of p = 0.05 and p = 0.01 in a *t*-test compared to the 0 hour time point. The level of ornithine is generally increased and spermidine and putrescine are generally decreased, indicating that eflornithine is still able to inhibit ODC in the combination therapy.

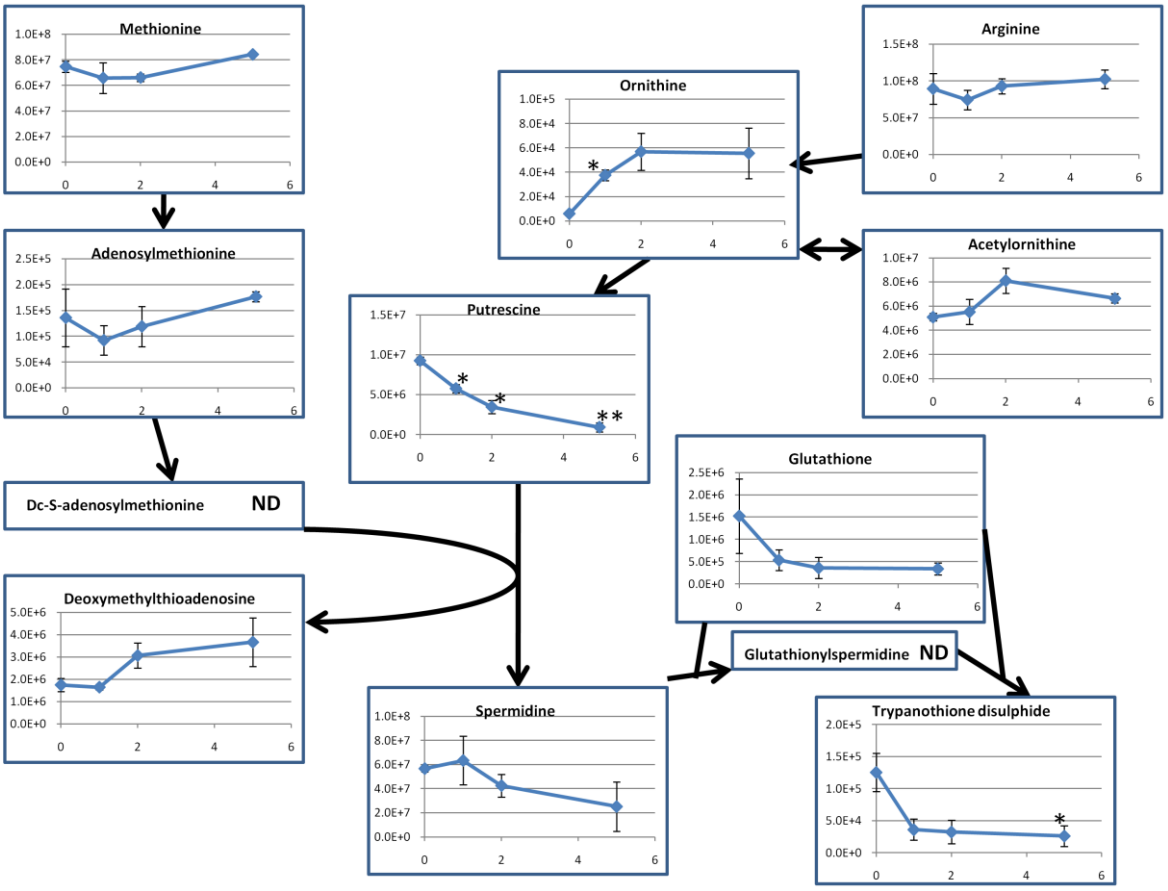

Figure 4-24. Polyamine metabolite changes in NECT. X-axes indicate the time in hours since drug addition. Y-axes indicate the relative intensity (area under the curve) of each metabolite. ND: not detected. Methionine (M+H: 150.0581, RT: 14.5 minutes), S-adenosylmethionine (M+H: 399.1444, RT: 32.7 minutes), methylthioadenosine (M+H: 298.0968, RT: 11.1 minutes), arginine (M+H: 175.1190, RT: 28.7 minutes), ornithine (M+H: 133.0971, RT: 28.8 minutes), acetylornithine (M+H: 175.1077, RT: 18.0 minutes), spermidine (M+H: 146.1652, RT: 33.7 minutes), glutathione (M+H: 308.0910, RT: 16.7 minutes) and trypanothione disulphide (M+H: 722.2960, RT: 30.0 minutes). * denotes significance at a p = 0.05 level and ** denotes significance at a p = 0.01 level in a *t*-test comparing levels to the 0 hour time point. N = 3.

An untargeted analysis of the NECT metabolome revealed 36 significantly altered metabolites after five hours (p = 0.05) (Table 4-8). Interestingly, where ethanolamines were increased in the nifurtimox monotherapy, in the combination therapy the one ethanolamine with a significant alteration (at p = 0.05) shows decreased intensity levels, as do the other lipids. AMP and uracil (in UMP) maintain their increase in intensity and the sugars maintain their decrease in intensity in line with the nifurtimox monotherapy.

M/Z	RT	Formula	Isomers	Name	Ratio	p-value
135.0544	16.4	$C_5H_5N_5$	1	Adenine	3.03	0.001
715.5148	6.9	$C_{39}H_{74}NO_8P$	11	Phosphoethanolamine (14:0/20:2)	0.72	0.002
134.0579	7.8	$C_5H_{10}O_4$	6	Deoxyribose	0.18	0.002
134.0580	7.4	$C_5H_{10}O_4$	6	(R)-2,3-Dihydroxy-3-methylbutanoate	0.18	0.002
88.1001	36.1	$C_4H_{12}N_2$	1	Putrescine	0.11	0.003
71.0735	35.8	C_4H_9N	2	3-Buten-1-amine	0.18	0.005
86.0368	14.8	$C_4H_6O_2$	7	Diacetyl	1.67	0.006
550.4962	5.1	$C_{35}H_{66}O_4$	1	1-O-(1Z-Tetradecenyl)-2-(9Z-octadecenoyl)-sn-glycerol	0.51	0.006
70.0531	18.2	$C_3H_6N_2$	3	beta-Aminopropionitrile	1.29	0.007
266.0903	7.4	$C_{12}H_{14}N_2O_5$	1	p-aminobenzoyl glutamate	2.73	0.008
264.1045	34.3	$C_{12}H_{17}N_4O_S$	1	Thiamin	1.92	0.009
132.0899	28.8	$C_5H_{12}N_2O_2$	3	L-Ornithine	2.97	0.009
241.0926	6.5	$C_{21}H_{30}N_4O_{7S}$	4	Ala-Met-Phe-Asp	1.55	0.011
237.9952	9.5	$C_{12}H_8OCl_2$	6	2,6-Dichloro-4'-biphenylol	0.29	0.011
130.1107	36.1	$C_6H_{14}N_2O$	2	N-Acetylputrescine	1.69	0.012
520.1613	23.7	$C_{19}H_{32}N_6O_5S_3$	1	Cys-Met-Met-His	1.23	0.013
148.0735	5.5	$C_6H_{12}O_4$	14	(R)-2,3-Dihydroxy-3-methylpentanoate	1.58	0.013
713.4997	5.8	$C_{39}H_{72}NO_8P$	12	Phosphoethanolamine (16:0/18:3)	0.52	0.020
338.0232	6.4	$C_8H_8HgO_2$	1	mercuriphenyl acetate	0.56	0.021
408.3751	5.1	$C_{30}H_{48}$	2	4,4'-Diapophytoene	1.36	0.027
314.0590	5.5	$C_{10}H_{19}O_7PS$	1	Malaoxon	1.29	0.030
118.0268	6.6	$C_4H_6O_4$	7	Succinate	0.49	0.030
112.0274	7.9	$C_4H_4N_2O_2$	1	Uracil	1.93	0.031
446.3394	5.1	$C_{28}H_{46}O_4$	22	3-Dehydroteasterone	7.26	0.033
188.1160	17.9	$C_8H_{16}N_2O_3$	7	Glycyl-leucine	1.79	0.033
191.0616	6.0	$C_7H_{13}NO_3S$	1	N-Acetylmethionine	0.47	0.033
331.5544	20.3	$C_{21}H_{28}N_7O_{14}P_2$	1	NAD+	1.15	0.034
185.9928	20.9	$C_3H_7O_7P$	2	2-Phospho-D-glycerate	0.44	0.035
192.1011	17.0	$C_{17}H_{28}N_4O_6$	1	Ala-Thr-Pro-Pro	0.68	0.037
324.0358	14.3	$C_9H_{13}N_2O_9P$	4	3'-UMP	1.89	0.040
130.1107	36.4	$C_6H_{14}N_2O$	2	N-Acetylputrescine	1.52	0.042
347.0631	17.8	$C_{10}H_{14}N_5O_7P$	7	AMP	3.00	0.043
386.3555	5.2	$C_{27}H_{46}O$	14	[ST] cholest-7-en-3beta-ol	0.62	0.044
390.2271	5.2	$C_{20}H_{30}N_4O_4$	1	Lys-Phe-Pro	1.68	0.044
200.0300	6.5	$C_{12}H_8OS$	1	dibenzothiophene-5-oxide	1.38	0.044
202.1428	26.6	$C_8H_{18}N_4O_2$	3	NG,NG-Dimethyl-L-arginine	1.56	0.047

Table 4-8. Significantly changing metabolites with NECT. Peptides are shaded blue and lipids yellow. 'M/Z' relates to the detected mass charge ratio (peak height) corrected for positive or negative ionisation. Fold change relates to the ratio of the five hour sample intensity compared to 0 hour intensity.

The combination therapy showed the same changes as were present in each of the monotherapies alone. This indicates that both of the drugs are able to exert their individual effects, but means that the basis for the antagonism shown is still unknown. It is also of value in offering additional independent corroboration of changes seen in monotherapy.

There are also many metabolites with unknown identities. Dehydroteasterone is again present and shows the same upward trend as in the nifurtimox toxicity experiment. Other metabolites that have been identified here (such as mercuriphenyl acetate) are unlikely to be present in trypanosomes and therefore probably relate to other metabolites not in the regularly-used databases. These unusual metabolites will require further investigation.

A comparison of selected metabolites from the three toxic dose drug treatments was conducted (Table 4-9). Some metabolites show an additive effect when in combination (succinate, peptides, deoxyribose, spermidine, sedoheptulose phosphate and putrescine) as might be expected in a combination therapy. Some of the metabolites show opposite trends in eflornithine and nifurtimox (glucose 6-phosphate, dehydroteasterone, formyldihydrofolate, acetylornithine and AMP), meaning that the combination therapy shows a more moderate change. This is also true of the increase in ornithine levels, which is lessened in the combination therapy as compared to the eflornithine monotherapy. It is possible that a reduced impact on these metabolite levels may be responsible for the lack of synergy in the combination therapy.

	Ratio 1:5 hours		
Name	**Eflornithine**	**Nifurtimox**	**NECT**
Peptides (average)	1.22	1.07	1.61
Lipids (average)	1.17	1.04	0.97
Succinate	0.77	0.75	0.49
Uracil	1.08	2.62	1.93
D-Glucose 6-phosphate (average)	1.25	0.51	0.72
Deoxyribose	0.76	0.42	0.18
3-Dehydroteasterone	0.76	11.32	7.26
10-Formyldihydrofolate	1.59	0.73	0.85
Acetylputrescine	0.37	0.97	1.61
Cystathionine	2.75	1.09	1.13
Methylthioadenosine	2.23	1.11	2.06
Acetylornithine	3.03	0.93	1.25
Ornithine	4.21	1.11	2.97
Spermidine	0.82	0.87	0.45
AMP	0.82	3.61	3
Sedoheptulose	1.49	Not found	1.35
GMP	1.24	1.52	1.25
Sedoheptulose phosphate	2.14	1.82	6.17
Putrescine	0.13	0.94	0.11

Table 4-9. A comparison of metabolite levels in the three drug treatments. The ratio is the metabolite intensity at 5 hours compared to the intensity at the 0 hour time point. Blue shading indicates a decrease in metabolite levels, red and increase and yellow shading indicates that levels are not altered.

4.3 Discussion

At low levels of drug (sub IC_{50}) specific changes to the metabolome can be detected as was evidenced with eflornithine. The data reveal only very localised changes in the sub IC_{50} experiments, which is surprising considering the number of metabolites that are detected. It is clear with eflornithine that the specific changes are not disseminated through the metabolome revealing a degree of robustness within the metabolic network. A recovery was also noted between 48 and 72 hours further demonstrating that trypanosomes are able to react to changes within the polyamine pathway and regulate the expression or kinetics of the enzymes. Acetylated ornithine and putrescine were detected, with acetylornithine correlating particularly well with ornithine levels. This metabolite has an unknown function within trypanosomes and is investigated further in chapter five. This proof of principle reveals the power of metabolomics for predicting the MOA of compounds with a metabolic (enzyme inhibition) mode of action.

Changes to nifurtimox-treated cells (sub IC_{50} and at toxic doses) did not involve alterations to the polyamine pathway metabolites or thiols. It is unfortunate that the oxidation state of the metabolites cannot be measured on the platform used. Dr. Dong Hyun-Kim at the University of Glasgow is optimising a method to detect the oxidation state of all the thiols within the trypanosome. In this method reduced thiols are derivatised with bromobimane which, when conjugated to a thiol, fluoresces. The fluorescence, when read after samples have been separated by mass on a HPLC column, can inform the user as to the oxidation state of each thiol within a cell extract (Dr. Dong Hyun-Kim, personal communication and Petrotchenko *et al*. 2011).

No robust, linear, significant changes were detected with sub IC_{50} levels of nifurtimox. Any significant changes at 48 hours were likely due to the processing method as there was a correlation between time points that were processed on the same day. This is a clear demonstration of the paramount importance of standardising protocols as much as possible and quenching all metabolic samples at the same time.

The lack of changes to the nifurtimox sub IC_{50} metabolome could serve to demonstrate that nifurtimox does not act metabolically. The reactive open chain nitrile, predicted to be the active compound of nifurtimox after processing with type I nitroreductases (Hall *et al.,* 2011), could not be detected either alone or as an adduct to other metabolites, although the levels of nifurtimox were seen to be reduced between 24 and 48 hours. Higher doses of nifurtimox did not detect any of the intermediates of nifurtimox processing, but the open chain nitrile was detected after one hour. Levels of this active metabolite decreased, however, after the initial peak at one hour, suggesting that the processing of nifurtimox is somehow compromised or that the active metabolite is used more rapidly at later time points.

4.3.1 Eflornithine MOA

Eflornithine inhibited ODC relatively quickly with levels of ornithine and putrescine demonstrably altered after just five hours in drug. The drug was seen to be trypanostatic for 48 hours, before killing the parasites after compromising the membrane of the cell. It has been suggested that the irreversible transformation to non-dividing forms produces parasites that have a limited life span (Fairlamb and Cerami, 1992). Whether cells eventually die through apoptosis or through another form of lysis remains unexplained.

One interesting observation from the eflornithine toxicity experiment is that levels of trypanothione are not greatly reduced. The levels fall by approximately 50 %, similar to the decrease of 66 % seen by Fairlamb *et al*. (1987). It may be that this decrease is sufficient to exert the cytostatic effects of the drug or it may be that the reduction in levels of spermidine are more important. Spermidine is an essential polyamine known to modulate DNA stability, transcription, translation and apoptosis (Igarashi and Kashiwagi, 2010), but rescue experiments where spermidine is given exogenously to ODC knock down cells were unsuccessful (Xiao *et al.,* 2009).

Exogenous spermidine increases the life span of yeast, nematodes, flies and human immune cells in culture (Eisenberg *et al.,* 2009). The mechanism for this death delay is not known, but was suggested that it may involve remodelling of chromatin and upregulation of autophagy, increasing resistance to oxidative

stress (Eisenberg *et al.*, 2009). In human lymphocytes it has been shown that 60 % of total spermidine is ionically bound to RNA (Igarashi and Kashiwagi, 2010), which demonstrates its importance in these immune cells.

When spermidine levels in *T. cruzi* are reduced, lipid peroxidation was shown to be increased and the effects could not be rescued by trypanothione. Spermine was observed to be more effective at lipid peroxidation rescue (Hernandez *et al.*, 2006), but *T. b. brucei* are not capable of producing spermine (they do not contain a spermine synthase) and levels are very low or undetectable (Bacchi *et al.*, 1983;Fairlamb *et al.*, 1987). There is also no evidence seen of an increase in lipid peroxidation from our *T. b. brucei* data.

Spermidine conjugated to glutathione has been found to increase as cells move into stationary phase of the growth cycle, but it is unclear whether this is a trigger for cytostasis or not (Shim and Fairlamb, 1988). Glutathionylspermidine was not detected in our assays, but if more spermidine is present then it may be that more glutathionylspermidine is being produced as the cells become stationary either exerting the effects of eflornithine or because of the effects of eflornithine. However, Fairlamb *et al.* found no increase in glutathionylspermidine over 48 hours (levels remain at approximately 0.25 nmol/10^8 cells) despite the approximate three fold reduction in spermidine (Fairlamb *et al.*, 1987).

Free lipids decreased after 24 hours and the cells became more permeable after 48 hours. The decrease in lipids at 24 hours may indicate an attempt to maintain the integrity of the membrane.

An increase in sedoheptulose and sedoheptulose phosphate was an interesting observation in eflornithine-treated cells, especially as the transketolase required to produce the four or five carbon sugars required for the synthesis of seven carbon sugars is not present in bloodstream forms of the parasite (Stoffel *et al.*, 2011). It could be that eflornithine treated cells are differentiating into stumpy forms and transketolase is being expressed. Quantitative PCR analysis of transketolase expression would be useful to investigate this hypothesis. An alternative source of erythrose 4-phosphate is evident, however, as this four carbon sugar can be detected within bloodstream form cells and in procyclic

cells with the transketolase gene knocked out (Michael Barrett, unpublished). A possible alternative route could be through phosphoketolase (Ingram-Smith *et al.*, 2005), although this enzyme is usually bacterial and no orthologues could be found in the trypanosome gene databases. This phosphoketolase would convert fructose 6-phosphate to phosphoacetate and erythrose 4-phosphate. The Bringaud group at the Centre National de Recherche Scientifique, Bordeaux, have noted a high rate of conversion of glucose to acetate, in support of this hypothesis (Frédéric Bringaud, personal communication).

It is unclear whether the increases in sedoheptulose and sedoheptulose phosphate are a specific response to eflornithine treatment or whether they are a general reaction in dying cells. An assay with toxic doses of nifurtimox did not reveal changes in sedoheptulose or sedoheptulose phosphate. This may mean that the two drugs have different mechanisms of killing.

4.3.2 Nifurtimox toxicity

Toxic doses of nifurtimox revealed alterations to lipids (both increases and decreases), sugars (decreases in sugars and sugar phosphates) and uracil and purines (increases). More work will need to be done do ascertain why these metabolites' levels are altered with nifurtimox treatment. One way to investigate whether there has been an effect on glycolysis, the TCA cycle and the pentose phosphate pathway could be to provide exogenous ribose, succinate or sugar phosphates to the cells to see if the effects of nifurtimox can be lessened in an alamar blue assay. The decrease in deoxyribose could also be linked to DNA synthesis or breakdown, although there is a negative correlation between the DNA bases and deoxyribose.

4.3.3 NECT

The nifurtimox-eflornithine combination therapy, which was previously assumed to be synergistic, was shown to be mildly antagonistic *in vitro* although a metabolomic analysis revealed that both of the drugs were able to exert their effects in the combination therapy and nifurtimox was still reduced to its active form. The combination therapy has not, as yet, revealed any antagonism in the field, although its use has been limited so far. A synergistic effect *in vivo* may

not be evident *in vitro* if nifurtimox increases eflornithine entry into the brain allowing more of the drug to reach the late-stage trypanosomes. Studies have shown that very little eflornithine actually enters the brain on its own (CSF levels are recorded at 68.9 μM during the normal monotherapy treatment regime (Milord *et al.,* 1993)), or in combination with nifurtimox in mice (10 - 40 nM using an artificial plasma perfusion with 1 μM eflornithine (Sanderson *et al.,* 2008)). It is however possible that nifurtimox could allow more entry of eflornithine across the blood-brain barrier in humans.

Another reason why the drug combination is not synergistic *in vitro* may be that downstream effects of nifurtimox may only be possible in dividing cells so when growth arrest is induced by eflornithine, nifurtimox's efficiency is reduced. This hypothesis was confounded with the antagonism seen with the other trypanostatic compounds NA42 and NA134, adenosine analogues developed by Boris Rodenko (Rodenko *et al.,* 2007). Metabolomic studies of NECT, however, revealed no major differences in nifurtimox reduction or the metabolome when compared the drugs tested in isolation.

The power of using metabolomics to elucidate the mode of action of a drug is very clear; assays can be untargeted and can reveal the action of the drug at a range of doses and time points. The sensitivity of the assays is, however, a double-edged sword. The number of metabolites detected will inevitably lead to some metabolites showing significant alterations by chance rather than due to biological significance, if the number of replicates is not adequate. Care must also be taken to verify the identity of all mass identifications as there are many artefacts, isomers and fragments in the datasets, even after very stringent processing through the mzMatch and IDEOM softwares.

The confidence of identification can be increased through the use of heavy label tracking. Cells can be cultured in medium containing heavy atoms in the form of a starter metabolite and this can be tracked through the cell in a resting state and after perturbation with a drug. In the case of eflornithine, heavy nitrogen could be tracked through the polyamine pathway from a starting metabolite of arginine in the growth medium. Rates of nitrogen incorporation could then be measured and compared with and without drug. If a build up of ornithine is toxic to the cells and they therefore have to produce acetylornithine to store the

ornithine then this incorporation would be observed. This technique has been tested before in *E. coli* and was shown to be very effective in tracking heavy ammonia through the folate pathway after treatment with trimethoprim (Kwon *et al.*, 2008).

As metabolomics technologies and data processing softwares become more advanced, the utility of a metabolomics experiment to provide a read out of the perturbations in a cell system are likely to become more and more obvious to biologists. The relative ease and cost of sample preparation in comparison to proteomics, transcriptomics and genomics methods will be an attraction to many, but a great deal of skill and care is still required in the analysis of metabolic data.

The advantages of metabolomics in the prediction of a mode of action of a drug should be obvious to anyone working in the pharmaceutical industry, but the low cost and ease of these assays will allow any lab scientist with access to a high resolution mass spectrometer to produce a list of metabolites altered in perturbation of a system.

5. Ornithine Biosynthesis in *T. b. brucei*

5.1 Introduction

The unexpected discovery of N-acetylornithine in trypanosomes during eflornithine mode of action studies (section 4.2.1.2) prompted the further investigation of the polyamine pathway to ascertain whether a new pathway may contribute to the production of ornithine.

Ornithine is a basic amino acid closely related in structure and charge to arginine and lysine (Fig 5-1). It is the second metabolite in the polyamine pathway where it loses a carboxyl group through the action of ornithine decarboxylase to become putrescine, which is in turn converted to spermidine and conjugated to two molecules of glutathione to form trypanothione, the trypanosome's main thiol (Fairlamb and Cerami, 1992). A thiol pool is imperative to all cells to react with damaging free radicals and protect them from oxidative stress. Blocking the polyamine pathway with eflornithine (an inhibitor of ornithine decarboxylase) in trypanosomes results in a cessation of the cell cycle and ultimately cell death.

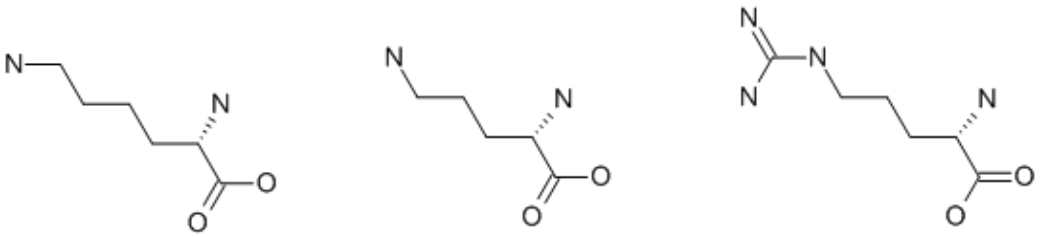

Figure 5-1. Lysine, ornithine and arginine (l-r). These basic amino acids are structurally related with a carboxyl group at one end and multiple amines at the other. Ornithine can be produced from arginine by the cleavage of a CN_2H_4 fragment, classically by the enzyme arginase.

The polyamine pathway in eukaryotes commences upon the uptake or synthesis of arginine. Arginine uptake has been shown to occur in *L. donovani* and in *T. cruzi*. In *L. donovani* the rate of uptake has been reported to occur via LdAAP3 (K_m 1.9 μM, V_{max} 16.9 pmol/min/10^6 cells) (Shaked-Mishan *et al.*, 2006) and in *T.*

cruzi via TcAAAP411 (K_m 30 μM) (Carrillo *et al.*, 2010). These rates are relatively low (c.f. a V_{max} of 1, 300 pmol/min/10^6 cells for high-rate glucose transport (Barrett *et al.*, 1998) or 6.4 pmol/min/10^6 cells for the low-rate transport of adenosine (Carter and Fairlamb, 1993), but the rate of arginine uptake and the fate of arginine within the African trypanosome has yet to be fully investigated.

Arginine is classically converted to ornithine by arginase, an enzyme of the urea cycle (Fig 5-2).

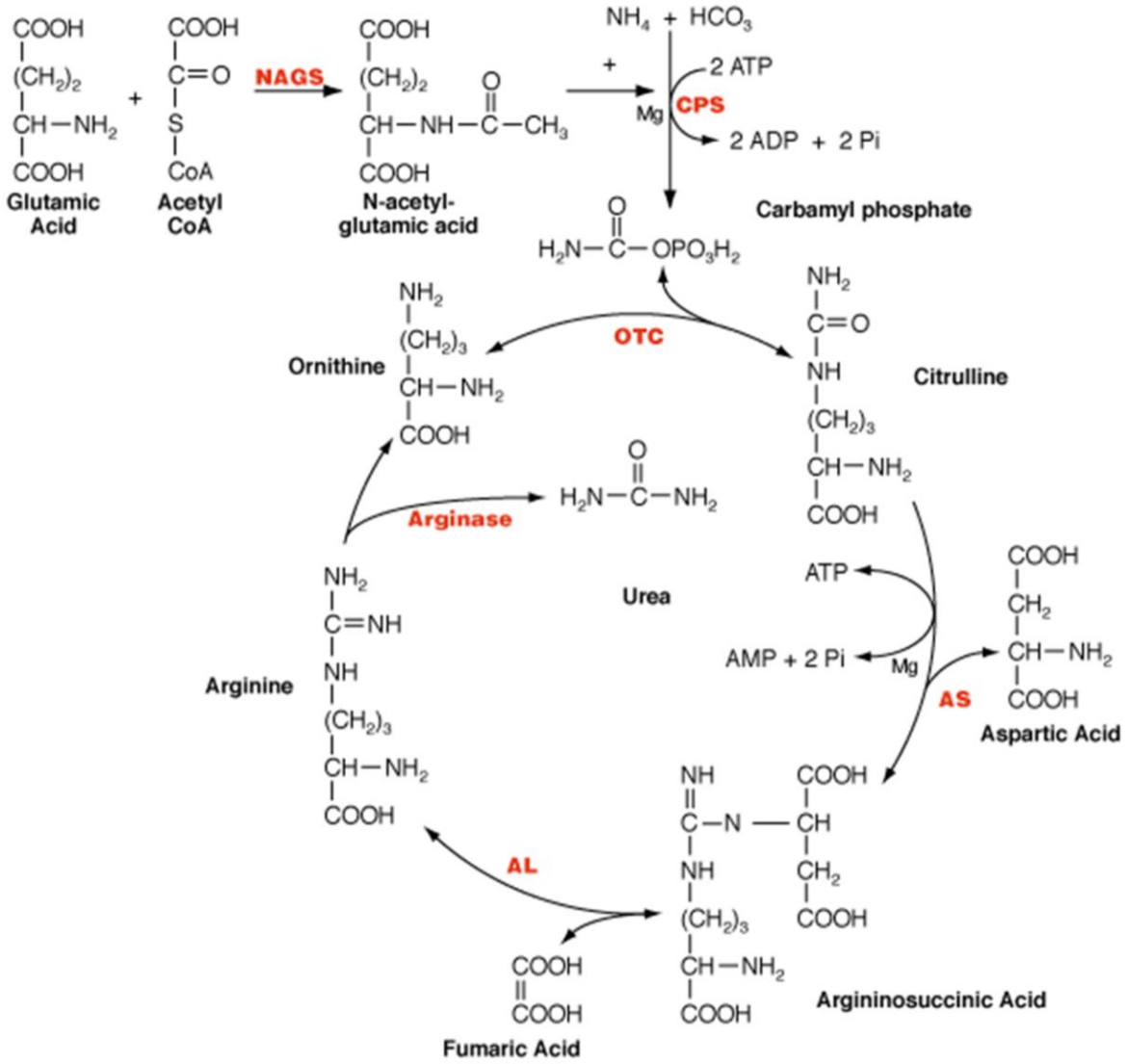

Figure 5-2.The urea cycle. Enzymes in red are NAGS: N-acetylglutamate synthetase, CPS: carbamoyl phosphate synthase, OTC: ornithine transcarbamoylase, AS: argininosuccinate synthetase and AL: argininosuccinate lyase. Adapted from Brusilow and Horwich (1995).

Vertebrates generally have two arginase enzymes (Arg I and Arg II, whereas microorganisms more often encode just one arginase (NCBI protein database). The branch at the top of the urea cycle (Fig 5-2) provides carbamoyl phosphate to produce citrulline from ornithine. If ornithine transcarbamoylase can operate in the reverse direction, then this may be an alternative source of ornithine, either from the uptake of citrulline or aspartate or indeed from arginine.

N-acetylornithine appears to correlate extremely closely with changes in ornithine levels after addition of eflornithine (see chapter 4). N-acetylation of ornithine as a sample preparation artefact is possible. However, it is clear that the acetylation is not an artefact of the ionisation process in these experiments for two reasons. One; acetylornithine and ornithine have different retention times and therefore any acetylation artefact must occur before entry into the column, which is unlikely as all enzymes are inactivated by the solvent. And two; when ornithine alone (or labelled ornithine in trypanosome growth medium) is added to the column, acetylornithine is not produced meaning a spontaneous non-enzymatic conversion is unlikely (data not shown). Furthermore, inspection of the *T. brucei* genome revealed the presence of a putative N-acetylornithine deacetylase (ArgE, Tb927.8.1910) predicted by sequence similarity to the *Leishmania* acetylornithine deacetylase-like genes LbrM.07.0280, LinJ.07.0430, LmjF.07.0270 and LmxM.07.0270. It is also syntenic with *T. b. gambiense* and *T. congolense* putative acetylornithine deacetylase genes. A putative aminoacylase (Tb927.1.3000) on TriTrypDB may also be able to acetylate ornithine, as has been seen in the *B. stearothermophilus* enzyme (which matches Tb927.1.3000 in a BLAST search with a score of p = 5.6e-61) (Sakanyan *et al.*, 1993).

N-acetylornithine is not a metabolite that has been observed in trypanosomes before. Indeed it has been predicted that only bacteria use N-acetylornithine in the conversion of glutamate to ornithine (Albrecht and Vogel 1964) (Fig 5-3). Although more recent data does predict a role of N-acetylglutamate synthase (NAGS) in mammals (a difference being that NAGS is inhibited in microbes and plants by arginine but stimulated in mammals (Caldovic *et al.*, 2010)). However, trypanosomes are not predicted to have any of the enzymes for the glutamate to ornithine pathway (aside from the putative acetylornithine deacetylase) annotated in the genome and simple BLAST searches of the bacterial protein sequences do not draw any hits (data not shown).

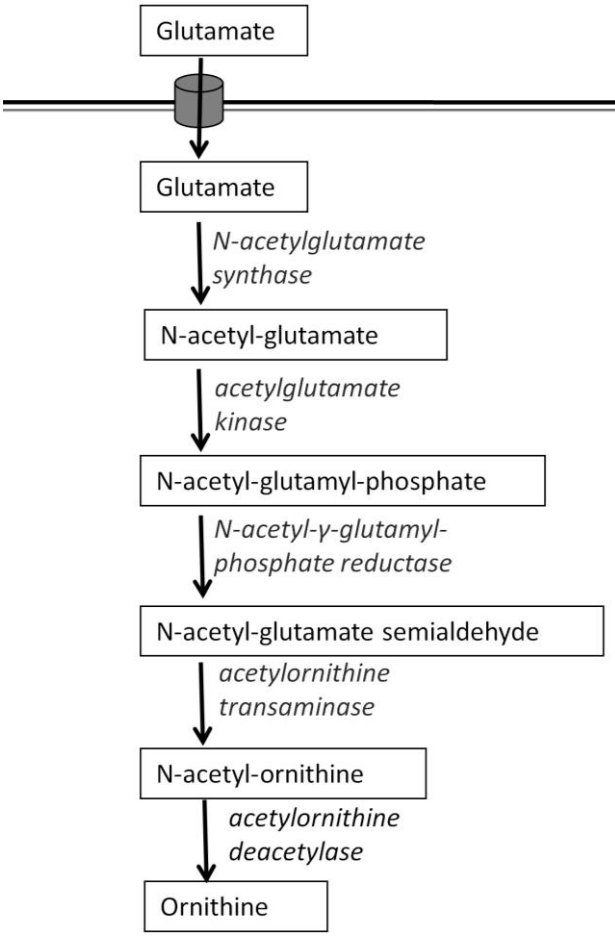

Figure 5-3. Ornithine biosynthesis from glutamate in *Escherichia coli*. The plasma membrane is represented by double line, metabolites are in boxes, enzymes are in italics. From Albrecht and Vogel (1964).

An enhanced understanding of the polyamine pathway may allow other synergistic compounds to be designed relieving the pressure on nifurtimox-eflornithine combination therapy (which has been shown not to be synergistic *in vitro*, so may not be the best combination to use in the field (see section 4.2.2 of this thesis)). The use of more combination therapies and more choice of drugs in general will reduce the risk of resistance occurring.

Arginase, the first enzyme in the classical ornithine synthesis pathway, has been studied in myriad organisms including *Helicobacter pylori* (Zhang *et al.*, 2011), *Staphyococcus saprophyticus* (Deutch, 2011), mammals (Cederbaum *et al.*, 2004) and fish (Joerink *et al.*, 2006;Srivastava and Ratha, 2010) but its role within trypanosomes is unknown. Arginase activity within the host has been shown to

be increased in the blood of mice upon trypanosome infection (Duleu *et al.*, 2004), but not in brain (Amrouni *et al.*, 2011).

Arginase has also been studied extensively in Leishmania species. It appears to be essential in *L. mexicana* promastigotes (Riley *et al.*, 2011), but not in *L. mexicana* amastigotes or *L. major* amastigotes (Gaur *et al.*, 2007;Muleme *et al.*, 2009). Furthermore, the recombinant protein has been expressed, purified and characterised biochemically (da Silva *et al.*, 2002;da Silva *et al.*, 2008). In *L. mexiana* and *L. braziliensis*, the arginase gene is located on chromosome 34 while in *L. major* and *L. infantum* it is on chromosome 35, which is the equivalent genomic position. The gene is missing in the syntenic region of *T. brucei*. Also within the arginase family of proteins are agmatinases and formiminoglutamases. There is an agmatinase-like gene predicted on chromosome 23 of the Leishmania species, and this does have a syntenic partner in *T. brucei* with the putative arginase at Tb927.8.2020 (also labelled as agmatinase in some databases, but as arginase in the *T. brucei* databases until 2010). Fomiminoglutamases hydrolyse N-formimidoyl-L-glutamate to L-glutamate and formamide and are not well researched in comparison to arginases and agmatinases.

5.2 Heavy isotope labelling

The non-targeted nature of global metabolomics can often reveal unexpected metabolites and pathways that are not predicted to be present from the genome of an organism. This is especially true in parasites as many more of the pathways are likely to result from salvaged precursors (Fairlamb, 1989).

The natural isotope pattern of metabolites is useful in the assignment of empirical formulae as the isotope ratio is unique to each element (Fig 5-4), but it can also be useful to track metabolites through a pathway. When done quantitatively and as a function of time this technique is known as fluxomics (Niittylae *et al.*, 2009).

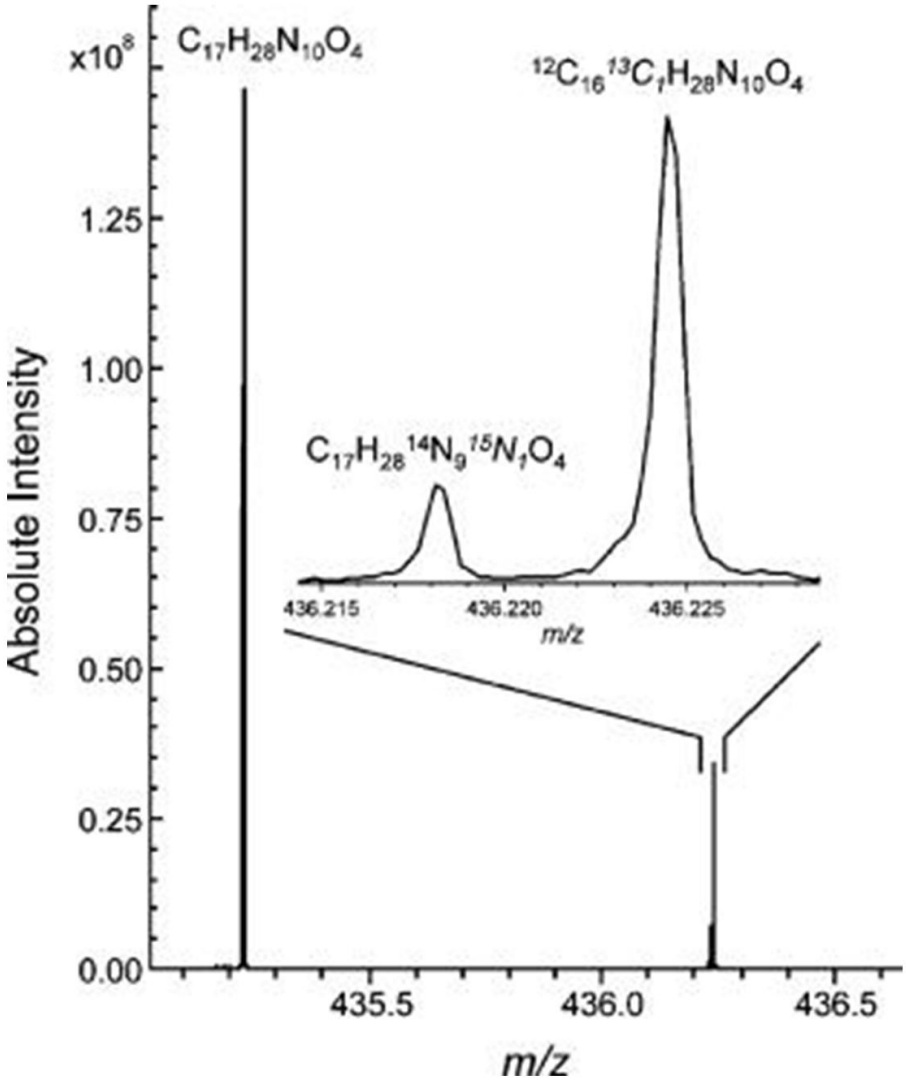

Figure 5-4. Isotope abundance patterns of guanamine (Miura *et al.*, 2010). Peaks related to the parent metabolite ($C_{17}H_{28}N_{10}O_4$) are detected approximately one atomic mass unit from the parent ion relating to the ^{13}C and the ^{15}N isotope. The ^{13}C and ^{15}N isotope labels can only be differentiated in high resolution instruments.

The McConville group in Melbourne, Australia, recently used ^{13}C labelled metabolites to interrogate central carbon metabolism in *L. mexicana* (Saunders *et al.*, 2011). They were able to track glucose, aspartate and alanine though glycolysis, the pentose phosphate pathway and the tricarboxylic acid cycle using NMR and GC-MS (Saunders *et al.*, 2011). These experiments provided a lot of information on the use of these pathways and gave indications as to the rates of these pathways; experiments that, without metabolomic techniques, would have taken a great deal more time and effort. In *T. b. brucei*, more focussed studies

using ^{13}C proline revealed differences in glucose metabolism depending on the carbon source used in procyclic forms (Coustou *et al.*, 2008).

In trypanosomes, Van Weelden *et al.* (2005) tracked radio-labelled glucose, glycerol, proline and threonine using HPLC to analyse catabolic and anabolic functions of the TCA cycle after growing procyclic trypanosomes in glucose-rich and glucose-deprived media. They found that the TCA cycle does not always operate as a cycle and instead distinct branches of the cycle provide separate anabolic and catabolic reactions. For example, in the presence or absence of glucose, proline is transported into the mitochondrion where it is broken down to ketoglutarate and ultimately succinate. The succinate is not further catabolised to fumarate, but is instead expelled from the cell (van Weelden *et al.*, 2005). Anabolic processes also occur from this "cycle". In glycerol and glucose-deprived medium the cells reduced succinate excretion and instead used the succinate to produce malate through fumarate. This malate was then thought to be used in the cytosol for production of phosphoenolpyruvate to provide energy for the cell. The formation of citrate from oxalacetate and pyruvate forms another branch of the cycle. The citrate is then used for the formation of acetyl-coA for fatty acid biosynthesis. The oxalacetate must, however, be formed through malate dehydrogenase (van Weelden *et al.*, 2005) meaning the malate branch of the cycle is not isolated from the other parts of the cycle.

To analyse ornithine biosynthesis, ^{15}N may be a more useful isotope label than ^{13}C as nitrogen is a less common element than carbon. This means that the natural isotope abundance will be lower compared to carbon, making the spectra easier to interpret. For tracking ornithine and subsequent polyamine synthesis it is also more beneficial to have the amine group labelled for following its fate through the polyamine pathway.

In this chapter I address the question: "how do trypanosomes obtain ornithine?". If ornithine can be produced via the deacetylation of N-acetylornithine then is N-acetylornithine part of an alternative route for ornithine production in trypanosomes? If this is the case, then what would be the role of arginase, a gene for which Tb927.8.2020 was annotated in the TriTrypDB as recently as

autumn 2010? The biosynthesis of ornithine is investigated using biochemical, bioinformatic and metabolomic techniques.

5.3 Results

In order to assess the contribution of arginase to the production of ornithine, Tb927.8.2020 (annotated as arginase in trypanosome gene databases until autumn 2010) was analysed at the sequence and biochemical levels.

5.3.1 Arginine uptake in bloodstream form T. b. brucei

In most eukaryotes arginine serves as a precursor to ornithine. We therefore measured the rate of uptake of this amino acid into trypanosomes. Arginine uptake in *T. b. brucei* appeared to show a biphasic uptake pattern suggesting that there were two transporters responsible for arginine transport; one low affinity and one high affinity. The low affinity transporter was analysed over a substrate range of 125 to 2,000 μM and the high affinity transporter over a substrate range of 1.25 to 80 μM arginine. The low affinity transporter gave an average apparent K_m of 1,169 ± 300 μM and a V_{max} of 91.6 ± 62.5 pmol/minute/10^6 cells. The high affinity transporter gave an apparent K_m of 26 ± 1.9 μM and V_{max} of 5.98 ± 2.78 pmol/minute/10^6 cells (Fig 5-5). Values are mean ± standard error of the mean.

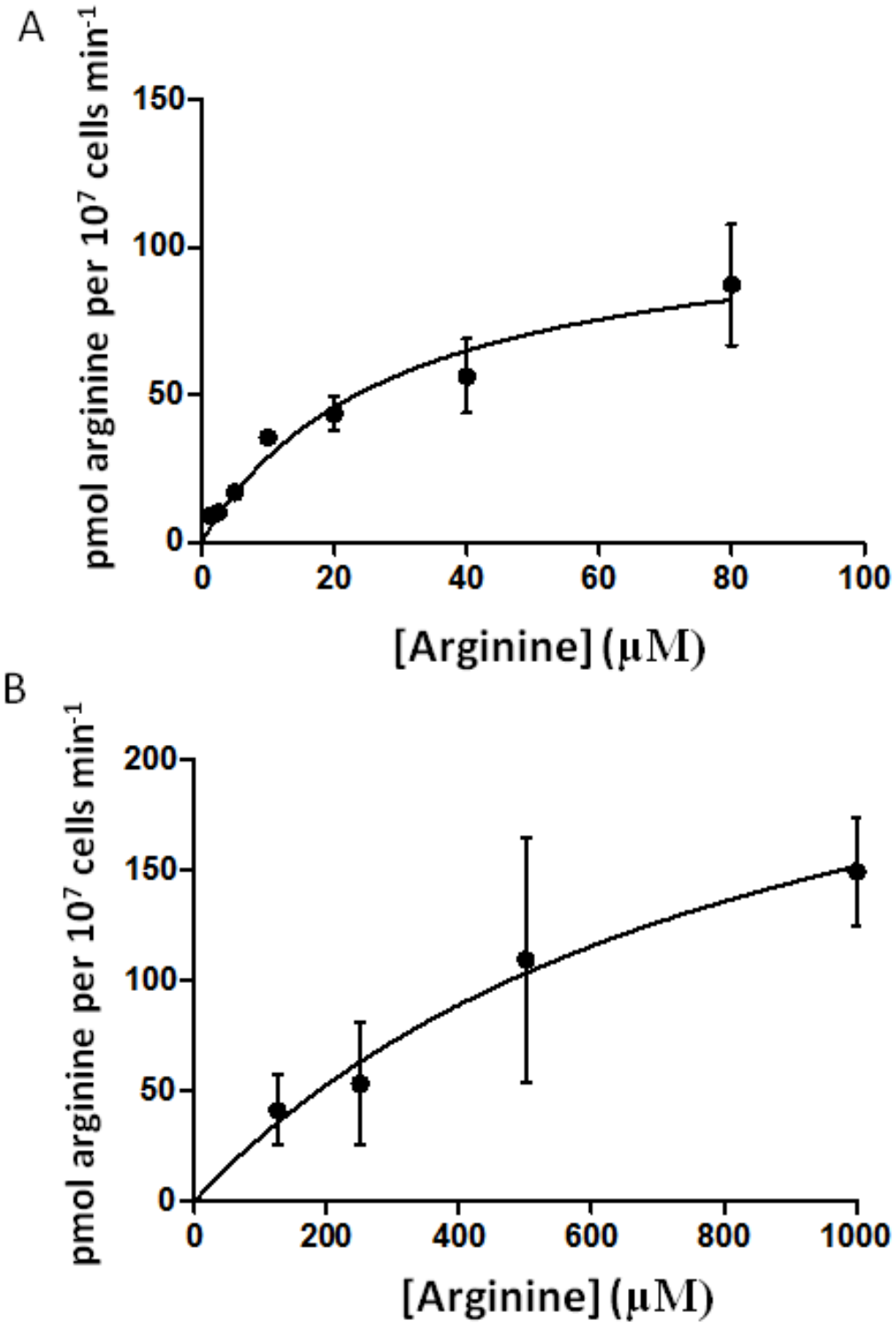

Figure 5-5. The uptake of arginine appears to use two transporters. A, Uptake via the high affinity transporter. B, Uptake via the low affinity transporter. Representative of two experiments for the low affinity and three experiments for the high affinity transporter. Error bars show standard error of the mean.

Both transporters show a higher K_m value than the *L. donovani* transporter (K_m 1.9 μM (Shaked-Mishan *et al.*, 2006)), but the high affinity transporter shows a

similar K_m to the measured constant in *T. cruzi* (30 μM (Carrillo *et al.*, 2010)). The higher Km would be expected as human blood serum levels range from 63 - 218 μM.

5.3.2 The trypanosome "arginase"

5.3.2.1 Arginase inhibitors do not work in *T. b. brucei*

Ornithine is classically created through the hydrolysis of arginine by arginase (EC: 3.5.3.1). If trypanosomes used this route, arginase inhibitors would be useful against HAT as they would be expected to synergise with eflornithine. Arginase inhibitors (2S-amino- 6-boronohexanoic acid, methyl 2S-amino- 6-boronohexanoic acid and 2S-amino- 6-boronohexanoic acid) were tested for activity against bloodstream-form trypanosomes. These compounds, which have shown activity against mammalian arginase (Christianson, 2005), did not kill trypanosomes in concentrations up to 100 μM (Kate Beckham, unpublished data). It may be that the concentrations of these inhibitors used were not high enough as another arginase inhibitor, N-hydroxy-nor-L-arginine, is used at 500 μM to inhibit macrophage arginase (Duleu *et al.*, 2004). However, purified Tb927.8.2020 (from heterologous expression in *E.coli*) enzyme produced no detectable arginase activity through mass spectrometry analysis of trypanosome growth medium with and without enzyme (Kate Beckham, unpublished data).

5.3.2.2 The *T. b. brucei* "arginase" gene is divergent from other conserved arginases

The gene in *T.b. brucei 927* was labelled as an arginase by sequence homology and synteny with a putative leishmania arginase is Tb927.8.2020 in TritrypDB. This gene has since been re-named as an agmatinase-like gene in some, but not all, of the databases as it is syntenic with an agmatinase-like gene in leishmania. The characterised *L. mexicana* arginase (LmxM.34.1480) (Riley *et al.*, 2011) is syntenic with *L. major, L. braziliensis* and *L. infantum* arginases, but is missing in *T. brucei*. The *T. b. gambiense* (Tbg972.8.1660), *T. congolense* (TcIL3000.8.2050) and *T. vivax* (TvY480.0801520) genes are still annotated as putative arginases.

Arginase amino acid sequences were compared between a range of species (Appendix 8-5) and a phylogenetic tree was produced using a neighbour-joining algorithm bootstrapped 1000 times (Fig 5-6). From the sequences included in the tree, the closest neighbours of Tb927.8.2020 were the *L. mexicana* agmatinase-like protein, which has not had its agmatinase activity confirmed, and the bacterium, *D. radiodurans,* agmatinase (a confirmed agmatinase (Ahn *et al.*, 2004)), but with the largest branch size in the tree with a distance of 2.227 (average substitutions per site) between the two genes, they are not close relatives.

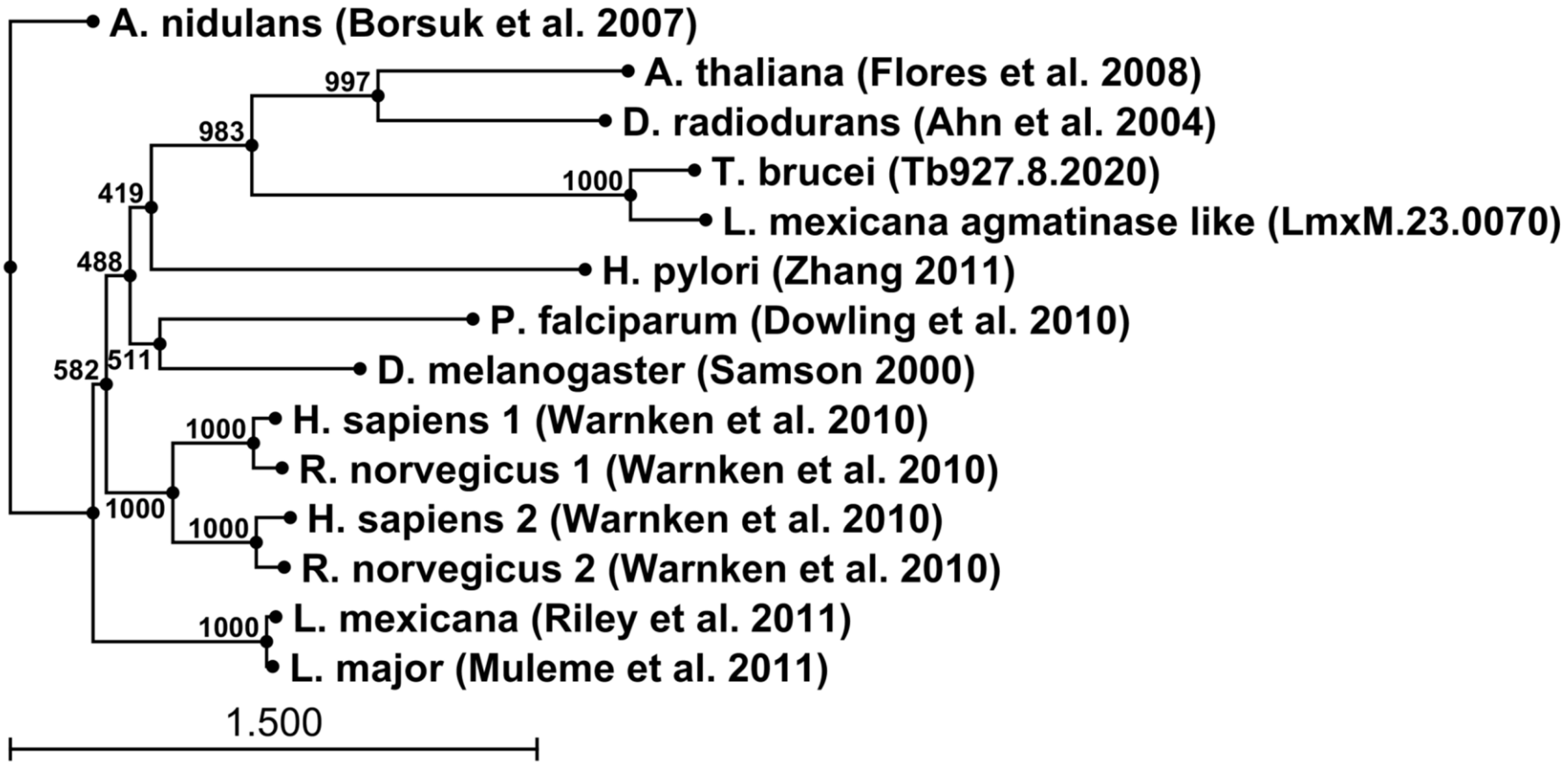

Figure 5-6. Cladogram of arginase amino acid sequences. A phylogenetic tree built on the amino acid sequences of confirmed arginases from a range of organisms. *T. b. brucei* shows the closest relationship to *Arabidopsis thaliana*. Numbers show bootstrap values out of 1000. The scale shows the branch length average as the rate of divergence (average number of substitutions per site). References for the confirmation of arginase activity are included in parentheses.

Work by Perozich *et al*. (1998) analysed the catalytic and structural residues in a range of amino acid sequences from the arginase family of proteins, which includes agmatinases and formiminoglutamases. Thirty one sequences were compared and the highly conserved residues were identified. These residues showed very little divergence (over 80 % conserved over the 31 family members) between family members and different species (Perozich *et al.*, 1998). The arginase alignment was compared to *T. b. brucei* at the sequence level. Many of the residues found to be structurally or functionally important by Perozich *et al*. were found to be missing in *T. brucei* (Table 5-1).

Conserved residue (human arginase 1 position)	Residue in Tb927.8.2020	Residue in LmxM.23.0070 (agmatinase-like)	Residue in LmxM34.1480 (arginase)	Function of residue in protein
Ser230	Ser222	Ser223	Ser241	Indirect metal binding
Asp274	Asp265	Asp266	Asp285	Indirect metal binding
His228	* Phe220	*Phe221	Met239*	Indirect metal binding
Pro14	* Asp18	Pro13	Pro21	Important for structural bends
Pro28	Pro25	Pro25	Pro35	Important for structural bends
Pro144	Pro160	Pro161	Pro157	Important for structural bends
Pro238	Pro230	Pro231	Pro249	Important for structural bends
Pro280	Pro271	Pro272	Pro291	Important for structural bends
Gly23	* -	*-	Gly30	Start of first α-helix
Gly142	* -	*-	Gly155	Important for structural bends
Gly178	Gly177	Gly178	Gly189	Hold metal ligands in place
Gly245	* Asp237	*Gln238	Gly256	Important for structural bends
Gly250	Gly242	Gly243	Gly261	Important for structural bends
His141	* -	*-	His154	Catalytic function
Asp100	Asp123	Asp124	Asp113	Structural
His101	* Gly124	*Gly125	His114	Metal-ligand
Asp234	* Ser226	Asp227	Asp245	Metal ligand
Glu256	* Asp248	*Asp249	Glu267	Subunit interaction
Arg255	Arg247	Arg248	Arg266	Structural
Ala243	Ala235	Ala236	Ala232	Structural
Arg180	Arg179	Arg180	Arg191	Hold metal ligands in place
Thr292	*Gly295	*Ser296	Thr303	Structural

Table 5-1. Highly conserved residues across the arginase family. Strictly conserved residues are shaded (from Perozich *et al.*, (1998)). Equivalent *T. b. brucei* residues predicted from an alignment in CLC workbench. * denotes a change from the conserved human residue. Tb927.8.2020 and LmxM.23.0700 show 225/332 Identity, Tb927.8.2020 and human arginase I show 58/332. Human arginase and *L. mexicana* arginase show 204/332 identity.

Of the four most highly conserved residues within the arginase family, three were altered or missing in Tb927.8.2020. Gly23 in the *H. sapiens* arginase begins the first α-helix in all the arginases compared in Perozich's study (1998) and is strictly conserved, but is absent in the *T. b. brucei* sequence.

His141 is present in all members of the arginase family apart from two formiminoglutamases. Mutations to this residue (Cavalli *et al.*, 1994;Vockley *et al.*, 1996) have shown that it probably serves a catalytic function. This is further supported by its side chain's close proximity to the water molecule which bridges two manganese atoms (discovered through site-directed mutagenesis). This residue is therefore thought to be a proton shuttle during the catalysis of arginine (Kanyo *et al.*, 1996; Perozich *et al.*, 1998). This residue is completely absent in the *T. b. brucei* sequence and the *L. mexicana* agmatinase-like sequence, but is replaced with a tryptophan in the *D. radiodurans* sequence. It is therefore unlikely that Tb927.8.2020 would be able to catalyse arginine metabolism in the same way as other arginases.

The side chain of Glu256 falls just 2.9 Ångströms away from the Arg255 of a different subunit and is therefore thought to be integral in interactions between arginase's multiple (rat and human arginases are homotrimers (Perozich *et al.*, 1998;Di Costanzo *et al.*, 2005)) subunit interactions. The *T. b. brucei* enzyme has substituted Glu256 for Asp248. As aspartate has a shorter side chain than glutamate this may mean that the subunits cannot complex together properly, but without a crystal structure of Tb927.8.2020, this cannot be tested.

Arg180 holds his101 and Asp234 in place for metal binding as well as helping to maintain the overall structure of the enzyme (Perozich *et al.*, 1998) and is conserved in the *T. b. brucei* enzyme.

Studies on the substrate specificity of arginase have found that hydrogen bonding between Thr135 and Asn130 are both essential to allow arginine binding in the active site. Agmatine binds 11 fold less well at this site. Site-directed mutagenesis of Asn130 to Asp130 reduces the binding affinity of arginine nine fold, while producing no effect on agmatine binding (Carvajal *et al.*, 1999; Alarcon *et al.*, 2006) . Tb927.8.2020 and LmxM.23.0070 (the leishmania agmatinase-like protein) both lack Thr135. A confirmed agmatinase from *D.*

radiodurans (an extremophilic bacterium (Ahn *et al.*, 2004)) does, however, have a threonine in this position. Tb927.8.2020 has a serine at position 130 and LmxM.23.0070 has a glutamate, while the *D. radiodurans* agmatinase is missing this residue altogether providing further evidence that the predicted enzymes are not able to bind arginine.

The main difference found between human arginase and the *D. radiodurans* agmatinase appears to be in loops four and five flanking the active site (Shishova *et al.*, 2009). Residues from loops four and five in the *D. radiodurans* agmatinase (Asn153,Tthr155, Gly183, Asp187 and Ala190) do not, however, match the loops in the leishmania agmatinase-like sequence (-, -, Cys181, Ser183 and Asp186) or Tb927.8.2020 (-, -, Gln180, Ser182 and Asp185).

Tb927.8.2020 has many residues in common with the *L. mexicana* agmatinase-like protein sequence, which are different to the conserved arginase family residues and from the *D. radiodurans* agmatinase. This would suggest that trypanosome and leishmania genes do not code for arginases or agmatinases. No structural or activity research on formiminoglutaminases could be found in the literature so confirmed amino acid sequences could not be obtained and aligned with Tb927.8.2020. The function of this putative enzyme remains unknown. It would be interesting to knock out the gene to see if a function can be ascribed to it. The protein could also be heterologously expressed and characterised using metabolomic approaches.

5.3.2.3 *T. b. brucei* has negligible arginase activity

The overwhelming sequence data evidence suggests that TB927.8.2020 is not an arginase, or indeed a member of the greater arginase family, which includes agmatinase and formininoglutaminase. It does not, however, prove that there is an absence of arginase activity in bloodstream form *T. b. brucei*. To quantify arginase activity within the bloodstream form trypanosome a commercial arginase assay kit was used comparing the amount of urea produced over two hours in a cell extract. *T. b. brucei* extracts were compared to *L. mexicana* and published rat and human extracts. Results are summarised in table 5-2.

Species	Arginase activity (Units/L)
T. brucei brucei	*0.128* ± 0.206
L. mexicana	*19.704* ± 0.841
R. norvegicus plasma (from literature in assay kit)	*322*
H. sapiens plasma (from literature in assay kit)	*0.88*

Table 5-2 Arginase activities of *T. b. brucei* and *L. mexicana*. A unit is defined as 1 µmole of arginine converted to ornithine and urea per minute at pH 9.5 and 37ºC. N = 3. Results show mean ± S.E.M (n = 3).

T. b. brucei has very low arginase activity in bloodstream forms. It has been shown that some parasites upregulate arginase activity upon infection of a mammalian host in order to diminish arginine pools, decreasing the ability of nitric oxide synthase to produce toxic nitric oxide (an alternative product of arginine metabolism) from arginine (e.g. *Salmonella* (Lahiri *et al.*, 2008), *L. mexicana* (Gaur *et al.*, 2007), *L. major* (Iniesta *et al.*, 2005), *Helicobacter pylori* (Gobert *et al.*, 2001) and hepatitis C (Cao *et al.*, 2009)). Upregulation of arginase to increase conversion of host arginine to ornithine has also been observed in *P. falciparum*-infected red blood cells (Olszewski *et al.*, 2009). These adaptations protect pathogens from toxic nitric oxide and increase the amount of ornithine available to make polyamines, further protecting them from oxidative stress. This does not seem to be the case in trypanosomes, however, because inducible nitric oxide synthase knock outs in mice have no effect on *T. cruzi* infections (Cummings and Tarleton, 2004) and arginase activity does not even seem to be present in *T. b. brucei*. Duleu *et al.*(2004) have shown that mice are more susceptible to trypanosome infection if arginase I and II expression by macrophages is increased, the increase in expression appearing to be induced by the trypanosomes (Duleu *et al.*, 2004). The arginase activity was shown to result in a reduction in nitric oxide production, probably through the diversion of arginine away from nitric oxide synthase (Duleu *et al.*, 2004), but would also result in more ornithine for uptake by the trypanosome.

Foetal calf serum used in the lab is heat inactivated at 55 °C for half an hour, but it has been shown that bovine arginase only loses half its activity at 77 °C over 10 minutes (Rossi *et al.*, 1983). The arginase activity detected in trypanosomes is very low and there could potentially be arginase activity carried over from the foetal calf serum (FCS) that the cells are grown in. Arginase assays on heat-inactivated (-0.204 units/L (a negative value is likely due to variation around a level of 0, rather than a decrease in urea)) and non heat-inactivated FCS (0.469 units/L) (one unit is defined as 1 µmole of arginine converted to ornithine and urea per minute at pH 9.5 and 37 °C) revealed similar low levels of activity to the *T. b. brucei* cells, which are likely to be negligible variance around zero activity.

Another test was used to ascertain whether there is arginase activity in the medium or not. Isotopically labelled arginine (four ^{15}N labels) was added to HMI-9 with 10 % FCS (heat inactivated) and to FCS (heat inactivated) alone and left for two hours (Fig 5-7). Cells washed four times in CBSS were also tested for one hour.

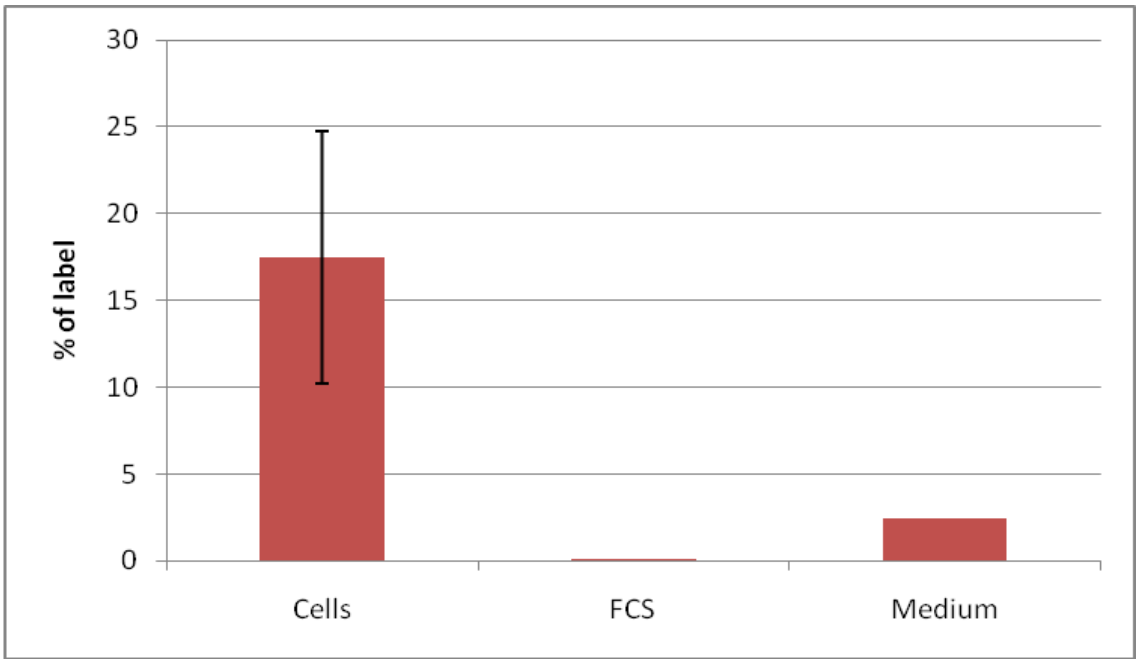

Figure 5-7. Heavy ornithine production from heavy arginine in medium. FCS: foetal calf serum, medium is the trypanosome growth medium (HMI-9 + 10 % FCS), Values show the percentage of label (2 labels, M+H: 135.0988, RT: 25.7 minutes) compared to non-labelled ornithine (M+H: 133.1047, RT: 25.7 minutes). N = 3. Error bars show the standard error of the mean.

Labelled ornithine was detected in the washed cell sample and in the HMI-9 + FCS sample albeit at very low levels, but not in the FCS alone. There should be no enzymatic activity in the HMI-9 so it must be the FCS that is causing the conversion, but why there is no conversion in the FCS alone is unclear. It is possible that there are cofactors required for arginase activity that are available in the medium, but not in the FCS. Manganese is known to be required for arginase activity and is an essential component of the arginase activity kit. It is also possible that arginase inhibitors present in the serum are diluted out in the whole medium, allowing previously blocked activity to recommence.

Labelled ornithine was detected in the cell samples that had been washed thoroughly (three replicates) (Fig 5-7), confirming that cells are able to convert arginine to ornithine, although without producing urea, which would have been detected in the assay kit.

5.3.3 The production of Ornithine

In the absence of arginase, there may be many routes biochemically able to produce ornithine. Some species of bacteria are able to convert glutamate to ornithine via acetylglutamate and acetylornithine (Fig 5-3) (Albrecht and Vogel, 1964). The only enzyme of this pathway found in trypanosomes, acetylornithine deacetylase (Tb927.8.1910) was successfully knocked out indicating that it is not essential in normal bloodstream form *in vitro* growth conditions (Eduard Kerkhoven, unpublished data). The recombinant protein was expressed in *E. coli,* purified and was shown to have significant deacetylase activity on several amino acids (Eduard Kerkhoven, Darren Creek and Felicity Lumb, unpublished data) but it remains to be seen whether N-acetylornithine, ornithine or polyamine levels are altered in the knock out line.

Heavy isotope distribution patterns were used with several amino acid precursors to determine the possible route(s) of ornithine biosynthesis. Data was collected in positive and negative ionisation modes, but polyamine relative levels were acquired from positive mode data as the amine groups are more readily ionised in positive mode. An untargeted approach using the IDEOM software was used to search for labelled metabolites (see section 2.2.3.1),

followed by a more quantitave analysis of the relative intensities of the metabolites using Thermo QuanBrowser.

5.3.3.1 Glutamate distribution

To assess whether glutamate might serve as a precursor of ornithine via the bacterial-like pathway (Fig 5-3) in *T. b. brucei,* ^{15}N labelled glutamate was added to bloodstream form cells in CBSS buffer and the isotope distribution was analysed after two hours. Glutamate was not taken into the cells to any appreciable level (data not shown) over the time frame (two hours) and the conditions (in CBSS at room temperature) used so no isotope distribution was observable. This could indicate a lack of glutamate transport, although glutamate transport in *T. b. brucei* has been measured in the past at a relatively low K_m of 158 μM and a V_{max} of 36 pmol/minute/10^6 cells (Hasne, 2000) (which is between the values of the two arginine transporters measured here).

The uptake of glutamate in *L. mexicana* was also seen to be very low in nutrient-rich conditions with more glutamate produced (from glucose, aspartate and alanine) through the TCA cycle than taken up (Saunders *et al.*, 2011). Abrogation of the TCA cycle using sodium fluoroacetate, resulting in growth arrest, is rescued by exogenous glutamate underlining the importance of glutamate to normal cell growth in these parasites (Saunders *et al.*, 2011). It is thought that the glutamate transporter is expressed at low levels during periods of nutritional abundance to prevent leakage of intracellular glutamate, but that this transporter can be upregulated when required.

Trypanosome intracellular glutamate pools may also be replenished through synthesis from other amino acids (and possibly glucose if the Saunders data is corroborated) rather than through uptake.

5.3.3.2 Glutamine distribution

Glutamate can be produced via the removal of an amine group from glutamine by glutamine synthetase (EC 6.3.1.2) or glutaminase (EC 3.5.1.2 or 3.5.1.38). To test this theory, ^{15}N-labelled glutamine was applied to bloodstream form cells. The isotope distribution is shown in figure 5-8.

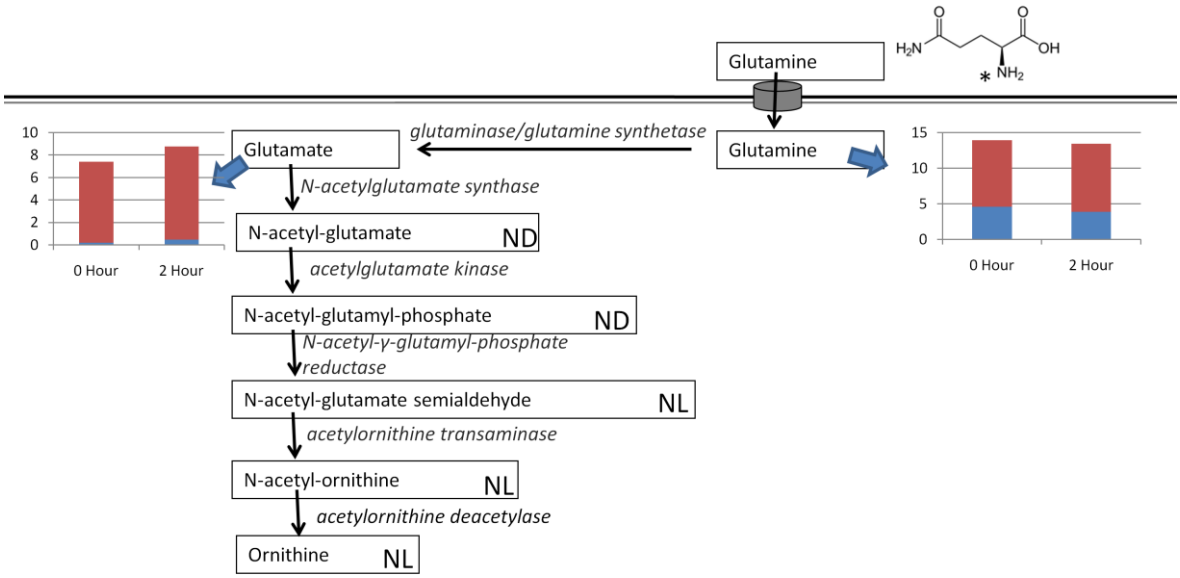

Figure 5-8. The isotope distribution of glutamine in ornithine biosynthesis. Metabolites are shown in boxes, enzymes in italics. Bar charts show the relative intensity (area under the curve (divided by 10^7)) of ^{14}N (red) and ^{15}N (blue) metabolites. ND: not detected, NL: not labelled. Glutamine is detected at M+H: 147.0764 (^{14}N) or 148.0734 (^{15}N), RT: 15.7 minutes. Glutamate is detected at M+H: 148.0604 (^{14}N), 149.0575 (^{15}N), RT: 14.6 minutes. N-acetylglutamate semialdehyde: M+H: 190.0710, RT: 5.5 minutes, acetylornithine: M+H: 175.1077, RT: 14.5 minutes, ornithine: M+H: 133.0972, RT: 22.9 minutes. N = 3.

Glutamate was labelled after two hours at 5 % of the ^{14}N isotope level. As the ^{15}N natural isotope abundance is 1 % and no labelled glutamate was detected in the control (HMI-9 plus FCS without cells) samples (data not shown), then this represents a significant amount of label and shows glutamine is taken into trypanosomes and converted to glutamate.

Human glutaminase is thought to exist in two isoforms, termed the kidney and liver glutaminases (Erdmann *et al.*, 2009). In most mammals kidney glutaminase is known to be localised to the mitochondrion while liver glutaminase was shown to be localised to the nuclei of rat and monkey brains (Olalla *et al.*, 2002). A simple search for glutaminase in TriTrypdb reveals no annotated trypanosome gene and a BLAST search with rat glutaminase produces no trypanosome hits. A BLAST search with *Ferrimonas balearica* DSM 9799 glutaminase gives a very high p-value of 0.993 with a *T. b. brucei* gene termed “kinetoplastid-specific dual specificity phosphatase, putative” (Tb427.10.10670). It is very unlikely that this protein would have any glutamine deaminase function.

If glutaminase were present and were also located in the mitochondrion of *T. b. brucei,* separating the glutamate from other polyamine pathway enzymes (in *L. major,* trypanothione synthetase is located in the cytosol (Oza *et al.*, 2005) and the trypanothione peroxidise system in *T. brucei* has been shown to be cytosolic (Tetaud *et al.*, 2001) although the location of all the enzymes in *T. brucei* have yet to be determined), then further conversion to ornithine may be prevented. This would only be true, however, if glutamate were to be retained within an organelle, which is unlikely as it in required in many cellular processes including protein synthesis.

Glutamine synthetases are ubiquitous and are found in all domains of life with three isoforms distinguishable by length (360, 450 and 730 amino acids) and many organisms having multiple isoforms (van Rooyen *et al.*, 2011). A putative glutamine amidotransferase is annotated in TriTrypdb at Tb927.7.2100. Amidotransferases usually add an NH_2 group to an acceptor (rather than removing the NH_3 from glutamine) but it is possible that they could work in the reverse direction and remove an amide if thermodynamically favourable (Keq > 800 (Benzinger and Hems, 1956)). Tb927.7.2100 appears to be expressed in bloodstream and insect stages of the *T. brucei* life cycle (from TriTrypDB) but exhibits no loss of fitness when knocked down (Alsford *et al.,* 2011).

Other members of the pathway in figure 5-3 including acetylglutamate and N-acetyl-glutamyl phosphate could not be detected with the mass spectrometry platform used. This may be due to low levels in the trypanosome, poor ionisation or poor stability, or they may be absent. N-acetyl-glutamate semialdehyde, acetylornithine and ornithine were unlabelled after two hours, which is probably due to the non-existence of the pathway, although the conditions of the experiment (cells in CBSS at room temperature for two hours) might also influence this. In all, the fact that the orthologues of the key enzymes are absent, as are the key intermediates added to the fact that ^{15}N-glutamine does not distribute to ornithine suggests that this pathway is unlikely in *T. b. brucei*.

5.3.3.3 Proline distribution

Another route to produce glutamate commences with the uptake of proline. Proline dehydrogenase (Tb927.7.210) converts L-proline to L-1-pyrroline 5-

carboxylate, which is then oxidised by pyrroline 5-carboxylate dehydrogenase (putative at Tb927.10.3210). This also occurs within the mitochondrion (Coustou *et al.*, 2008), so if glutamate is not further metabolised into the polyamine pathway then this would support the theory that glutamate is isolated from the polyamine pathway enzymes.

The ^{15}N amine distribution from proline was analysed in bloodstream form trypanosomes to detect conversions to glutamate and ascertain whether proline-derived glutamate can be converted further to ornithine (Fig 5-9). Procyclic form trypanosomes were also studied for comparative purposes.

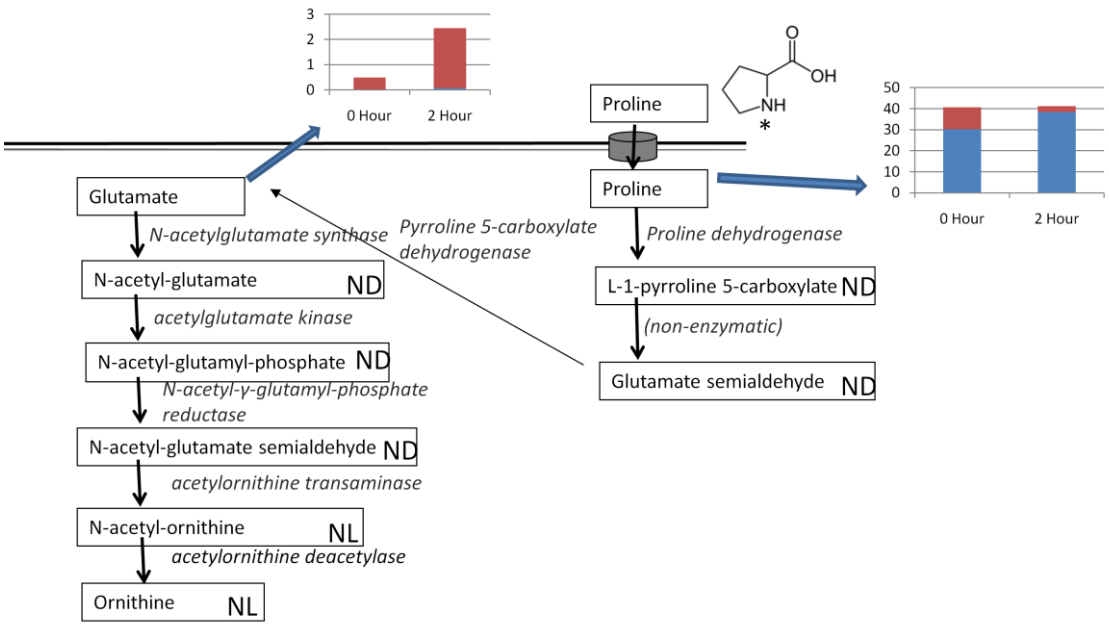

Figure 5-9. The isotope distribution of proline in ornithine biosynthesis. Metabolites are shown in boxes, enzymes in italics. Bar charts show the relative intensity (area under the curve (divided by 10^7)) of ^{14}N (red) and ^{15}N (blue) metabolites. ND: not detected, NL: not labelled. Proline is detected at M+H: 116.0706 (^{14}N) or 117.0676 (^{15}N), RT: 16.6 minutes. Glutamate is detected at M+H: 148.0604 (^{14}N), 149.0575 (^{15}N), RT: 17.9 minutes. Acetylornithine is at M+H: 175.1077, RT: 17.9 minutes and ornithine is at M+H: 133.0972, RT: 27.5 minutes. N = 3

In bloodstream form trypanosomes the ^{15}N label from proline was detected in glutamate, but at only 3.1 % of the ^{14}N label after two hours. This represents a slight increase from 1.9 % at 0 hours and ^{15}N glutamate is not detected in the CBSS buffer. The fact that heavy glutamate is only detected at 0.17 % in samples where no label was added indicates that the 1.9 % seen may be due to a very fast uptake of proline and conversion to glutamate at the “0 hour” time point.

The first stage in the processing of the 0 hour time point involves a cooled centrifugation step (method 2.2.1) that should stop enzyme activity, but samples do not cool immediately in the centrifuge and are still in contact with the medium including heavy substrate so some enzymatic activity may still be taking place. However, since levels of heavy glutamate after two hours are still not very high, a rapid conversion seems unlikely and the high background at the 0 time point remains unexplained.

Levels of unlabelled glutamate in the two hour samples are increased. This may indicate a back-conversion of glutamate from another metabolite or from protein and may explain why the percentage of ^{15}N label is relatively low. The increase in glutamate is mirrored in many amino acids (methionine, ornithine, arginine, leucine/isoleucine, valine, tyrosine and glutamine) but not all (phenylalanine, tryptophan, histidine and lysine do not change and alanine, serine, asparagine and threonine show a decreasing trend). If the increase in glutamate were due to an increase in protein degradation then you would expect all amino acids to display a similar trend, but this is not the case so the increase is more likely due to a metabolic change. The decreases in amino acids are probably due to a decrease in uptake from medium, as CBSS has no amino acid additives.

Saunders *et al.* recently showed that the TCA cycle is used to sustain levels of glutamate within *L. mexicana* promastigotes (the insect stages). Glucose, aspartate and alanine were all converted to glutamate under normal culture conditions and inhibition of mitochondrial aconitase (required to convert citrate to ketoglutarate) caused a depletion in glutamate that lead to growth arrest that was rescued with exogenous glutamate (Sauders *ét al.*, 2011). It may be that when trypanosomes are kept in glutamate-free medium (CBSS) for too long then they too need to produce more glutamate through the TCA cycle and through glutamine and proline. The uptake of glutamate in bloodstream form trypanosomes does not appear to be very efficient (see section 1.3.3.1) so levels may have to be maintained through anabolic or catabolic processes within the trypanosome.

The IDEOM software also detected the heavy label in alanine (M+H: 90.0549 (^{14}N), 91.0519 (^{15}N), RT: 18.0 minutes) at 28 % of the unlabelled after two hours.

Alanine could be an artefact caused by the fragmentation of proline or glutamate. If this were the case then the retention time of alanine (18.0 minutes) would match the retention time of proline (16.6 minutes) or glutamate (17.9 minutes). As the retention times of glutamate and alanine are very similar, it cannot be determined whether the alanine is a fragment of glutamate or if it occurs enzymatically, but as the percentage of incorporation is higher than that for glutamate it can be assumed that the alanine peaks are not fragments. It has been shown that glutamate donates a nitrogen to pyruvate to produce alanine through L-alanine aminotransferase (Tb927.1.3950) (Fig 5-10) in procyclic trypanosomes, but this mechanism is not thought to exist in bloodstream forms of the parasite (Coustou *et al.*, 2008). Derek Nolan's lab in Dublin, Ireland found that alanine aminotransferase knockouts could not be created in bloodstream-forms, although high levels of RNA knock down resulted in no growth phenotype (Spitznagel *et al.*, 2009), which indicates that alanine aminotransferase is important to bloodstream form trypanosomes, but very low levels are sufficient to maintain metabolic activity.

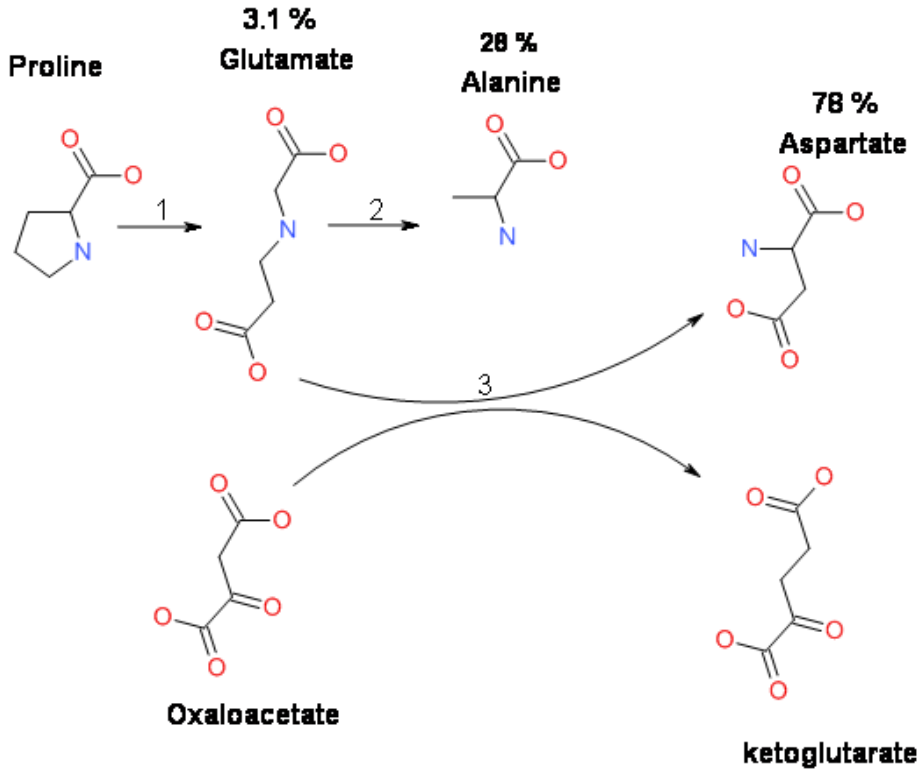

Figure 5-10. The amine group from proline can be tracked to glutamate, aspartate and alanine in bloodstream cells. 1: Pyrroline dehydrogenase and Pyrroline carboxylate dehydrogenase, 2: TCA cycle to pyruvate and alanine aminotransferase, 3: aspartate aminotransferase. Percentages show the incorporation of heavy label as a percentage of unlabelled amino acid after two hours in heavy proline.

Other data from our laboratory shows that ^{13}C-labelled glucose produces high levels of alanine in bloodstream form trypanosomes (Jana Anderson, University of Glasgow) as did early NMR experiments by Neil Mackenzie (Mackenzie *et al.*, 1983). This suggests that the endpoint of bloodstream form glycolysis may not always be pyruvate as has previously been thought (Opperdoes and Borst, 1977;Bakker *et al.*, 1997;Bringaud *et al.*, 2006).

Glutamine was also found to be labelled after two hours of ^{15}N-proline exposure in bloodstream form parasites, but at levels of incorporation at only 1.3 % of unlabelled, the levels were not significantly higher than the expected natural isotope abundance of 1 %. Aspartate (M+H: 134.0447 (^{14}N), 135.0417 (^{15}N), RT: 18.63 minutes) was heavily labelled at 78 % of unlabelled after two hours. Oxaloacetate can be transaminated from any donor amino acid by L-aspartate aminotransferase (Tb927.10.3660) to form aspartate. If oxaloacetate is generated from glutamate then ketoglutarate would be formed that could feed into the TCA cycle producing energy or other metabolites. This may be the case in procyclic forms, where aspartate was labelled at 118 % of unlabelled, but in bloodstream forms the TCA cycle is not thought to be active (Durieux *et al.*, 1991). Recent evidence, however, indicates that many of the enzymes of the TCA cycle are active, at least in cultured bloodstream forms (Jana Anderson, unpublished data), hence it is possible that the cycle is operative in cultured forms of the bloodstream-form parasite. Ketoglutarate (not detectable with our mass spectrometry method due to its high acidity) is a metabolite that is involved in many reactions, but usually as an end product, so the reasons for its hypothesised production increase in bloodstream forms is unclear.

In procyclic forms of the parasite the same experimental setup resulted in greater incorporation of the label into glutamate (75 % of unlabelled), which could be tracked further into glutathione (17 %) and trypanothione disulphide (10 %). Glutamine was also labelled at 4.7 % and alanine had a greater incorporation than bloodstream forms at 81 %. Procyclic forms of the parasite have been shown to use proline as a carbon source when glucose is not available, reflective of the nutrient situation in the tsetse midgut (Coustou *et al.*, 2008). The proline is converted to glutamate and further to ketoglutarate (Coustou *et al.*, 2008), which enters the tricarboxylic acid cycle. This may provide energy for the cell or may be part of a reduced cycle providing, for example, citrate to be

converted to acetate for lipid synthesis (van Weelden *et al.*, 2005). The greater incorporation of label into glutamate is likely to be due to this different energy source requirement in procyclic trypanosomes and the increased glutamate was able to disseminate its amine group down the polyamine pathway into glutathione and trypanothione. Unfortunately, incorporation into the tricarboxylic acid cycle cannot be tracked as the heavy nitrogen is lost on aspartate during the formation ketoglutarate.

The proline to glutamate pathway is in the mitochondrion of procyclic form trypanosomes. From this data it is clear that compartmentalisation of this pathway does not hinder further progress to trypanothione in insect stages. Glutamate was labelled in both stages of the parasite, but the label was not incorporated into ornithine in either stage. This does not disprove the existence of a glutamate to ornithine pathway in trypanosomes, but shows that it was not active in the conditions used and makes it less likely that acetylornithine is produced in this way.

5.3.3.4 Lysine distribution

Gaston *et al*. (2011) showed recently that lysine can be used to produce methylornithine through PylB, which may in turn become demethylated to become ornithine in the pyrrolysine pathway (Fig 5-11). ^{15}N-lysine was therefore assessed for its potential contribution to the polyamine pathway with a conceivable route through methylornithine in *T. brucei*.

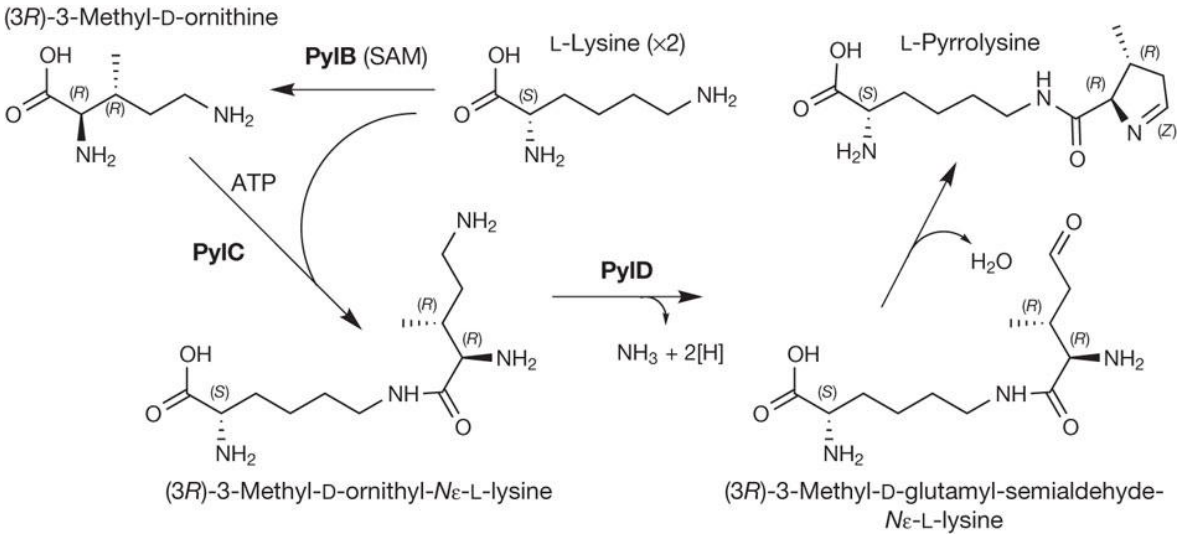

Figure 5-11. Lysine can be converted to methylornithine via PylB in *Methanosarcina spp*. SAM: S-adenosyl methionine, used in the conversion of lysine to methylornithine. From (Gaston *et al.,* 2011).

The heavy label was not found to be passed on to any of the polyamine metabolites during the two hour assay, nor was it passed on to any other metabolite detected by IDEOM. As methylornithine has the same mass as lysine (it is a stereoisomer) and a very similar predicted retention time on the HILIC column (a retention factor of 2.5 compared to 2.4 for lysine (from the Sequant retention time predictor at www.sequant.com/prediction)), it was not possible to ascertain whether heavy methylornithine had been obtained. A retention time more specific for the University of Glasgow metabolomic platform could be obtained by running a standard for methylornithine through the apparatus, but as it is likely that this would be difficult to separate from lysine and ornithine was not labelled in this experiment this avenue was not pursued.

A search for genes annotated with pyrrolysine or PylB in kinetoplastids revealed no hits and a BLAST search with the *Methanosarcina barkeri* PylB protein sequence (GenBank accession: AAL40868.1) produced just one hit of a probability of 0.73 with a *T. vivax* hypothetical gene (TvY486_0044100). A BLAST search of the *T. vivax* hypothetical gene on the NCBI database produced no significant hits. It appears that this route of ornithine production does not exist in *T. b. brucei*.

5.3.3.5 Ornithine distribution

No labelling of ornithine from glutamate, glutamine, proline or lysine was found. If the acetylornithine deacetylase enzyme works reversibly, then another possible means to seek the source of ornithine involves adding labelled ornithine to cells to allow the pathway involved in its production to be identified. Ornithine labelled with two heavy nitrogens was added to cells and was found to be taken up into the trypanosomes and converted to acetylornithine (Fig 5-12).

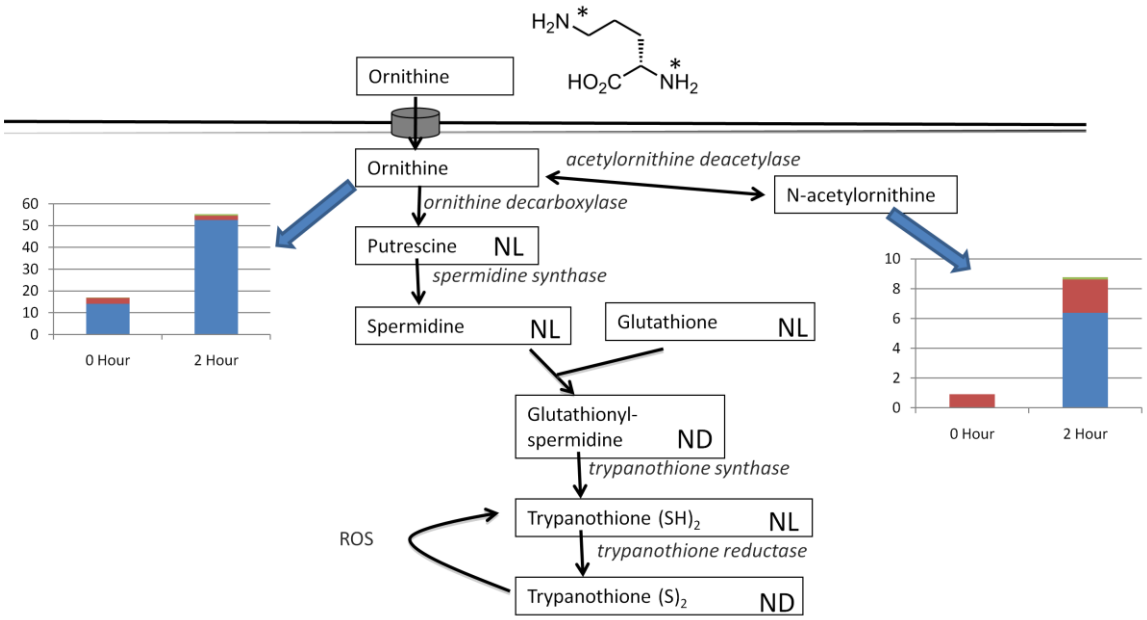

Figure 5-12. The isotope distribution of ornithine. Metabolites are shown in boxes, enzymes in italics. Bar charts show the relative intensity (area under the curve (divided by 10^6)) of ^{14}N (red), ^{15}N (green) and $2^{*15}N$ (blue) metabolites. ND: not detected, NL: not labelled. Ornithine is detected at M+H: 133.0972, (^{14}N), 134.0942 (^{15}N), or 135.0912 ($2^{*15}N$), RT: 22.8 minutes. Acetylornithine is detected at M+H: 175.1077 (^{14}N), 176.1048 (^{15}N), or 177.1018 ($2^{*15}N$), RT: 14.4 minutes. Spermidine is detected at M+H: 146.1652, (^{14}N), 147.1622 (^{15}N), or 148.1592 ($2^{*15}N$), RT: 37.7 minutes. Spermidine was not detected with $3^{*15}N$. Glutathione is detected at M+H: 308.0911, RT: 13.4 minutes and trypanothione disulphide at M+H: 722.2960, RT: 23.5 minutes. N = 3.

The acetylornithine was labelled at 287 % of unlabelled after two hours. This is a very significant back-conversion when compared to 0.7 % at 0 hours, which is interesting as acetylornithine deacetylase was thought to favour the deacetylation direction, with a Keq for amino acids usually in the range of 3 – 33 (NIST database (Goldberg *et al.*, 2004)), meaning you would need around 3 - 33

fold more ornithine to reverse the direction of the reaction. However, there may be other acetylases and acetyltransferases yet to be annotated within the *T. b. brucei* genome and clearly ornithine is being acetylated at a high rate in these experimental conditions. The relative levels of ornithine and acetylornithine support a Keq of around 100 (ornithine is detected at approximately 100 times the intensity of acetylornithine, data not shown) if there is no compartmentalisation of the two metabolites.

Acetylornithine has the same mass as the glycine-valine dipeptide, prolinyl-glycine and ethyl-glutamine (175.1077 (^{14}N) or 177.1018 (2*^{15}N)), but the retention times are different at 14.4 minutes for acetylornithine, a calculated 11 minutes for the dipeptide and prolinyl-glycine and 12 minutes for ethyl-glutamine (using RT calculator, developed by Darren Creek, University of Glasgow). Further confirmation that the detected mass relates to acetylornithine and not its isomers comes from a targeted analysis of the valine, proline, glutamine and glycine amino acids separately, which revealed no ^{15}N incorporations making it highly unlikely that the amino acid derivatives were labelled and confirming that the mass detected was acetylornithine.

It is interesting that the total levels of both ornithine and acetylornithine increase over the two hours in CBSS. It may be that the cells are stressed in this buffer solution and are therefore taking in increased ornithine for the production of trypanothione, although thiol production using the heavy metabolites is not observed in the two hour time frame.

No metabolite further back along the glutamate to ornithine pathway (Fig 5-3) was labelled. This may be because this pathway is not in use or because the conditions and length of time used in the assay were not conducive to their labelling, but the most likely reason is that this pathway is absent in bloodstream form trypanosomes.

Arginine was detected as its natural isotope, but a heavy isotope (of one, two or four labelled nitrogens) was not detected.

Chapter 3 of this thesis showed that ornithine is transported into bloodstream form trypanosomes. Whether this transport would be sufficient to provide all the

amines for the polyamine pathway is unclear although a metabolic model of the polyamine pathway, developed by Dr. Xu Gu, University of Glasgow, suggests that it would be (Dr. X u Gu, personal communication). Ornithine was quantified in HMI-9 + FCS by spiking a range of concentrations of 2*^{15}N ornithine into HMI-9 for mass spectrometry. The absolute concentration of ornithine in HMI-9 + FCS could then be ascertained using a calibration curve for the known concentrations of the heavy isotope. Ornithine in HMI-9 + FCS was found to be at 77 µM from this method (Fig 5-13). Published levels of ornithine in human adult blood are 54-100 µM (HMDB) and in CSF the levels are around 5 µM (HMDB).

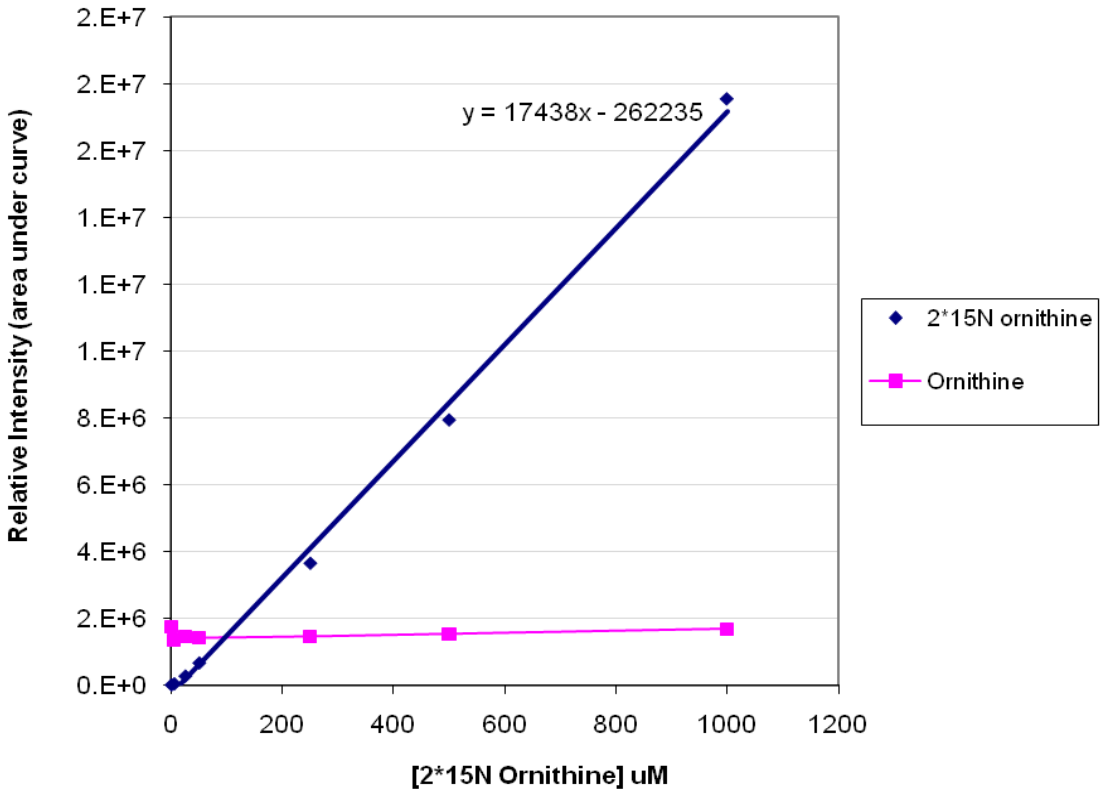

Figure 5-13. Ornithine quantification in medium. Ornithine levels (M+H : 133.0972, RT: 22.2 minutes) in HMI-9 + 10 % FCS were quantified using a calibration curve of 2*^{15}N ornithine (M+H : 135.0912, RT: 22.2 minutes) spiked into HMI-9 + FCS over a range of concentrations. Ornithine levels were found to be at 77 µM.

The level of ornithine in blood is similar to the reported arginine concentration of 70 µM found within trypanosomes (Smith *et al.*, 2009). It seems possible therefore that sufficient ornithine could be transported into the trypanosome directly, bypassing the need for an arginase enzyme.

Ornithine uptake into bloodstream form trypanosomes was measured with an estimated V_{max} (the curve was not adequately level for an accurate measurement) of 40 pmol/min/10^6 cells and a K_m of approximately 300 µM (Fig 5-14).

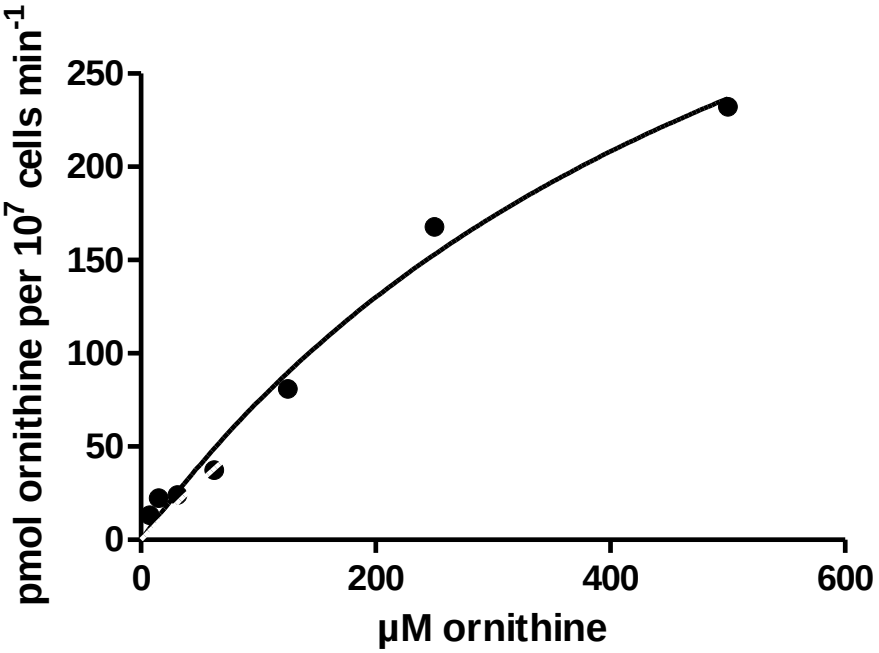

Figure 5-14. Ornithine uptake in bloodstream form *T. b. brucei.* One of two repeats is shown. Levels shown are for 10^7 cells.

The K_m of a transporter is usually similar to the concentration of the substrate in the natural medium, allowing maximum efficiency of uptake, so this K_m is very high when compared to the measured level of ornithine in blood and in HMI-9 + FCS and may not be very accurate. The measurement of ornithine uptake may be complicated if there are several transporters contributing to the total uptake rate. This would explain why the uptake curve was not saturated in increasing ornithine concentrations. More analysis of ornithine uptake is required.

A longer-term analysis of ornithine amine incorporation would allow an assessment of how much ornithine contributes to the overall production of glutathionylspermidine and trypanothione. Ornithine is found in the serum used to produce the trypanosome growth medium. An attempt was made to create ornithine-free medium using ornithine transcarbamoylase (6 units per 500 ml medium) and 700 µM carbamoyl phosphate. Ornithine transcarbamoylase adds a

carbamoyl group to ornithine to create citrulline and is thought to greatly favour the citrulline direction thermodynamically (Reichard and Reichard, 1958). 2*^{15}N-ornithine was then added to the medium with cells and the incorporation was analysed over four hours. Interestingly, heavy putrescine could not be detected in the cells over the four hour time course, but heavy spermidine (M+H: 148.1593, RT: 42.0 minutes) increased steadily (Fig 5-15). This suggests that putrescine is a transient metabolite in these cells and the flux favours storage of spermidine.

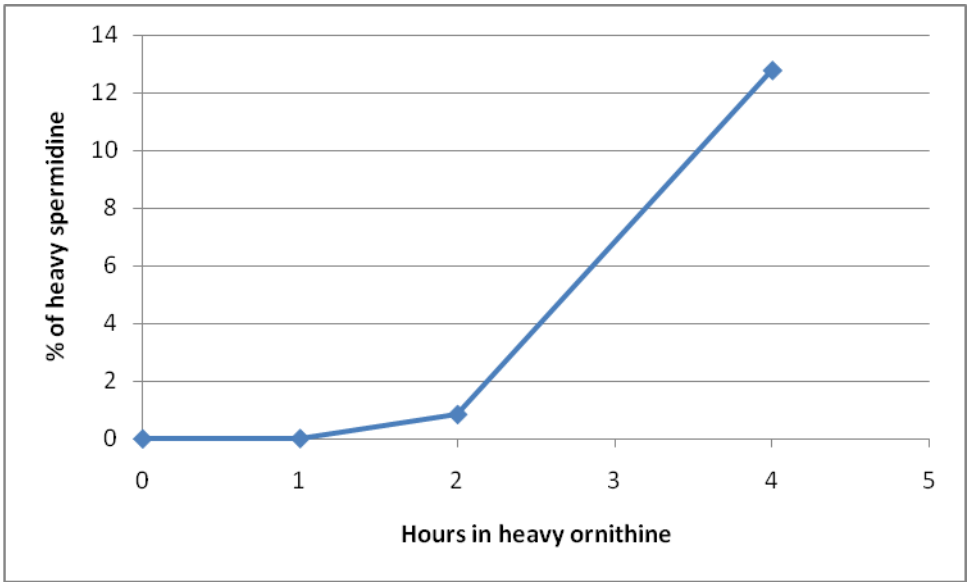

Figure 5-15. Spermidine is labelled from ornithine over four hours. Results are shown as a percentage of labelling. This study was performed just once so error bars are not available.

The Bacchi *et al.* and Fairlamb *et al.* studies measured levels of putrescine and spermidine. The Bacchi study found natural levels of putrescine at an average of 6.95 ± 2.22 nmol per mg protein (average of four ± s.e.m), four times lower than the spermidine levels (Bacchi *et al.*, 1983). The Fairlamb study found levels of putrescine to be around three times lower than spermidine (Fairlamb *et al.*, 1987). This supports the theory that putrescine is not stored, but is instead rapidly converted to spermidine, although some labelled putrescine would still be expected. This assay for longer term incorporation in rich medium will need to be repeated, possibly over a longer period.

Heavy trypanothione (with two heavy nitrogen labels M+H: 724.2901) was detected at 1.7 % of the ^{14}N isotope after one hour and 1.8 % after two hours.

The heavy label was however, undetectable after four hours in heavy ornithine. As the heavy spermidine levels were high after four hours, the lack of heavy trypanothione is interesting. The cells were not under stress as they were growing in normal growth medium so were perhaps not producing any new trypanothione, but why the levels of heavy trypanothione already made should decrease is unclear. The trypanothione must have been metabolised, either back to spermidine or through some, as yet unidentified, pathway. From the mode of action studies with toxic doses of eflornithine in the previous chapter (section 4.2.1.3) it was seen that trypanothione levels are not depleted significantly as the cells are dying whereas spermidine levels are. It was therefore thought that decreases in spermidine may be more important in eflornithine trypanocidal action than trypanothione. Maintaining high levels of spermidine in these experiments may therefore be attained by catalysis of the less important trypanothione. Glutathione levels in this assay decrease to approximately 30 % of the 0 hour level after four hours, in contradiction to this hypothesis, although the glutathione may also be catalysed to produce other metabolites, such as cysteine.

5.3.3.6 Arginine distribution

Since it seems that arginine can produce ornithine within the trypanosomes, in spite of an apparent absence of arginase, a more detailed analysis of the fate of arginine was performed. The role of arginine within the trypanosome was investigated using arginine labelled with four heavy nitrogen atoms (Fig 5-16).

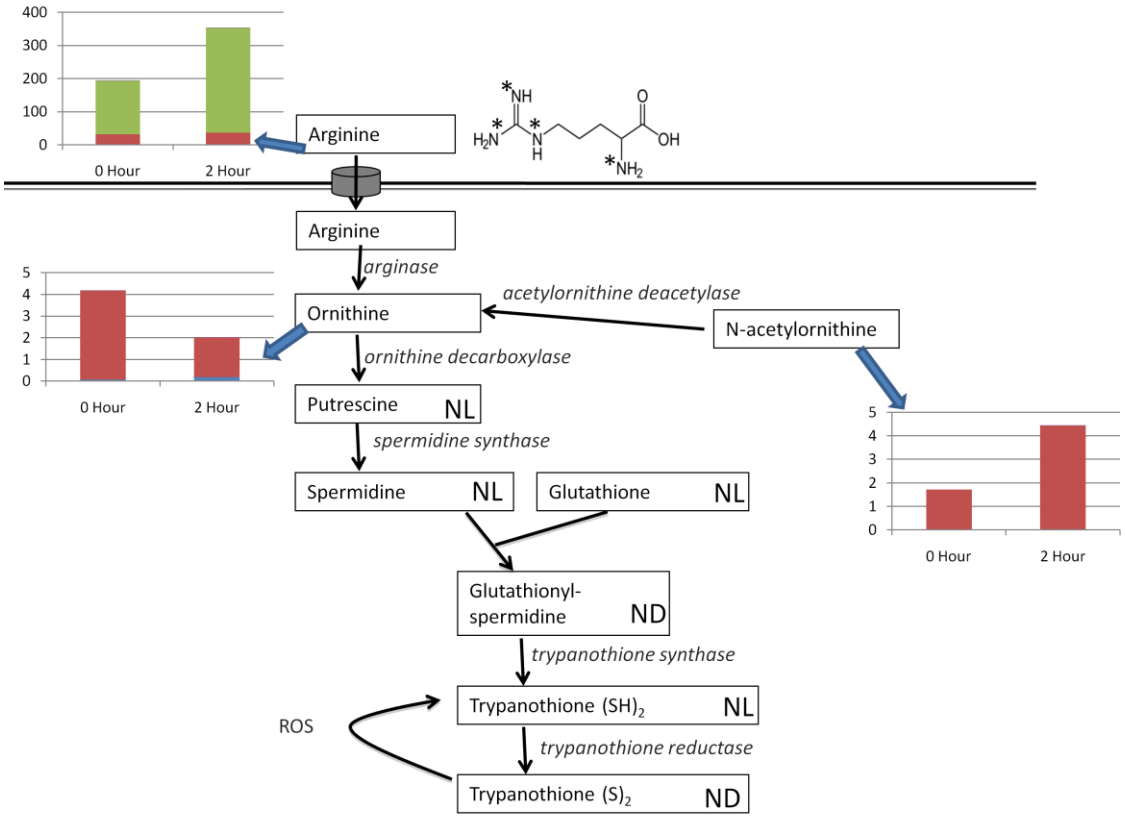

Figure 5-16. The isotope distribution of arginine. Metabolites are shown in boxes, enzymes in italics. Bar charts show the relative intensity (area under the curve (divided by 10^6)) of ^{14}N (red), ^{15}N (purple), $2^*{}^{15}N$ (blue) and $4^*{}^{15}N$ (green) metabolites. ND: not detected, NL: not labelled. Arginine is detected at M+H: 175.1190 (^{14}N), 176.1160 (^{15}N), 177.1131 ($2^*{}^{15}N$), 179.1073 ($4^*{}^{15}N$), RT: 22.1 minutes. Ornithine is detected at M+H: 133.0972, (^{14}N), 134.0942 (^{15}N), or 135.0912 ($2^*{}^{15}N$), RT: 22.8 minutes. Acetylornithine is detected at M+H: 175.1077 (^{14}N), 176.1048 (^{15}N), or 177.1018 ($2^*{}^{15}N$), RT: 14.3 minutes. Spermidine: M+H: 146.1654, RT: 37.9 minutes, glutathione: M+H: 308.0911, RT: 13.4 minutes, trypanothione disulphide: M+H: 722.2960, RT: 23.6 minutes. N = 3

Arginine was converted to ornithine (10 % of unlabelled) and further into acetylornithine (0.7 %) (confirmation was obtained that the potential isomer constituents for acetylornithine (glycine and valine) were not labelled (see section 5.3.3.5)). As there is no arginase activity within the trypanosome it is unclear how this conversion could take place. It is possible that there is an as yet unknown mechanism to convert arginine to ornithine without creating urea (urea would have been detected in the arginase activity kit).

A targeted analysis of the urea cycle intermediates was undertaken to ascertain whether this cycle could be working in reverse to produce ornithine from arginine via argininosuccinate and citrulline. ^{14}N peaks for citrulline were of very

low intensities (an average 14, 000 (area under the curve) where one would normally consider anything with an intensity below 10, 000 as noise), so labelled peaks would not have been expected. Argininosuccinate could not be detected on our mass spectrometry platform, although it would be thought to be detected in either positive or negative ionisation mode, so its levels must be below the limit of detection or not present at all. The absence of detectable argininosuccinate and the lack of label detected in citrulline mean that it cannot be determined whether the ornithine produced was a result of the urea cycle (Fig 5-2) working in reverse or through some other mechanism.

The IDEOM software detected labelling in 4*^{15}N CDP ethanolamine (M+H: 449.0423, RT: 22.2 minutes), 4*^{15}N arginine phosphate (M+H: 257.0586, RT: 21.3 minutes), 3*^{15}N imidazole ethanamine (M+H: 115.0778, RT: 22.2 minutes) and 3*^{15}N piperazine carboxamide (M+H: 133.0883, RT: 22.2 minutes) as well as the ornithine and acetylornithine already discussed. The retention times of the masses labelled as imidazole ethanamine and piperazine carboxamide are similar to that of arginine (22.1 minutes) making it likely that they are fragments, adducts or other artefacts of the very abundant arginine peak. CDP ethanolamine, also has a similar retention time to arginine, but does not appear to be a fragment or be a related to arginine through an adduct multimer of a fragment. CDP ethanolamine may therefore be labelled with four heavy amide groups from arginine, although its synthesis from arginine is not obvious. The mass for the labelled CDP-ethanolamine if around 10 times higher than the mass of unlabelled CDP-ethanolamine, which is unlikely to occur naturally as arginine would have to be catabolised to small amine-containing compounds to reconstitute to CDP-ethanolamine. This mass is therefore thought not to be labelled CDP-ethanolamine, but is unexplained.

Arginine phosphate has a retention time that differs by nearly one minute from arginine meaning that this is probably a real peak and arginine has been phosphorylated in these cells. There are three arginine kinase genes present in *T. b. brucei* (Tb.09.160.4560, Tb.09.160.4570 and Tb.09.160.4590), which are syntenic with a proven arginine kinase in *T. cruzi* (Pereira *et al.*, 2003).

A longer term assay in HMI-9 showed that ornithine is only produced from heavy arginine at very low levels over four hours (Fig 5-17), and heavy acetylornithine

was not produced at all. The retention times of ornithine and arginine are very similar in this assay (RT: 25.2 minutes for arginine, 25.7 for ornithine) meaning that the heavy ornithine seen could also be a fragment of arginine. This suggests that ornithine and acetylornithine are only made from the catalysis of arginine during stress conditions (e.g. in CBSS, where ornithine is lacking). Citrulline levels were much higher in this analysis, and ^{15}N citrulline was detected at 0.3 % of light, although this was constant over all time points suggesting that the levels detected were merely the natural isotope.

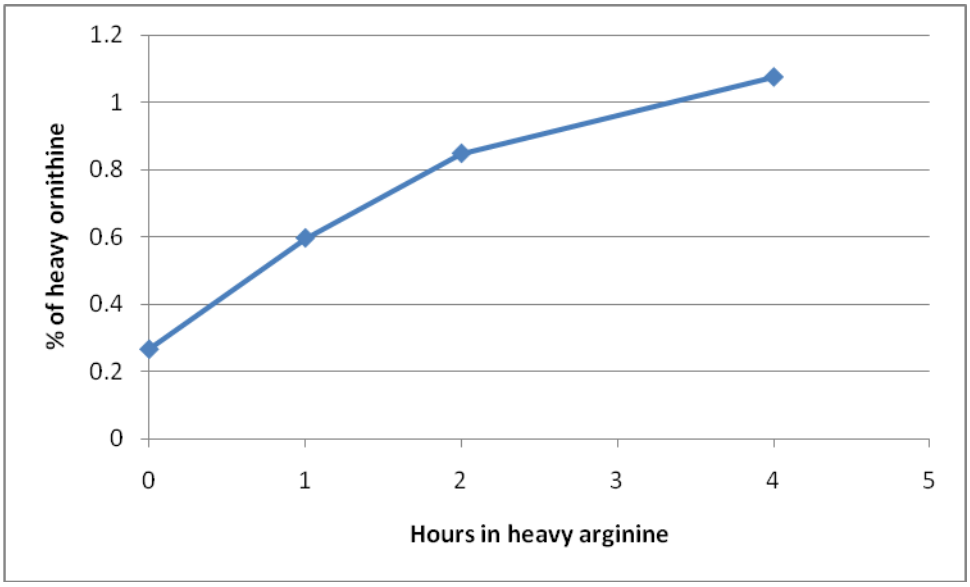

Figure 5-17. Ornithine is produced from heavy arginine over four hours, but only at very low levels. N = 1.

Of the enzymes in the urea cycle, only Tb927.8.2020 (proven not to be an arginase) and a putative aspartate carbamoyltransferase (Tb427.05.3820) could be found with text searches. A BLAST search with this carbamoyltransferase protein sequence confirmed that it held a high degree of similarity with carbamoyltransferases from many other organisms. The argininosuccinate lyase or synthase could not be found in TriTrypDB from BLAST searches with gene orthologues from a range of other organisms. Arginine deiminase is predicted to be able to convert arginine to citrulline directly releasing ammonia instead of the urea released in the production of ornithine (detected in the arginase assay). This bypasses the need for argininosuccinate lyase and argininosuccinate synthase (Morada *et al.*, 2011). A *T. congolense* gene in TriTrypDB is an orthologue of a group of bacterial glutamine deiminases (81 % identity with a

Pseudomonas gene), but a match in *T. b. brucei* could not be found. A BLAST search with a *Helicobacter mustelae* deiminase produced a tenuous match with Tb427tmp.211.1070, a hypothetical protein, but with a p value of just 0.996, it is not a good match.

Apart from in the case of arginine deiminase, citrulline is only known to be made from ornithine-containing compounds (acetylornithine can be converted to acetylcitrulline and then deacetylated, or succinylornithine can be converted to succinylcitrulline and desuccinated). Uptake of citrulline in trypanosomes cannot be ruled out, indeed a protein predicted to transport ornithine and citrulline exists in mammals termed ORNT1 (Tonazzi and Indiveri, 2011;Camacho *et al.*, 2006), although BLAST searches in kinetoplasta revealed no orthologues.

5.4 Discussion

Bloodstream form *T. b. brucei* take in ornithine. This ornithine uptake would be unnecessary if the arginase enzyme were functioning. The lower rate of arginine uptake compared to *Leishmania*, which have relatively high levels of arginase activity, suggests that *T. brucei* require less arginine than other trypanosomatids.

Ornithine was found to be present in the bloodstream form *T. brucei* growth medium at a level of 77 μM. It was thought that there may be arginase activity in the foetal calf serum used to prepare the trypanosome growth medium, which would produce the ornithine. The arginase assay and use of heavy arginine failed to substantiate this claim, as FCS alone was not seen to produce ornithine from arginine, although growth medium with 10 % FCS was able to produce a small amount. This may be due to cofactors in the growth medium or to the dilution of inhibitors in the FCS.

Levels in human serum are similar to the 77 μM seen in the medium, but in cerebrospinal fluid are significantly less at around 5 μM (HMDB). The levels in tsetse haemolymph have not been measured. The metabolism of trypanosomes in CSF or in haemolymph is not well understood, although it is known that in the haemolymph (procyclic forms) trypanosomes rely much more on amino acid metabolism than glucose for energy (Coustou *et al.*, 2008).

In summary of the amino acid label distributions, glutamate and lysine were either not taken into the cell or were not converted to any other amine-containing metabolites. The amine group from glutamine was incorporated into glutamate only. Proline was converted to glutamate, alanine, aspartate and glutamine in bloodstream-forms and further to glutathione and trypanothione disulphide in procyclic-forms. Ornithine was found to only label acetylornithine when in CBSS for two hours, but in HMI-9, spermidine and trypanothione disulphide were found to be labelled. Arginine labelled ornithine and acetylornithine when in CBSS, where ornithine is absent, but not when in ornithine-rich HMI-9, and arginine phosphate. Glutamate is not thought to be converted to ornithine and it seems likely that ornithine can be both taken up

through transport and synthesised from arginine. We can hypothesise from the evidence presented here that ornithine uptake is sufficient for polyamine synthesis in normal growth conditions but when no ornithine is present it can be synthesised from arginine.

An interesting hypothesis for the reason that *T. b. brucei* do not encode an arginase within their genome is put forward by Canepa *et al.* (2011). Vertebrates use creatine phosphate as the main phosphagen for energy storage. *T. brucei*, Leishmania and *T. cruzi* parasites do not encode a creatine kinase (TriTrypDB), however, and are thought to use arginine phosphate instead as a stored source of energy. Arginine kinase would compete directly with arginase for arginine and it was suggested that trypanosomes and other arginase-lacking organisms evolved other ways to produce ornithine in order to create high levels of arginine phosphate for stored energy. *T. brucei* encodes at least three arginine kinases (Tb09.160.4560 (not essential (Alsford *et al.*, 2011)), Tb09.160.4570 and Tb09.160.4590) and *T. cruzi* has one annotated (Tc00.1047053507241.30) and several putative arginine kinases, but leishmania do not have any annotated. The fact that leishmania possess an arginase, but no arginine kinase and neither of the trypanosomes have an arginase, but do have arginine kinases supports this arginine competition hypothesis. It should be noted that arginine phosphate has been observed in leishmania, although whether this phosphorylation occurs through arginine kinase or through an unspecific phosphatase is not verified (Malcolm McConville, personal communication). Further evidence for the hypothesis comes from studies in our lab that show arginine phosphate increasing upon introduction of the oxidative stress inducer, methylene blue (Dong-Hyun Kim, unpublished data).

The absence of arginase in African trypanosomes is clear, but heavy arginine was still seen to be converted to ornithine although the way that this conversion takes place is unclear. The shortest routes from arginine to ornithine are through the urea cycle, requiring the cycle to operate in the opposite direction to normal or through arginine deiminase. The other intermediates in the urea cycle could not be detected, however, or were detected at very low levels, so proof of this theory could not be obtained. A different mass spectrometry platform (such as using a pHILIC column for the chromatography, which has been shown to provide better separation for succinate (Dr. Gavin Blackburn, University of

Strathclyde)) may allow better detection of arginosuccinate and citrulline to analyse incorporations from heavy arginine. Although if the problem is one of low abundance then simply using more cells may help.

5.4.1 A role for acetylornithine

Acetylornithine is produced from ornithine at detectable levels within a two hour time span, but the mechanism for this conversion is unclear. It was hypothesised that acetylornithine was produced from glutamate as a consequence of *T. b. brucei's* lack of arginase activity. This hypothesis could not be proven in the time scale and conditions used and the pathway is unlikely to be present in bloodstream form trypanosomes.

Ornithine is transported into cells and converted to acetylornithine rapidly, reaching a labelled level three times that of unlabelled after two hours in CBSS with heavy ornithine. The reasons for this conversion are unclear. In *Mycobacterium tuberculosis* it was shown that acetylornithine deacetylase reversibly transfers the acetyl group of acetylornithine to glutamate as part of arginine biosynthesis (Sankaranarayanan *et al.*, 2010), but this pathway is thought to be confined to bacterial species and metabolites further along the pathway from acetylornithine were not observed in *T. b. brucei*. There may be other enzymes capable of the acetylation of ornithine that have yet to be verified in the *T. brucei* genome.

If arginine to ornithine conversion were not possible, and uptake was the only source of ornithine, then it might be advantageous to store some ornithine as acetylornithine for use when blood levels are lower. However, arginine was observed to produce ornithine when exogenous ornithine was lacking through an alternative route to the classical arginase pathway. This route may be the urea cycle working in reverse, but could not be determined as levels of citrulline are too low for accurate measurement and argininosuccinate cannot be analysed on the mass spectrometry platform used. Furthermore, argininosuccinate lyase and synthase (or arginine deiminase) gene sequences could not be found within the *T. brucei* genome. The lack of gene sequences homologous to identified genes does not rule out their existence, however, especially in the case of arginine deiminase, where very few genes have been characterised.

The data appears to show that stress, either through eflornithine (section 4.2.1) or through nutritional deprivation (e.g. in CBSS) increases the production of acetylornithine. It has been shown in human cells that acetylation of polyamines occurs more in cancerous cells compared to healthy cells (Kingsnorth and Wallace, 1985) and these acetylated polyamines (spermidine and spermine) are involved in the generation of reactive oxygen species leading to apoptosis (Wallace *et al.*, 2003). The enzymes required for this free radical production include an acetyltransferase and a polyamine oxidase. A polyamine oxidase could not be found in trypanosomes through BLAST searches with known polyamine oxidases, however, so the apoptosis mechanism may not be present in trypanosomes.

5.4.2 The use of heavy labelling to interrogate pathways

The advantages of using heavy labelling to interrogate pathways are clear. The mzMatch and IDEOM softwares were very useful for producing untargeted analyses of each experiment. They did not, however, always identify all of the metabolites that were labelled in each experiment. This is probably due to the rigorous filters built into the softwares that aim only to report those peaks with a high reproducibility, which may not always be appropriate for smaller scale biological experiments where creating a lot of power by increasing numbers of replicates isn't always possible or cost effective. A targeted approach was therefore also used to look for metabolites that were missed by the automated programmes. This is much more time consuming and requires a prior hypothesis to determine which metabolites to seek. More labelled metabolites were reported using a targeted approach.

Levels of labelled metabolites were often relatively low in these experiments, which is probably reflective of the conditions used. The leishmania ^{13}C labelling experiments performed by Saunders *et al.* (2011) were undertaken in a completely defined medium, which included amino acids, vitamins, heme, bovine serum albumin (BSA) and fatty acids (bound to the BSA). This more complete medium is likely to contain many more cofactors and essential nutrients for efficient labelling. Labelling in the leishmania experiments was also conducted for two days prior to quenching, allowing an equilibrium of labelled

to non-labelled atoms to be reached providing more detailed information on which metabolites are taken up from medium and which are produced through anabolic and catabolic reactions within the parasite. The van Weelden experiments were also conducted in rich medium replacing metabolites under test with heavy isotopes (van Weelden *et al.,* 2005). The labelling in the experiments described in this chapter was mainly conducted in CBSS buffer solution at room temperature. This is sufficient to keep bloodstream form cells alive for up to eight hours, but the cells may not be metabolising as they normally would and may lack essential precursors and cofactors. The creation of drop out medium is quite time-consuming, however, and adaptation to the medium may be required by the parasites as was seen in the van Weelden experiments (van Weelden *et al.,* 2005). A minimal defined medium for bloodstream form trypanosomes has not been created before, but is a priority for future metabolomics experiments. The relative ease of conducting experiments in CBSS and the lack of necessity of an adaptation stage means that parasites can be assayed with their metabolic machinery in a natural state. The medium also contains much fewer contaminating metabolites so cells do not require a washing step, which can be stressful to the cells and cause reactionary metabolism. Both protocols are therefore useful and complementary for measuring short term and longer term incorporations.

One of the major disadvantages of mass spectrometry over nuclear magnetic resonance is that it is not quantitative. Here, we have shown that metabolites can be quantified using a calibration curve of the heavy isotope (Fig 5-13). A replete labelled metabolome could be created by growing a culture of cells on a labelled carbon source for several generations until every carbon in the metabolome were labelled as has be done previously by Kiefer *et al.* with *M. Extorquens* (2008). This metabolite mixture, could have each metabolite quantified and be used to spike into samples with unknown metabolite levels for quantification. This is an aim for the metabolomics community in the near future and is being validated in our laboratory by Dr. Dong-Hyun Kim.

6. Final Conclusions

The main findings of this thesis are:

- Eflornithine resistance is rapidly selected in the laboratory (chapter 3).
- *In vitro* resistance to eflornithine is due to the loss of TbAAT6, an amino acid transporter able to transport eflornithine into bloodstream form trypanosomes (chapter 3).
- Metabolomic methods to predict the mode of action of drugs against *T. brucei* work in untargeted analyses (chapter 4).
- Acetylornithine is produced in large quantities from ornithine and levels correlate highly with ornithine when the polyamine pathway is perturbed (chapter 4 and 5).
- Ornithine is not produced from arginine under normal growth conditions, but is when cells are in buffer solution lacking nutrients (chapter 5).
- Tb927.8.2020, previously annotated as arginase, is not an arginase (chapter 5).
- Sedoheptulose, sedoheptulose phosphate and erythrose phosphate are present in *in vitro* grown bloodstream form *T. b. brucei*, suggesting some aldolase or transketolase action or possibly a novel phosphoketolase (chapter 4).
- Nifurtimox-eflornithine combination therapy is not synergistic *in vitro* as has been shown in isobologram and metabolomic analyses (chapter 4).

Studies into the mode of drug action and resistance in trypanosomes are of paramount importance if we are to achieve the aim of bringing this treatable disease under control. The drugs in use against HAT are insufficient due to lack of efficacy against late stage disease (pentamidine and suramin), unacceptable toxicity (melarsoprol) and emerging resistance (eflornithine and melarsoprol).

The latest therapy for use against HAT is the drug combination NECT. The uptake of this new therapy has been much more rapid than the uptake of eflornithine alone was in the 1990s, mainly due to the reduced quantities required and therefore the reduction in transportation costs.

The emergence of resistance to eflornithine is of real concern and may thwart the use of the new combination therapy as nifurtimox monotherapy is ineffective at the dose used in the combination therapy. Tests for resistance in the field would therefore be extremely useful for assigning treatment regimes to patients.

We present here a substantial body of evidence that an amino acid transporter, TbAAT6, is lost in eflornithine resistance *in vitro* and can be responsible for resistance when knocked down by RNAi. The natural substrate for this transporter is not known, but as the transporter is not essential in bloodstream forms of the parasite it is expected that the natural substrate would have multiple modes of entry to the cell or is able to be synthesised *de novo* by the parasite. It would be interesting to find out the natural substrate of TbAAT6. It is possible that this transporter is not essential in the artificial growth medium used in the laboratory, but in a different environment (e.g. *in vivo*) may have increased importance, although the fact that the resistance phenotype was retained in mice would contradict this argument. A different resistance mechanism may occur in the field. A cell line selected for eflornithine resistance was created by Frank Jennings (University of Glasgow) by passage through eflornithine treated mice. It will be interesting to test this cell line for the absence of TbAAT6.

In the field the loss of TbAAT6 may have more detrimental effects on the parasite than it would in an *in vitro* environment. The human-infective strains may have different nutrient requirements or human blood may have a different nutrient availability than mouse blood that prevents the loss of TbAAT6. The monomorphic strains in the laboratory are also not passed through the tsetse fly vector so if TbAAT6 is essential for growth in the tsetse midgut or survival in the tsetse salivary glands, for example, then the resistance phenotype would not be passed on in the field. Studies on the essentiality of TbAAT6 in procyclic form trypanosomes were inconclusive. A TbAAT6 RNAi line showed no growth

phenotype when induced, but levels of gene knockdown were not measured. Another RNAi line for TbAAT6 created by David Horn's laboratory in London did reveal a lethal phenotype in a large scale RNAi assay (Baker *et al.*, 2010), but on further, more targeted analyses, the knock down was found not to be essential in procyclic forms (David Horn, personal communication). It is of note that recent evidence suggests a role for TbAAT6 in proline uptake (Doris Rentsch, personal communication), which would be likely to have a negative effect, if lost, in procyclic forms of the parasite given their dependence on proline as an energy source. Growth curves for the procyclic TbAAT6 RNAi line should therefore be attempted in SDM80 medium, which lacks glucose, allowing proline to be used as an energy source.

Attempts to assess the status of TbAAT6 in field isolates of eflornithine refractory parasites in blood samples were unsuccessful. The levels of parasitaemia in these samples were known to be very low. Methods of concentrating parasites for PCR in the field have been developed (Buscher *et al.* 2009) as have more sensitive PCR methods (Ahmed *et al.*, 2011) so it will be a priority in the field to optimise the protocols for testing the TbAAT6 status.

Determining the mode of action of new active compounds against HAT is also going to be important for licensing, prediction of toxicity and the prediction of synergism with other compounds. Here we show a method for determining the mode of action of trypanocides using a metabolic approach. Eflornithine was used as a proof of principle with sub IC_{50} doses causing very localised changes to the metabolic network and higher doses causing many more changes as the cells are dying from the drug. The fact that the analysis was untargeted, but still picked out the metabolites that would be most expected to changes with eflornithine addition is very promising.

For our studies of eflornithine toxicity it appears that spermidine levels may be more important than trypanothione in the mode of action of the drug. This is supported by the fact that spermidine levels are much more greatly affected than levels of trypanothione as the cells are dying (Fig 4-6) and that heavy trypanothione is converted back to spermidine in cells grown in HMI-9 (Fig 5-15). In similar experiments, administering eflornithine in drinking water to dehydrated rats, trypanothione levels were found to decrease (66% (Fairlamb *et*

al., 1987) and *in vitro* studies saw levels reduced to 40 % of untreated. In fact, our experiments did see a 40 % reduction in trypanothione disulphide after 48 hours, but as the cells were losing their integrity at this point and the majority of metabolite levels are reduced, the reduction was not seen to be significant. As the other three studies only looked at a small range of metabolites, with no non-polyamine controls, it cannot be concluded whether their studies also suffered from a loss of cell wall integrity. The Phillips study saw a depletion in all metabolite levels tested apart from decarboxylated S-adenosylmethionine after three days at sub-IC_{50} levels (Xiao *et al.,* 2009). In our studies, it is not thought that the membrane has been damaged at this drug level, but we do begin to see a recovery of treated cells at 72 hours (when the Phillips metabolite levels are recorded).

After 24 hours in drug, trypanothione disulphide levels are only reduced to 75 % of the normal levels (Fig 4-6), whereas spermidine has suffered a much more profound loss to 33 % of normal growth levels. Phillips noted that adding exogenous spermidine rescued tryps that had knocked down ODC expression (Xiao *et al.,* 2009), but it is unclear whether this spermidine was used to produce more trypanothione or not. It would be interesting to attempt an add back of trypanothione to treated cells, but whether this thiol would be taken into the cell is unknown and it may simply result in the back-conversion to spermidine. Trypanothione synthase has been shown to be essential (Wyllie *et al.*, 2009) and pharmacological inhibition of trypanothione reductase has been shown to be very effective (Olin-Sandoval *et al.,* 2010) but while trypanothione is essential to the cell, depleted levels of the thiol may not be the reason that trypanosomes die from eflornithine.

Similar analyses with nifurtimox were more complex. It is unknown how nifurtimox kills trypanosomes, but it was thought to induce oxidative stress, which might have explained why it was thought to be synergistic with eflornithine as trypanosomes with reduced polyamines would be less able to detoxify reactive oxygen intermediates (Michael Barrett, personal communication). However, our studies have shown that the two drugs are not synergistic *in vitro* and that nifurtimox does not significantly affect any of the polyamines or other thiols in sub IC_{50} or toxicity assays. The apparent lack of synergy may be seen if nifurtimox is only effective on dividing cells and

eflornithine treatment causes trypanosomes to enter a static, non-dividing state. A type I nitroreductase has been shown to be important in the processing of the nifurtimox pro-drug to its active compound (Hall *et al.*, 2011). This enzyme is NADH dependent and may only be active in growing cells, however our data shows that nifurtimox is still reduced to its active form in the combination therapy. Studies with other trypanostatic drugs show a similar antagonism, although this antagonism is not as pronounced as with eflornithine. The reasons for the reduced action in combination may be more complex than a requirement for growing cells in nifurtimox action.

Acetylornithine and acetylputrescine were seen to highly correlate with ornithine and putrescine in the eflornithine mode of action studies. It was hypothesised that acetylornithine may be involved in the production of ornithine through a bacterial pathway commencing on the uptake of glutamate. This pathway could have been required to produce ornithine for polyamine synthesis as arginase activity is not seen in *T. b. brucei*. Glutamate was not seen to be transported into trypanosomes in our metabolite tracking assays, however, and glutamate produced from glutamine or proline was not traceable to ornithine in bloodstream forms. Uptake of ornithine was detected and may be sufficient to produce all of the ornithine required for the production of polyamines (with acetylornithine as a possible storage metabolite). Arginine to ornithine conversion was detected, even though no arginase activity can be detected in trypanosomes and the gene previously thought to encode an arginase was shown not to have many of the arginase catalytic residues. The mechanism for this conversion has not been discovered through metabolite tracking. Possible mechanisms include the urea cycle working in reverse to convert arginine to ornithine via argininosuccinate and citrulline or through arginine deiminase conversion of arginine to citrulline and to ornithine. It would be useful to investigate these theories further using heavy citrulline, longer-term assays and metabolomic platforms that can assay argininosuccinate levels.

Arginase is thought to be important in many parasitic organisms to divert arginine away from host nitric oxide synthases reducing the amount of toxic nitric oxide in the parasite's environment. Trypanosomes lacking arginase may therefore be vulnerable to nitric oxide when grown inside their vertebrate host. A high level of conversion of arginine to arginine phosphate in *T. b. brucei*, seen

in arginine tracking experiments, may therefore be used to divert arginine from nitric oxide synthase.

There are three arginine kinases in trypanosomes, which appear to have been acquired through horizontal gene transfer from arthropod vectors. Vertebrates lack arginine kinases (Hoffman and Ellington, 2011), possibly because they are in direct competition with high rates of arginase activity. Vertebrates therefore use creatine phosphate as a phosphagen store, where *T. brucei* uses arginine phosphate.

In *T. cruzi,* it was shown that over expression of arginine kinase improved their capability to deal with oxidative stress (Pereira *et al.,* 2003) and H_2O_2 treatment results in a time-dependent increase in arginine kinase expression (Miranda *et al.,* 2006). A knockout of one arginine kinase in *T. b. brucei* produced no growth phenotype. Attempts are being made in our laboratory to knockout all three arginine kinases in *T. b. brucei*.

These results together suggest that the trypanosomatids lack an arginase as they use arginine phosphate as a phosphagen store to deal with oxidative stress and high rates of arginine kinase activity are not compatible with high arginase activity.

The untargeted nature of metabolomics can reveal many interesting leads in a large dataset. Acetylornithine was one such metabolite that had an unexpected presence in the trypanosome data and was investigated further. Other metabolites that were thought not to be present in bloodstream form parasites were sedoheptulose and sedoheptulose phosphate, which will require further investigations. Malate is also consistently seen in bloodstream form data in this laboratory. As the TCA cycle is not thought to be operative in bloodstream stages, malate was an unexpected discovery. Studies that looked at the absence of a TCA cycle in bloodstream stages used parasites grown in animals rather than *in vitro* (Ryley, 1956; Grant and Fulton, 1957; Ryley, 1962) so it may be that a difference in culture conditions (e.g. more amino acids in the medium) induces a metabolic shift in these parasites. Alternatively, these metabolites may be evidence that there is some mitochondrial energy generation after all. More analyses, using heavy labelled glucose are being undertaken in our laboratory.

More analysis of nifurtimox's mode of action is also warrented. Our analyses reveal no changes in polyamine or thiol levels, although significant changes in sugar, sugar phosphate and DNA base levels are observed.

Automatic processing methods failed to highlight metabolites that had small, but robust changes across the drug perturbation time courses. Groups of related metabolites (such as sedoheptulose and sedoheptulose phosphate) were also not highlighted as being significant in the automated processing. A group at INRA-ENVT, Toulouse, are using metabolic network modelling to map metabolic changes, helping to highlight areas of the network that are changed, rather than looking at individual metabolite levels (Jourdan *et al.*, 2010), which may help to highlight small changes that occur in a group of related metabolites.

The uses of metabolomic studies are not limited to the description of drug mode of action, but can be used to ascribe metabolic phenotypes to any kind of cellular perturbation such as gene knockouts to ascribe gene function, effects of nutrient starvation and describing resistance mechanisms as was used in the comparison of wildtype and eflornithine resistant trypanosomes in this thesis (section 3.2.2). Combining these metabolomics approaches with heavy isotope labelling of metabolites will provide extra power to the data, aiding in the identification of metabolites and as a measure of the rate of flux through pathways.

6.1 Future work

An assessment of the status of TbAAT6 in eflornithine treatment areas will be important to determine whether loss of TbAAT6 confers resistance to eflornithine in *T. b. gambiense* in a field setting.

The role of acetylornithine in *T. brucei* has not been determined. As there are several potential enzymes capable of the acetylation of ornithine, knocking each one out and tracking heavy labelled ornithine through the pathway would be time consuming. If acetylornithine has a role in providing ornithine when exogenous levels are reduced and before the arginine production commences then studying levels as cells adapt to ornithine depleted medium would be useful. Depletion of ornithine in medium using ornithine carbamoyl transferase

was not successful in this thesis, but may work after some optimisation. Otherwise a defined medium could be created.

The mechanism by which arginine is converted to ornithine is yet to be verified. Using higher numbers of cells to analyse whether ^{15}N isotope labels from arginine are transferred to citrulline or argininosuccinate will be informative. A more detailed search for the enzymes of the urea cycle or the arginine deiminase may also reveal the way by which arginine can form ornithine in the absence of arginase.

Further analysis of nifurtimox MOA will be a priority for the future as will be further analysis of nifurtimox and eflornithine action in combination. This will be imperative to advise on the implementation of the combination therapy in the field, which is being taken up at a much faster rate than eflornithine was as a monotherapy.

It would be interesting to determine how the oxidation states of thiols within the drug treated trypanosomes are altered during treatment. Methods to measure the oxidation state of the thiols are available and are being optimised for use in our metabolomic platform (Dong Hyun-Kim, University of Glasgow), but methods are complicated and involve the rapid derivitisation of the oxidised and reduced thiols to prevent further changes when cells are lysed. These methods will be particularly useful in further studies into nifurtimox's mode of action to ascertain why the drug is antagonistic with eflornithine.

7. References

Abdel-Hameed DM and Hassanein O (2004) Evaluation of Semi-Quantitative PCR and IgG & IgM ELISA in Diagnosis of Toxoplasmosis in Females With Miscarriage. *J Egypt Soc Parasitol* **34**:559-570.

Ahmed HA, MacLeod E T, Hide G, Welburn S C and Picozzi K (2011) The Best Practice for Preparation of Samples From FTA(R)Cards for Diagnosis of Blood Borne Infections Using African Trypanosomes As a Model System. *Parasit Vectors* **4**:68.

Ahn HJ, Kim K H, Lee J, Ha J Y, Lee H H, Kim D, Yoon H J, Kwon A R and Suh S W (2004) Crystal Structure of Agmatinase Reveals Structural Conservation and Inhibition Mechanism of the Ureohydrolase Superfamily. *J Biol Chem* **279**:50505-50513.

Aksoy S, Gibson W C and Lehane M J (2003) Interactions Between Tsetse and Trypanosomes With Implications for the Control of Trypanosomiasis. *Adv Parasitol* **53**:1-83.

Alarcon R, Orellana M S, Neira B, Uribe E, Garcia J R and Carvajal N (2006) Mutational Analysis of Substrate Recognition by Human Arginase Type I Agmatinase Activity of the N130D Variant. *FEBS J* **273**:5625-5631.

Albert MA, Haanstra J R, Hannaert V, Van Roy J, Opperdoes F R, Bakker B M and Michels P A (2005) Experimental and in Silico Analyses of Glycolytic Flux Control in Bloodstream Form *Trypanosoma brucei*. *J Biol Chem* **280**:28306-28315.

Albrecht AM and Vogel H J (1964) Acetylornithine Delta-Transaminase. Partial Purification and Repression Behavior. *J Biol Chem* **239**:1872-1876.

Alibu VP, Richter C, Voncken F, Marti G, Shahi S, Renggli C K, Seebeck T, Brun R and Clayton C (2006) The Role of *Trypanosoma brucei* MRPA in Melarsoprol Susceptibility. *Mol Biochem Parasitol* **146**:38-44.

Allen J, Davey H M, Broadhurst D, Rowland J J, Oliver S G and Kell D B (2004) Discrimination of Modes of Action of Antifungal Substances by Use of Metabolic Footprinting. *ApplEnviron Microbiol*. **70**:6157-6165.

Alsford S and Horn D (2008) Single-Locus Targeting Constructs for Reliable Regulated RNAi and Transgene Expression in *Trypanosoma brucei*. Mol *Biochem Parasitol*. **161**:76-79.

Alsford S, Turner D J, Obado S O, Sanchez-Flores A, Glover L, Berriman M, Hertz-Fowler C and Horn D (2011) High-Throughput Phenotyping Using Parallel Sequencing of RNA Interference Targets in the African Trypanosome. *Genome Res* **21**:915-924.

Amrouni D, Meiller A, Gautier-Sauvigne S, Piraud M, Bouteille B, Vincendeau P, Buguet A and Cespuglio R (2011) Cerebral Changes Occurring in Arginase and Dimethylarginine Dimethylaminohydrolase (DDAH) in a Rat Model of Sleeping Sickness. *PLoS One* **6**:e16891.

Aranibar N, Singh B K, Stockton G W and Ott K H (2001) Automated Mode-of-Action Detection by Metabolic Profiling. *Biochem Biophys Res Commun*. **286**:150-155.

Ariyanayagam MR and Fairlamb A H (2001) Ovothiol and Trypanothione As Antioxidants in Trypanosomatids. *Mol Biochem Parasitol*. **115**:189-198.

Askonas BA, Corsini A C, Clayton C E and Ogilvie B M (1979) Functional Depletion of T- and B-Memory Cells and Other Lymphoid Cell Subpopulations-During Trypanosomiasis. *Immunology* **36**:313-321.

Bacchi CJ (1993) Resistance to Clinical Drugs in African Trypanosomes. *Parasitol Today* **9**:190-193.

Bacchi CJ, Garofalo J, Ciminelli M, Rattendi D, Goldberg B, McCann P P and Yarlett N (1993) Resistance to Dl-Alpha-Difluoromethylornithine by Clinical Isolates of *Trypanosoma brucei rhodesiense* - Role of S-Adenosylmethionine. *Biochem Pharmacol*. **46**:471-481.

Bacchi CJ, Garofalo J, Mockenhaupt D, McCann P P, Diekema K A, Pegg A E, Nathan H C, Mullaney E A, Chunosoff L, Sjoerdsma A and Hutner S H (1983) In Vivo Effects of Alpha-DL-Difluoromethylornithine on the Metabolism and Morphology of *Trypanosoma brucei brucei*. *Mol Biochem Parasitol*. **7**:209-225.

Bacchi CJ, Goldberg B, Garofalo-Hannan J, Rattendi D, Lyte P and Yarlett N (1995) Fate of Soluble Methionine in African Trypanosomes: Effects of Metabolic Inhibitors. *Biochem J* **309**:737-743.

Baker N, Alsford S and Horn D (2011) Genome-Wide RNAi Screens in African Trypanosomes Identify the Nifurtimox Activator NTR and the Eflornithine Transporter AAT6. *Mol Biochem Parasitol*. **176**:55-7

Bakker BM, Krauth-Siegel R L, Clayton C, Matthews K, Girolami M, Westerhoff H V, Michels P A, Breitling R and Barrett M P (2010) The Silicon Trypanosome. *Parasitology* **137**:1333-1341.

Bakker BM, Mensonides F I, Teusink B, van Hoek P, Michels P A and Westerhoff H V (2000) Compartmentation Protects Trypanosomes From the Dangerous Design of Glycolysis. *Proc Natl Acad Sci U S A* **97**:2087-2092.

Bakker BM, Michels P A, Opperdoes F R and Westerhoff H V (1997) Glycolysis in Bloodstream Form *Trypanosoma brucei* Can Be Understood in Terms of the Kinetics of the Glycolytic Enzymes. *J Biol Chem* **272**:3207-3215.

Balasegaram M, Harris S, Checchi F, Ghorashian S, Hamel C and Karunakara U (2006) Melarsoprol Versus Eflornithine for Treating Late-Stage Gambian Trypanosomiasis in the Republic of the Congo. *Bull World Health Organ* **84**:783-791.

Balmer O, Beadell J S, Gibson W and Caccone A (2011) Phylogeography and Taxonomy of *Trypanosoma brucei*. *PLoS Negl Trop Dis* **5**:961.

Bando K, Kunimatsu T, Sakai J, Kimura J, Funabashi H, Seki T, Bamba T and Fukusaki E (2010) GC-MS-Based Metabolomics Reveals Mechanism of Action for Hydrazine Induced Hepatotoxicity in Rats. *J Appl Toxicol*.**31:**524-535.

Barfield CA, Barney R S, Crudder C H, Wilmoth J L, Stevens D S, Mora-Garcia S, Yanovsky M J, Weigl B H and Yanovsky J (2011) A Highly Sensitive Rapid Diagnostic Test for Chagas Disease That Utilizes a Recombinant *Trypanosoma cruzi* Antigen. *IEEE Trans Biomed Eng* **58**:814-817.

Barrett MP (1999) The Fall and Rise of Sleeping Sickness. *Lancet* **353**:1113-1114.

Barrett MP (2006) The Rise and Fall of Sleeping Sickness. *Lancet* **367**:1377-1378.

Barrett MP, Boykin D W, Brun R and Tidwell R R (2007) Human African Trypanosomiasis: Pharmacological Re-Engagement With a Neglected Disease. *Br J Pharmacol*. **152**:1155-1171.

Barrett MP and Fairlamb A H (1999) The Biochemical Basis of Arsenical-Diamidine Crossresistance in African Trypanosomes. *Parasitol Today* **15**:136-140.

Barrett MP and Gilbert I H (2006) Targeting of Toxic Compounds to the Trypanosome's Interior. *Adv Parasitol* **63**:125-183.

Barrett MP, Tetaud E, Seyfang A, Bringaud F and Baltz T (1998) Trypanosome Glucose Transporters. *Mol Biochem Parasitol* **91**:195-205.

Barrett MP, Vincent IM, Burchmore RJ, Kazibwe AJ, Matovu E (2011) Drug Resistance in Human African Trypanosomiasis. *Future Microbiol*. **6**:1037-47.

Barry JD, Hajduk S L, Vickerman K and Le Ray D (1979) Detection of Multiple Variable Antigen Types in Metacyclic Populations of *Trypanosoma brucei*. *Trans R Soc Trop Med Hyg* **73**:205-208.

Basselin M, Denise H, Coombs G H and Barrett M P (2002) Resistance to Pentamidine *in Leishmania mexicana* Involves Exclusion of the Drug From the Mitochondrion. *Antimicrob Agents Chemother* **46**: 3731-3738.

Beckonert O, Keun H C, Ebbels T M, Bundy J, Holmes E, Lindon J C and Nicholson J K (2007) Metabolic Profiling, Metabolomic and Metabonomic Procedures for NMR Spectroscopy of Urine, Plasma, Serum and Tissue Extracts. *Nat Protoc* **2**:2692-2703.

Bellofatto V, Fairlamb A H, Henderson G B and Cross G A (1987) Biochemical Changes Associated With Alpha-Difluoromethylornithine Uptake and Resistance in *Trypanosoma brucei*. *Mol Biochem Parasitol* **25**:227-238.

Benne R, Van den B J, Brakenhoff J P, Sloof P, Van Boom J H and Tromp M C (1986) Major Transcript of the Frameshifted CoxII Gene From Trypanosome Mitochondria Contains Four Nucleotides That Are Not Encoded in the DNA. *Cell* **46**:819-826.

Benzinger TH and Hems R (1956) Reversibility and Equilibrium of the Glutaminase Reaction Observed Calorimetrically to Find the Free Energy of Adenosine Triphosphate Hydrolysis. *Proc Natl Acad Sci USA*. **42**:896-900.

Berger BJ, Carter N S and Fairlamb A H (1995) Characterisation of Pentamidine-Resistant *Trypanosoma brucei brucei*. *Mol Biochem Parasitol* **69**:289-298.

Berrang-Ford L, Berke O, Sweeney S and Abdelrahman L (2010) Sleeping Sickness in Southeastern Uganda: a Spatio-Temporal Analysis of Disease Risk, 1970-2003. *Vector Borne Zoonotic Dis* **10**:977-988.

Berriman M, Ghedin E, Hertz-Fowler C, Blandin G, Renauld H, Bartholomeu D C, Lennard N J, Caler E, Hamlin N E, Haas B, Bohme W, Hannick L, Aslett M A, Shallom J, Marcello L, Hou L H, Wickstead B, Alsmark U C M, Arrowsmith C, Atkin R J, Barron A J, Bringaud F, Brooks K, Carrington M, Cherevach I, Chillingworth T J, Churcher C, Clark L N, Corton C H, Cronin A, Davies R M, Doggett J, Djikeng A, Feldblyum T, Field M C, Fraser A, Goodhead I, Hance Z, Harper D, Harris B R, Hauser H, Hostetter J, Ivens A, Jagels K, Johnson D, Johnson J, Jones K, Kerhornou A X, Koo H, Larke N, Landfear S, Larkin C, Leech V, Line A, Lord A, MacLeod A, Mooney P J, Moule S, Martin D M A, Morgan G W, Mungall K, Norbertczak H, Ormond D, Pai G, Peacock C S, Peterson J, Quail M A, Rabbinowitsch E, Rajandream M A, Reitter C, Salzberg S L, Sanders M, Schobel S, Sharp S, Simmonds M, Simpson A J, Talton L, Turner C M R, Tait A, Tivey A R, Van Aken S, Walker D, Wanless D, Wang S L, White B, White O, Whitehead S, Woodward J, Wortman J, Adams M D, Embley T M, Gull K, Ullu E, Barry J D, Fairlamb A H, Opperdoes F, Barret B G, Donelson J E, Hall N, Fraser C M, Melville S E and El Sayed N M (2005) The Genome of the African Trypanosome *Trypanosoma brucei*. *Science* **309**:416-422.

Besteiro S, Barrett M P, Riviere L and Bringaud F (2005) Energy Generation in Insect Stages of *Trypanosoma brucei*: Metabolism in Flux. *Trends Parasitol*. **21**:185-191.

Biebinger S, Wirtz L E, Lorenz P and Clayton C (1997) Vectors for Inducible Expression of Toxic Gene Products in Bloodstream and Procyclic *Trypanosoma brucei*. *Mol Biochem Parasitol*. **85**:99-112.

Bitonti AJ, Bacchi C J, McCann P P and Sjoerdsma A (1986a) Uptake of Alpha-Difluoromethylornithine by *Trypanosoma brucei brucei*. *Biochem Pharmacol*. **35**:351-354.

Bitonti AJ, Crossdoersen D E and McCann P P (1988) Effects of Alpha-Difluoromethylornithine on Protein-Synthesis and Synthesis of the Variant-Specific Glycoprotein (Vsg) in *Trypanosoma-brucei-brucei*. *Biochem J.* **250**:295-298.

Bitonti AJ, Dumont J A and McCann P P (1986b) Characterization of *Trypanosoma brucei brucei* S-Adenosyl-L-Methionine Decarboxylase and Its Inhibition by Berenil, Pentamidine and Methylglyoxal Bis(Guanylhydrazone). *Biochem J.* **237**:685-689.

Bitonti AJ, McCann P P and Sjoerdsma A (1986c) Necessity of Antibody Response in the Treatment of African Trypanosomiasis With Alpha-Difluoromethylornithine. *Biochem Pharmacol.* **35**:331-334.

Blum B, Bakalara N and Simpson L (1990) A Model for RNA Editing in Kinetoplastid Mitochondria: "Guide" RNA Molecules Transcribed From Maxicircle DNA Provide the Edited Information. *Cell* **60**:189-198.

Blum J, Nkunku S and Burri C (2001) Clinical Description of Encephalopathic Syndromes and Risk Factors for Their Occurrence and Outcome During Melarsoprol Treatment of Human African Trypanosomiasis. *Trop Med Int Health* **6**:390-400.

Bochud-Allemann N and Schneider A (2002) Mitochondrial Substrate Level Phosphorylation Is Essential for Growth of Procyclic *Trypanosoma brucei*. *J Biol Chem.* **277**:32849-32854.

Boiani M, Piacenza L, Hernandez P, Boiani L, Cerecetto H, Gonzalez M and Denicola A (2010) Mode of Action of Nifurtimox and N-Oxide-Containing Heterocycles Against *Trypanosoma cruzi*: Is Oxidative Stress Involved? *Biochem Pharmacol.* **79:**1736-45.

Borst P and Ouellette M (1995) New Mechanisms of Drug Resistance in Parasitic Protozoa. *Annu Rev Microbiol* **49**:427-460.

Boulange AF, Khamadi S A, Pillay D, Coetzer T H and Authie E (2011) Production of Congopain, the Major Cysteine Protease of *Trypanosoma (Nannomonas) congolense*, in *Pichia pastoris* Reveals Unexpected Dimerisation at Physiological PH. *Protein Expr Purif* **75**:95-103.

Bowes AE, Samad A H, Jiang P, Weaver B and Mellors A (1993) The Acquisition of Lysophosphatidylcholine by African Trypanosomes. *J Biol Chem* **268**:13885-13892.

Bray PG, Barrett M P, Ward S A and De Koning H P (2003) Pentamidine Uptake and Resistance in Pathogenic Protozoa: Past, Present and Future. *Trends Parasitol* **19**:232-239.

Breitling R, Pitt A R and Barrett M P (2006) Precision Mapping of the Metabolome. *Trends Biotechnol*. **24**:543-548.

Bridges DJ, Gould M K, Nerima B, Maser P, Burchmore R J S and De Koning H P (2007) Loss of the High-Affinity Pentamidine Transporter Is Responsible for High Levels of Cross-Resistance Between Arsenical and Diamidine Drugs in African Trypanosomes. *Mol Pharmacol*. **71**:1098-1108.

Bringaud F, Riviere L and Coustou V (2006) Energy Metabolism of Trypanosomatids: Adaptation to Available Carbon Sources. *Mol Biochem Parasitol*. **149**:1-9.

Brun R, Blum J, Chappuis F and Burri C (2010) Human African Trypanosomiasis. *Lancet* **375**:148-159.

Brun R and Schonenberger M (1981) Stimulating Effect of Citrate and Cis-Aconitate on the Transformation of *Trypanosoma brucei* Bloodstream Forms to Procyclic Forms *in Vitro*. *Z Parasitenkd* **66**:17-24.

Brun R, Schumacher R, Schmid C, Kunz C and Burri C (2001) The Phenomenon of Treatment Failures in Human African Trypanosomiasis. *Trop Med Int Health* **6**:906-914.

Brusilow SW and Horwich A L (1995) Amino acids, in The Metabolic and Molecular Bases of Inherited Disease (Scriver CR, Beaudet AL, Sly WS and Valle D eds)85, McGraw-Hill, New York.

Burkard GS, Jutzi P and Roditi I (2010) Genome-Wide RNAi Screens in Bloodstream Form Trypanosomes Identify Drug Transporters. *Mol Biochem Parasitol*. **175**:91-4.

Burri C and Brun R (2003) Eflornithine for the Treatment of Human African Trypanosomiasis. *Parasitol Res* **90** Supp 1:S49-S52.

Buscher P, Mumba N D, Kabore J, Lejon V, Robays J, Jamonneau V, Bebronne N, Van d, V and Bieler S (2009) Improved Models of Mini Anion Exchange Centrifugation Technique (MAECT) and Modified Single Centrifugation (MSC) for Sleeping Sickness Diagnosis and Staging. *PLoS Negl Trop Dis* **3**:e471.

Caldovic L, Ah M N, Shi D, Morizono H, Yudkoff M and Tuchman M (2010) N-Acetylglutamate Synthase: Structure, Function and Defects. *Mol Genet Metab* **100** Suppl 1:S13-S19.

Camacho JA, Mardach R, Rioseco-Camacho N, Ruiz-Pesini E, Derbeneva O, Andrade D, Zaldivar F, Qu Y and Cederbaum S D (2006) Clinical and Functional Characterization of a Human ORNT1 Mutation (T32R) in the Hyperornithinemia-Hyperammonemia-Homocitrullinuria (HHH) Syndrome. *Pediatr Res* **60**:423-429.

Canepa GE, Carrillo C, Miranda M R, Saye M and Pereira C A (2011) Arginine Kinase in *Phytomonas*, a Trypanosomatid Parasite of Plants. *Comp Biochem Physiol B Biochem Mol Biol*.**160**:40-3.

Canepa GE, Silber A M, Bouvier L A and Pereira C A (2004) Biochemical Characterization of a Low-Affinity Arginine Permease From the Parasite *Trypanosoma cruzi*. *FEMS Microbiol Lett* **236**:79-84.

Cao W, Sun B, Feitelson M A, Wu T, Tur-Kaspa R and Fan Q (2009) Hepatitis C Virus Targets Over-Expression of Arginase I in Hepatocarcinogenesis. *Int J Cancer* **124**:2886-2892.

Careri M and Mangia A (2011) Trends in Analytical Atomic and Molecular Mass Spectrometry in Biology and the Life Sciences. *Anal Bioanal Chem* **399**:2585-2595.

Carrillo C, Canepa G E, Giacometti A, Bouvier L A, Miranda M R, los Milagros C M and Pereira C A (2010) *Trypanosoma cruzi* Amino Acid Transporter TcAAAP411 Mediates Arginine Uptake in Yeasts. *FEMS Microbiol Lett* **306**:97-102.

Carter NS and Fairlamb A H (1993) Arsenical-Resistant Trypanosomes Lack An Unusual Adenosine Transporter. *Nature* **361**:173-176.

Carvajal N, Lopez V, Salas M, Uribe E, Herrera P and Cerpa J (1999) Manganese Is Essential for Catalytic Activity of *Escherichia coli* Agmatinase. *Biochem Biophys Res Commun* **258**:808-811.

Cavalli RC, Burke C J, Kawamoto S, Soprano D R and Ash D E (1994) Mutagenesis of Rat Liver Arginase Expressed in *Escherichia coli*: Role of Conserved Histidines. *Biochemistry* **33**:10652-10657.

Cederbaum SD, Yu H, Grody W W, Kern R M, Yoo P and Iyer R K (2004) Arginases I and II: Do Their Functions Overlap? *Mol Genet Metab* **81** Suppl 1:S38-S44.

Chappuis F, Udayraj N, Stietenroth K, Meussen A and Bovier P A (2005) Eflornithine Is Safer Than Melarsoprol for the Treatment of Second-Stage *Trypanosoma brucei gambiense* Human African Trypanosomiasis. *Clin Infect Dis.* **41**:748-751.

Chen J, Rauch C A, White J H, Englund P T and Cozzarelli N R (1995) The Topology of the Kinetoplast DNA Network. *Cell* **80**:61-69.

Choi Y, Park H Y, Park S J, Park S J, Kim S K, Ha C, Im S J and Lee J H (2011) Growth Phase-Differential Quorum Sensing Regulation of Anthranilate Metabolism in *Pseudomonas aeruginosa*. *Mol Cells*. **32**:57-65

Christianson DW (2005) Arginase: Structure, Mechanism, and Physiological Role in Male and Female Sexual Arousal. *Acc Chem Res* **38**:191-201.

Clasquin MF, Melamud E, Singer A, Gooding J R, Xu X, Dong A, Cui H, Campagna S R, Savchenko A, Yakunin A F, Rabinowitz J D and Caudy A A (2011) Riboneogenesis in Yeast. *Cell* **145**:969-980.

Clayton CE and Michels P (1996) Metabolic Compartmentation in African Trypanosomes. *Parasitol Today* **12**:465-471.

Clayton CE, Sacks D L, Ogilvie B M and Askonas B A (1979) Membrane Fractions of Trypanosomes Mimic the Immunosuppressive and Mitogenic Effects of Living Parasites on the Host. *Parasite Immunol* **1**:241-249.

Clyne T, Kinch L N and Phillips M A (2002) Putrescine Activation of *Trypanosoma cruzi* S-Adenosylmethionine Decarboxylase. *Biochemistry* **41**:13207-13216.

Comini MA, Guerrero S A, Haile S, Menge U, Lunsdorf H and Flohe L (2004) Validation of *Trypanosoma brucei* Trypanothione Synthetase As Drug Target. *Free Radic Biol Med* **36**:1289-1302.

Cottret L, Wildridge D, Vinson F, Barrett M P, Charles H, Sagot M F and Jourdan F (2010) MetExplore: a Web Server to Link Metabolomic Experiments and Genome-Scale Metabolic Networks. *Nucleic Acids Res* **38**:W132-W137.

Coustou V, Besteiro S, Biran M, Diolez P, Bouchaud V, Voisin P, Michels P A, Canioni P, Baltz T and Bringaud F (2003) ATP Generation in the *Trypanosoma brucei* Procyclic Form: Cytosolic Substrate Level Is Essential, but Not Oxidative Phosphorylation. *J Biol Chem* **278**:49625-49635.

Coustou V, Besteiro S, Riviere L, Biran M, Biteau N, Franconi J M, Boshart M, Baltz T and Bringaud F (2005) A Mitochondrial NADH-Dependent Fumarate Reductase Involved in the Production of Succinate Excreted by Procyclic *Trypanosoma brucei*. *J Biol Chem.* **280**:16559-16570.

Coustou V, Biran M, Breton M, Guegan F, Riviere L, Plazolles N, Nolan D, Barrett M P, Franconi J M and Bringaud F (2008) Glucose-Induced Remodeling of Intermediary and Energy Metabolism in Procyclic *Trypanosoma brucei. J Biol Chem* **283**:16342-16354.

Cross GA (1975) Identification, Purification and Properties of Clone-Specific Glycoprotein Antigens Constituting the Surface Coat of *Trypanosoma brucei. Parasitology* **71**:393-417.

Crowe JS, Barry J D, Luckins A G, Ross C A and Vickerman K (1983) All Metacyclic Variable Antigen Types of *Trypanosoma congolense* Identified Using Monoclonal Antibodies. *Nature* **306**:389-391.

Cubbon S, Antonio C, Wilson J and Thomas-Oates J (2010) Metabolomic Applications of HILIC-LC-MS. *Mass Spectrom Rev* **29**:671-684.

Cummings KL and Tarleton R L (2004) Inducible Nitric Oxide Synthase Is Not Essential for Control of *Trypanosoma cruzi* Infection in Mice. *Infect Immun* **72**:4081-4089.

Czichos J, Nonnengaesser C and Overath P (1986) *Trypanosoma brucei*: Cis-Aconitate and Temperature Reduction As Triggers of Synchronous Transformation of Bloodstream to Procyclic Trypomastigotes *in Vitro*. *Exp Parasitol* **62**:283-291.

da Silva ER, Castilho T M, Pioker F C, Tomich de Paula Silva CH and Floeter-Winter L M (2002) Genomic Organisation and Transcription Characterisation of the Gene Encoding *Leishmania (Leishmania) amazonensis* Arginase and Its Protein Structure Prediction. *Int J Parasitol* **32**:727-737.

da Silva ER, da Silva M F, Fischer H, Mortara R A, Mayer M G, Framesqui K, Silber A M and Floeter-Winter L M (2008) Biochemical and Biophysical Properties of a Highly Active Recombinant Arginase *From Leishmania (Leishmania) amazonensis* and Subcellular Localization of Native Enzyme. *Mol Biochem Parasitol* **159**:104-111.

Daniels JP, Gull K and Wickstead B (2010) Cell Biology of the Trypanosome Genome. *Microbiol Mol Biol Rev* **74**:552-569.

Danielsson AP, Moritz T, Mulder H and Spegel P (2010) Development and Optimization of a Metabolomic Method for Analysis of Adherent Cell Cultures. *Anal Biochem* **404**:30-39.

Darghouth D, Koehl B, Junot C and Romeo P H (2010) Metabolomic Analysis of Normal and Sickle Cell Erythrocytes. *Transfus Clin Biol* **17**:148-150.

Davis RH, Lieu P and Ristow J L (1994) Neurospora Mutants Affecting Polyamine-Dependent Processes and Basic-Amino-Acid Transport Mutants Resistant to the Polyamine Inhibitor, Alpha-Difluoromethylornithine. *Genetics* **138**:649-655.

De Koning HP (2001) Uptake of Pentamidine in *Trypanosoma brucei brucei* Is Mediated by Three Distinct Transporters: Implications for Cross-Resistance With Arsenicals. *Mol Pharmacol* **59**:586-592.

De Koning HP, Anderson L F, Stewart M, Burchmore R J, Wallace L J and Barrett M P (2004) The Trypanocide Diminazene Aceturate Is Accumulated Predominantly Through the TbAT1 Purine Transporter: Additional Insights on Diamidine Resistance in African Trypanosomes. *Antimicrob Agents Chemother* **48**:1515-1519.

De Koning HP and Jarvis S M (1999) Adenosine Transporters in Bloodstream Forms of *Trypanosoma brucei brucei*: Substrate Recognition Motifs and Affinity for Trypanocidal Drugs. *Mol Pharmacol* **56**:1162-1170.

de la Fuente J, Rodriguez M, Redondo M, Montero C, Garcia-Garcia J C, Mendez L, Serrano E, Valdes M, Enriquez A, Canales M, Ramos E, Boue O, Machado H,

Lleonart R, de Armas C A, Rey S, Rodriguez J L, Artiles M and Garcia L (1998) Field Studies and Cost-Effectiveness Analysis of Vaccination With Gavac Against the Cattle Tick *Boophilus microplus*. *Vaccine* **16**:366-373.

De Ravin SS, Zarember K A, Long-Priel D, Chan K C, Fox S D, Gallin J I, Kuhns D B and Malech H L (2010) Tryptophan/Kynurenine Metabolism in Human Leukocytes Is Independent of Superoxide and Is Fully Maintained in Chronic Granulomatous Disease. *Blood* **116**:1755-1760.

Dean S, Marchetti R, Kirk K and Matthews K R (2009) A Surface Transporter Family Conveys the Trypanosome Differentiation Signal. *Nature* **459**:213-217.

Delespaux V and De Koning H P (2007) Drugs and Drug Resistance in African Trypanosomiasis. *Drug Resist Updat* **10**:30-50.

Denery JR, Nunes A A, Hixon M S, Dickerson T J and Janda K D (2010) Metabolomics-Based Discovery of Diagnostic Biomarkers for Onchocerciasis. *PLoS Negl Trop Dis* **4**: e824.

Deutch CE (2011) L-Proline Nutrition and Catabolism in *Staphylococcus saprophyticus*. *Antonie Van Leeuwenhoek* **99**:781-793.

Di Costanzo L, Sabio G, Mora A, Rodriguez P C, Ochoa A C, Centeno F and Christianson D W (2005) Crystal Structure of Human Arginase I at 1.29-A Resolution and Exploration of Inhibition in the Immune Response. *Proc Natl Acad Sci U S A* **102**:13058-13063.

Docampo R and Moreno S N (1984) Free Radical Metabolites in the Mode of Action of Chemotherapeutic Agents and Phagocytic Cells on *Trypanosoma cruzi*. *Rev Infect Dis* **6**:223-238.

Docampo R, Moreno S N, Stoppani A O, Leon W, Cruz F S, Villalta F and Muniz R F (1981) Mechanism of Nifurtimox Toxicity in Different Forms of *Trypanosoma cruzi*. *Biochem Pharmacol* **30**:1947-1951.

Docampo R and Stoppani A O (1979) Generation of Superoxide Anion and Hydrogen Peroxide Induced by Nifurtimox in *Trypanosoma cruzi*. *Arch Biochem Biophys* **197**:317-321.

Dorman FL, Whiting J J, Cochran J W and Gardea-Torresdey J (2010) Gas Chromatography. *Anal Chem* **82**:4775-4785.

Doyle JJ, Hirumi H, Hirumi K, Lupton E N and Cross G A (1980) Antigenic Variation in Clones of Animal-Infective *Trypanosoma brucei* Derived and Maintained *in Vitro*. *Parasitology* **80**:359-369.

Duleu S, Vincendeau P, Courtois P, Semballa S, Lagroye I, Daulouede S, Boucher J L, Wilson K T, Veyret B and Gobert A P (2004) Mouse Strain Susceptibility to

Trypanosome Infection: an Arginase-Dependent Effect. *J Immunol* **172**:6298-6303.

Dunn WB (2008) Current Trends and Future Requirements for the Mass Spectrometric Investigation of Microbial, Mammalian and Plant Metabolomes. *Phys Biol* **5**:011001.

Durieux PO, Schutz P, Brun R and Kohler P (1991) Alterations in Krebs Cycle Enzyme Activities and Carbohydrate Catabolism in Two Strains of *Trypanosoma brucei* During *in Vitro* Differentiation of Their Bloodstream to Procyclic Stages. *Mol Biochem Parasitol* **45**:19-27.

Ebikeme, C. E. Amino Acid Transporters in *Trypanosoma brucei brucei* (2008) University of Glasgow Thesis/Dissertation: 86-87

Eisenberg T, Knauer H, Schauer A, Buttner S, Ruckenstuhl C, Carmona-Gutierrez D, Ring J, Schroeder S, Magnes C, Antonacci L, Fussi H, Deszcz L, Hartl R, Schraml E, Criollo A, Megalou E, Weiskopf D, Laun P, Heeren G, Breitenbach M, Grubeck-Loebenstein B, Herker E, Fahrenkrog B, Frohlich K U, Sinner F, Tavernarakis N, Minois N, Kroemer G and Madeo F (2009) Induction of Autophagy by Spermidine Promotes Longevity. *Nat Cell Biol* **11**:1305-1314.

Ellman GL (1959) Tissue Sulfhydryl Groups. *Arch Biochem Biophys* **82**:70-77.

Enanga B, Ariyanayagam M R, Stewart M L and Barrett M P (2003) Activity of Megazol, a Trypanocidal Nitroimidazole, Is Associated With DNA Damage. *Antimicrob Agents Chemother* **47**:3368-3370.

Erdmann N, Tian C, Huang Y, Zhao J, Herek S, Curthoys N and Zheng J (2009) In Vitro Glutaminase Regulation and Mechanisms of Glutamate Generation in HIV-1-Infected Macrophage. *J Neurochem* **109**:551-561.

Esser KM, Schoenbechler M J and Gingrich J B (1982) *Trypanosoma rhodesiense* Blood Forms Express All Antigen Specificities Relevant to Protection Against Metacyclic (Insect Form) Challenge. *J Immunol* **129**:1715-1718.

Ezeani MC, Okoro H, Anosa V O, Onyenekwe C C, Meludu S C, Dioka C E and Azikiwe C C (2008) Immunodiagnosis of Bovine Trypanosomiasis in Anambra and Imo States, Nigeria, Using Enzyme-Linked Immunosorbent Assay: Zoonotic Implications to Human Health. *J Vector Borne Dis* **45**:292-300.

Fairlamb AH (1989) Novel Biochemical Pathways in Parasitic Protozoa. *Parasitology* **99** Suppl:S93-112.

Fairlamb AH (2002) Metabolic Pathway Analysis in Trypanosomes and Malaria Parasites. *Philos Trans R Soc Lond B Biol Sci.* **357**:101-107.

Fairlamb AH and Cerami A (1992) Metabolism and Functions of Trypanothione in the Kinetoplastida. *Annu Rev Microbiol* **46**:695-729.

Fairlamb AH, Henderson G B, Bacchi C J and Cerami A (1987) *In Vivo* Effects of Difluoromethylornithine on Trypanothione and Polyamine Levels in Bloodstream Forms of *Trypanosoma brucei*. *Mol Biochem Parasitol* **24**:185-191.

Fairlamb AH, Henderson G B and Cerami A (1989) Trypanothione Is the Primary Target for Arsenical Drugs Against African Trypanosomes. *Proc Natl Acad Sci U S A* **86**:2607-2611.

Fan TW, Lane A N, Higashi R M, Farag M A, Gao H, Bousamra M and Miller D M (2009) Altered Regulation of Metabolic Pathways in Human Lung Cancer Discerned by (13)C Stable Isotope-Resolved Metabolomics (SIRM). *Mol Cancer* **8**:41.

Farooq U and Mahajan R C (2004) Drug Resistance in Malaria. *J Vector Borne Dis* **41**:45-53.

Feagin JE, Abraham J M and Stuart K (1988) Extensive Editing of the Cytochrome c Oxidase III Transcript in *Trypanosoma brucei*. *Cell* **53**:413-422.

Fenn K and Matthews K R (2007) The Cell Biology of *Trypanosoma brucei* Differentiation. *Curr Opin Microbiol* **10**:539-546.

Field MC and Carrington M (2009) The Trypanosome Flagellar Pocket. *Nat Rev Microbiol* **7**:775-786.

Franz G and Robinson A S (2011) Molecular Technologies to Improve the Effectiveness of the Sterile Insect Technique. *Genetica* **139**:1-5.

Furuya T, Kessler P, Jardim A, Schnaufer A, Crudder C and Parsons M (2002) Glucose Is Toxic to Glycosome-Deficient Trypanosomes. *Proc Natl Acad Sci U S A* **99**:14177-14182.

Gaston MA, Zhang L, Green-Church K B and Krzycki J A (2011) The Complete Biosynthesis of the Genetically Encoded Amino Acid Pyrrolysine From Lysine. *Nature* **471**:647-650.

Gaur U, Roberts S C, Dalvi R P, Corraliza I, Ullman B and Wilson M E (2007) An Effect of Parasite-Encoded Arginase on the Outcome of Murine Cutaneous Leishmaniasis. *J Immunol* **179**:8446-8453.

Ghoda L, Sidney D, Macrae M and Coffino P (1992) Structural Elements of Ornithine Decarboxylase Required for Intracellular Degradation and Polyamine-Dependent Regulation. *Mol Cell Biol* **12**:2178-2185.

Gibson W (2002) Will the Real *Trypanosoma brucei rhodesiense* Please Step Forward? *Trends Parasitol* **18**:486-490.

Gobert AP, McGee D J, Akhtar M, Mendz G L, Newton J C, Cheng Y, Mobley H L and Wilson K T (2001) *Helicobacter pylori* Arginase Inhibits Nitric Oxide

Production by Eukaryotic Cells: a Strategy for Bacterial Survival. *Proc Natl Acad Sci U S A* **98**:13844-13849.

Goldberg RN, Tewari Y B and Bhat T N (2004) Thermodynamics of Enzyme-Catalyzed Reactions--a Database for Quantitative Biochemistry. *Bioinformatics* **20**:2874-2877.

Gonzalez-Martin G, Thambo S, Paulos C, Vasquez I and Paredes J (1992) The Pharmacokinetics of Nifurtimox in Chronic Renal Failure. *Eur J Clin Pharmacol* **42**:671-673.

Grant PT and Fulton J D (1957) The Catabolism of Glucose by Strains of *Trypanosoma rhodesiense*. *Biochem J* **66**:242-250.

Griffin JL (2006) The Cinderella Story of Metabolic Profiling: Does Metabolomics Get to Go to the Functional Genomics Ball? *Philos Trans R Soc Lond B Biol Sci* **361**:147-161.

Grishin NV, Osterman A L, Brooks H B, Phillips M A and Goldsmith E J (1999) X-Ray Structure of Ornithine Decarboxylase From *Trypanosoma brucei*: the Native Structure and the Structure in Complex With Alpha-Difluoromethylornithine. *Biochemistry* **38**:15174-15184.

Grondin K, Roy G and Ouellette M (1996) Formation of Extrachromosomal Circular Amplicons With Direct or Inverted Duplications in Drug-Resistant *Leishmania tarentolae*. *Mol Cell Biol* **16**:3587-3595.

Guerra-Giraldez C, Quijada L and Clayton C E (2002) Compartmentation of Enzymes in a Microbody, the Glycosome, Is Essential in *Trypanosoma brucei*. *J Cell Sci* **115**:2651-2658.

Haanstra JR, Kerkhoven E J, van Tuijl A, Blits M, Wurst M, van Nuland R, Albert M A, Michels P A, Bouwman J, Clayton C, Westerhoff H V and Bakker B M (2011) A Domino Effect in Drug Action: From Metabolic Assault Towards Parasite Differentiation. *Mol Microbiol* **79**:94-108.

Haanstra JR, van Tuijl A, Kessler P, Reijnders W, Michels P A, Westerhoff H V, Parsons M and Bakker B M (2008) Compartmentation Prevents a Lethal Turbo-Explosion of Glycolysis in Trypanosomes. *Proc Natl Acad Sci U S A* **105**:17718-17723.

Haberkorn A, Harder A and Greif G (2001) Milestones of Protozoan Research at Bayer. *Parasitol Res* **87**:1060-1062.

Hall BS, Bot C and Wilkinson S R (2011) Nifurtimox Activation by Trypanosomal Type I Nitroreductases Generates Cytotoxic Nitrile Metabolites. *J Biol Chem*. **286**:13088-95.

Hamilton PB, Gibson W C and Stevens J R (2007) Patterns of Co-Evolution Between Trypanosomes and Their Hosts Deduced From Ribosomal RNA and Protein-Coding Gene Phylogenies. *Mol Phylogenet Evol* **44**:15-25.

Hammarton TC (2007) Cell Cycle Regulation in *Trypanosoma brucei*. *Mol Biochem Parasitol* **153**:1-8.

Hasne M and Barrett M P (2000a) Drug Uptake Via Nutrient Transporters in *Trypanosoma brucei*. *J Appl Microbiol* **89**:697-701.

Hasne, M. P. Amino acid transporters in *Trypanosoma brucei brucei* (2000) University of Glasgow Thesis/Dissertation.

Hasne MP and Barrett M P (2000b) Transport of Methionine in *Trypanosoma brucei brucei*. *Mol Biochem Parasitol* **111**:299-307.

Hasne MP, Coppens I, Soysa R and Ullman B (2010) A High-Affinity Putrescine-Cadaverine Transporter From *Trypanosoma cruzi*. *Mol Microbiol* **76**:78-91.

Hasne MP and Ullman B (2005) Identification and Characterization of a Polyamine Permease From the Protozoan Parasite *Leishmania major*. *J Biol Chem* **280**:15188-15194.

Heby O, Persson L and Rentala M (2007) Targeting the Polyamine Biosynthetic Enzymes: a Promising Approach to Therapy of African Sleeping Sickness, Chagas' Disease, and Leishmaniasis. *Amino Acids* **33**:359-366.

Hernandez SM, Sanchez M S and de Tarlovsky M N (2006) Polyamines As a Defense Mechanism Against Lipoperoxidation in *Trypanosoma cruzi*. *Acta Trop* **98**:94-102.

Hirumi H, Doyle J J and Hirumi K (1977) Cultivation of Blood-Stream *Trypanosoma-brucei*. *Bull World Health Organ* **55**:405-409.

Hoare CA (1973) Letter: "*Trypanosoma brucei*-Subgroup". *Trans R Soc Trop Med Hyg* **67**:421-422.

Hoffman GG and Ellington W R (2011) Arginine Kinase Isoforms in the Closest Protozoan Relative of Metazoans. *Comp Biochem Physiol Part D Genomics Proteomics* **6**:171-177.

Holsbeeks I, Lagatie O, Van Nuland A, Van de Velde S and Thevelein J M (2004) The Eukaryotic Plasma Membrane As a Nutrient-Sensing Device. *Trends Biochem Sci* **29**:556-564.

Horn D and Barry J D (2005) The Central Roles of Telomeres and Subtelomeres in Antigenic Variation in African Trypanosomes. *Chromosome Res* **13**:525-533.

Huang J and van der Ploeg L H (1991) Maturation of Polycistronic Pre-MRNA in *Trypanosoma brucei*: Analysis of Trans Splicing and Poly(A) Addition at Nascent RNA Transcripts From the Hsp70 Locus. *Mol Cell Biol* **11**:3180-3190.

Hughes B (2010) 2009 FDA Drug Approvals. *Nat Rev Drug Discov* **9**:89-92.

Huynh TT, Huynh V T, Harmon M A and Phillips M A (2003) Gene Knockdown of Gamma-Glutamylcysteine Synthetase by RNAi in the Parasitic Protozoa *Trypanosoma brucei* Demonstrates That It Is an Essential Enzyme. *J Biol Chem* **278**:39794-39800.

Igarashi K and Kashiwagi K (2010) Modulation of Cellular Function by Polyamines. *Int J Biochem Cell Biol* **42**:39-51.

Imboden MA, Laird P W, Affolter M and Seebeck T (1987) Transcription of the Intergenic Regions of the Tubulin Gene Cluster of *Trypanosoma brucei*: Evidence for a Polycistronic Transcription Unit in a Eukaryote. *Nucleic Acids Res* **15**:7357-7368.

Ingram-Smith C, Gorrell A, Lawrence S H, Iyer P, Smith K and Ferry J G (2005) Characterization of the Acetate Binding Pocket in the *Methanosarcina thermophila* Acetate Kinase. *J Bacteriol* **187**:5059.

Iniesta V, Carcelen J, Molano I, Peixoto P M, Redondo E, Parra P, Mangas M, Monroy I, Campo M L, Nieto C G and Corraliza I (2005) Arginase I Induction During *Leishmania major* Infection Mediates the Development of Disease. *Infect Immun* **73**:6085-6090.

Inoue N, Narumi D, Mbati P A, Hirumi K, Situakibanza N T and Hirumi H (1998) Susceptibility of Severe Combined Immuno-Deficient (SCID) Mice to *Trypanosoma brucei gambiense* and *T. b. rhodesiense*. *Trop Med Int Health* **3**:408-412.

Iten M, Mett H, Evans A, Enyaru J C, Brun R and Kaminsky R (1997) Alterations in Ornithine Decarboxylase Characteristics Account for Tolerance of *Trypanosoma brucei rhodesiense* to D,L-Alpha-Difluoromethylornithine. *Antimicrob Agents Chemother* **41**:1922-1925.

Jackson AP (2007) Origins of Amino Acid Transporter Loci in Trypanosomatid Parasites. *BMC Evol Biol* **7**:26.

Jackson LK, Baldwin J, Akella R, Goldsmith E J and Phillips M A (2004) Multiple Active Site Conformations Revealed by Distant Site Mutation in Ornithine Decarboxylase. *Biochemistry* **43**:12990-12999.

Janne J, Alhonenhongisto L, Seppanen P and Siimes M (1981) Use of Polyamine Antimetabolites in Experimental-Tumors and in Human-Leukemia. *Med Biol* **59**:448-457.

Janssens PG and De Muynck A (1977) Clinical Trials With "Nifurtimox" in African Trypanosomiasis. *Ann Soc Belg Méd Trop.* **57**:475-480.

Jansson-Lofmark R, Romsing S, Albers E and Ashton M (2010) Determination of Eflornithine Enantiomers in Plasma by Precolumn Derivatization With O-Phthalaldehyde-N-Acetyl-L-Cysteine and Liquid Chromatography With UV Detection. *Biomed Chromatogr* **24**:768-773.

Jeganathan S, Sanderson L, Dogruel M, Rodgers J, Croft S and Thomas S A (2011) The Distribution of Nifurtimox Across the Healthy and Trypanosome-Infected Murine Blood-Brain and Blood-Cerebrospinal Fluid Barriers. *J Pharmacol Exp Ther* **336**:506-515.

Jenkins H, Hardy N, Beckmann M, Draper J, Smith A R, Taylor J, Fiehn O, Goodacre R, Bino R J, Hall R, Kopka J, Lane G A, Lange B M, Liu J R, Mendes P, Nikolau B J, Oliver S G, Paton N W, Rhee S, Roessner-Tunali U, Saito K, Smedsgaard J, Sumner L W, Wang T, Walsh S, Wurtele E S and Kell D B (2004) A Proposed Framework for the Description of Plant Metabolomics Experiments and Their Results. *Nat Biotechnol* **22**:1601-1606.

Jennings FW (1993) Combination Chemotherapy of Cns Trypanosomiasis. *Acta Tropica* **54**:205-213.

Joerink M, Forlenza M, Ribeiro C M, de Vries B J, Savelkoul H F and Wiegertjes G F (2006) Differential Macrophage Polarisation During Parasitic Infections in Common Carp (Cyprinus carpio L.). *Fish Shellfish Immunol* **21**:561-571.

Jokiranta TS, Jokipii L and Meri S (1995) Complement Resistance of Parasites. *Scand J Immunol* **42**:9-20.

Jordan AM (1985) Tsetse Eradication Plans for Southern Africa. *Parasitol Today* **1**:121-123.

Jourdan F, Cottret L, Huc L, Wildridge D, Scheltema R, Hillenweck A, Barrett M P, Zalko D, Watson D G and Debrauwer L (2010) Use of Reconstituted Metabolic Networks to Assist in Metabolomic Data Visualization and Mining. *Metabolomics* **6**:312-321.

Kamleh A, Barrett M P, Wildridge D, Burchmore R J, Scheltema R A and Watson D G (2008) Metabolomic Profiling Using Orbitrap Fourier Transform Mass Spectrometry With Hydrophilic Interaction Chromatography: a Method With Wide Applicability to Analysis of Biomolecules. *Rapid Commun Mass Spectrom* **22**:1912-1918.

Kanyo ZF, Scolnick L R, Ash D E and Christianson D W (1996) Structure of a Unique Binuclear Manganese Cluster in Arginase. *Nature* **383**:554-557.

Kato H, Gomez E A, Caceres A G, Uezato H, Mimori T and Hashiguchi Y (2010) Molecular Epidemiology for Vector Research on Leishmaniasis. *Int J Environ Res Public Health* **7**:814-826.

Kell DB (2006) Systems Biology, Metabolic Modelling and Metabolomics in Drug Discovery and Development. *Drug Discov Today* **11**:1085-1092.

Kell DB, Brown M, Davey H M, Dunn W B, Spasic I and Oliver S G (2005) Metabolic Footprinting and Systems Biology: The Medium Is the Message. *Nature Rev Microbiol*. **3**:557-565.

Kelly JM, Taylor M C, Smith K, Hunter K J and Fairlamb A H (1993) Phenotype of Recombinant *Leishmania donovani* and *Trypanosoma cruzi* Which Over-Express Trypanothione Reductase. Sensitivity Towards Agents That Are Thought to Induce Oxidative Stress. *Eur J Biochem* **218**:29-37.

Kiefer P, Portais J C and Vorholt J A (2008) Quantitative Metabolome Analysis Using Liquid Chromatography-High-Resolution Mass Spectrometry. *Anal Biochem* **382**:94-100.

Kim HK and Verpoorte R (2010) Sample Preparation for Plant Metabolomics. *Phytochem Anal* **21**:4-13.

Kingsnorth AN and Wallace H M (1985) Elevation of Monoacetylated Polyamines in Human Breast Cancers. *Eur J Cancer Clin Oncol* **21**:1057-1062.

Kwon YK, Lu W, Melamud E, Khanam N, Bognar A and Rabinowitz J D (2008) A Domino Effect in Antifolate Drug Action in *Escherichia coli*. *Nat Chem Biol* **4**:602-608.

L'Hostis C, Geindre M and Deshusses J (1993) Active Transport of L-Proline in the Protozoan Parasite *Trypanosoma brucei brucei*. *Biochem J* **291**:297-301.

LaCount DJ, Bruse S, Hill K L and Donelson J E (2000) Double-Stranded RNA Interference in *Trypanosoma brucei* Using Head-to-Head Promoters. *Mol Biochem Parasitol* **111**:67-76.

Lahiri A, Das P and Chakravortty D (2008) Arginase Modulates *Salmonella* Induced Nitric Oxide Production in RAW264.7 Macrophages and Is Required for *Salmonella* Pathogenesis in Mice Model of Infection. *Microbes Infect* **10**:1166-1174.

Lanteri CA, Stewart M L, Brock J M, Alibu V P, Meshnick S R, Tidwell R R and Barrett M P (2006) Roles for the *Trypanosoma brucei* P2 Transporter in DB75 Uptake and Resistance. *Mol Pharmacol*. **70**:1585-1592.

Lanteri CA, Trumpower B L, Tidwell R R and Meshnick S R (2004) DB75, a Novel Trypanocidal Agent, Disrupts Mitochondrial Function in *Saccharomyces cerevisiae*. *Antimicrob Agents Chemother* **48**:3968-3974.

Laxman S, Riechers A, Sadilek M, Schwede F and Beavo J A (2006) Hydrolysis Products of CAMP Analogs Cause Transformation of *Trypanosoma brucei* From Slender to Stumpy-Like Forms. *Proc Natl Acad Sci U S A* **103**:19194-19199.

Le Ray D, Barry J D and Vickerman K (1978) Antigenic Heterogeneity of Metacyclic Forms of *Trypanosoma brucei*. *Nature* **273**:300-302.

Le Roch KG, Johnson J R, Ahiboh H, Chung D W, Prudhomme J, Plouffe D, Henson K, Zhou Y, Witola W, Yates J R, Mamoun C B, Winzeler E A and Vial H (2008) A Systematic Approach to Understand the Mechanism of Action of the Bisthiazolium Compound T4 on the Human Malaria Parasite, *Plasmodium falciparum*. *BMC Genomics* **9**:513.

Legros D, Fournier C, Gastellu E M, Maiso F and Szumilin E (1999) Therapeutic Failure of Melarsoprol Among Patients Treated for Late Stage *T.b. gambiense* Human African Trypanosomiasis in Uganda. *Bull Soc Pathol Exot* **92**:171-172.

Leprohon P, Legare D, Raymond F, Madore E, Hardiman G, Corbeil J and Ouellette M (2009) Gene Expression Modulation Is Associated With Gene Amplification, Supernumerary Chromosomes and Chromosome Loss in Antimony-Resistant *Leishmania infantum*. *Nucleic Acids Res* **37**:1387-1399.

Levin VA, Csejtey J and Byrd D J (1983) Brain, CSF, and Tumor Pharmacokinetics of Alpha-Difluoromethylornithine in Rats and Dogs. *Cancer Chemother Pharmacol* **10**:196-199.

Li F, Hua S B, Wang C C and Gottesdiener K M (1996) Procyclic *Trypanosoma brucei* Cell Lines Deficient in Ornithine Decarboxylase Activity. Mol *Biochem Parasitol*. **78**:227-236.

Li JV, Saric J, Wang Y, Utzinger J, Holmes E and Balmer O (2011) Metabonomic Investigation of Single and Multiple Strain *Trypanosoma brucei brucei* Infections. *Am J Trop Med Hyg* **84**:91-98.

Li SQ, Fung M C, Reid S A, Inoue N and Lun Z R (2007) Immunization With Recombinant Beta-Tubulin From *Trypanosoma evansi* Induced Protection Against *T. evansi, T. equiperdum* and *T. b. brucei* Infection in Mice. *Parasite Immunol* **29**:191-199.

Li SQ, Yang W B, Ma L J, Xi S M, Chen Q L, Song X W, Kang J and Yang L Z (2009) Immunization With Recombinant Actin From *Trypanosoma evansi* Induces Protective Immunity Against *T. evansi, T. equiperdum* and *T. b. brucei* Infection. *Parasitol Res* **104**:429-435.

Lietze VU, Abd-Alla A M, Vreysen M J, Geden C J and Boucias D G (2011) Salivary Gland Hypertrophy Viruses: a Novel Group of Insect Pathogenic Viruses. *Annu Rev Entomol* **56**:63-80.

Lubega GW, Ochola D O and Prichard R K (2002) *Trypanosoma brucei*: Anti-Tubulin Antibodies Specifically Inhibit Trypanosome Growth in Culture. *Exp Parasitol*. **102**:134-142.

Mackenzie NE, Hall J E, Flynn I W and Scott A I (1983) 13C Nuclear Magnetic Resonance Studies of Anaerobic Glycolysis in *Trypanosoma brucei Spp*. *Biosci Rep* **3**:141-151.

MacLeod A, Tait A and Turner C M (2001) The Population Genetics of *Trypanosoma brucei* and the Origin of Human Infectivity. *Philos Trans R Soc Lond B Biol Sci*. **356**:1035-1044.

Makarov A, Denisov E, Kholomeev A, Baischun W, Lange O, Strupat K and Horning S (2006) Performance Evaluation of a Hybrid Linear Ion Trap/Orbitrap Mass Spectrometer. *Anal Chem*. **78**:2113-2120.

Mamas M, Dunn W B, Neyses L and Goodacre R (2011) The Role of Metabolites and Metabolomics in Clinically Applicable Biomarkers of Disease. *Arch Toxicol* **85**:5-17.

Marciano D, Maugeri D A, Cazzulo J J and Nowicki C (2009) Functional Characterization of Stage-Specific Aminotransferases From Trypanosomatids. *Mol Biochem Parasitol*. **166**:172-182.

Maser P, Sutterlin C, Kralli A and Kaminsky R (1999) A Nucleoside Transporter From *Trypanosoma brucei* Involved in Drug Resistance. *Science* **285**:242-244.

Mashego MR, Rumbold K, De Mey M, Vandamme E, Soetaert W and Heijnen J J (2007) Microbial Metabolomics: Past, Present and Future Methodologies *Biotechnol Lett*. **29**:1-16.

Masson P, Alves A C, Ebbels T M, Nicholson J K and Want E J (2010) Optimization and Evaluation of Metabolite Extraction Protocols for Untargeted Metabolic Profiling of Liver Samples by UPLC-MS. *Anal Chem* **82**:7779-7786.

Mathis AM, Holman J L, Sturk L M, Ismail M A, Boykin D W, Tidwell R R and Hall J E (2006) Accumulation and Intracellular Distribution of Antitrypanosomal Diamidine Compounds DB75 and DB820 in African Trypanosomes. *Antimicrob Agents Chemother*. **50**:2185-2191.

Matovu, E. 2011. Ref Type: Personal Communication

Matovu E, Geiser F, Schneider V, Maser P, Enyaru J C, Kaminsky R, Gallati S and Seebeck T (2001) Genetic Variants of the TbAT1 Adenosine Transporter From African Trypanosomes in Relapse Infections Following Melarsoprol Therapy. *Mol Biochem Parasitol*. **117**:73-81.

Matthews KR and Gull K (1994) Evidence for an Interplay Between Cell Cycle Progression and the Initiation of Differentiation Between Life Cycle Forms of African Trypanosomes. *J Cell Biol*. **125**:1147-1156.

Maya JD, Repetto Y, Agosin M, Ojeda J M, Tellez R, Gaule C and Morello A (1997) Effects of Nifurtimox and Benznidazole Upon Glutathione and Trypanothione Content in Epimastigote, Trypomastigote and Amastigote Forms of *Trypanosoma cruzi*. *Mol Biochem Parasitol*. **86**:101-106.

McCulloch R and Horn D (2009) What Has DNA Sequencing Revealed About the VSG Expression Sites of African Trypanosomes? *Trends Parasitol*. **25**:359-363.

Merkel P, Beck A, Muhammad K, Ali S A, Schonfeld C, Voelter W and Duszenko M (2007) Spermine Isolated and Identified As the Major Trypanocidal Compound From the Snake Venom of *Eristocophis Macmahoni* Causes Autophagy in *Trypanosoma brucei*. *Toxicon*. **50**:457-469.

Michels PA, Bringaud F, Herman M and Hannaert V (2006) Metabolic Functions of Glycosomes in Trypanosomatids. *Biochim Biophys Acta* **1763**:1463-1477.

Milord F, Loko L, Ethier L, Mpia B and Pepin J (1993) Eflornithine Concentrations in Serum and Cerebrospinal Fluid of 63 Patients Treated for *Trypanosoma brucei gambiense* Sleeping Sickness. *Trans R Soc Trop Med Hyg*. **87**:473-477.

Miranda MR, Canepa G E, Bouvier L A and Pereira C A (2006) *Trypanosoma cruzi*: Oxidative Stress Induces Arginine Kinase Expression. *Exp Parasitol*. **114**:341-344.

Miura D, Tsuji Y, Takahashi K, Wariishi H and Saito K (2010) A Strategy for the Determination of the Elemental Composition by Fourier Transform Ion Cyclotron Resonance Mass Spectrometry Based on Isotopic Peak Ratios. *Anal Chem*. **82**:5887-5891.

Monsaingeon M, Perel Y, Simonnet G and Corcuff J B (2003) Comparative Values of Catecholamines and Metabolites for the Diagnosis of Neuroblastoma. *Eur J Pediatr*. **162**:397-402.

Morada M, Smid O, Hampl V, Sutak R, Lam B, Rappelli P, Dessi D, Fiori P L, Tachezy J and Yarlett N (2011) Hydrogenosome-Localization of Arginine Deiminase in *Trichomonas vaginalis*. *Mol Biochem Parasitol*. **176**:51-54.

Moreno B, Urbina J A, Oldfield E, Bailey B N, Rodrigues C O and Docampo R (2000) 31P NMR Spectroscopy of *Trypanosoma brucei, Trypanosoma cruzi*, and *Leishmania major*. Evidence for High Levels of Condensed Inorganic Phosphates. *J Biol Chem*. **275**:28356-28362.

Moreno T, Pous J, Subirana J A and Campos J L (2010) Coiled-Coil Conformation of a Pentamidine-DNA Complex. *Acta Crystallogr D Biol Crystallogr*. **66**:251-257.

Muhammad G, Saqib M, Sajid M S and Naureen A (2007) *Trypanosoma evansi* Infections in Himalayan Black Bears (*Selenarctos thibetanus*). *J Zoo Wildl Med.* **38**:97-100.

Muleme HM, Reguera R M, Berard A, Azinwi R, Jia P, Okwor I B, Beverley S and Uzonna J E (2009) Infection With Arginase-Deficient *Leishmania major* Reveals a Parasite Number-Dependent and Cytokine-Independent Regulation of Host Cellular Arginase Activity and Disease Pathogenesis. *J Immunol.* **183**:8068-8076.

Murray PK, Jennings F W, Murray M and Urquhart G M (1974a) The Nature of Immunosuppression in *Trypanosoma brucei* Infections in Mice. I. The Role of the Macrophage. *Immunology* **27**:815-824.

Murray PK, Jennings F W, Murray M and Urquhart G M (1974b) The Nature of Immunosuppression in *Trypanosoma brucei* Infections in Mice. II. The Role of the T and B Lymphocytes. *Immunology* **27**:825-840.

Narui K, Noguchi N, Saito A, Kakimi K, Motomura N, Kubo K, Takamoto S and Sasatsu M (2009) Anti-Infectious Activity of Tryptophan Metabolites in the L-Tryptophan-L-Kynurenine Pathway. *Biol Pharm Bull.* **32**:41-44.

Nerima B, Nilsson D and Maser P (2010) Comparative Genomics of Metabolic Networks of Free-Living and Parasitic Eukaryotes. *BMC Genomics* **11**:217.

Niittylae T, Chaudhuri B, Sauer U and Frommer W B (2009) Comparison of Quantitative Metabolite Imaging Tools and Carbon-13 Techniques for Fluxomics. *Methods Mol Biol.* **553**:355-372.

Nogge G and Giannetti M (1980) Specific Antibodies: a Potential Insecticide. *Science* **209**:1028-1029.

O'Kane RL, Vina J R, Simpson I, Zaragoza R, Mokashi A and Hawkins R A (2006) Cationic Amino Acid Transport Across the Blood-Brain Barrier Is Mediated Exclusively by System Y(+). *Am J Physiol-Endocrinol Metab.* **291**:E412-E419.

Odiit M, Coleman P G, Liu W C, McDermott J J, Fevre E M, Welburn S C and Woolhouse M E (2005) Quantifying the Level of Under-Detection of *Trypanosoma brucei rhodesiense* Sleeping Sickness Cases. *Trop Med Int Health* **10**:840-849.

Olalla L, Gutierrez A, Campos J A, Khan Z U, Alonso F J, Segura J A, Marquez J and Aledo J C (2002) Nuclear Localization of L-Type Glutaminase in Mammalian Brain. *J Biol Chem.* **277**:38939-38944.

Oldiges M, Lutz S, Pflug S, Schroer K, Stein N and Wiendahl C (2007) Metabolomics: Current State and Evolving Methodologies and Tools. *Appl MicrobiolBiotechnol.* **76**:495-511.

Olin-Sandoval V, Moreno-Sanchez R and Saavedra E (2010) Targeting Trypanothione Metabolism in Trypanosomatid Human Parasites. *Curr Drug Targets* **11**:1614-1630.

Olszewski KL, Mather M W, Morrisey J M, Garcia B A, Vaidya A B, Rabinowitz J D and Llinas M (2010) Branched Tricarboxylic Acid Metabolism in *Plasmodium falciparum*. *Nature* **466**:774-778.

Olszewski KL, Morrisey J M, Wilinski D, Burns J M, Vaidya A B, Rabinowitz J D and Llinas M (2009) Host-Parasite Interactions Revealed by *Plasmodium falciparum* Metabolomics. *Cell Host Microbe* **5**:191-199.

Opigo J and Woodrow C (2009) NECT Trial: More Than a Small Victory Over Sleeping Sickness. *Lancet* **374**:7-9.

Opperdoes FR, Baudhuin P, Coppens I, De Roe C, Edwards S W, Weijers P J and Misset O (1984) Purification, Morphometric Analysis, and Characterization of the Glycosomes (Microbodies) of the Protozoan Hemoflagellate *Trypanosoma brucei*. *J Cell Biol*. **98**:1178-1184.

Opperdoes FR and Borst P (1977) Localization of Nine Glycolytic Enzymes in a Microbody-Like Organelle in *Trypanosoma Brucei*: the Glycosome. *FEBS Lett*. **80**:360-364.

Outchkourov NS, Roeffen W, Kaan A, Jansen J, Luty A, Schuiffel D, van Gemert G J, van d, V, Sauerwein R W and Stunnenberg H G (2008) Correctly Folded Pfs48/45 Protein of *Plasmodium falciparum* Elicits Malaria Transmission-Blocking Immunity in Mice. *Proc Natl Acad Sci U S A* **105**:4301-4305.

Oza SL, Shaw M P, Wyllie S and Fairlamb A H (2005) Trypanothione Biosynthesis in *Leishmania major*. *Mol Biochem Parasitol*. **139**:107-116.

Paine MF, Wang M Z, Generaux C N, Boykin D W, Wilson W D, De Koning H P, Olson C A, Pohlig G, Burri C, Brun R, Murilla G A, Thuita J K, Barrett M P and Tidwell R R (2010) Diamidines for Human African Trypanosomiasis. *Curr Opin Investig Drugs* **11**:876-883.

Pal A, Hall B S and Field M C (2002) Evidence for a Non-LDL-Mediated Entry Route for the Trypanocidal Drug Suramin in *Trypanosoma brucei*. *Mol Biochem Parasitol*. **122**:217-221.

Pegg AE (2006) Regulation of Ornithine Decarboxylase. *J Biol Chem*. **281**:14529-14532.

Pepin J and Milord F (1994) The Treatment of Human African Trypanosomiasis. *Adv Parasitol*. **33**:1-47.

Pereira CA, Alonso G D, Ivaldi S, Silber A M, Alves M R M, Torres H N and Flawia M M (2003) Arginine Kinase Overexpression Improves *Trypanosoma cruzi* Survival Capability. *Febs Lett*. **554**:201-205.

Perozich J, Hempel J and Morris S M, Jr. (1998) Roles of Conserved Residues in the Arginase Family. *Biochim Biophys Acta* **1382**:23-37.

Petrotchenko EV, Yamaguchi N, Pasek D A, Borchers C H and Meissner G (2011) Mass Spectrometric Analysis and Mutagenesis Predict Involvement of Multiple Cysteines in Redox Regulation of the Skeletal Muscle Ryanodine Receptor Ion Channel Complex. *Res Rep Biol*. **2011**:13-21.

Phillips MA, Coffino P and Wang C C (1987) Cloning and Sequencing of the Ornithine Decarboxylase Gene From *Trypanosoma brucei* - Implications for Enzyme Turnover and Selective Difluoromethylornithine Inhibition. *J Biol Chem*. **262**:8721-8727.

Phillips MA and Wang C C (1987) A *Trypanosoma brucei* Mutant Resistant to Alpha-Difluoromethylornithine. *Mol Biochem Parasitol*. **22**:9-17.

Poulin R, Lu L, Ackermann B, Bey P and Pegg A E (1992) Mechanism of the Irreversible Inactivation of Mouse Ornithine Decarboxylase by Alpha-Difluoromethylornithine - Characterization of Sequences at the Inhibitor and Coenzyme Binding-Sites. *J Biol Chem*. **267**:150-158.

Priotto G, Kasparian S, Mutombo W, Ngouama D, Ghorashian S, Arnold U, Ghabri S, Baudin E, Buard V, Kazadi-Kyanza S, Ilunga M, Mutangala W, Pohlig G, Schmid C, Karunakara U, Torreele E and Kande V (2009) Nifurtimox-Eflornithine Combination Therapy for Second-Stage African *Trypanosoma brucei gambiense* Trypanosomiasis: a Multicentre, Randomised, Phase III, Non-Inferiority Trial. *Lancet* **374**:56-64.

Priotto G, Pinoges L, Fursa I B, Burke B, Nicolay N, Grillet G, Hewison C and Balasegaram M (2008) Safety and Effectiveness of First Tine Eflornithine for *Trypanosoma brucei gambiense* Sleeping Sickness in Sudan: Cohort Study. *BMJ* **336**:705-708A.

Psychogios N, Hau D D, Peng J, Guo A C, Mandal R, Bouatra S, Sinelnikov I, Krishnamurthy R, Eisner R, Gautam B, Young N, Xia J, Knox C, Dong E, Huang P, Hollander Z, Pedersen T L, Smith S R, Bamforth F, Greiner R, McManus B, Newman J W, Goodfriend T and Wishart D S (2011) The Human Serum Metabolome. *PLoS One* **6**:e16957.

Qu N, Ignatenko N A, Yamauchi P, Stringer D E, Levenson C, Shannon P, Perrin S and Gerner E W (2003) Inhibition of Human Ornithine Decarboxylase Activity by Enantiomers of Difluoromethylornithine. *Biochem J* **375**:465-470.

Radwanska M, Guirnalda P, De Trez C, Ryffel B, Black S and Magez S (2008) Trypanosomiasis-Induced B Cell Apoptosis Results in Loss of Protective Anti-Parasite Antibody Responses and Abolishment of Vaccine-Induced Memory Responses. *PLoS Pathog* **4**:e1000078.

Raz B, Iten M, Grether-Buhler Y, Kaminsky R and Brun R (1997) The Alamar Blue Assay to Determine Drug Sensitivity of African Trypanosomes (*T.b. rhodesiense* and *T.b. gambiense*) *in Vitro*. *Acta Tropica* **68**:139-147.

Reichard H and Reichard P (1958) Determination of Ornithine Carbamyl Transferase in Serum. *J Lab Clin Med* **52**:709-717.

Reuner B, Vassella E, Yutzy B and Boshart M (1997) Cell Density Triggers Slender to Stumpy Differentiation of *Trypanosoma brucei* Bloodstream Forms in Culture. *Mol Biochem Parasitol* **90**:269-280.

Riley E, Roberts S C and Ullman B (2011) Inhibition Profile of *Leishmania mexicana* Arginase Reveals Differences With Human Arginase I. *Int J Parasitol* **41**:545-552.

Rocha G, Martins A, Gama G, Brandao F and Atouguia J (2004) Possible Cases of Sexual and Congenital Transmission of Sleeping Sickness. *Lancet* **363**:247.

Rodenko B, van der Burg A M, Wanner M J, Kaiser M, Brun R, Gould M, De Koning H P and Koomen G J (2007) 2,N6-Disubstituted Adenosine Analogs With Antitrypanosomal and Antimalarial Activities. *Antimicrob Agents Chemother* **51**:3796-3802.

Rossi V, Grandi C, Dalzoppo D and Fontana A (1983) Spectroscopic Study on the Structure and Stability of Beef Liver Arginase. *Int J Pept Protein Res* **22**:239-250.

Ryley Y JF (1956) Studies on the Metabolism of the Protozoa. 7. Comparative Carbohydrate Metabolism of Eleven Species of Trypanosome. *Biochem J* **62**:215-222.

Ryley JF (1962) Studies on the Metabolism of the Protozoa. 9. Comparative Metabolism of Blood-Stream and Culture Forms of *Trypanosoma rhodesiense*. *Biochem J* **85**:211-223.

Sakanyan V, Desmarez L, Legrain C, Charlier D, Mett I, Kochikyan A, Savchenko A, Boyen A, Falmagne P, Pierard A and . (1993) Gene Cloning, Sequence Analysis, Purification, and Characterization of a Thermostable Aminoacylase From *Bacillus stearothermophilus*. *Appl Environ Microbiol* **59**:3878-3888.

Sambrook J and Russell D W (2001) Preparation and Analysis of Eukaryotic Genomic DNA, in Molecular Cloning6.39-6.58, Cold Spring Harbor Laboratory Press, New York.

Sanderson L, Dogruel M, Rodgers J, Bradley B and Thomas S A (2008) The Blood-Brain Barrier Significantly Limits Eflornithine Entry into *Trypanosoma brucei brucei* Infected Mouse Brain. *J Neurochem* **107**:1136-1146.

Sands M, Kron M A and Brown R B (1985) Pentamidine: a Review. *Rev Infect Dis* **7**:625-634.

Sankaranarayanan R, Cherney M M, Garen C, Garen G, Niu C, Yuan M and James M N (2010) The Molecular Structure of Ornithine Acetyltransferase From *Mycobacterium tuberculosis* Bound to Ornithine, a Competitive Inhibitor. *J Mol Biol* **397**:979-990.

Sansone SA, Fan T, Goodacre R, Griffin J L, Hardy N W, Kaddurah-Daouk R, Kristal B S, Lindon J, Mendes P, Morrison N, Nikolau B, Robertson D, Sumner L W, Taylor C, van der W M, van Ommen B and Fiehn O (2007) The Metabolomics Standards Initiative. *Nat Biotechnol* **25**:846-848.

Saraiva EM, de Figueiredo B A, Santos F N, Borja-Cabrera G P, Nico D, Souza L O, Oliveira Mendes-Aguiar C, de Souza E P, Fampa P, Parra L E, Menz I, Dias J G, Jr., de Oliveira S M and Palatnik-de-Sousa C B (2006) The FML-Vaccine (Leishmune) Against Canine Visceral Leishmaniasis: a Transmission Blocking Vaccine. *Vaccine* **24**:2423-2431.

Saunders EC, DE Souza D P, Naderer T, Sernee M F, Ralton J E, Doyle M A, Macrae J I, Chambers J L, Heng J, Nahid A, Likic V A and McConville M J (2010) Central Carbon Metabolism of *Leishmania* Parasites. *Parasitology* **137**:1303-1313.

Saunders EC, Ng W W, Chamber J M, Ng M, Naderer T, Kroemer J O, Likic V A and McConville M J (2011) Isoptopomer Profiling of *Leishmania Mexicana* Promastigotes Reveals Important Roles for Succinate Fermentation and Aspartate Uptake in TCA Cycle Anaplerosis, Glutamate Synthesis and Growth. *J Biol Chem*. **286**:27706-17.

Scheltema RA, Jankevics A, Jansen R C, Swertz M A and Breitling R (2011) PeakML/MzMatch: a File Format, Java Library, R Library, and Tool-Chain for Mass Spectrometry Data Analysis. *Anal Chem* **83**:2786-2793.

Scheltema RA, Kamleh A, Wildridge D, Ebikeme C, Watson D G, Barrett M P, Jansen R C and Breitling R (2008) Increasing the Mass Accuracy of High-Resolution LC-MS Data Using Background Ions: a Case Study on the LTQ-Orbitrap. *Proteomics* **8**:4647-4656.

Schwede A and Carrington M (2010) Bloodstream Form Trypanosome Plasma Membrane Proteins: Antigenic Variation and Invariant Antigens. *Parasitology* **137**:2029-2039.

Schwede A, Manful T, Jha B A, Helbig C, Bercovich N, Stewart M and Clayton C (2009) The Role of Deadenylation in the Degradation of Unstable MRNAs in Trypanosomes. *Nucleic Acids Res* **37**:5511-5528.

Scott AG, Tait A and Turner C M (1996) Characterisation of Cloned Lines of *Trypanosoma brucei* Expressing Stable Resistance to MelCy and Suramin. *Acta Trop* **60**:251-262.

Scott AG, Tait A and Turner C M (1997) *Trypanosoma brucei*: Lack of Cross-Resistance to Melarsoprol in Vitro by Cymelarsan-Resistant Parasites. *Exp Parasitol* **86**:181-190.

Serricchio M and Butikofer P (2011) *Trypanosoma Brucei*: a Model Micro-Organism to Study Eukaryotic Phospholipid Biosynthesis. *FEBS J* **278**:1035-1046.

Shahi SK, Krauth-Siegel R L and Clayton C E (2002) Overexpression of the Putative Thiol Conjugate Transporter TbMRPA Causes Melarsoprol Resistance in *Trypanosoma brucei*. *Mol Microbiol* **43**:1129-1138.

Shaked-Mishan P, Suter-Grotemeyer M, Yoel-Almagor T, Holland N, Zilberstein D and Rentsch D (2006) A Novel High-Affinity Arginine Transporter From the Human Parasitic Protozoan *Leishmania donovani*. *Mol Microbiol* **60**:30-38.

Shim H and Fairlamb A H (1988) Levels of Polyamines, Glutathione and Glutathione-Spermidine Conjugates During Growth of the Insect Trypanosomatid *Crithidia fasciculata*. *J Gen Microbiol* **134**:807-817.

Shin MH, Lee d Y, Liu K H, Fiehn O and Kim K H (2010) Evaluation of Sampling and Extraction Methodologies for the Global Metabolic Profiling of *Saccharophagus degradans*. *Anal Chem* **82**:6660-6666.

Shishova EY, Di Costanzo L, Emig F A, Ash D E and Christianson D W (2009) Probing the Specificity Determinants of Amino Acid Recognition by Arginase. *Biochemistry* **48**:121-131.

Simarro PP, Diarra A, Ruiz Postigo J A, Franco J R and Jannin J G (2011) The Human African Trypanosomiasis Control and Surveillance Programme of the World Health Organization 2000-2009: the Way Forward. *PLoS Negl Trop Dis* **5**:e1007.

Simarro PP, Jannin J and Cattand P (2008) Eliminating Human African Trypanosomiasis: Where Do We Stand and What Comes Next? *PLoS Medicine* **5**:174-180.

Smith CA, Want E J, O'Maille G, Abagyan R and Siuzdak G (2006) XCMS: Processing Mass Spectrometry Data for Metabolite Profiling Using Nonlinear Peak Alignment, Matching, and Identification. *Anal Chem* **78**:779-787.

Smith TK, Vasileva N, Gluenz E, Terry S, Portman N, Kramer S, Carrington M, Michaeli S, Gull K and Rudenko G (2009) Blocking Variant Surface Glycoprotein Synthesis in *Trypanosoma brucei* Triggers a General Arrest in Translation Initiation. *PLoS One* **4**:e7532.

Snyder C, Chollet J, Santo-Tomas J, Scheurer C and Wittlin S (2007) In Vitro and in Vivo Interaction of Synthetic Peroxide RBx11160 (OZ277) With Piperaquine in *Plasmodium* Models. *Exp Parasitol*. **115**:296-300.

Soignet SL, Tong W P, Hirschfeld S and Warrell R P, Jr. (1999) Clinical Study of an Organic Arsenical, Melarsoprol, in Patients With Advanced Leukemia. Cancer *Chemother Pharmacol* **44**:417-421.

Sokolova AY, Wyllie S, Patterson S, Oza S L, Read K D and Fairlamb A H (2010) Cross-Resistance to Nitro-Drugs and Implications for the Treatment of Human African Trypanosomiasis. *Antimicrob Agents Chemother.*. **54**:2893-900.

Spitznagel D, Ebikeme C, Biran M, Nic a' B N, Bringaud F, Henehan G T and Nolan D P (2009) Alanine Aminotransferase of *Trypanosoma brucei*--a Key Role in Proline Metabolism in Procyclic Life Forms. *FEBS J* **276**:7187-7199.

Sreekumar A, Poisson L M, Rajendiran T M, Khan A P, Cao Q, Yu J, Laxman B, Mehra R, Lonigro R J, Li Y, Nyati M K, Ahsan A, Kalyana-Sundaram S, Han B, Cao X, Byun J, Omenn G S, Ghosh D, Pennathur S, Alexander D C, Berger A, Shuster J R, Wei J T, Varambally S, Beecher C and Chinnaiyan A M (2009) Metabolomic Profiles Delineate Potential Role for Sarcosine in Prostate Cancer Progression. *Nature* **457**:910-914.

Srivastava S and Ratha B K (2010) Does Fish Represent an Intermediate Stage in the Evolution of Ureotelic Cytosolic Arginase I? *Biochem Biophys Res Commun* **391**:1-5.

Stanghellini A and Josenando T (2001) The Situation of Sleeping Sickness in Angola: a Calamity. *Trop Med Int Health* **6**:330-334.

Steenkamp DJ (2002) Trypanosomal Antioxidants and Emerging Aspects of Redox Regulation in the Trypanosomatids. *Antioxid Redox Signal*. **4**:105-121.

Stewart ML, Burchmore R J, Clucas C, Hertz-Fowler C, Brooks K, Tait A, MacLeod A, Turner C M, De Koning H P, Wong P E and Barrett M P (2010) Multiple Genetic Mechanisms Lead to Loss of Functional TbAT1 Expression in Drug-Resistant Trypanosomes. *Eukaryot Cell* **9**:336-343.

Stewart ML, Krishna S, Burchmore R J, Brun R, De Koning H P, Boykin D W, Tidwell R R, Hall J E and Barrett M P (2005) Detection of Arsenical Drug Resistance in *Trypanosoma brucei* With a Simple Fluorescence Test. *Lancet* **366**:486-487.

Stoffel SA, Alibu V P, Hubert J, Ebikeme C, Portais J C, Bringaud F, Schweingruber M E and Barrett M P (2011) Transketolase in *Trypanosoma brucei*. *Mol Biochem Parasitol*. **179**:1-7.

Sun L, Li H M, Seufferheld M J, Walters K R, Jr., Margam V M, Jannasch A, Diaz N, Riley C P, Sun W, Li Y F, Muir W M, Xie J, Wu J, Zhang F, Chen J Y, Barker E L, Adamec J and Pittendrigh B R (2011) Systems-Scale Analysis Reveals Pathways Involved in Cellular Response to Methamphetamine. *PLoS One* **6**:e18215.

Sundar S (2001) Drug Resistance in Indian Visceral Leishmaniasis. *Trop Med Int Health* **6**:849-854.

t'Kindt R, Jankevics A, Scheltema R A, Zheng L, Watson D G, Dujardin J C, Breitling R, Coombs G H and Decuypere S (2010) Towards an Unbiased Metabolic

Profiling of Protozoan Parasites: Optimisation of a *Leishmania* Sampling Protocol for HILIC-Orbitrap Analysis. *Anal Bioanal Chem* **398**:2059-2069.

Taylor NS, Weber R J, White T A and Viant M R (2010) Discriminating Between Different Acute Chemical Toxicities Via Changes in the Daphnid Metabolome. *Toxicol Sci* **118**:307-317.

Teixeira AR, Gomes C, Lozzi S P, Hecht M M, Rosa A C, Monteiro P S, Bussacos A C, Nitz N and McManus C (2009) Environment, Interactions Between *Trypanosoma cruzi* and Its Host, and Health. *Cad Saude Publica* **25** Suppl 1:S32-S44.

Teka IA, Kazibwe A J, El Sabbagh N, Al Salabi M I, Ward C P, Eze A A, Munday J C, Maeser P, Matovu E, Barrett M P and De Koning H P (2011) The Diamidine Diminazene Aceturate Is a Substrate for the High Affinity Pentamidine Transporter: Implications for the Development of High Resistance Levels in Trypanosomes. *Mol Pharmacol*. **80**:110-6.

Tetaud E, Giroud C, Prescott A R, Parkin D W, Baltz D, Biteau N, Baltz T and Fairlamb A H (2001) Molecular Characterisation of Mitochondrial and Cytosolic Trypanothione-Dependent Tryparedoxin Peroxidases in *Trypanosoma brucei*. *Mol Biochem Parasitol*. **116**:171-183.

Theobald U, Mailinger W, Baltes M, Rizzi M and Reuss M (1997) In Vivo Analysis of Metabolic Dynamics in *Saccharomyces cerevisiae*. Experimental Observations. *Biotechnol Bioeng*. **55**:305-316.

Tielens AG and van Hellemond J J (1998) Differences in Energy Metabolism Between Trypanosomatidae. *Parasitol Today* **14**:265-272.

Tonazzi A and Indiveri C (2011) Effects of Heavy Metal Cations on the Mitochondrial Ornithine/Citrulline Transporter Reconstituted in Liposomes. *Biometals*. **24**:1205-15.

Torr SJ, Hargrove J W and Vale G A (2005) Towards a Rational Policy for Dealing With Tsetse. *Trends Parasitol*. **21**:537-541.

Torreele E, Bourdin Trunz B, Tweats D, Kaiser M, Brun R, Mazué G, Bray MA, Pécoul B (2010). Fexinidazole-a new oral nitroimidazole drug candidate entering clinical development for the treatment of sleeping sickness. *PLoS Negl Trop Dis*. **4**:e923.

Urwyler S, Studer E, Renggli C K and Roditi I (2007) A Family of Stage-Specific Alanine-Rich Proteins on the Surface of Epimastigote Forms of *Trypanosoma brucei*. *Mol Microbiol*. **63**:218-228.

Van Den Abbeele J, Claes Y, van Bockstaele D, Le Ray D and Coosemans M (1999) *Trypanosoma brucei Spp*. Development in the Tsetse Fly: Characterization of the Post-Mesocyclic Stages in the Foregut and Proboscis. *Parasitology* **118**:469-478.

van der Spek H, Arts G J, Zwaal R R, Van den B J, Sloof P and Benne R (1991) Conserved Genes Encode Guide RNAs in Mitochondria of *Crithidia fasciculata*. *EMBO J.* **10**:1217-1224.

van Rooyen JM, Abratt V R, Belrhali H and Sewell T (2011) Crystal Structure of Type III Glutamine Synthetase: Surprising Reversal of the Inter-Ring Interface. *Structure* **19**:471-483.

van Weelden SW, van Hellemond J J, Opperdoes F R and Tielens A G (2005) New Functions for Parts of the Krebs Cycle in Procyclic *Trypanosoma brucei*, a Cycle Not Operating As a Cycle. *J Biol Chem.* **280**:12451-12460.

Vansterkenburg EL, Coppens I, Wilting J, Bos O J, Fischer M J, Janssen L H and Opperdoes F R (1993) The Uptake of the Trypanocidal Drug Suramin in Combination With Low-Density Lipoproteins by *Trypanosoma brucei* and Its Possible Mode of Action. *Acta Trop.* **54**:237-250.

Vassella E, Probst M, Schneider A, Studer E, Renggli C K and Roditi I (2004) Expression of a Major Surface Protein of *Trypanosoma brucei* Insect Forms Is Controlled by the Activity of Mitochondrial Enzymes. *Mol Biol Cell* **15**:3986-3993.

Vassella E, Reuner B, Yutzy B and Boshart M (1997) Differentiation of African Trypanosomes Is Controlled by a Density Sensing Mechanism Which Signals Cell Cycle Arrest Via the CAMP Pathway. *J Cell Sci.* **110**:2661-2671.

VICKERMA.K and Luckins A G (1969) Localization of Variable Antigens in Surface Coat of *Trypanosoma brucei* Using Ferritin Conjugated Antibody. *Nature* **224**:1125.

Vickers TJ, Murta S M F, Mandell M A and Beverley S M (2009) The Enzymes of the 10-Formyl-Tetrahydrofolate Synthetic Pathway Are Found Exclusively in the Cytosol of the Trypanosomatid Parasite *Leishmania major*. *Mol Biochem Parasitol.* **166**:142-152.

Vincent IM, Creek D, Watson D G, Kamleh M A, Woods D J, Wong P E, Burchmore R J and Barrett M P (2010) A Molecular Mechanism for Eflornithine Resistance in African Trypanosomes. *PLoS Pathog.* **6**:e1001204.

Viode C, Bettache N, Cenas N, Krauth-Siegel R L, Chauviere G, Bakalara N and Perie J (1999) Enzymatic Reduction Studies of Nitroheterocycles. *Biochem Pharmacol.* **57**:549-557.

Visser N and Opperdoes F R (1980) Glycolysis in *Trypanosoma Brucei*. *Eur J Biochem.* **103**:623-632.

Vockley JG, Goodman B K, Tabor D E, Kern R M, Jenkinson C P, Grody W W and Cederbaum S D (1996) Loss of Function Mutations in Conserved Regions of the Human Arginase I Gene. *Biochem Mol Med.* **59**:44-51.

Vogt RN, Spies H S C and Steenkamp D J (2001) The Biosynthesis of Ovothiol A (N-1-Methyl-4-Mercaptohistidine) - Identification of S-(4 '-L-Histidyl)-L-Cysteine Sulfoxide As an Intermediate and the Products of the Sulfoxide Lyase Reaction. *Eur J Biochem*. **268**:5229-5241.

Voorheis HP (1980) Fatty Acid Uptake by Bloodstream Forms of *Trypanosoma brucei* and Other Species of the Kinetoplastida. *Mol Biochem Parasitol*. **1**:177-186.

Vreysen MJ, Saleh K M, Ali M Y, Abdulla A M, Zhu Z R, Juma K G, Dyck V A, Msangi A R, Mkonyi P A and Feldmann H U (2000) *Glossina austeni* (Diptera: Glossinidae) Eradicated on the Island of Unguja, Zanzibar, Using the Sterile Insect Technique. *J Econ Entomol*. **93**:123-135.

Wallace HM, Fraser A V and Hughes A (2003) A Perspective of Polyamine Metabolism. *Biochem J*. **376**:1-14.

Wang CC (1995) Molecular Mechanisms and Therapeutic Approaches to the Treatment of African Trypanosomiasis. *Annu Rev Pharmacol Toxicol*. **35**:93-127.

Wang Y, Utzinger J, Saric J, Li J V, Burckhardt J, Dirnhofer S, Nicholson J K, Singer B H, Brun R and Holmes E (2008) Global Metabolic Responses of Mice to *Trypanosoma brucei brucei* Infection. *Proc Natl Acad Sci U S A* **105**:6127-6132.

Watson DG (2010) The Potential of Mass Spectrometry for the Global Profiling of Parasite Metabolomes. *Parasitology* **137**:1409-1423.

Wilkinson SR, Taylor MC, Horn D, Kelly JM, Cheeseman I (2008) A mechanism for cross-resistance to nifurtimox and benznidazole in trypanosomes. *Proc Natl Acad Sci U S A*. **105**:5022-7.

Willadsen P, Bird P, Cobon G S and Hungerford J (1995) Commercialisation of a Recombinant Vaccine Against *Boophilus microplus*. *Parasitology* **110** Suppl:S43-S50.

Wishart DS, Lewis M J, Morrissey J A, Flegel M D, Jeroncic K, Xiong Y, Cheng D, Eisner R, Gautam B, Tzur D, Sawhney S, Bamforth F, Greiner R and Li L (2008) The Human Cerebrospinal Fluid Metabolome. *J Chromatogr B Analyt Technol Biomed Life Sci*. **871**:164-173.

World Health Organisation (2006) Weekly epidemiological record. **8:**69-80. Ref Type: Report

Wu L, Mashego M R, van Dam J C, Proell A M, Vinke J L, Ras C, van Winden W A, van Gulik W M and Heijnen J J (2005) Quantitative Analysis of the Microbial Metabolome by Isotope Dilution Mass Spectrometry Using Uniformly 13C-Labeled Cell Extracts As Internal Standards. *Anal Biochem*. **336**:164-171.

Wyllie S, Oza S L, Patterson S, Spinks D, Thompson S and Fairlamb A H (2009) Dissecting the Essentiality of the Bifunctional Trypanothione Synthetase-Amidase in *Trypanosoma brucei* Using Chemical and Genetic Methods. *Mol Microbiol*. **74**:529-540.

Xiao Y, McCloskey D E and Phillips M A (2009) RNA Interference-Mediated Silencing of Ornithine Decarboxylase and Spermidine Synthase Genes in *Trypanosoma brucei* Provides Insight into Regulation of Polyamine Biosynthesis. *Eukaryotic Cell* **8**:747-755.

Yarlett N and Bacchi C J (1988) Effect of Dl-Alpha-Difluoromethylornithine on Methionine Cycle Intermediates in *Trypanosoma brucei brucei*. *MolBiochem Parasitol*. **27**:1-10.

Yeh I, Hanekamp T, Tsoka S, Karp P D and Altman R B (2004) Computational Analysis of *Plasmodium Falciparum* Metabolism: Organizing Genomic Information to Facilitate Drug Discovery. *Genome Res*. **14**:917-924.

Yi ZB, Yu Y, Liang Y Z and Zeng B (2007) Evaluation of the Antimicrobial Mode of Berberine by LC/ESI-MS Combined With Principal Component Analysis. *J Pharm Biomed Anal*. **44**:301-304.

Yun O, Priotto G, Tong J, Flevaud L and Chappuis F (2010) NECT Is Next: Implementing the New Drug Combination Therapy for *Trypanosoma brucei gambiense* Sleeping Sickness. *PLoS Negl Trop Dis* **4**:e720.

Zhang J, Zhang X, Mao X, Zou Q and Li D (2011) Crystallization and Preliminary Crystallographic Studies of *Helicobacter pylori* Arginase. *Acta Crystallogr Sect F Struct Biol Cryst Commun*. **67**:707-709.

Zhou J, Shen J, Liao D, Zhou Y and Lin J (2004) Resistance to Drug by Different Isolates *Trypanosoma evansi* in China. *Acta Trop*. **90**:271-275.

Ziegelbauer K, Quinten M, Schwarz H, Pearson T W and Overath P (1990) Synchronous Differentiation of *Trypanosoma brucei* From Bloodstream to Procyclic Forms *in Vitro*. *Eur J Biochem*. **192**:373-378.

8. Appendix

8.1 A comparison of wildtype and DFMOR1 metabolite levels

Putative metabolite	Formula	m/z	Polarity	RT (minutes)	DFMOR1 vs WT	P value	WT intensity	WT sd	DFMOR1 insensity	DFMOR 1 sd
5'-Methylthioadenosine	C11H15N5O3S	298.0971	+	8.1	1.3	0.34	524	162	697	220
glutathionylspermidine	C17H34N6O5S	435.2378	+	32.25	0.8	0.61	7	5	6	2
L-Ornithine	C5H12N2O2	133.0978	+	21.98	0.5	0.47	76	70	39	25
N-acetylglutamate semialdehyde	C7H11NO4	174.0754	+	10.07	1.0	0.98	801	71	805	199
N-Acetylornithine	C7H14N2O3	175.1077	+	14.16	0.9	0.81	123	78	111	29
Putrescine	C4H12N2	89.10727	+	29.82	0.9	0.50	399	32	361	76
S-Adenosyl-L-methionine	C15H22N6O5S	399.1455	+	25.13	1.1	0.90	12	4	12	8
Spermidine	C7H19N3	146.1653	+	41.61	1.1	0.86	1301	330	1361	437
Trypanothione disulfide	C27H47N9O10S2	722.295	+	23.15	1.0	0.97	87	17	88	35
3-Methyl-2-oxobutanoic acid	C5H8O3	115.0401	-	6.07	1.0	0.94	1172	542	1218	817
4-Aminobutanoate	C4H9NO2	102.0561	-	14.03	1.2	0.63	372	128	442	192
4-Trimethylammoniobutanoate	C7H15NO2	146.1176	+	9.21	1.0	0.92	102	24	104	26
8-Methoxykynurenate	C11H9NO4	218.0459	-	10.01	0.9	0.60	21	3	18	7
Adenine	C5H5N5	136.0617	+	11.72	1.0	0.96	2423	1242	2378	1110
Anthranilate	C7H7NO2	138.0554	+	14	0.2	0.01	322	41	70	2
Benzoate	C7H6O2	123.0443	+	6.48	1.3	0.26	11	2	15	4
Carnitine	C7H15NO3	162.1124	+	13.54	1.2	0.58	1111	477	1318	337
Choline phosphate	C5H14NO4P	184.0734	+	19.66	1.4	0.29	1572	344	2270	861
CMP-N-trimethyl-2-	C14H26N4O10P2	473.1199	+	20.1	1.1	0.54	47	12	52	5

aminoethylphosphonate										
D-Glucosamine 6-phosphate	C6H14NO8P	258.0382	-	15.84	1.7	0.09	23	2	38	9
Glutathione	C10H17N3O6S	308.0908	+	13.19	1.2	0.79	6	3	7	1
Imidazole-4-acetaldehyde	C5H6N2O	111.0552	+	16.5	1.4	0.21	19	4	27	8
L-Arginine phosphate	C6H15N4O5P	255.0852	+	19.77	1.2	0.75	177	93	204	104
L-Cystathionine	C7H14N2O4S	223.0748	+	18.72	1.1	0.40	105	14	118	20
N4-Acetylaminobutanal	C6H11NO2	130.0867	+	11.21	0.9	0.27	82	7	75	7
N-acetyl-D-glucosamine-6-phosphate	C8H16NO9P	324.0462	+	14.99	1.3	0.49	26	7	33	15
O-Acetylcarnitine	C9H17NO4	204.1227	+	11.11	1.2	0.54	160	20	190	69
Phenylpyruvate	C9H8O3	163.0401	-	5.52	0.9	0.42	1527	186	1331	315
trans-4-Hydroxy-L-proline	C5H9NO3	132.066	+	14.23	0.8	0.24	147	31	110	34
(R)-Lactate	C3H6O3	89.02428	-	6.67	1.2	0.53	110	15	127	37
(S)-Malate	C4H6O5	133.0141	-	8.43	1.2	0.67	232	112	277	129
2-Oxoglutarate	C5H6O5	145.0142	-	8.57	1.4	0.61	624	447	885	664
citrate	C6H8O7	191.0197	-	9.4	1.0	0.69	54	3	53	5
D-glucose-6-phosphate	C6H13O9P	283.0183	+	17.54	1.1	0.48	28	7	31	1
D-Ribose	C5H10O5	149.0455	-	9.99	1.2	0.56	113	18	132	48
D-Xylulose 5-phosphate	C5H11O8P	229.0121	-	15.68	0.6	0.56	32	30	20	9
Fumarate	C4H4O4	115.0037	-	8.36	1.1	0.79	56	30	63	31
Glycerol	C3H8O3	93.05456	+	9.67	1.1	0.59	1347	182	1478	329
L-Arabinono-1-5-lactone	C5H8O5	149.0446	+	7.4	0.9	0.83	53	15	50	16
L-Gulonate	C6H12O7	195.0508	-	9.99	1.2	0.64	43	4	51	23
Succinate	C4H6O4	117.0193	-	6.67	1.4	0.35	1376	776	1935	399
sucrose	C12H22O11	341.1085	-	13.69	0.9	0.30	87	10	78	10
NAD+	C21H27N7O14P2	686.0977	+	16.48	1.1	0.64	10	2	11	3
(R)-3-Hydroxybutanoate	C4H8O3	103.0401	-	7.35	0.8	0.39	97	34	75	16
Acetoacetate	C4H6O3	101.0244	-	8.57	1.4	0.62	391	273	545	411

sn-glycero-3-Phosphocholine	C8H20NO6P	280.0924	+	17.4	1.2	0.31	8225	1659	10195	2371
sn-glycero-3-Phosphoethanolamine	C5H14NO6P	238.0453	+	15.69	3.0	0.26	184	24	559	420
sn-Glycerol 3-phosphate	C3H9O6P	171.0063	-	15.3	1.1	0.39	16855	2616	18707	2078
Choline	C5H13NO	104.1069	+	14.33	1.5	0.44	21503	9814	31658	17553
D-glucose	C6H12O6	203.0524	+	12.98	1.2	0.61	434	209	517	148
Folate	C19H19N7O6	442.1476	+	9.05	1.1	0.77	218	28	229	53
Hypoxanthine	C5H4N4O	137.0463	+	9.05	1.2	0.38	56986	5515	65670	13145
Nicotinamide	C6H6N2O	123.0556	+	8.03	1.1	0.61	1418	191	1575	426
Orthophosphate	H3O4P	98.9845	+	15.25	1.3	0.71	81	33	101	80
Pantothenate	C9H17NO5	220.118	+	6.64	1.3	0.35	854	70	1146	423
Phenol Red	C19H14O5S	355.0635	+	5.72	1.0	0.88	3344	749	3490	1407
Pyridoxal	C8H9NO3	168.0651	+	11.72	1.2	0.58	551	95	647	244
Pyruvate	C3H4O3	87.0087	-	7.56	1.0	0.90	7542	979	7795	3000
riboflavin	C17H20N4O6	377.1453	+	7.55	1.0	0.99	69	22	70	27
Thiamine	C12H16N4OS	265.1117	+	23.08	1.4	0.63	1859	992	2539	1950
Thymidine	C10H14N2O5	241.0829	-	7.09	0.9	0.82	149	111	127	111
Glycine	C2H5NO2	76.03952	+	15.32	1.2	0.70	1438	1010	1697	180
L-Alanine	C3H7NO2	90.05495	+	14.23	1.2	0.64	70091	8050	85201	48225
L-Arginine	C6H14N4O2	175.119	+	21.27	1.1	0.66	15235	1185	16992	5865
L-Asparagine	C4H8N2O3	133.0612	+	15.62	1.3	0.79	655	783	824	682
L-Aspartate	C4H7NO4	134.0454	+	14.54	1.5	0.35	400	82	586	268
L-Cysteine	C3H7NO2S	122.0273	+	13.77	1.0	0.90	70	14	73	32
L-Cystine	C6H12N2O4S2	241.0309	+	18.83	1.3	0.67	204	41	259	186
L-Glutamate	C5H9NO4	148.0604	+	14.07	1.6	0.47	12005	4459	19255	14178
L-Glutamine	C5H10N2O3	147.0769	+	15.13	1.2	0.32	45949	9107	54379	8961
L-Histidine	C6H9N3O2	156.0769	+	20.4	1.1	0.62	6667	939	7592	2696
L-isoleucine	C6H13NO2	132.1023	+	10.63	1.1	0.16	61077	5032	67409	3399

L-Leucine	C6H13NO2	132.1023	+	11.01	1.1	0.13	62113	3927	69326	5241
L-Lysine	C6H14N2O2	147.1132	+	21.54	1.2	0.41	15797	871	18169	3981
L-Methionine	C5H11NO2S	150.0577	+	11.51	1.1	0.16	16088	927	17713	1297
L-Phenylalanine	C9H11NO2	166.0855	+	10.12	1.3	0.41	23713	10449	30500	6702
L-Proline	C5H9NO2	116.0707	+	13.77	0.9	0.71	20439	1913	18966	5750
L-Serine	C3H7NO3	106.0503	+	15.13	1.3	0.58	1978	944	2574	1399
L-Threonine	C4H9NO3	120.0655	+	14.44	1.2	0.53	21012	1797	24219	7361
L-Tryptophan	C11H12N2O2	205.0969	+	10.56	1.2	0.22	6121	147	7119	994
L-Tyrosine	C9H11NO3	182.0812	+	12.21	1.0	0.30	26322	918	25564	556
L-Valine	C5H11NO2	118.0865	+	12.4	1.1	0.13	49695	1108	56337	4685
Nicotinate	C6H5NO2	124.0398	+	7.38	1.2	0.74	284	150	338	211
N-Ribosylnicotinamide	C11H14N2O5	255.0971	+	14.44	0.6	0.44	22	9	12	18
ubiquinone-8	C49H74O4	727.5696	+	7.68	0.9	0.69	13	4	12	1
3',5'-Cyclic AMP	C10H12N5O6P	330.0601	+	15.94	0.8	0.26	28	7	22	5
Adenosine	C10H13N5O4	268.1035	+	10.32	0.7	0.39	84	41	56	26
AMP	C10H14N5O7P	348.0712	+	15.3	1.7	0.62	174	97	301	377
dTMP	C10H15N2O8P	321.0492	-	12.15	1.0	0.96	23	14	24	18
Guanine	C5H5N5O	152.0565	+	11.9	0.7	0.01	494	34	345	36
IMP	C10H13N4O8P	347.0394	-	14.99	1.1	0.76	29	5	34	20
UMP	C9H13N2O9P	323.0279	-	14.61	1.0	0.92	74	26	71	35
Uracil	C4H4N2O2	113.0347	+	7.62	1.2	0.64	389	96	474	262
Uridine	C9H12N2O6	243.0621	-	10.6	1.0	0.86	65	15	63	17
Xanthine	C5H4N4O2	153.0407	+	8.54	1.2	0.64	1741	95	1998	825

Appendix 8-1. Putative metabolite identification based on accurate mass match in KEGG (tbr) and/or trypanocyc databases. Common fragments, adducts and false identifications have been removed from putative identification list based on retention time and reproducibility. Results were obtained using a boiling ethanol extraction method. Data analysed by Dr. Darren Creek.

8.2 ODC sequences

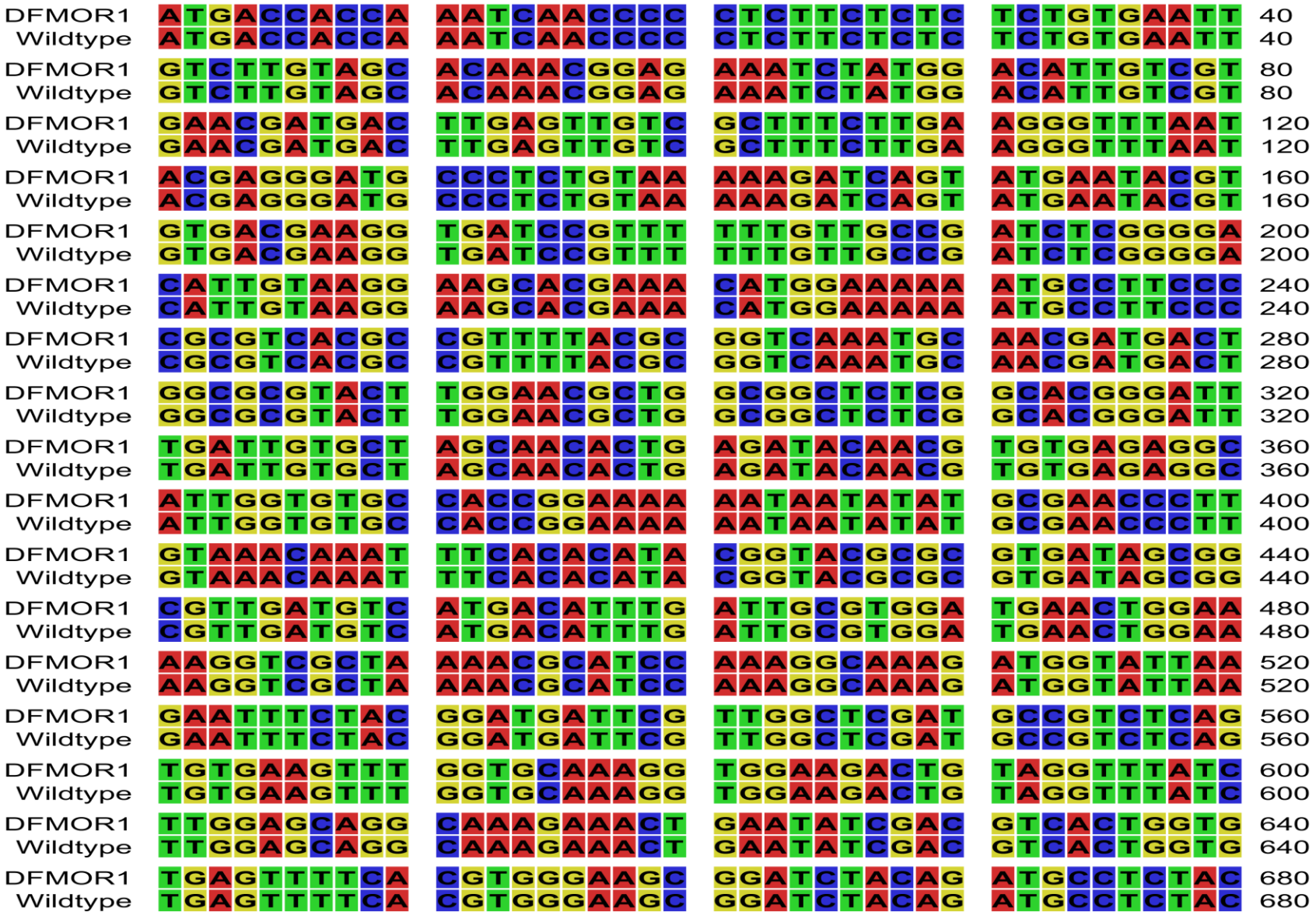
DFMOR1 ATGACCACCA AATCAACCCC CTCTTCTCTC TCTGTGAATT 40
Wildtype ATGACCACCA AATCAACCCC CTCTTCTCTC TCTGTGAATT 40
DFMOR1 GTCTTGTAGC ACAAACGGAG AAATCTATGG ACATTGTCGT 80
Wildtype GTCTTGTAGC ACAAACGGAG AAATCTATGG ACATTGTCGT 80
DFMOR1 GAACGATGAC TTGAGTTGTC GCTTTCTTGA AGGGTTTAAT 120
Wildtype GAACGATGAC TTGAGTTGTC GCTTTCTTGA AGGGTTTAAT 120
DFMOR1 ACGAGGGATG CCCTCTGTAA AAAGATCAGT ATGAATACGT 160
Wildtype ACGAGGGATG CCCTCTGTAA AAAGATCAGT ATGAATACGT 160
DFMOR1 GTGACGAAGG TGATCCGTTT TTTGTTGCCG ATCTCGGGGA 200
Wildtype GTGACGAAGG TGATCCGTTT TTTGTTGCCG ATCTCGGGGA 200
DFMOR1 CATTGTAAGG AAGCACGAAA CATGGAAAAA ATGCCTTCCC 240
Wildtype CATTGTAAGG AAGCACGAAA CATGGAAAAA ATGCCTTCCC 240
DFMOR1 CGCGTCACGC CGTTTTACGC GGTCAAATGC AACGATGACT 280
Wildtype CGCGTCACGC CGTTTTACGC GGTCAAATGC AACGATGACT 280
DFMOR1 GGCGCGTACT TGGAACGCTG GCGGCTCTCG GCACGGGATT 320
Wildtype GGCGCGTACT TGGAACGCTG GCGGCTCTCG GCACGGGATT 320
DFMOR1 TGATTGTGCT AGCAACACTG AGATACAACG TGTGAGAGGC 360
Wildtype TGATTGTGCT AGCAACACTG AGATACAACG TGTGAGAGGC 360
DFMOR1 ATTGGTGTGC CACCGGAAAA AATAATATAT GCGAACCCTT 400
Wildtype ATTGGTGTGC CACCGGAAAA AATAATATAT GCGAACCCTT 400
DFMOR1 GTAAACAAAT TTCACACATA CGGTACGCGC GTGATAGCGG 440
Wildtype GTAAACAAAT TTCACACATA CGGTACGCGC GTGATAGCGG 440
DFMOR1 CGTTGATGTC ATGACATTTG ATTGCGTGGA TGAACTGGAA 480
Wildtype CGTTGATGTC ATGACATTTG ATTGCGTGGA TGAACTGGAA 480
DFMOR1 AAGGTCGCTA AAACGCATCC AAAGGCAAAG ATGGTATTAA 520
Wildtype AAGGTCGCTA AAACGCATCC AAAGGCAAAG ATGGTATTAA 520
DFMOR1 GAATTTCTAC GGATGATTCG TTGGCTCGAT GCCGTCTCAG 560
Wildtype GAATTTCTAC GGATGATTCG TTGGCTCGAT GCCGTCTCAG 560
DFMOR1 TGTGAAGTTT GGTGCAAAGG TGGAAGACTG TAGGTTTATC 600
Wildtype TGTGAAGTTT GGTGCAAAGG TGGAAGACTG TAGGTTTATC 600
DFMOR1 TTGGAGCAGG CAAAGAAACT GAATATCGAC GTCACTGGTG 640
Wildtype TTGGAGCAGG CAAAGAAACT GAATATCGAC GTCACTGGTG 640
DFMOR1 TGAGTTTTCA CGTGGGAAGC GGATCTACAG ATGCCTCTAC 680
Wildtype TGAGTTTTCA CGTGGGAAGC GGATCTACAG ATGCCTCTAC 680

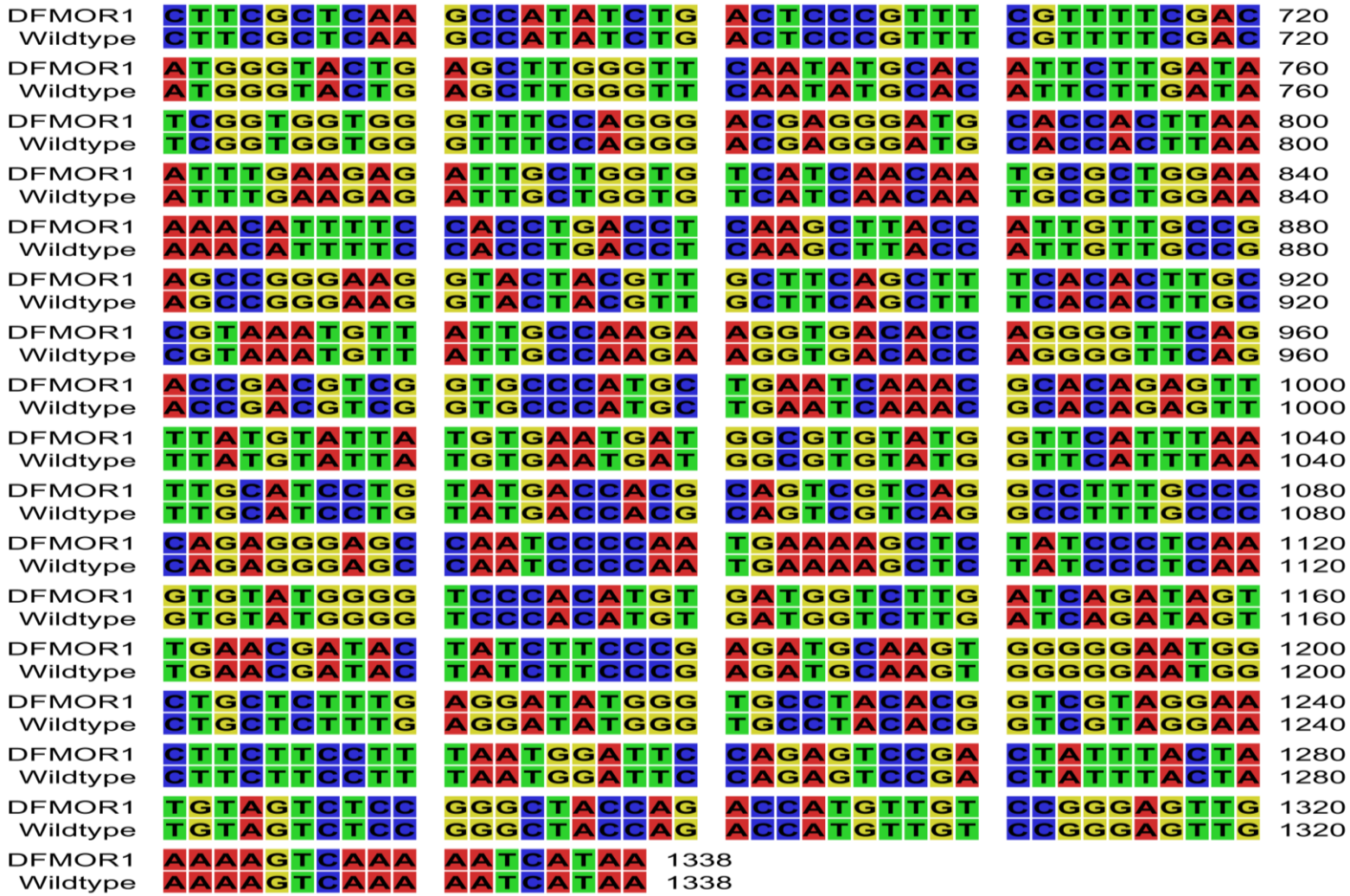

Appendix 8-2. Wildtype and DFMOR1 ornithine decarboxylase gene sequences. Alignments were performed in CLC workbench

8.3 Publication

8.4 Eflornithine toxicity metabolomics

Mass	RT	Formula	Isomers	Name	Confidence	Map	Database	KEGG ID	Ratio to 0 hours					*t*-test c.f. 0 hours				
									0	1	5	24	48	0	1	5	24	48
70.078332	5.0469	C5H10	1	butylene	5	0	Metacyc	0	1.00	1.18	1.30	1.15	0.82	1	0.634125	0.427277	0.575067	0.704181
71.07355159	8.4818	C4H9N	2	3-Buten-1-amine	5	0	KEGG	C12244	1.00	0.98	1.18	1.10	0.70	1	0.863118	0.202028	0.693717	0.078595
75.0684074	13.559	C3H9NO	6	1-Aminopropan-2-ol	7	0	KEGG	C05771	1.00	0.97	0.80	0.94	0.60	1	0.82697	0.393381	0.744036	0.103096
84.06868681	21.205	C8H16N4	1	α -allenylagmatine	7	0	Metacyc	0	1.00	1.23	1.54	1.06	0.65	1	0.69664	0.345428	0.924549	0.513892
85.0526942	7.4384	C4H7NO	2	Acetone cyanohydrin	8	0	KEGG_Metacyc	C02659	1.00	0.92	0.95	1.02	0.52	1	0.761345	0.859046	0.955599	0.123493
89.0840235	12.873	C4H11NO	1	N-dimethylethanolamine	5	0	Metacyc	0	1.00	1.12	1.30	1.03	0.67	1	0.5502	0.428372	0.880447	0.181951
91.03494999	7.1482	C6H15O4P	2	Diisopropyl phosphate	7	0	KEGG_Metacyc	C03113	1.00	1.17	0.99	1.01	0.75	1	0.560627	0.98328	0.980567	0.551029
96.0209418	15.488	C5H4O2	3	Furfural	5	0	KEGG_Metacyc	C14279	1.00	1.39	**1.47**	1.01	**0.57**	1	0.249909	0.038424	0.941319	0.042535
96.02104747	13.978	C5H4O2	3	Furfural	7	0	KEGG_Metacyc	C14279	1.00	**1.62**	1.59	1.05	1.20	1	0.027024	0.188952	0.76766	0.446719
100.0160082	7.0715	C4H4O3	1	2-oxobut-3-enanoate	7	0	Metacyc	0	1.00	1.16	1.01	0.71	**0.65**	1	0.493586	0.971938	0.055007	0.017564

101.0475954	22.701	C4H7NO2	5	L-Azetidine 2-carboxylic acid	5	0	KEGG_Metacyc	C08267	1.00	1.35	**2.11**	1.31	3.53	1	0.285774	0.034532	0.05703	0.105179
101.0476624	8.2098	C4H7NO2	5	Diacetylmonoxime	5	0	KEGG	C07509	1.00	0.95	1.19	0.91	0.58	1	0.761491	0.681935	0.585473	0.103482
102.0316104	12.528	C4H6O3	8	4-Hydroxycrotonicacid	7	0	HMDB	0	1.00	0.93	0.92	0.90	0.45	1	0.705855	0.628008	0.56106	0.080527
114.0793108	13.92	C5H10N2O	2	L-proline amide	5	0	Metacyc	0	1.00	1.05	**1.61**	1.46	0.77	1	0.808707	0.028996	0.322668	0.556492
118.026516	6.8109	C4H6O4	7	Methyl oxalate	7	0	KEGG	C10900	1.00	1.18	1.07	0.48	0.75	1	0.726021	0.886789	0.178561	0.442272
118.0783489	5.2111	C9H10	1	alpha-Methylstyrene	5	0	KEGG	C14395	1.00	1.33	0.92	0.79	0.81	1	0.134649	0.625079	0.28545	0.331549
120.0421038	12.469	C4H8O4	9	D-Erythrulose	5	0	KEGG_Metacyc	C02022	1.00	0.85	0.92	0.88	0.50	1	0.113431	0.482462	0.4688	0.128689
120.0939521	5.2043	C9H12	6	1,2,4-Trimethylbenzene	5	0	KEGG_Metacyc	C14533	1.00	0.91	1.07	0.66	1.32	1	0.839451	0.913894	0.469542	0.510923
129.090209	21.085	C5H11N3O	3	(S)-piperazine-2-carboxamide	5	0	Metacyc	0	1.00	1.09	0.97	0.81	**0.42**	1	0.674482	0.834381	0.183441	0.012082
132.0420883	13.656	C5H8O4	16	Deoxyribonolactone	5	0	KEGG_Metacyc_HMDB	C02674	1.00	0.99	0.90	1.04	0.44	1	0.95434	0.603325	0.852489	0.087293
133.0198058	14.327	C4H7NO2S	1	L-thiazolidine-4-carboxylate	7	0	Metacyc	0	1.00	0.88	0.93	0.74	**0.23**	1	0.537497	0.705901	0.208635	0.015844
133.0739415	11.555	C5H11NO3	4	N-hydroxyvaline	7	0	Metacyc	0	1.00	1.31	**2.54**	1.33	1.55	1	0.233449	0.035914	0.166323	0.432521
136.0385148	9.6823	C5H4N4O	3	allopurinol	7	0	KEGG_Metacyc	D00224	1.00	0.97	1.13	1.24	0.53	1	0.837326	0.654804	0.132303	0.210125

143.0945952	11.475	C7H13NO2	2	Stachydrine	5	0	KEGG_Metacyc_HMDB	C10172	1.00	1.26	1.23	1.13	0.61	1	0.59154	0.41875	0.684286	0.159903
144.020399	13.412	C4H5ClN4	1	4-chloro-2,6-diaminopyrimidine	5	0	Metacyc	0	1.00	0.83	1.73	0.54	0.34	1	0.830939	0.446435	0.590904	0.479563
145.0526682	10.417	C9H7NO	7	1(2H)-Isoquinolinone	5	0	KEGG_Metacyc	C06324	1.00	0.97	1.01	1.03	0.71	1	0.835857	0.942874	0.803917	0.083175
145.0526955	5.5904	C9H7NO	7	3-Methyleneoxindole	7	0	KEGG_Metacyc	C02796	1.00	0.95	1.26	0.62	2.85	1	0.957671	0.796361	0.633312	0.098083
147.0354367	12.08	C5H9NO2S	1	Thiomorpholine 3-carboxylate	7	0	KEGG_Metacyc	C03901	1.00	0.85	0.82	0.75	**0.24**	1	0.493396	0.417517	0.269623	0.023949
147.0529295	8.9641	C5H9NO4	14	N-hydroxy-N-isopropyloxamate	5	0	Metacyc	0	1.00	1.42	1.21	1.20	**0.40**	1	0.256934	0.366208	0.504955	0.009296
150.0347506	6.0837	C5H10O3S	1	2-hydroxy-4-methylthiobutanoate	7	0	Metacyc	0	1.00	0.63	0.55	0.89	2.98	1	0.480743	0.389752	0.832972	0.22346
154.0028197	22.936	C3H7O5P	3	Hydroxyacetone phosphate	7	0	KEGG_Metacyc	C03505	1.00	1.04	0.60	0.71	0.32	1	0.952585	0.462427	0.59593	0.258695
161.051023	10.235	C6H11NO2S	1	allylcysteine	5	0	KEGG_Metacyc	C16759	1.00	0.77	0.82	0.73	0.23	1	0.503276	0.572943	0.426422	0.09713
161.1051428	12.009	C7H15NO3	2	(S)-Carnitine	5	0	KEGG_Metacyc	C15025	1.00	1.24	1.30	0.99	0.33	1	0.510281	0.427127	0.97518	0.053845
163.0841351	15.97	C6H13NO4	9	D-Fucosamine	5	0	KEGG	C15478	1.00	1.06	1.19	0.78	**0.35**	1	0.641203	0.350911	0.101448	0.048004
165.0649576	11.134	C6H7N5O	5	3-Methylguanine	5	0	KEGG_HMDB	C02230	1.00	0.98	1.04	1.08	0.41	1	0.951714	0.876563	0.848232	0.091496
166.0056098	24.333	C8H14NO9S2	1	Glucocapparin	7	0	KEGG	C08404	1.00	1.00	0.99	1.04	1.06	1	0.992692	0.558797	0.262851	0.105449

166.0837783	11.506	C6H14O5	2	L-rhamnitol	7	0	Metacyc	0	1.00	1.04	0.90	1.07	0.71	1	0.807772	0.601081	0.660415	0.156004
173.116487	8.4428	C7H15N3O2	2	ε-guanidinocaproate	5	0	Metacyc	0	1.00	1.18	1.33	1.40	0.85	1	0.379217	0.143226	0.187356	0.302301
173.9988349	10.375	C6H6O4S	2	Phenol sulfate	5	0	KEGG	C02180	1.00	0.97	1.05	0.77	0.92	1	0.939806	0.905403	0.391649	0.743218
174.0521807	14.825	C7H10O5	6	2-oxopimelate	3	0	KEGG_Metacyc	C16588	1.00	**1.56**	0.81	1.29	1.01	1		0.526415	0.422061	0.960101
174.1003254	11.013	C7H14N2O3	5	N5-Ethyl-L-glutamine	7	0	KEGG_Metacyc	C01047	1.00	1.18	1.17	1.10	**0.46**	1	0.29463	0.211287	0.770782	0.018273
176.0949178	11.145	C10H12N2O	4	N-hydroxyl-tryptamine	5	0	KEGG_Metacyc	C17203	1.00	1.01	1.43	1.08	0.85	1	0.983143	0.57542	0.850721	0.716202
179.057972	6.2229	C9H9NO3	6	N-Acetylanthranilate	5	0	KEGG_Metacyc	C06332	1.00	1.13	0.94	1.21	0.76	1	0.623717	0.694018	0.104343	0.071617
179.0945812	7.7623	C10H13NO2	5	(-)-Salsolinol	5	0	KEGG_HMDB	C09642	1.00	1.26	0.85	1.88	0.84	1	0.496047	0.677197	0.087506	0.662875
181.0408041	15.399	C5H11NO4S	1	DL-Methionine sulfone	5	0	Metacyc	0	1.00	1.07	1.13	0.99	0.55	1	0.82195	0.735569	0.96629	0.225551
181.9800701	5.1317	C15H12O2Cl4	1	Tetrachlorobisphenol A	7	0	KEGG	C14528	1.00	1.00	1.04	1.04	1.07	1	0.989512	0.830073	0.849885	0.66016
187.168336	22.006	C9H21N3O	2	N1-Acetylspermidine	7	0	KEGG_Metacyc_HMDB	C00612	1.00	1.09	2.30	3.16	0.79	1	0.82996	0.106486	0.08882	0.695554
188.0793979	9.427	C7H12N2O4	2	N-Acetylglutamine	5	0	HMDB	0	1.00	1.09	1.10	0.54	0.23	1	0.810092	0.817796	0.130376	0.055708
192.0631344	8.2021	C7H12O6	6	5D-5-O-Methyl-2,3,5/4,6-pentahydroxycyclohexanone	5	0	KEGG_Metacyc	C01295	1.00	0.68	0.85	0.81	0.85	1	0.209044	0.443126	0.3708	0.592007

192.0634636	10.409	C7H12O6	6	Valiolone	5	0	KEGG	C12113	1.00	0.66	0.69	0.81	0.97	1	0.335149	0.331383	0.560837	0.919164
195.1107177	18.394	C7H17NO5	1	**N-methyl glucamine**	9	0	IntStd	0	1.00	1.01	1.00	0.98	0.40	1	0.938139	0.990473	0.897538	0.111504
197.0800038	8.3143	C8H11N3O3	3	Methyl5-(but-3-en-1-yl)amino-1,3,4-oxadiazole-2-carboxylate	7	0	KEGG	C12245	1.00	1.39	0.88	1.23	0.55	1	0.240146	0.574122	0.371007	0.090305
197.0800627	9.0288	C8H11N3O3	3	N-Acetyl-L-histidine	7	0	KEGG_Metacyc	C02997	1.00	0.96	1.06	1.16	0.57	1	0.9156	0.869136	0.701264	0.218669
202.1430106	19.115	C8H18N4O2	3	NG,NG-Dimethyl-L-arginine	7	0	KEGG_Metacyc_HMDB	C03626	1.00	0.99	1.04	1.17	0.60	1	0.970384	0.849317	0.488578	0.204041
203.058007	5.7289	C11H9NO3	2	Anibine	7	0	KEGG	C10127	1.00	1.58	1.54	0.85	0.88	1	0.112729	0.278827	0.529757	0.705786
203.0792501	14.125	C8H13NO5	2	2-acetamidoglucal	5	0	Metacyc	0	1.00	0.97	1.32	0.96	0.54	1	0.857593	0.462333	0.846084	0.224221
204.1109014	20.63	C8H16N2O4	5	N5-(L-1-Carboxyethyl)-L-ornithine	7	0	KEGG_Metacyc	C04210	1.00	0.65	1.97	**7.02**	22.59	1	0.455385	0.146532	0.015804	0.42495
210.073691	13.382	C7H14O7	4	alpha-D-Mannoheptulopyranose	7	0	KEGG	C08236	1.00	1.21	1.73	2.69	2.94	1	0.402414	0.120416	0.072898	0.170693
212.0082638	22.963	C5H9O7P	3	phosphinomethylmalate	5	0	Metacyc	0	1.00	0.62	1.21	0.62	0.94	1	0.1951	0.417103	0.194008	0.897457
217.0773166	5.9664	C9H15NO3S	2	captopril	7	0	KEGG_Metacyc	D00251	1.00	0.82	0.92	1.08	0.95	1	0.794072	0.913315	0.911074	0.960537
222.0562995	5.2318	C8H14O5S	2	2-(3'-methylthio)propylmalate	5	0	KEGG_Metacyc	C17214	1.00	**3.07**	**2.00**	2.46	0.60	1			0.122493	0.549402
224.0898741	10.187	C9H12N4O3	1	Temurin	7	0	HMDB	0	1.00	0.81	0.83	0.91	0.78	1	0.571894	0.622054	0.790006	0.778894

228.1109936	14.143	C10H16N2O4	2	(S)-ATPA	5	0	KEGG	C13733	1.00	1.01	1.03	1.14	0.40	1	0.96528	0.9361	0.596403	0.099543
232.2191697	5.1611	C17H28	1	sterone-ring	5	0	Metacyc	0	1.00	1.16	1.70	0.94	1.49	1	0.776274	0.336746	0.918379	0.347875
240.0451467	19.712	C21H20O13	1	Gossypin	7	0	KEGG	C10051	1.00	1.16	1.50	19.86	1.04	1	0.435738	0.078762	0.414398	0.877012
242.0189623	26.8	C6H11O8P	2	D-myo-Inositol 1,2-cyclic phosphate	7	0	KEGG_Metacyc_HMDB	C04299	1.00	1.07	1.26	0.87	0.42	1	0.8319	0.609951	0.648083	0.165457
242.0191874	25.431	C6H11O8P	2	6-deoxy-5-ketofructose-1-phosphate	7	0	Metacyc	0	1.00	0.82	1.30	1.12	0.55	1	0.484251	0.454783	0.661309	0.294726
245.1626781	6.5512	C12H23NO4	4	N-(octanoyl)-L-homoserine	7	0	Metacyc	0	1.00	0.88	1.23	1.15	0.99	1	0.339888	0.245787	0.35944	0.983487
246.0501309	22.42	C6H15O8P	3	Glycerophosphoglycerol	7	0	KEGG_Metacyc	C03274	1.00	0.72	0.93	0.74	**0.31**	1	0.095295	0.681431	0.122287	0.04886
246.0853381	10.099	C9H14N2O6	2	5-6-Dihydrouridine	7	0	HMDB	0	1.00	0.78	0.83	0.67	0.60	1	0.547296	0.621991	0.344185	0.331265
249.0861147	8.0532	C10H19NO2S2	2	S-Acetyldihydrolipoamide	8	0	KEGG_Metacyc_HMDB	C01136	1.00	0.76	0.91	0.88	0.46	1	0.457662	0.781359	0.811644	0.15975
266.0901539	7.6191	C12H14N2O5	1	p-aminobenzoyl glutamate	5	0	Metacyc	0	1.00	0.72	1.02	1.25	0.69	1	0.491135	0.926909	0.565528	0.225241
267.0565166	7.517	C12H13NO4S	1	Oxycarboxin	7	0	KEGG	C10956	1.00	0.77	1.83	1.36	0.69	1	0.548217	0.375004	0.562419	0.479889
267.0952714	12.485	C9H17NO8	2	Miserotoxin	5	0	KEGG	C08507	1.00	0.81	0.94	0.92	0.50	1	0.17337	0.675569	0.667518	0.159403
268.0792831	14.053	C9H16O9	4	2-keto-3-deoxy-D-glycero-D-galacto-nononate	5	0	Metacyc	0	1.00	1.00	1.08	1.01	0.82	1	0.992963	0.871904	0.979457	0.689147

268.0793033	14.788	C9H16O9	4	2(alpha-D-Mannosyl)-D-glycerate	6	0	KEGG_Metacyc	C11544	1.00	1.00	1.11	1.00	0.62	1	0.994406	0.716864	0.997135	0.398454
268.9702295	16.102	C12H17BrN2O13P2	1	uridine-5'-diphosphate bromoacetol	7	0	Metacyc	0	1.00	1.00	0.75	0.90	**0.16**	1	0.99923	0.438637	0.692949	0.035191
272.0295876	25.362	C7H13O9P	2	α-(2,6-anhydro-3-deoxy-D-arabino-heptulopyranosid)onate 7-phosphate	7	0	Metacyc	0	1.00	1.25	1.93	4.08	5.38	1	0.438776	0.266953	0.069677	0.12366
272.0836695	5.2406	C19H12O2	2	7,8-benzoflavone	5	0	Metacyc	0	1.00	1.11	1.45	0.68	1.52	1	0.786178	0.411591	0.401488	0.556827
272.2350553	5.1962	C16H32O3	18	16-hydroxypalmitate	7	0	Metacyc_HMDB	0	1.00	1.08	0.83	1.52	0.92	1	0.845672	0.563368	0.278421	0.827833
274.1569707	5.0438	C17H22O3	3	Podocarpic acid	5	0	KEGG	C09171	1.00	1.15	0.78	1.43	1.93	1	0.851108	0.262879	0.697879	0.41472
288.0957234	7.6254	C13H21O3PS	1	Iprobenfos	7	0	KEGG	C15230	1.00	1.01	0.90	0.95	0.74	1	0.974588	0.640808	0.853734	0.682603
291.0953494	12.143	C11H17NO8	3	2,7-Anhydro-alpha-N-acetylneuraminic acid	7	0	KEGG_Metacyc	C04521	1.00	0.91	0.84	0.70	0.45	1	0.861851	0.774676	0.555202	0.320306
292.1673902	5.112	C17H24O4	2	Trichodermin	5	0	KEGG	C09741	1.00	0.91	0.78	0.95	1.32	1	0.88694	0.391762	0.917248	0.451433
299.0614812	8.129	C16H13NO3S	2	8-Anilino-1-naphthalene sulfonic acid	5	0	KEGG	C11326	1.00	**0.49**	0.64	0.80	0.67	1	0.030176	0.18711	0.407955	0.238073
309.1058359	12.456	C11H19NO9	5	α-N-acetylneuraminate	5	0	Metacyc	0	1.00	0.97	1.16	1.03	0.57	1	0.919092	0.649903	0.918093	0.361247
311.1214921	12.456	C12H17N5O5	2	N2-N2-Dimethylguanosine	5	0	HMDB	0	1.00	0.64	0.69	0.94	0.63	1	0.104246	0.139832	0.842791	0.343049
311.1327388	13.352	C19H18FNO2	1	Citalopram alcohol	5	0	KEGG	C16611	1.00	0.96	0.83	0.99	0.36	1	0.879765	0.455813	0.980641	0.060325

316.0922 59	6.47 16	C18H17FO2 S	1	SC-57666	5	0	KEGG	C11706	1. 00	0. 70	0. 83	0.9 1	0.5 7	1	0.548 289	0.729 952	0.828 583	0.354 924
324.1054 532	14.8 05	C12H20O10	4	D-Fructofuranose 1,2':2,3'-dianhydride	5	0	KEGG	C04420	1. 00	1. 02	0. 88	1.1 0	**0.3 6**	1	0.909 756	0.580 213	0.633 003	0.000 346
324.1054 813	14.0 93	C12H20O10	4	Bis-D-fructose 2',1:2,1'- dianhydride	5	0	KEGG_Metacyc	C04333	1. 00	1. 03	1. 12	1.0 0	0.5 1	1	0.937 195	0.820 381	0.991 211	0.211 181
327.2772 009	7.54 33	C19H37NO3	1	Margaroylglycine	5	0	HMDB	0	1. 00	0. 78	1. 37	1.0 4	0.7 4	1	0.167 797	0.145 388	0.800 963	0.118 838
335.1326 531	18.8 87	C12H21N3O 8	3	N4-(Acetyl-beta-D- glucosaminyl)asparagine	5	0	KEGG_Metacyc_H MDB	C04540	1. 00	0. 80	1. 21	**1.6 1**	0.7 8	1	0.081 372	0.169 107	0.002 777	0.447 288
336.2664 03	7.95 83	C21H36O3	3	5beta-Pregnane- 3alpha,17alpha,20alpha- triol	7	0	KEGG	C14680	1. 00	1. 07	1. 62	1.1 8	1.8 4	1	0.763 623	0.179 987	0.338 032	0.109 107
340.1428 826	5.47 97	C19H20N2O 4	1	N2,N5-Dibenzoyl-L- ornithine	7	0	KEGG_Metacyc	C03712	1. 00	1. 24	1. 98	1.3 4	1.1 7	1	0.356 911	0.186 239	0.411 856	0.483 927
343.0949 409	7.82 68	C20H13N3O 3	1	violacein	5	0	Metacyc	0	1. 00	0. 97	1. 80	1.4 8	1.9 9	1	0.881 258	0.120 773	0.155 153	0.109 857
348.0468 978	23.8 91	C10H13N4O 8P	3	dXMP	7	0	Metacyc	0	1. 00	**0. 36**	0. 56	0.8 1	0.3 5	1	0.002 082	0.061 747	0.529 548	0.060 089
358.0839 662	17.5 05	C14H18N2O 7S	1	Miraxanthin-I	5	0	KEGG	C08554	1. 00	1. 09	1. 00	1.0 0	**0.6 2**	1	0.453 113	0.976 269	0.977 162	0.016 392
371.1330 4	8.12 4	C34H46O18	1	Acanthoside D	7	0	KEGG	C10543	1. 00	1. 21	1. 18	1.5 9	0.4 8	1	0.659 224	0.802 41	0.235 051	0.274 651
395.3033 943	5.96 64	C23H41NO4	1	9,12- Hexadecadienoylcarnitin e	7	0	HMDB	0	1. 00	1. 43	1. 16	1.2 7	1.7 8	1	0.354 919	0.508 258	0.340 272	0.341 842
402.1637 112	12.6 29	C18H22N6O 5	1	7,8-H2pterin-6-ylmethyl- l-(4-aminophenyl)-1- deoxy-D-ribitol	7	0	Metacyc	0	1. 00	1. 10	0. 98	0.8 1	0.7 3	1	0.787 686	0.949 644	0.590 995	0.454 863

411.1357015	15.22	C19H25NO7S	1	13E-Tetranor-16-carboxy-LTE4	5	0	HMDB	0	1.00	1.06	0.91	0.78	0.47	1	0.903296	0.743925	0.45707	0.140551
416.2325259	7.553	C21H37O6P	1	CPA(18:2(9Z,12Z)/0:0)	7	0	HMDB	0	1.00	0.51	**3.20**	**0.51**	1.07	1	0.074709	0.010547		0.940876
418.0188999	17.461	C10H16N2O12P2	2	P1-uridyl-P2-methyl diphosphate	5	0	Metacyc	0	1.00	0.99	1.01	0.99	0.61	1	0.629177	0.880008	0.658014	0.32814
464.0544052	11.21	C16H20N2O10S2	1	4-hydroxy-3-indolylmethyl-glucosinolate	5	0	Metacyc	0	1.00	0.85	0.84	0.89	0.79	1	0.53247	0.53223	0.610693	0.380933
466.1002404	15.685	C17H19N6O8P	1	N-Adenylylanthranilate	5	0	KEGG Metacyc	C03293	1.00	1.03	1.35	0.89	**0.33**	1	0.741864	0.420408	0.369789	0.014152
519.3322938	6.2574	C26H50NO7P	3	1-Linoleoylglycerophosphocholine	7	0	KEGG Metacyc	C04100	1.00	1.27	1.34	1.01	0.52	1	0.580698	0.177902	0.977935	0.373137
521.3484407	10.177	C26H52NO7P	11	1-Oleoylglycerophosphocholine	5	0	KEGG Metacyc	C03916	1.00	0.99	1.03	1.23	0.25	1	0.973847	0.938 79	0.557075	0.095175
522.8906005	16.555	C10H12MoN5O8PS2	1	molybdenum cofactor	5	0	Metacyc	0	1.00	0.96	0.92	0.91	0.72	1	0.550021	0.188187	0.067217	0.292406
541.0600152	22.114	C15H21N5O13P2	1	Cyclic ADP-ribose	5	0	KEGG	C13050	1.00	1.08	1.24	1.16	1.23	1	0.203417	0.217 81	0.210 45	0.686 69
713.2393339	20.75	C30H35N9O12	1	pteroyl-γ-glutamyl-γ-glutamylglutamate	7	0	Metacyc	0	1.00	1.17	1.32	0.83	0.63	1	0.452253	0.181148	0.235773	0.141124
798.4452476	5.2764	C38H72O13P2	1	Phosphatidylglycerophosphate (dihexadec-9-enoyl, n-C16:1)	7	0	Metacyc HMDB	0	1.00	1.11	1.14	0.74	0.81	1	0.897605	0.867915	0.714944	0.836 52
826.2473785	20.513	C39H42N2O18	1	Pradimicin C	5	0	KEGG	C06786	1.00	1.57	1.38	1.69	2.28	1	0.150219	0.254315	0.097476	0.051756
839.5678431	8.0363	C46H82NO10P	1	1-22:1-2-18:3-phosphatidylserine	5	0	Metacyc	0	1.00	1.09	1.06	0.46	0.87	1	0.786995	0.878824	0.128706	0.733625

858.5264227	9.1964	C45H79O13P	15	1-18:2-2-18:2-phosphatidylinositol	5	0	Metacyc	0	1.00	1.19	1.42	0.63	0.95	1	0.717098	0.479097	0.350537	0.887444
882.5260657	8.7356	C55H70N4O6	1	geranylgeranyl-bacteriopheophytin	7	0	Metacyc	0	1.00	1.07	1.20	0.77	0.71	1	0.831809	0.562132	0.442091	0.45074
75.03172565	17.856	C2H5NO2	3	**Glycine**	8	Amino Acid Metabolism	KEGG_Metacyc_HMDB	C00037	1.00	0.92	1.04	0.97	1.78	1	0.728559	0.805247	0.863682	0.571137
75.03205583	17.635	C2H5NO2	3	**Glycine**	10	Amino Acid Metabolism	KEGG_Metacyc_HMDB	C00037	1.00	1.10	1.12	0.96	1.68	1	0.513584	0.482724	0.764805	0.573817
83.07344968	12.777	C5H9N	4	Piperideine	6	Amino Acid Metabolism	KEGG_Metacyc	C06181	1.00	1.06	1.17	0.99	1.03	1	0.100421	0.50876	0.793944	0.77839
87.03196475	21.81	C3H5NO2	3	2-Aminoacrylate	6	Amino Acid Metabolism	KEGG_Metacyc_HMDB	C02218	1.00	0.96	0.98	1.20	0.83	1	0.77113	0.86432	0.307104	0.33235
101.0476288	12.484	C4H7NO2	5	1-Aminocyclopropane-1-carboxylate	6	Amino Acid Metabolism	KEGG_Metacyc	C01234	1.00	0.86	0.88	0.92	0.46	1	0.418718	0.540624	0.697378	0.071123
101.0476699	13.444	C4H7NO2	5	1-Aminocyclopropane-1-carboxylate	8	Amino Acid Metabolism	KEGG_Metacyc	C01234	1.00	1.24	2.10	1.04	1.17	1	0.331532	0.109984	0.766067	0.662039
103.063268	10.15	C4H9NO2	14	L-3-Amino-isobutanoate	8	Amino Acid Metabolism	KEGG_Metacyc_HMDB	C03284	1.00	1.02	1.20	1.04	0.96	1	0.898317	0.12969	0.711772	0.697356
103.0633214	13.871	C4H9NO2	14	N,N-Dimethylglycine	8	Amino Acid Metabolism	KEGG_Metacyc_HMDB	C01026	1.00	1.08	1.21	0.88	0.47	1	0.703783	0.192087	0.493241	0.072584

103.0997349	12.698	C5H13NO	1	**Choline**	8	Amino Acid Metabolism	KEGG_Metacyc_HMDB	C00114	1.00	0.75	0.78	0.86	0.42	1	0.423809	0.440833	0.634004	0.110935
105.0426156	17.84	C3H7NO3	3	**L-Serine**	10	Amino Acid Metabolism	KEGG_Metacyc_HMDB	C00065	1.00	0.98	1.08	0.88	0.39	1	0.935052	0.709764	0.484327	0.064556
113.0477073	17.252	C5H7NO2	6	(S)-1-Pyrroline-5-carboxylate	8	Amino Acid Metabolism	KEGG_Metacyc_HMDB	C03912	1.00	1.00	0.95	0.93	0.45	1	0.987897	0.690287	0.644385	0.132085
113.0589894	11.899	C4H7N3O	1	Creatinine	6	Amino Acid Metabolism	KEGG_Metacyc_HMDB	C00791	1.00	1.01	1.14	1.02	0.48	1	0.931868	0.648881	0.913262	0.150689
115.0633425	15.222	C5H9NO2	4	**L-Proline**	10	Amino Acid Metabolism	KEGG_Metacyc_HMDB	C00148	1.00	1.16	1.05	0.85	0.62	1	0.61534	0.755397	0.284958	0.093756
116.0472565	7.9619	C5H8O3	9	3-Methyl-2-oxobutanoic acid	8	Amino Acid Metabolism	KEGG_Metacyc_Lipidmaps_HMDB	C00141	1.00	1.15	1.03	0.75	0.48	1	0.628032	0.899828	0.419158	0.189707
116.047397	7.602	C5H8O3	9	3-Methyl-2-oxobutanoic acid	6	Amino Acid Metabolism	KEGG_Metacyc_Lipidmaps_HMDB	C00141	1.00	1.09	0.93	1.31	0.89	1	0.88666	0.857419	0.498617	0.816796
117.0790085	15.928	C5H11NO2	16	Betaine	6	Amino Acid Metabolism	KEGG_Metacyc_HMDB	C00719	1.00	1.12	1.26	0.82	**0.22**	1	0.549914	0.240908	0.403854	0.009846
117.0790202	12.509	C5H11NO2	16	**L-Valine**	10	Amino Acid Metabolism	KEGG_Metacyc_HMDB	C00183	1.00	1.03	1.21	0.99	0.57	1	0.673486	0.433641	0.942341	0.221488

119.0583313	16.4498	C4H9NO3	11	**L-Threonine**	10	Amino Acid Metabolism	KEGG_Metacyc_HMDB	C00188	1.00	0.93	1.03	0.71	0.57	1	0.793861	0.883601	0.228408	0.25915
121.0195631	21.684	C3H7NO2S	2	L-Cysteine	6	Amino Acid Metabolism	KEGG_Metacyc_HMDB	C00097	1.00	1.17	0.87	1.25	0.43	1	0.739041	0.814585	0.663012	0.318521
121.0196705	15.4428	C3H7NO2S	2	L-Cysteine	6	Amino Acid Metabolism	KEGG_Metacyc_HMDB	C00097	1.00	0.56	0.68	0.54	0.27	1	0.390879	0.513755	0.372122	0.21101
122.0366543	5.6279	C7H6O2	6	**Benzoate**	10	Amino Acid Metabolism	KEGG_Metacyc_HMDB	C00180	1.00	0.88	0.77	0.64	1.67	1	0.883535	0.772934	0.645854	0.541623
125.9984717	18.749	C2H6O4S	1	2-Hydroxyethanesulfonate	7	Amino Acid Metabolism	KEGG_Metacyc_HMDB	C05123	1.00	0.60	0.86	1.18	**0.69**	1	0.490883	0.570867	0.211502	
125.9984832	21.155	C2H6O4S	1	2-Hydroxyethanesulfonate	7	Amino Acid Metabolism	KEGG_Metacyc_HMDB	C05123	1.00	1.08	1.22	0.95	0.78	1	0.818237	0.37337	0.822578	0.625561
128.0586255	14.01	C5H8N2O2	3	gamma-Amino-gamma-cyanobutanoate	8	Amino Acid Metabolism	KEGG_Lipidmaps	C05715	1.00	0.95	1.09	0.89	0.46	1	0.847378	0.757941	0.715952	0.133653
129.0424814	8.2111	C5H7NO3	6	L-1-Pyrroline-3-hydroxy-5-carboxylate	8	Amino Acid Metabolism	KEGG_Metacyc_HMDB	C04281	1.00	1.02	0.93	0.95	0.48	1	0.960096	0.847451	0.888024	0.219807
129.0790666	13.732	C6H11NO2	9	L-Pipecolate	6	Amino Acid Metabolism	KEGG_Metacyc_HMDB	C00408	1.00	1.12	1.23	1.11	0.65	1	0.258548	0.141509	0.517607	0.166833

129.0791039	9.1032	C6H11NO2	9	N4-Acetylaminobutanal	8	Amino Acid Metabolism	KEGG_Metacyc_HMDB	C05936	1.00	1.10	1.48	0.97	0.75	1	0.673857	0.140946	0.883434	0.26408
130.0628575	6.3315	C6H10O3	17	(S)-3-Methyl-2-oxopentanoic acid	8	Amino Acid Metabolism	KEGG_Metacyc_Lipidmaps_HMDB	C00671	1.00	1.15	0.98	0.72	0.35	1	0.729051	0.92402	0.261046	0.065725
130.1107031	13.257	C6H14N2O	2	N-Acetylputrescine	8	Amino Acid Metabolism	KEGG_Metacyc_HMDB	C02714	1.00	0.86	**0.37**	**0.14**	**0.21**	1	0.273961	0.017161	0.002133	0.001308
131.0583101	16.534	C5H9NO3	14	L-Glutamate 5-semialdehyde	8	Amino Acid Metabolism	KEGG_Metacyc_HMDB	C01165	1.00	1.17	1.23	0.96	**0.40**	1	0.505968	0.34537	0.82122	0.02761
131.0695572	13.298	C4H9N3O2	2	Creatine	8	Amino Acid Metabolism	KEGG_Metacyc_HMDB	C00300	1.00	1.00	1.14	0.90	0.39	1	0.983499	0.355984	0.587822	0.068262
132.0535468	17.878	C4H8N2O3	6	**L-Asparagine**	8	Amino Acid Metabolism	KEGG_Metacyc_HMDB	C00152	1.00	1.01	1.07	0.81	**0.28**	1	0.979556	0.776941	0.295019	0.024518
132.0896542	21.084	C5H12N2O2	6	D-Ornithine	6	Amino Acid Metabolism	KEGG_Metacyc_HMDB	C00515	1.00	0.73	0.93	0.85	0.53	1	0.502443	0.844566	0.719465	0.303021
132.089964	21.894	C5H12N2O2	6	**L-Ornithine**	10	Amino Acid Metabolism	KEGG_Metacyc_HMDB	C00077	1.00	1.56	4.21	**4.80**	1.58	1	0.393104	0.150035	0.009421	0.623776
133.0374959	18.565	C4H7NO4	4	D-Aspartate	8	Amino Acid Metabolism	KEGG_Metacyc_HMDB	C00402	1.00	0.96	1.02	1.00	2.22	1	0.788111	0.850485	0.961434	0.531397

133.0375688	17.518	C4H7NO4	4	**L-Aspartate**	10	Amino Acid Metabolism	KEGG_Metacyc_HMDB	C00402	1.00	1.17	1.06	1.10	2.13	1	0.069805	0.429623	0.411483	0.496793
140.0584644	11.275	C6H8N2O2	7	Methylimidazoleacetic acid	6	Amino Acid Metabolism	KEGG_HMDB	C05828	1.00	1.20	1.21	1.15	0.39	1	0.332059	0.486773	0.686206	0.068149
144.1262145	21.706	C7H16N2O	2	1-(3-aminopropyl)-4-aminobutanal	6	Amino Acid Metabolism	Metacyc_HMDB	0	1.00	1.18	1.04	1.15	0.30	1	0.496112	0.917541	0.676099	0.073657
145.037247	7.8656	C5H7NO4	2	2-Oxoglutaramate	8	Amino Acid Metabolism	KEGG_Metacyc_HMDB	C00940	**1.00**	**1.50**	**0.53**	**0.90**	**0.00**			#DIV/0!	#DIV/0!	
145.07374	13.729	C6H11NO3	9	6-Amino-2-oxohexanoate	8	Amino Acid Metabolism	KEGG_Metacyc_HMDB	C03239	1.00	1.43	1.22	1.10	1.49	1	0.604845	0.696194	0.812255	0.609259
145.0740399	12.044	C6H11NO3	9	[FA oxo,amino(6:0)] 3-oxo-5S-amino-hexanoic acid	6	Amino Acid Metabolism	KEGG_Metacyc_Lipidmaps_HMDB	C03656	1.00	0.99	1.02	0.90	0.70	1	0.969547	0.933875	0.518418	0.14729
145.1102213	7.9107	C7H15NO2	6	3-Dehydroxycarnitine	3	Amino Acid Metabolism	KEGG_HMDB	C05543	1.00	1.04	0.99	1.14	0.65	1	0.91417	0.984112	0.446792	0.118267
145.1579035	32.407	C7H19N3	1	**Spermidine**	10	Amino Acid Metabolism	KEGG_Metacyc_HMDB	C00315	1.00	1.06	0.82	**0.34**	**0.38**	1	0.716374	0.337029	0.017641	0.049361
146.0691481	17.489	C5H10N2O3	6	D-Glutamine	8	Amino Acid Metabolism	KEGG_Metacyc_HMDB	C00819	1.00	1.12	1.07	0.96	**0.64**	1	0.488214	0.343581	0.752088	0.002548

146.1054877	21.493	C6H14N2O2	7	**L-Lysine**	10	Amino Acid Metabolism	KEGG_Metacyc_HMDB	C00047	1.00	1.09	0.98	1.10	0.43	1	0.578487	0.920193	0.62738	0.095112
147.0531062	15.941	C5H9NO4	14	**L-Glutamate**	10	Amino Acid Metabolism	KEGG_Metacyc_HMDB	C00025	1.00	0.93	1.01	0.78	**0.40**	1	0.418064	0.966706	0.104566	0.030941
148.0193168	7.8134	C5H8O3S	1	[FA oxo,methyl(4:0)] 2-oxo-4-methylthio-butanoic acid	6	Amino Acid Metabolism	KEGG_Metacyc_Lipidmaps_HMDB	C01180	1.00	1.14	1.14	0.69	0.89	1	0.687029	0.697973	0.400782	0.731432
149.0476693	7.9834	C8H7NO2	8	5,6-Dihydroxyindole	8	Amino Acid Metabolism	KEGG_Metacyc_HMDB	C05578	1.00	0.92	1.14	1.76	0.89	1	0.778045	0.662968	0.119811	0.591067
149.0510691	11.9	C5H11NO2S	5	**L-Methionine**	10	Amino Acid Metabolism	KEGG_Metacyc_HMDB	C00073	1.00	1.05	1.12	0.99	0.52	1	0.476176	0.41114	0.866686	0.141857
152.0470606	6.1079	C8H8O3	25	3,4-Dihydroxyphenylacetaldehyde	6	Amino Acid Metabolism	KEGG_Metacyc_HMDB	C04043	1.00	1.11	0.88	1.14	2.09	1	0.812576	0.752266	0.701506	0.469963
154.0375511	11.965	C6H6N2O3	2	Imidazol-5-yl-pyruvate	6	Amino Acid Metabolism	KEGG_Metacyc	C03277	1.00	1.06	0.99	0.96	**0.39**	1	0.723318	0.953544	0.797123	0.033767
155.069543	20.697	C6H9N3O2	4	**L-Histidine**	8	Amino Acid Metabolism	KEGG_Metacyc_HMDB	C00135	1.00	1.11	1.07	0.97	0.48	1	0.257022	0.410611	0.706034	0.104644
160.1210176	20.94	C7H16N2O2	6	N6-Methyl-L-lysine	7	Amino Acid Metabolism	KEGG_Metacyc_HMDB	C02728	1.00	1.00	1.34	1.01	0.96	1	0.988582	0.336039	0.968468	0.923941

161.0686934	14.348	C6H11NO4	10	O-Acetyl-L-homoserine	6	Amino Acid Metabolism	KEGG_Metacyc	C01077	1.00	1.03	1.01	1.04	0.52	1	0.81499	0.958733	0.854818	0.092445
163.066601	8.2584	C6H13NO2S	6	S-Methyl-L-methionine	8	Amino acid Metabolism	KEGG_Metacyc	C03172	1.00	1.07	**1.66**	1.21	0.85	1	0.733321	0.029809	0.353113	0.471972
164.0471121	6.4412	C9H8O3	13	4-Coumarate	6	Amino Acid Metabolism	KEGG_Metacyc_HMDB	C00811	1.00	1.09	0.87	1.06	0.80	1	0.831667	0.759457	0.890527	0.724838
164.0471262	6.9435	C9H8O3	13	enol-Phenylpyruvate	8	Amino Acid Metabolism	KEGG_Metacyc_HMDB	C02763	1.00	0.91	1.03	1.18	0.80	1	0.839787	0.946885	0.687004	0.730882
164.0471304	5.5891	C9H8O3	13	**Phenylpyruvate**	10	Amino Acid Metabolism	KEGG_Metacyc_HMDB	C00166	1.00	1.12	1.29	0.70	1.00	1	0.843296	0.666209	0.528899	0.996263
164.0471512	7.5899	C9H8O3	13	trans-3-Hydroxycinnamate	8	Amino Acid Metabolism	KEGG_HMDB	C12621	1.00	0.80	1.56	1.71	0.38	1	0.606727	0.457337	0.403003	0.205673
165.0790108	10.069	C9H11NO2	7	D-Phenylalanine	8	Amino Acid Metabolism	KEGG_Metacyc	C02265	1.00	1.03	0.98	0.97	**0.35**	1	0.872975	0.865766	0.839619	0.015531
166.0626351	5.8031	C9H10O3	17	3-(3-Hydroxy-phenyl)-propanoic acid	8	Amino Acid Metabolism	KEGG_Metacyc_HMDB	C11457	1.00	0.81	0.72	0.80	0.95	1	0.369038	0.283511	0.355058	0.926631
169.0850364	20.852	C7H11N3O2	4	N(pi)-Methyl-L-histidine	8	Amino Acid Metabolism	KEGG_Metacyc_HMDB	C01152	1.00	0.94	0.60	0.84	0.09	1	0.924619	0.511853	0.797319	0.213838

173.0687 43	11.009	C7H11NO4	6	N-Acetyl-L-glutamate 5-semialdehyde	6	Amino Acid Metabolism	KEGG_Metacyc_HMDB	C01250	1.00	1.00	1.11	0.90	0.66	1	0.988681	0.486682	0.350343	0.157045
174.0524488	7.6097	C7H10O5	6	(2S)-2-Isopropyl-3-oxosuccinate	6	Amino Acid Metabolism	KEGG_Metacyc_HMDB	C04236	1.00	**0.32**	0.58	1.33	0.43	1	0.040502	0.128011	0.415464	0.070865
174.0526751	10.608	C7H10O5	6	Shikimate	8	Amino Acid Metabolism	KEGG_Metacyc_HMDB	C00493	1.00	0.53	0.49	0.82	0.40	1	0.331466	0.178213	0.573091	0.130723
174.1003737	16.156	C7H14N2O3	5	**N-Acetylornithine**	10	Amino Acid Metabolism	KEGG_Metacyc_HMDB	C00437	1.00	2.19	**3.03**	**4.84**	2.27	1	0.050287	0.036044	0.000599	0.353974
174.1117071	21.093	C6H14N4O2	2	**L-Arginine**	10	Amino Acid Metabolism	KEGG_Metacyc_HMDB	C00062	1.00	1.00	0.93	0.81	**0.42**	1	0.978096	0.629636	0.139127	0.01421
175.0956056	18.068	C6H13N3O3	3	L-Citrulline	6	Amino Acid Metabolism	KEGG_Metacyc_HMDB	C00327	1.00	1.05	1.12	0.92	0.39	1	0.611893	0.52529	0.555833	0.318392
176.0680727	7.5159	C7H12O5	7	(2S)-2-Isopropylmalate	8	Amino Acid Metabolism	KEGG_Metacyc_HMDB	C02504	1.00	2.07	2.75	**4.36**	**9.67**	1	0.389894	0.325621	0.025701	0.007046
179.0579641	5.9517	C9H9NO3	6	Hippurate	8	Amino Acid Metabolism	KEGG_Metacyc_HMDB	C01586	1.00	1.05	0.91	0.91	0.96	1	0.846502	0.712376	0.71114	0.958745
180.0419742	6.0632	C9H8O4	11	trans-2,3-Dihydroxycinnamate	6	Amino Acid Metabolism	KEGG	C12623	1.00	0.71	1.20	0.82	0.68	1	0.362642	0.677076	0.53676	0.535507

180.0423144	10.643	C9H8O4	11	2-Hydroxy-3-(4-hydroxyphenyl)propenoate	8	Amino Acid Metabolism	KEGG_HMDB	C05350	1.00	0.62	0.55	0.55	1.54	1	0.66855	0.610232	0.593708	0.555856
181.0739738	12.749	C9H11NO3	11	**L-Tyrosine**	10	Amino Acid Metabolism	KEGG_Metacyc_HMDB	C00082	1.00	1.07	1.07	1.05	0.49	1	0.394449	0.683319	0.668347	0.138856
187.0844247	10.708	C8H13NO4	6	6-Acetamido-2-oxohexanoate	8	Amino Acid Metabolism	KEGG_Metacyc_HMDB	C05548	1.00	0.93	1.10	2.21	3.39	1	0.874843	0.834677	0.157029	0.112062
188.1161357	14.779	C8H16N2O3	7	N6-Acetyl-L-lysine	8	Amino Acid Metabolism	KEGG_Metacyc_HMDB	C02727	1.00	1.17	2.11	**1.91**	19.78	1	0.554791	0.118024	0.042217	0.336475
188.1274009	20.63	C7H16N4O2	5	Homoarginine	5	Amino Acid Metabolism	KEGG_Metacyc_HMDB	C01924	1.00	1.19	1.14	0.84	0.61	1	0.323985	0.673497	0.499883	0.075273
188.1524946	22.275	C9H20N2O2	2	**N6,N6,N6-Trimethyl-L-lysine**	10	Amino Acid Metabolism	KEGG_Metacyc_HMDB	C03793	1.00	1.08	1.43	1.21	8.34	1	0.80823	0.26505	0.609872	0.360921
189.082353	7.8688	C8H15NO2S	1	Prenyl-L-cysteine	7	Amino Acid Metabolism	KEGG_Metacyc_HMDB	C06751	1.00	0.78	0.78	0.77	0.15	1	0.491333	0.485315	0.452297	0.062444
190.0475227	8.1275	C7H10O6	4	[FA hydroxy(7:1/2:0)] 2,4-dihydroxy-2-heptenedioc acid	8	Amino Acid Metabolism	KEGG_Lipidmaps	C06201	1.00	1.27	0.87	1.18	0.48	1	0.366933	0.535371	0.456501	0.075715
192.06306	12.747	C7H12O6	6	Quinate	6	Amino Acid Metabolism	KEGG_Metacyc_HMDB	C00296	1.00	0.88	0.94	0.82	0.42	1	0.780997	0.873083	0.63904	0.218927

193.0736536	5.87 15	C10H11NO3	10	**Phenylacetylglycine**	10	Amino Acid Metabolism	KEGG_Metacyc_HMDB	C05598	1.00	1.27	0.98	0.84	1.38	1	0.320475	0.9329	0.547261	0.563921
195.0894833	8.51 01	C10H13NO3	6	L-Tyrosine methyl ester	7	Amino Acid Metabolism	KEGG_Metacyc	C03404	1.00	0.96	1.38	1.12	0.85	1	0.620961	0.060782	0.424846	0.440221
197.0181051	14.1 93	C5H11NO3S2	1	CysteineMercaptoethanol disulfide	7	Amino Acid Metabolism	Medium	0	1.00	1.07	1.13	1.13	0.68	1	0.700256	0.675796	0.566739	0.152318
200.9761462	24.3 78	C3H7NO5S2	1	S-Sulfo-L-cysteine	8	Amino Acid Metabolism	KEGG_Metacyc_HMDB	C05824	1.00	0.91	0.83	0.71	0.43	1	0.827853	0.681248	0.487495	0.231808
203.0581144	7.61 21	C11H9NO3	2	Indolepyruvate	6	Amino Acid Metabolism	KEGG_Metacyc	C00331	1.00	0.62	0.91	1.05	0.30	1	0.447513	0.854227	0.928806	0.225847
203.0794057	12.4 56	C8H13NO5	2	N2-Acetyl-L-aminoadipate	6	Amino Acid Metabolism	KEGG_Metacyc	C12986	1.00	1.12	1.57	0.90	0.55	1	0.673 39	0.238647	0.7108	0.168527
204.0899275	10.4 1	C11H12N2O2	6	D-Tryptophan	7	Amino Acid Metabolism	KEGG_Metacyc_HMDB	C00525	1.00	0.98	1.06	1.02	0.42	1	0.864306	0.768238	0.905333	0.052053
206.0423822	7.69 52	C7H10O7	5	2-Hydroxybutane-1,2,4-tricarboxylate	6	Amino Acid Metabolism	KEGG_Metacyc_HMDB	C01251	1.00	1.20	1.85	2.09	**0.16**	1	0.866643	0.629404	0.558543	
216.1109603	13.2 8	C9H16N2O4	3	gamma-Glutamyl-gamma-aminobutyraldehyde	8	Amino Acid Metabolism	KEGG_Metacyc	C15700	1.00	**1.61**	1.33	1.04	1.18	1	0.038 96	0.157765	0.860753	0.625814

218.1054578	7.9577	C12H14N2O2	7	N-Acetylserotonin	6	Amino Acid Metabolism	KEGG_Metacyc_HMDB	C00978	1.00	1.06	1.57	1.23	0.49	1	0.904648	0.671344	0.601624	0.280945
219.1107345	7.4568	C9H17NO5	1	**Pantothenate**	8	Amino Acid Metabolism	KEGG_Metacyc_HMDB	C00864	1.00	1.00	0.75	2.11	0.30	1	0.994799	0.518881	0.134886	0.138208
222.067408	21.208	C7H14N2O4S	4	**L-Cystathionine**	10	Amino Acid Metabolism	KEGG_Metacyc_HMDB	C02291	1.00	1.27	**2.75**	1.35	6.72	1	0.487528	0.011421	0.364	0.407904
226.1063409	21.142	C9H14N4O3	3	Carnosine	6	Amino Acid Metabolism	KEGG_Metacyc_HMDB	C00386	1.00	0.99	1.38	1.01	0.50	1	0.971237	0.191404	0.970322	0.168008
240.0238094	21.664	C6H12N2O4S2	2	**L-Cystine**	10	Amino Acid Metabolism	medium_KEGG_Metacyc_HMDB	C00491	1.00	1.08	1.02	1.33	0.62	1	0.800953	0.955404	0.359051	0.439 05
243.085432	14.965	C9H13N3O5	4	gamma-Glutamyl-beta-cyanoalanine	6	Amino Acid Metabolism	KEGG	C05711	1.00	0.91	1.05	0.95	0.63	1	0.612643	0.891162	0.785 25	0.114165
254.077895	22.839	C6H15N4O5P	1	L-Arginine phosphate	8	Amino Acid Metabolism	KEGG_Metacyc	C05945	1.00	0.94	0.63	0.50	1.16	1	0.913484	0.479458	0.343202	0.894794
259.0455123	23.253	C6H14NO8P	8	**D-Glucosamine 6-phosphate**	10	Amino Acid Metabolism	KEGG_Metacyc_HMDB	C00352	1.00	0.83	0.82	**0.72**	**0.25**	1	0.113599	0.130355	0.043784	0.025682
283.0456131	23.527	C8H14NO8P	2	N2-Acetyl-L-aminoadipyl-delta-phosphate	8	Amino Acid Metabolism	KEGG_Metacyc	C12987	1.00	0.82	1.01	0.85	0.57	1	0.454564	0.969616	0.475604	0.279756

297.0896303	7.8281	C11H15N5O3S	2	**5'-Methylthioadenosine**	10	Amino Acid Metabolism	KEGG_Metacyc_HMDB	C00170	1.00	1.04	**2.23**	1.58	1.90	1	0.90405	0.013431	0.119082	0.259158
301.0559498	23.529	C8H16NO9P	9	N-Acetyl-D-glucosamine 6-phosphate	6	Amino Acid Metabolism	KEGG_Metacyc_HMDB	C00357	1.00	0.82	1.14	0.92	0.62	1	0.465479	0.593864	0.714984	0.387613
307.0836059	15.335	C10H17N3O6S	3	Glutathione	8	Amino Acid Metabolism	KEGG_Metacyc_HMDB	C00051	1.00	0.31	0.81	0.34	6.52	1	0.387548	0.769227	0.401926	0.529393
360.6442388	22.725	C27H47N9O10S2	1	**Trypanothione disulfide**	10	Amino Acid Metabolism	KEGG_Metacyc	C03170	1.00	1.04	1.12	0.77	1.05	1	0.894586	0.693922	0.301565	0.953291
398.1370824	22.731	C15H23N6O5S	1	**S-Adenosyl-L-methionine**	8	Amino Acid Metabolism	KEGG_Metacyc_HMDB	C00019	1.00	1.87	2.99	1.46	5.07	1	0.331569	0.223152	0.385124	0.421883
426.0879557	20.708	C13H22N4O8S2	2	**S-glutathionyl-L-cysteine**	7	Amino Acid Metabolism	KEGG_Metacyc_HMDB	C05526	1.00	1.29	1.32	1.18	0.29	1	0.497399	0.590517	0.621429	0.050185
430.066111	17.96	C11H20N4O10P2	1	CMP-2-aminoethylphosphonate	6	Amino Acid Metabolism	KEGG	C05673	1.00	0.97	1.09	0.62	**0.31**	1	0.943886	0.835436	0.311651	
529.0863367	15.956	C16H25N3O13P2	1	dTDP-3-amino-2,3,6-trideoxy-D-threo-hexopyranos-4-ulose	5	Biosynthesis of Polyketides and Nonribosomal Peptides	KEGG	C12318	1.00	0.74	0.65	0.50	**0.29**	1	0.243204	0.214394	0.062201	
564.0399605	14.92	C15H22N2O17P2	1	UDP-3-ketoglucose	5	Biosynthesis of Polyketid	KEGG_Metacyc	C12210	1.00	1.08	1.04	1.05	0.53	1	0.41667	0.74361	0.705659	0.29059

						es and Nonribosomal Peptides												
564.0402487	15.408	C15H22N2O17P2	1	UDP-3-ketoglucose	5	Biosynthesis of Polyketides and Nonribosomal Peptides	KEGG_Metacyc	C12210	1.00	0.97	1.03	1.09	0.62	1	0.875516	0.957549	0.522122	0.327214
139.0996766	10.843	C8H13NO	2	Tropinone	6	Biosynthesis of Secondary Metabolites	KEGG_Metacyc	C00783	1.00	**1.34**	1.25	1.20	0.97	1	0.047208	0.203686	0.279248	0.670853
180.0420271	9.1234	C9H8O4	11	3,4-Dihydroxy-trans-cinnamate	6	Biosynthesis of Secondary Metabolites	KEGG_Metacyc_HMDB	C01197	1.00	0.96	0.95	0.97	0.46	1	0.908333	0.888079	0.940345	0.202371
240.1472942	11.146	C12H20N2O3	2	Slaframine	7	Biosynthesis of Secondary Metabolites	KEGG	C06185	1.00	1.10	1.25	0.79	0.60	1	0.696642	0.273718	0.238733	0.283451
575.0576022	20.781	C15H24N5O13P3	1	Isopentenyladenosine-5'-triphosphate	6	Biosynthesis of Secondary Metabolites	KEGG_Metacyc	C16424	1.00	0.47	0.86	0.95	0.94	1	0.152864	0.35958	0.209909	0.745236
74.03648069	7.0682	C3H6O2	7	Propanoate	8	Carbohydrate Metabolis	KEGG_Metacyc_Lipidmaps_HMDB	C00163	1.00	1.18	0.91	1.17	0.68	1	0.574293	0.802096	0.838495	0.096531

						m												
88.016165	10.313	C3H4O3	3	3-Oxopropanoate	8	Carbohydrate Metabolism	KEGG_Metacyc_HMDB	C00222	1.00	0.99	1.08	1.06	1.03	1	0.965495	0.803114	0.833497	0.935977
88.0523716	7.9548	C4H8O2	7	Butanoic acid	6	Carbohydrate Metabolism	KEGG_Metacyc_Lipidmaps_HMDB	C00246	1.00	1.21	1.02	0.72	0.52	1	0.497407	0.933254	0.366743	0.213932
92.0472785	10.414	C3H8O3	1	**Glycerol**	10	Carbohydrate Metabolism	KEGG_Metacyc_HMDB	C00116	1.00	0.75	0.88	0.73	0.74	1	0.680472	0.863503	0.646627	0.719116
104.0109036	9.3772	C3H4O4	3	2-Hydroxy-3-oxopropanoate	6	Carbohydrate Metabolism	KEGG_Metacyc_HMDB	C01146	1.00	1.11	0.62	0.91	0.39	1	0.8705	0.189446	0.838831	0.087102
106.0266802	10.382	C3H6O4	2	D-Glycerate	8	Carbohydrate Metabolism	KEGG_Metacyc_HMDB	C00258	1.00	1.18	1.33	1.24	0.89	1	0.587828	0.450149	0.282779	0.830782
116.0108466	10.933	C4H4O4	3	Maleic acid	8	Carbohydrate Metabolism	KEGG_Metacyc_HMDB	C01384	1.00	0.63	0.81	0.82	0.15	1	0.714458	0.867897	0.861676	0.421888
118.0265153	7.4839	C4H6O4	7	**Succinate**	10	Carbohydrate Metabolism	KEGG_Metacyc_Lipidmaps_HMDB	C00042	1.00	1.03	0.77	1.97	0.36	1	0.959651	0.665279	0.087222	0.197364
120.0420987	13.809	C4H8O4	9	L-Erythrulose	7	Carbohydrate Metabolism	KEGG_Metacyc_HMDB	C02045	1.00	1.07	0.90	1.04	0.48	1	0.612066	0.556272	0.832325	0.104175
120.0421255	9.4349	C4H8O4	9	**D-Erythrose**	9	Carbohydrate Metabolis	KEGG_Metacyc_HMDB	C01796	1.00	1.00	0.75	1.42	1.10	1	0.997714	0.476617	0.332107	0.891675

						m												
120.0421298	8.8675	C4H8O4	9	D-Threose	5	Carbohydrate Metabolism	KEGG_Metacyc	C06463	1.00	1.07	0.83	1.28	0.94	1	0.798028	0.589664	0.538208	0.834814
130.0265697	9.5123	C5H6O4	7	Mesaconate	8	Carbohydrate Metabolism	KEGG_Metacyc_HMDB	C01732	1.00	0.76	0.58	0.85	0.63	1	0.424308	0.10707	0.535247	0.240829
132.0420728	11.353	C5H8O4	16	2-Acetolactate	8	Carbohydrate Metabolism	KEGG_Metacyc_HMDB	C00900	1.00	1.08	1.15	0.77	0.60	1	0.796353	0.484058	0.127733	0.277135
134.0213676	12.388	C4H6O5	4	(R)-Malate	8	Carbohydrate Metabolism	KEGG_Metacyc	C00497	1.00	1.97	1.47	2.49	0.33	1	0.498521	0.679002	0.38015	0.371731
134.0214013	9.9032	C4H6O5	4	**(S)-Malate**	10	Carbohydrate Metabolism	KEGG_Metacyc_HMDB	C00149	1.00	1.60	1.62	1.88	0.51	1	0.419621	0.595632	0.244588	0.461454
136.0370266	13.639	C4H8O5	3	[FA trihydroxy(4:0)] 2,3,4-trihydroxy-butanoic acid	8	Carbohydrate Metabolism	KEGG_Metacyc_Lipidmaps_HMDB	C01620	1.00	1.05	0.90	1.06	**0.32**	1	0.790082	0.601415	0.805403	0.036713
146.0212658	13.115	C5H6O5	7	Methyloxaloacetate	7	Carbohydrate Metabolism	KEGG_Metacyc	C06030	1.00	0.98	0.82	0.50	0.16	1	0.93988	0.704203	0.178823	0.064036
148.0369113	9.7792	C5H8O5	18	2-Dehydro-3-deoxy-L-arabinonate	8	Carbohydrate Metabolism	KEGG_Metacyc	C00684	1.00	0.38	0.52	0.49	2.41	1	0.096491	0.171806	0.139775	0.551199
148.0369496	8.0977	C5H8O5	18	D-Xylonolactone	8	Carbohydrate Metabolis	KEGG_Metacyc_HMDB	C02266	1.00	0.54	0.61	0.76	0.91	1	0.061374	0.140676	0.262961	0.866824

						m												
150.0525442	13.205	C5H10O5	37	L-Xylulose	8	Carbohydrate Metabolism	KEGG_Metacyc_HMDB	C00312	1.00	1.13	0.92	1.09	0.76	1	0.470123	0.715802	0.646082	0.400656
150.0525174	15.667	C5H10O5	37	L-Arabinose	8	Carbohydrate Metabolism	KEGG_Metacyc_HMDB	C00259	1.00	0.83	0.80	1.22	0.70	1	0.65669	0.522875	0.676399	0.360859
150.0525998	15.42	C5H10O5	37	D-Xylulose	6	Carbohydrate Metabolism	KEGG_Metacyc_HMDB	C00310	1.00	1.09	0.96	1.07	**0.63**	1	0.322362	0.4656	0.324536	0.024474
152.0681534	13.413	C5H12O5	4	Xylitol	8	Carbohydrate Metabolism	KEGG_Metacyc_HMDB	C00379	1.00	1.01	0.93	1.05	0.47	1	0.930375	0.625606	0.730117	0.104144
167.9819679	29.399	C3H5O6P	3	Phosphoenolpyruvate	8	Carbohydrate Metabolism	KEGG_Metacyc_HMDB	C00074	1.00	1.18	1.11	1.09	2.74	1	0.625719	0.719187	0.73278	0.479932
169.9977043	24.677	C3H7O6P	7	Glycerone phosphate	8	Carbohydrate Metabolism	KEGG_Metacyc_HMDB	C00111	1.00	0.83	1.04	0.82	0.36	1	0.612688	0.911873	0.569776	0.117206
178.0475097	10.053	C6H10O6	26	2-Dehydro-3-deoxy-D-gluconate	6	Carbohydrate Metabolism	KEGG_Metacyc_HMDB	C00204	1.00	0.95	1.00	1.04	2.44	1	0.949319	0.997503	0.961234	0.338665
178.0476917	10.325	C6H10O6	26	D-Glucono-1,5-lactone	6	Carbohydrate Metabolism	KEGG_Metacyc_HMDB	C00198	1.00	0.89	1.04	1.21	2.32	1	0.872413	0.948015	0.710531	0.369213
179.0792696	19.069	C6H13NO5	10	D-Glucosamine	8	Carbohydrate Metabolis	KEGG_Metacyc_HMDB	C00329	1.00	0.99	1.01	0.90	1.42	1	0.950768	0.980767	0.603699	0.699567

						m												
180.0631853	15.466	C6H12O6	57	**D-Glucose**	10	Carbohydrate Metabolism	KEGG_Metacyc_HMDB	C00221	1.00	1.00	0.97	1.05	**0.61**	1	0.942574	0.612766	0.542489	0.024934
182.0787896	14.591	C6H14O6	6	D-Sorbitol	8	Carbohydrate Metabolism	KEGG_Metacyc_HMDB	C00794	1.00	1.04	0.98	1.03	0.46	1	0.772558	0.908746	0.852507	0.119168
185.9926006	29.526	C3H7O7P	3	**3-Phospho-D-glycerate**	8	Carbohydrate Metabolism	KEGG_Metacyc_HMDB	C00197	1.00	1.00	1.14	0.92	1.79	1	0.993341	0.651246	0.740094	0.577487
192.0268113	20.265	C6H8O7	12	5-Dehydro-4-deoxy-D-glucarate	8	Carbohydrate Metabolism	KEGG_Metacyc	C00679	1.00	0.97	1.16	1.23	0.52	1	0.932152	0.707587	0.662417	0.301227
194.0429735	10.333	C6H10O7	16	3-Dehydro-L-gulonate	6	Carbohydrate Metabolism	KEGG_Metacyc_HMDB	C00618	1.00	0.86	1.06	0.93	1.25	1	0.787566	0.920771	0.873887	0.657679
196.0579592	19.294	C6H12O7	11	D-Mannonate	6	Carbohydrate Metabolism	KEGG_Metacyc	C00514	1.00	1.56	1.53	1.45	1.59	1	0.576385	0.530027	0.652202	0.698064
196.0579617	21.526	C6H12O7	11	L-Gulonate	8	Carbohydrate Metabolism	KEGG_Metacyc_HMDB	C00800	1.00	1.57	1.38	1.41	0.47	1	0.590794	0.618699	0.669073	0.463276
196.058024	16.028	C6H12O7	11	**D-Gluconic acid**	10	Carbohydrate Metabolism	KEGG_Metacyc_HMDB	C00257	1.00	1.77	2.07	0.92	0.46	1	0.432663	0.050011	0.891259	0.169167
196.0580602	11.494	C6H12O7	11	D-Galactonate	6	Carbohydrate Metabolis	KEGG_Metacyc	C00880	1.00	0.98	1.03	0.87	0.38	1	0.922061	0.870138	0.261785	0.056091

						m												
196.0581737	11.044	C6H12O7	11	D-Altronate	6	Carbohydrate Metabolism	KEGG_Metacyc	C00817	1.00	1.02	1.08	0.95	0.68	1	0.877826	0.67795	0.695991	0.193462
200.0082395	26.609	C4H9O7P	4	Erythrulose 1-phosphate	5	Carbohydrate Metabolism	KEGG_Metacyc	C03394	1.00	0.89	1.34	1.17	0.61	1	0.663347	0.431433	0.553328	0.306144
221.0899117	12.458	C8H15NO6	7	N-Acetyl-D-mannosamine	6	Carbohydrate Metabolism	KEGG_Metacyc_HMDB	C00645	1.00	1.18	1.21	1.18	0.57	1	0.363694	0.571467	0.455676	0.135775
230.0187896	24.9	C5H11O8P	16	**D-Ribose 5-phosphate**	10	Carbohydrate Metabolism	KEGG_Metacyc_HMDB	C00117	1.00	1.30	0.98	0.85	0.15	1	0.625922	0.966402	0.665774	0.103503
230.0191227	24.663	C5H11O8P	16	**D-Ribose 5-phosphate**	10	Carbohydrate Metabolism	KEGG_Metacyc_HMDB	C00117	1.00	1.22	0.95	0.70	0.15	1	0.752766	0.925627	0.483998	0.134018
260.0294049	25.255	C6H13O9P	46	**D-Fructose 6-phosphate**	10	Carbohydrate Metabolism	KEGG_Metacyc_HMDB	C00085	1.00	0.85	1.23	1.04	0.52	1	0.535691	0.510014	0.848026	0.190325
260.0294061	25.723	C6H13O9P	46	**D-Glucose 6-phosphate**	10	Carbohydrate Metabolism	KEGG_Metacyc_HMDB	C00092	1.00	0.86	1.25	1.18	0.55	1	0.618308	0.523993	0.55305	0.233539
260.0294387	26.577	C6H13O9P	46	D-Mannose 1-phosphate	6	Carbohydrate Metabolism	KEGG_Metacyc_HMDB	C00636	1.00	0.87	1.17	1.13	0.56	1	0.625255	0.623085	0.655989	0.224182
290.0400955	25.377	C7H15O10P	6	D-Sedoheptulose 7-phosphate	8	Carbohydrate Metabolis	KEGG_Metacyc	C05382	1.00	1.36	2.14	5.04	6.01	1	0.240439	0.306621	0.064381	0.135491

						m												
566.0538362	1.6692	C15H24N2O17P2	3	UDP-glucose	8	Carbohydrate Metabolism	KEGG_Metacyc_HMDB	C00029	1.00	1.51	0.86	0.43	1.42	1	0.509128	0.575176	0.390809	0.168314
75.06840155	10.706	C3H9NO	6	Trimethylamine N-oxide	7	Energy Metabolism	KEGG_Metacyc_HMDB	C01104	1.00	1.20	1.18	1.02	0.52	1	0.552274	0.657178	0.948813	0.250581
97.97673489	23.063	H3O4P	1	**Orthophosphate**	10	Energy Metabolism	KEGG_Metacyc_HMDB	C00009	1.00	0.95	0.96	0.93	1.42	1	0.652783	0.730895	0.542838	0.644291
97.97692148	23.974	H3O4P	1	**Orthophosphate**	8	Energy Metabolism	KEGG_Metacyc_HMDB	C00009	1.00	0.75	0.98	0.97	0.60	1	0.155198	0.918629	0.6711	0.139972
210.0738113	14.883	C7H14O7	4	Sedoheptulose	7	Energy Metabolism	KEGG_Metacyc_HMDB	C02076	1.00	1.14	1.49	2.43	2.15	1	0.36803	0.242563	0.135181	0.334786
331.5545142	22.116	C21H28N7O14P2	1	**NAD+**	10	Energy Metabolism	KEGG_Metacyc_HMDB	C00003	1.00	1.03	1.12	1.12	1.26	1	0.701147	0.140105	0.40709	0.622005
371.537434	35.009	C21H29N7O17P3	1	NADP+	8	Energy Metabolism	KEGG_Metacyc_HMDB	C00006	1.00	1.60	1.48	0.95	0.88	1	0.230438	0.362686	0.805544	0.464516
238.0688926	10.991	C8H14O8	1	3-Deoxy-D-manno-octulosonate	8	Glycan Biosynthesis and Metabolism	KEGG_Metacyc	C01187	1.00	0.90	1.01	0.81	0.86	1	0.763222	0.988527	0.55747	0.68747
104.0472933	6.6101	C4H8O3	13	(R)-3-Hydroxybutanoate	6	Lipid Metabolism	KEGG_Metacyc_Lipidmaps_HMDB	C01089	1.00	0.95	0.90	1.05	0.80	1	0.822558	0.438856	0.841109	0.157643
125.0144842	17.101	C2H7NO3S	1	Taurine	8	Lipid Metabolism	KEGG_Metacyc_HMDB	C00245	1.00	1.07	1.11	0.82	3.49	1	0.674996	0.501873	0.318364	0.497409

145.1101564	10.8116	C7H15NO2	6	Acetylcholine	8	Lipid Metabolism	KEGG_Metacyc_HMDB	C01996	1.00	1.23	1.13	1.20	0.41	1	0.698204	0.761688	0.69109	0.196857
155.03477	16.032	C3H10NO4P	3	N-Methylethanolamine phosphate	8	Lipid Metabolism	KEGG_Metacyc	C01210	1.00	1.02	1.15	1.02	0.56	1	0.699451	0.382032	0.832323	0.126413
157.0349275	15.74	C10H20O7P2	6	[PR] Geranyl pyrophosphate	8	Lipid Metabolism	KEGG_Metacyc_Lipidmaps_HMDB	C00341	1.00	1.02	1.08	0.98	**0.46**	1	0.761551	0.561866	0.847465	0.013938
169.0502829	20.532	C4H12NO4P	1	Phosphodimethylethanolamine	6	Lipid Metabolism	KEGG_Metacyc	C13482	1.00	0.72	0.89	0.73	0.47	1	0.26643	0.661699	0.271459	0.098246
172.013379	24.073	C3H9O6P	3	**sn-Glycerol 3-phosphate**	10	Lipid Metabolism	KEGG_Metacyc_HMDB	C00093	1.00	0.72	0.96	0.89	0.41	1	0.123612	0.836163	0.221332	0.105165
183.0661188	23.152	C5H14NO4P	1	**Choline phosphate**	10	Lipid Metabolism	KEGG_Metacyc_HMDB	C00588	1.00	0.68	1.20	1.05	0.52	1	0.40532	0.644749	0.894764	0.186811
215.0556647	18.688	C5H14NO6P	1	sn-glycero-3-Phosphoethanolamine	8	Lipid Metabolism	KEGG_Metacyc_HMDB	C01233	1.00	0.80	1.13	1.02	0.86	1	0.494138	0.554227	0.938379	0.790859
244.0536445	24.73	C14H26N4O11P2	1	CDP-choline	8	Lipid Metabolism	KEGG_Metacyc_HMDB	C00307	1.00	**1.98**	2.07	1.46	1.03	1	0.02547	0.062135	0.256781	0.942611
254.224439	5.1859	C16H30O2	19	(9Z)-Hexadecenoic acid	8	Lipid Metabolism	KEGG_Lipidmaps_HMDB	C08362	1.00	1.25	**0.67**	1.15	1.26	1	0.349256		0.558452	0.652708
257.1029335	20.69	C8H20NO6P	1	**sn-glycero-3-Phosphocholine**	10	Lipid Metabolism	KEGG_Metacyc_HMDB	C00670	1.00	0.89	0.81	1.10	**0.31**	1	0.630889	0.249187	0.718823	0.022042
400.3340084	5.181	C27H44O2	35	7alpha-Hydroxycholest-4-en-3-one	8	Lipid Metabolism	KEGG_Metacyc_Lipidmaps_HMDB	C05455	1.00	1.03	0.84	1.14	0.60	1	0.961055	0.763038	0.831479	0.462567
449.3140325	5.6096	C26H43NO5	6	Glycodeoxycholate	7	Lipid Metabolism	KEGG_Metacyc_HMDB	C05464	1.00	1.17	1.15	0.97	0.73	1	0.439951	0.585418	0.874929	0.233325

472.1123978	24.169	C14H27N4O10P2	1	CMP-N-trimethyl-2-aminoethylphosphonate	5	Lipid Metabolism	KEGG	C05674	1.00	0.95	1.23	0.96	0.73	1	0.785325	0.581692	0.711936	0.308727
102.0679991	6.231	C5H10O2	5	Pentanoate	5	Lipids: Fatty Acyls	KEGG_Metacyc_Lipidmaps_HMDB	C00803	1.00	1.77	1.37	0.85	0.57	1	0.300613	0.406168	0.362641	0.476977
102.068014	6.5289	C5H10O2	5	3-Methylbutanoic acid	5	Lipids: Fatty Acyls	KEGG_Metacyc_Lipidmaps_HMDB	C08262	1.00	0.65	0.76	0.67	0.56	1	0.265576	0.371014	0.26394	0.170685
116.0837259	5.3602	C6H12O2	16	Hexanoic acid	5	Lipids: Fatty Acyls	KEGG_Metacyc_Lipidmaps_HMDB	C01585	1.00	0.74	1.09	0.77	0.85	1	0.337825	0.324316	0.366897	0.584676
118.0629005	6.1219	C5H10O3	12	5-Hydroxypentanoate	7	Lipids: Fatty Acyls	KEGG_Metacyc_Lipidmaps	C02804	1.00	0.88	0.82	1.03	0.89	1	0.671799	0.512058	0.902602	0.790339
132.0420156	6.3802	C5H8O4	16	Glutarate	6	Lipids: Fatty Acyls	KEGG_Metacyc_Lipidmaps_HMDB	C00489	1.00	0.88	0.87	1.09	0.85	1	0.722758	0.655646	0.77917	0.609837
146.0573895	6.2233	C6H10O4	16	Adipate	8	Lipids: Fatty Acyls	KEGG_Metacyc_Lipidmaps_HMDB	C06104	1.00	0.85	0.71	0.96	0.50	1	0.710116	0.455931	0.915329	0.24786
148.0733023	7.6208	C6H12O4	14	[FA methyl,hydroxy(5:0)] 3R-methyl-3,5-dihydroxy-pentanoic acid	8	Lipids: Fatty Acyls	KEGG_Metacyc_Lipidmaps_HMDB	C00418	1.00	1.19	1.08	0.91	2.32	1	0.720434	0.827222	0.794914	0.503826
160.0730941	5.8548	C7H12O4	4	[FA (7:0/2:0)] Heptanedioic acid	8	Lipids: Fatty Acyls	KEGG_Metacyc_Lipidmaps_HMDB	C02656	1.00	1.06	0.96	1.05	0.95	1	0.794477	0.805116	0.820758	0.925327
174.0887057	5.6392	C8H14O4	3	Suberic acid	7	Lipids: Fatty Acyls	KEGG_Metacyc_Lipidmaps_HMDB	C08278	1.00	1.03	0.82	1.08	0.72	1	0.92318	0.432479	0.888289	0.248245
202.1202786	5.4619	C10H18O4	2	[FA (10:0/2:0)] Decanedioic acid	7	Lipids: Fatty Acyls	KEGG_Metacyc_Lipidmaps_HMDB	C08277	1.00	1.08	0.86	0.84	0.53	1	0.843558	0.588361	0.698207	0.139939
216.1726041	5.2652	C12H24O3	11	12-Hydroxydodecanoic acid	5	Lipids: Fatty Acyls	KEGG_Metacyc_Lipidmaps_HMDB	C08317	1.00	3.75	1.08	2.91	0.40	1	0.514836	0.934236	0.082992	0.297678

217.1314263	8.4132	C10H19NO4	1	O-Propanoylcarnitine	7	Lipids: Fatty Acyls	KEGG_Lipidmaps_HMDB	C03017	1.00	0.89	0.99	1.07	0.65	1	0.642312	0.974457	0.81381	0.209235
222.0890082	5.3393	C12H14O4	8	[FA (12:4/2:0)] 2E,4E,8E,10E-Dodecatetraenedioic acid	7	Lipids: Fatty Acyls	Lipidmaps	0	1.00	0.97	0.75	0.96	0.52	1	0.943756	0.439224	0.873993	0.17728
231.1470116	8.0076	C11H21NO4	3	O-Butanoylcarnitine	7	Lipids: Fatty Acyls	KEGG_Lipidmaps_HMDB	C02862	1.00	1.01	1.25	1.03	1.13	1	0.977337	0.624623	0.905247	0.714038
281.271819	7.5436	C18H35NO	1	[FA (18:1)] 9Z-octadecenamide	7	Lipids: Fatty Acyls	Metacyc_Lipidmaps_HMDB	0	1.00	0.87	1.42	1.14	0.86	1	0.25547	0.186435	0.28417	0.228666
290.1882148	5.1827	C18H26O3	6	[FA hydroxy(18:1/2:0)] 8-hydroxy-13Z-octadecene-9,11-diynoic acid	7	Lipids: Fatty Acyls	Lipidmaps	0	1.00	1.12	1.17	1.45	4.25	1	0.811139	0.778915	0.430677	0.56866
298.2508203	5.1576	C18H34O3	46	2-Oxooctadecanoic acid	5	Lipids: Fatty Acyls	KEGG_Metacyc_Lipidmaps	C00869	1.00	1.36	1.01	0.85	0.95	1	0.316023	0.967658	0.269272	0.850494
300.2662744	5.1667	C18H36O3	27	[FA hydroxy(18:0)] 2S-hydroxy-octadecanoic acid	5	Lipids: Fatty Acyls	KEGG_Metacyc_Lipidmaps	C03045	1.00	1.08	0.87	1.42	0.84	1	0.82999	0.564035	0.211043	0.583054
316.2613015	5.2454	C18H36O4	19	[FA hydroxy(18:0)] 9,10-dihydroxy-octadecanoic acid	5	Lipids: Fatty Acyls	Metacyc_Lipidmaps	0	1.00	1.57	0.82	1.09	0.82	1	0.563171	0.568678	0.762721	0.578084
342.3133048	5.1973	C21H42O3	6	[FA hydroxy(21:0)] 21-hydroxy-heneicosanoic acid	5	Lipids: Fatty Acyls	Lipidmaps	0	1.00	0.81	1.22	1.18	0.57	1	0.593139	0.530038	0.569233	0.239135
354.2767186	5.0584	C21H38O4	5	[FA methoxy,trihydrox] 1-methoxy-9S,11R,15S-trihydroxy-5Z,13E-prostadiene	5	Lipids: Fatty Acyls	Lipidmaps	0	1.00	0.73	1.74	0.71	1.06	1	0.300106	0.159238	0.384484	0.919149
370.3081784	5.0535	C22H42O4	3	2-monooleoylglycerol	7	Lipids: Glycerolipids	Metacyc_HMDB	0	1.00	1.14	1.70	2.18	0.74	1	0.772698	0.209961	0.288736	0.626306
465.3216509	6.0962	C23H48NO6P	3	[PE (18:1)] 1-(9Z-octadecenyl)-sn-glycero-3-phosphoethanolamine	7	Lipids: Glycerophospholipids	Lipidmaps	0	1.00	0.76	0.96	1.27	0.55	1	0.600366	0.920622	0.496126	0.279504

465.3216902	7.6259	C23H48NO6P	3	[PC (15:1)] 1-(1Z-pentadecenyl)-sn-glycero-3-phosphocholine	5	Lipids: Glycerophospholipids	Lipidmaps	0	1.00	0.72	0.94	1.04	0.22	1	0.573511	0.887913	0.925319	0.154969
465.3217736	10.439	C23H48NO6P	3	[PE (18:1)] 1-(1Z-octadecenyl)-sn-glycero-3-phosphoethanolamine	3	Lipids: Glycerophospholipids	Lipidmaps	0	1.00	1.17	1.04	0.79	0.58	1	0.677678	0.923524	0.613402	0.406451
477.2852667	6.1053	C23H44NO7P	2	LysoPE(0:0/18:2(9Z,12Z))	5	Lipids: Glycerophospholipids	HMDB	0	1.00	1.43	1.21	1.53	1.16	1	0.412269	0.523133	0.278695	0.549135
479.3374523	10.263	C24H50NO6P	5	[PC (16:1)] 1-(1Z-hexadecenyl)-sn-glycero-3-phosphocholine	7	Lipids: Glycerophospholipids	KEGG_Lipidmaps_HMDB	C04230	1.00	1.15	1.16	0.86	0.47	1	0.769615	0.809992	0.749306	0.302416
493.316589	10.453	C24H48NO7P	3	[PC (16:0)] 1-(9Z-hexadecenoyl)-sn-glycero-3-phosphocholine	5	Lipids: Glycerophospholipids	Metacyc_Lipidmaps	0	1.00	1.25	1.28	0.93	0.14	1	0.666642	0.553686	0.87234	0.092238
493.3529031	6.1038	C25H52NO6P	1	[PC (17:1)] 1-(1Z-heptadecenyl)-sn-glycero-3-phosphocholine	5	Lipids: Glycerophospholipids	Lipidmaps	0	1.00	0.86	1.02	1.00	0.96	1	0.40311	0.721001	0.986906	0.937058
493.3529632	10.144	C25H52NO6P	1	[PC (17:1)] 1-(1Z-heptadecenyl)-sn-glycero-3-phosphocholine	7	Lipids: Glycerophospholipids	Lipidmaps	0	1.00	0.86	1.28	0.95	0.52	1	0.739594	0.632647	0.882471	0.234662
495.3322661	10.352	C24H50NO7P	5	[PC (16:0)] 1-hexadecanoyl-sn-glycero-3-phosphocholine	7	Lipids: Glycerophospholipids	KEGG_Lipidmaps_HMDB	C04230	1.00	1.14	0.97	1.82	0.25	1	0.848007	0.95346	0.298474	0.160232
507.3685676	6.1938	C26H54NO6P	6	[PC (18:1)] 3-(9E-octadecenyl)-sn-glycero-1-phosphocholine	5	Lipids: Glycerophospholipids	Lipidmaps	0	1.00	0.62	0.92	1.13	0.42	1	0.20721	0.810358	0.737753	0.111192

507.3687814	9.90009	C26H54NO6P	6	[PC (18:1)] 1-(11Z-octadecenyl)-sn-glycero-3-phosphocholine	5	Lipids: Glycerophospholipids	Lipidmaps	0	1.00	0.98	1.33	1.07	0.85	1	0.960415	0.483594	0.825822	0.703256
509.3477356	10.216	C25H52NO7P	8	LysoPC(17:0)	7	Lipids: Glycerophospholipids	KEGG_HMDB	C04230	1.00	0.97	0.91	1.39	0.33	1	0.961503	0.898331	0.483528	0.159313
509.384499	10.3398	C26H56NO6P	8	LysoPC(O-18:0)	7	Lipids: Glycerophospholipids	KEGG_HMDB	C04317	1.00	0.82	0.88	1.17	0.80	1	0.588623	0.689805	0.603072	0.535622
519.3323177	10.255	C26H50NO7P	3	[PC (18:2)] 1-(9Z,12Z-octadecadienoyl)-sn-glycero-3-phosphocholine	5	Lipids: Glycerophospholipids	KEGG_Lipidmaps_HMDB	C04230	1.00	1.32	1.09	1.42	0.15	1	0.547197	0.787519	0.39824	0.08464
521.3482982	6.2306	C26H52NO7P	11	LysoPC(18:1(9Z))	5	Lipids: Glycerophospholipids	KEGG_HMDB	C04230	1.00	0.90	1.06	1.09	0.30	1	0.744423	0.881478	0.752691	0.059741
523.3636768	6.2162	C26H54NO7P	9	LysoPC(18:0)	7	Lipids: Glycerophospholipids	KEGG_HMDB	C04230	1.00	0.90	1.39	1.19	**0.40**	1	0.812268	0.72656	0.62707	
523.3637702	10.087	C26H54NO7P	9	[PC (18:0)] 1-octadecanoyl-sn-glycero-3-phosphocholine	5	Lipids: Glycerophospholipids	Metacyc_Lipidmaps	0	1.00	0.86	0.72	1.46	0.41	1	0.784217	0.558458	0.415952	0.24111
535.3999381	9.7609	C28H58NO6P	1	[PC (18:2)] 1-octadecyl-2-(1E-ethenyl)-sn-glycero-3-phosphocholine	5	Lipids: Glycerophospholipids	Lipidmaps	0	1.00	0.93	1.72	1.09	0.79	1	0.68649	0.261438	0.644806	0.534804
537.4157468	10.184	C28H60NO6P	7	[PC (10:2/10:2)] 1-decyl-2-decyl-sn-glycero-3-phosphocholine	5	Lipids: Glycerophospholipids	Lipidmaps	0	1.00	0.99	1.10	1.08	0.81	1	0.935816	0.579824	0.631981	0.704313

565.4470169	9.9738	C30H64NO6P	4	[PC (10:2/12:2)] 1-decyl-2-dodecyl-sn-glycero-3-phosphocholine	7	Lipids: Glycerophospholipids	Lipidmaps	0	1.00	0.99	1.43	0.93	**2.43**	1	0.979025	0.535447	0.869882	0.036569
567.3322247	6.1898	C30H50NO7P	2	[PC (22:6)] 1-(4E,7E,10E,13E,16E,19E-docosahexaenoyl)-sn-glycero-3-phosphocholine	5	Lipids: Glycerophospholipids	Lipidmaps	0	1.00	1.07	1.08	0.86	0.38	1	0.916177	0.845337	0.664122	0.143354
567.3324132	9.961	C30H50NO7P	2	[PC (22:6)] 1-(4Z,7Z,10Z,13Z,16Z,19Z-docosahexaenoyl)-sn-glycero-3-phosphocholine	5	Lipids: Glycerophospholipids	KEGG_Lipidmaps_HMDB	C04230	1.00	1.45	1.10	1.03	0.33	1	0.493973	0.76002	0.93983	0.138942
569.3481185	6.18	C30H52NO7P	2	LysoPC(22:5(7Z,10Z,13Z,16Z,19Z))	5	Lipids: Glycerophospholipids	KEGG_HMDB	C04230	1.00	1.24	1.20	1.01	0.42	1	0.623234	0.512841	0.972748	0.098071
569.3483693	9.8645	C30H52NO7P	2	LysoPC(22:5(4Z,7Z,10Z,13Z,16Z))	7	Lipids: Glycerophospholipids	KEGG_HMDB	C04230	1.00	1.29	1.15	1.04	0.37	1	0.535227	0.666664	0.916813	0.132337
571.3636937	6.1722	C30H54NO7P	1	LysoPC(22:4(7Z,10Z,13Z,16Z))	5	Lipids: Glycerophospholipids	KEGG_HMDB	C04230	1.00	1.18	1.18	0.95	**0.86**	1	0.617234	0.577612	0.852763	
571.3640486	9.8354	C30H54NO7P	1	LysoPC(22:4(7Z,10Z,13Z,16Z))	5	Lipids: Glycerophospholipids	KEGG_HMDB	C04230	1.00	1.30	1.60	1.10	0.40	1	0.393849	0.207352	0.779071	0.056892
675.5209773	5.8444	C37H74NO7P	4	PE(14:0/P-18:0)	5	Lipids: Glycerophospholipids	KEGG_HMDB	C00350	1.00	1.33	**1.72**	**0.30**	0.71	1	0.37007			0.305268
687.520892	5.8351	C38H74NO7P	7	PC(14:1(9Z)/P-16:0)	5	Lipids: Glycerophospholipids	KEGG_HMDB	C00157	1.00	1.03	1.28	0.42	0.97	1	0.939691	0.709228	0.058409	0.917188

699.5203472	5.7549	C39H74NO7P	6	PE(16:1(9Z)/P-18:1(11Z))	5	Lipids: Glycerophospholipids	KEGG_HMDB	C00350	1.00	1.29	1.88	0.58	2.08	1	0.708382	0.484298	0.46822	0.160306
701.5364684	5.7845	C39H76NO7P	11	PE(16:0/P-18:1(11Z))	5	Lipids: Glycerophospholipids	KEGG_HMDB	C00350	1.00	1.04	1.37	0.30	1.27	1	0.960761	0.70532	0.294341	0.698427
713.5002379	5.7968	C39H72NO8P	12	[PE (16:0/18:3)] 1-hexadecanoyl-2-(9Z,12Z,15Z-octadecatrienoyl)-sn-glycero-3-phosphoethanolamine	5	Lipids: Glycerophospholipids	KEGG_Metacyc_Lipidmaps_HMDB	C00350	1.00	1.50	1.13	0.66	0.64	1	0.348561	0.696256	0.322782	0.341303
713.5361507	5.7432	C40H76NO7P	5	PC(14:1(9Z)/P-18:1(11Z))	5	Lipids: Glycerophospholipids	KEGG_HMDB	C00157	1.00	1.29	1.98	0.37	1.94	1	0.716966	0.479839	0.311083	0.245059
715.5155781	5.7944	C39H74NO8P	11	[PE (16:0/18:2)] 1-hexadecanoyl-2-(9Z,12Z-octadecadienoyl)-sn-glycero-3-phosphoethanolamine	5	Lipids: Glycerophospholipids	KEGG_Metacyc_Lipidmaps_HMDB	C00350	1.00	1.25	1.06	0.54	0.68	1	0.764748	0.932047	0.455335	0.577775
715.5517449	5.8853	C40H78NO7P	12	PC(14:0/P-18:1(11Z))	5	Lipids: Glycerophospholipids	KEGG_HMDB	C00157	1.00	1.08	1.41	0.47	1.32	1	0.903997	0.658292	0.368857	0.640894
717.5315514	5.8166	C39H76NO8P	17	[PE (16:0/18:1)] 1-Hexadecanoyl-2-(9Z-octadecenoyl)-sn-glycero-3-phosphoethanolamine	7	Lipids: Glycerophospholipids	KEGG_Metacyc_Lipidmaps_HMDB	C13877	1.00	1.21	0.76	0.26	0.49	1	0.783825	0.694345	0.245936	0.377113
717.5317166	7.7645	C39H76NO8P	17	[PE (16:0/18:1)] 1-hexadecanoyl-2-(11Z-octadecenoyl)-sn-glycero-3-phosphoethanolamine	5	Lipids: Glycerophospholipids	KEGG_Lipidmaps_HMDB	C00350	1.00	1.38	1.42	0.75	**0.13**	1	0.440851	0.440664	0.589252	

725.5360304	5.723	C41H76NO7P	13	PE(18:2(9Z,12Z)/P-18:1(11Z))	5	Lipids: Glycerophospholipids	KEGG_HMDB	C00350	1.00	1.36	1.74	0.50	1.65	1	0.663139	0.490034	0.4115	0.353989
727.5514799	5.751	C41H78NO7P	12	PE(18:1(11Z)/P-18:1(11Z))	7	Lipids: Glycerophospholipids	KEGG_HMDB	C00350	1.00	1.50	1.84	0.35	2.12	1	0.545492	0.464748	0.284731	0.121592
727.551843	7.627	C41H78NO7P	12	PE(18:1(11Z)/P-18:1(9Z))	7	Lipids: Glycerophospholipids	KEGG_HMDB	C00350	1.00	2.68	1.12	**2.80**	1.23	1	0.433895	0.653015	0.003583	0.60104
729.5314783	7.7851	C40H76NO8P	14	[PC (14:0/18:2)] 1-tetradecanoyl-2-(9Z,12Z-octadecadienoyl)-sn-glycero-3-phosphocholine	7	Lipids: Glycerophospholipids	KEGG_Lipidmaps_HMDB	C00157	1.00	1.19	1.36	0.62	0.41	1	0.786365	0.641939	0.516704	0.36279
729.5672056	5.903	C41H80NO7P	14	[PE (18:1/18:1)] 1-(1Z-octadecenyl)-2-(9Z-octadecenoyl)-sn-glycero-3-phosphoethanolamine	5	Lipids: Glycerophospholipids	Lipidmaps_HMDB	0	1.00	1.28	1.08	0.63	2.22	1	0.639784	0.911817	0.534774	0.107102
729.5675597	7.6423	C41H80NO7P	14	PC(15:0/P-18:1(11Z))	5	Lipids: Glycerophospholipids	KEGG_HMDB	C00157	1.00	2.22	0.78	1.99	1.13	1	0.490959	0.659934	0.135642	0.866352
731.5472838	7.7677	C40H78NO8P	14	[PC (14:0/18:1)] 1-tetradecanoyl-2-(11Z-octadecenoyl)-sn-glycero-3-phosphocholine	5	Lipids: Glycerophospholipids	KEGG_Lipidmaps_HMDB	C00157	1.00	1.02	1.32	0.59	0.34	1	0.95735	0.554693	0.364091	0.194978
731.5474698	6.1462	C40H78NO8P	14	[PC (14:0/18:1)] 1-tetradecanoyl-2-(9Z-octadecenoyl)-sn-glycero-3-phosphocholine	5	Lipids: Glycerophospholipids	KEGG_Lipidmaps_HMDB	C00157	1.00	0.95	1.11	0.60	**0.37**	1	0.907574	0.81434	0.296596	

733.5627549	7.7816	C40H80NO8P	24	[PC (16:0/16:0)] 1-hexadecanoyl-2-hexadecanoyl-sn-glycero-3-phosphocholine	7	Lipids: Glycerophospholipids	KEGG_Metacyc_Lipidmaps_HMDB	C00157	1.00	0.84	0.86	1.00	0.89	1	0.795191	0.811438	0.995203	0.882181
739.5145629	5.7514	C41H74NO8P	24	[PE (16:0/20:4)] 1-hexadecanoyl-2-(5Z,8Z,11Z,14Z-eicosatetraenoyl)-sn-glycero-3-phosphoethanolamine	7	Lipids: Glycerophospholipids	KEGG_Lipidmaps_HMDB	C00350	1.00	1.15	1.23	0.88	1.31	1	0.801922	0.70974	0.812394	0.529654
741.530292	5.7556	C41H76NO8P	20	[PE (18:1/18:2)] 1-(9Z-octadecenoyl)-2-(9Z,12Z-octadecadienoyl)-sn-glycero-3-phosphoethanolamine	5	Lipids: Glycerophospholipids	KEGG_Metacyc_Lipidmaps_HMDB	C00350	1.00	1.16	1.10	0.58	1.32	1	0.822046	0.892727	0.445088	0.674388
741.567093	6.1332	C42H80NO7P	10	PC(16:1(9Z)/P-18:1(11Z))	5	Lipids: Glycerophospholipids	KEGG_HMDB	C00157	1.00	1.00	1.20	0.92	1.67	1	0.996647	0.755854	0.884887	0.295038
741.5675547	7.6799	C42H80NO7P	10	[PC (16:1/18:2)] 1-(1Z-hexadecenyl)-2-(9Z,12Z-octadecadienoyl)-sn-glycero-3-phosphocholine	5	Lipids: Glycerophospholipids	Lipidmaps_HMDB	0	1.00	0.99	1.36	1.43	1.45	1	0.977539	0.344776	0.271805	0.335114
741.5677049	5.8071	C42H80NO7P	10	[PC (16:1/18:2)] 1-(1Z-hexadecenyl)-2-(9Z,12Z-octadecadienoyl)-sn-glycero-3-phosphocholine	5	Lipids: Glycerophospholipids	Lipidmaps_HMDB	0	1.00	1.47	1.14	0.61	2.27	1	0.400313	0.83576	0.477934	0.0832
743.5459829	5.7773	C41H78NO8P	18	[PE (18:0/18:2)] 1-octadecanoyl-2-(9Z,12Z-octadecadienoyl)-sn-glycero-3-phosphoethanolamine	5	Lipids: Glycerophospholipids	KEGG_Metacyc_Lipidmaps_HMDB	C00350	1.00	1.04	1.06	0.30	1.55	1	0.950691	0.921158	0.157188	0.34387
743.583105	6.1461	C42H82NO7P	14	[PC (16:2/18:2)] 1-hexadecyl-2-(9Z,12Z-octadecadienoyl)-sn-glycero-3-	5	Lipids: Glycerophospholipids	Lipidmaps_HMDB	0	1.00	0.90	0.89	0.64	0.84	1	0.886692	0.865994	0.558777	0.783958

				phosphocholine															
743.5831677	7.7486	C42H82NO7P	14	1-Hexadecanoyl-2-(9Z-octadecenoyl)-sn-glycero-3-phosphonocholine	5	Lipids: Glycerophospholipids	KEGG_Lipidmaps	C13876	1.00	1.02	1.28	1.02	0.89	1	0.972995	0.639141	0.974498	0.836425
748.5040202	7.3816	C43H73O8P	1	[GP (18:0/22:6)] 1-octadecanoyl-2-(4Z,7Z,10Z,13Z,16Z,19Z-docosahexaenoyl)-sn-glycero-3-phosphate	7	Lipids: Glycerophospholipids	Lipidmaps	0	1.00	0.63	1.31	**0.38**	0.39	1	0.277702	0.352688		0.135095
753.5665513	5.6986	C43H80NO7P	9	PE(20:2(11Z,14Z)/P-18:1(11Z))	5	Lipids: Glycerophospholipids	KEGG_HMDB	C00350	1.00	1.52	2.00	0.20	1.63	1	0.569283	0.439318	0.233636	0.402815
753.5670452	7.6906	C43H80NO7P	9	PE(20:2(11Z,14Z)/P-18:1(9Z))	5	Lipids: Glycerophospholipids	KEGG_HMDB	C00350	1.00	0.96	1.29	1.40	1.44	1	0.802771	0.455939	0.106835	0.516945
755.5469348	6.1302	C42H78NO8P	17	[PC (16:0/18:3)] 1-hexadecanoyl-2-(6Z,9Z,12Z-octadecatrienoyl)-sn-glycero-3-phosphocholine	5	Lipids: Glycerophospholipids	KEGG_Lipidmaps_HMDB	C00157	1.00	1.12	1.34	0.55	0.35	1	0.76654	0.416217	0.171392	0.083896
755.5470789	7.7269	C42H78NO8P	17	[PC (16:0/18:3)] 1-hexadecanoyl-2-(9Z,12Z,15Z-octadecatrienoyl)-sn-glycero-3-phosphocholine	5	Lipids: Glycerophospholipids	KEGG_Metacyc_Lipidmaps_HMDB	C00157	1.00	1.11	1.58	0.65	**0.38**	1	0.583187	0.058521	0.133192	0.044706
755.5823832	6.0967	C43H82NO7P	8	PE(20:1(11Z)/P-18:1(9Z))	5	Lipids: Glycerophospholipids	KEGG_HMDB	C00350	1.00	1.06	1.32	0.78	2.20	1	0.930856	0.72741	0.723094	0.148369

755.5827978	7.6537	C43H82NO7P	8	PE(20:1(11Z)/P-18:1(11Z))	5	Lipids: Glycerophospholipids	KEGG_HMDB	C00350	1.00	1.00	1.42	1.52	1.52	1	0.999265	0.450754	0.294476	0.468988
757.5624392	6.1389	C42H80NO8P	34	[PC (16:1/18:1)] 1-(9Z-hexadecenoyl)-2-(11Z-octadecenoyl)-sn-glycero-3-phosphocholine	5	Lipids: Glycerophospholipids	KEGG_Lipidmaps_HMDB	C00157	1.00	0.94	0.96	0.76	0.49	1	0.898856	0.922833	0.54551	0.228386
757.5626985	7.7231	C42H80NO8P	34	[PC (16:0/18:2)] 1-hexadecanoyl-2-(9Z,12Z-octadecadienoyl)-sn-glycero-3-phosphocholine	7	Lipids: Glycerophospholipids	KEGG_Metacyc_Lipidmaps_HMDB	C00157	1.00	0.89	1.16	0.95	0.43	1	0.762903	0.640092	0.870276	0.156968
759.5778148	7.7309	C42H82NO8P	20	[PC (16:0/18:1)] 1-hexadecanoyl-2-(11Z-octadecenoyl)-sn-glycero-3-phosphocholine	5	Lipids: Glycerophospholipids	KEGG_Lipidmaps_HMDB	C00157	1.00	0.89	1.02	0.73	0.39	1	0.773688	0.958933	0.510667	0.19313
759.5782113	6.1709	C42H82NO8P	20	[PC (16:0/18:1)] 1-hexadecanoyl-2-(9Z-octadecenoyl)-sn-glycero-3-phosphocholine	5	Lipids: Glycerophospholipids	KEGG_Metacyc_Lipidmaps_HMDB	C13875	1.00	0.91	0.95	0.47	0.55	1	0.896864	0.941919	0.388608	0.438446
763.5157444	5.678	C43H74NO8P	24	[PE (16:0/22:6)] 1-hexadecanoyl-2-(4Z,7Z,10Z,13Z,16Z,19Z-docosahexaenoyl)-sn-glycero-3-phosphoethanolamine	7	Lipids: Glycerophospholipids	KEGG_Lipidmaps_HMDB	C00350	1.00	1.08	0.68	0.94	0.60	1	0.850875	0.392047	0.866401	0.321093
767.5461738	5.8208	C43H78NO8P	31	[PE (18:0/20:4)] 1-octadecanoyl-2-(5Z,8Z,11Z,14Z-eicosatetraenoyl)-sn-glycero-3-phosphoethanolamine	5	Lipids: Glycerophospholipids	KEGG_Lipidmaps_HMDB	C00350	1.00	1.31	1.17	0.54	1.00	1	0.49179	0.72373	0.153695	0.99517

769.5631 18	7.7096	C43H80NO8P	21	PC(15:0/20:3(5Z,8Z,11Z))	5	Lipids: Glycerophospholipids	KEGG_HMDB	C00157	1.00	0.99	1.38	**0.65**	0.73	1	0.910785	0.054118	0.040403	0.687211
769.5983398	6.1504	C44H84NO7P	15	PC(18:1(11Z)/P-18:1(9Z))	7	Lipids: Glycerophospholipids	KEGG_HMDB	C00157	1.00	1.05	1.27	0.47	1.82	1	0.949527	0.756409	0.407539	0.410319
769.5986	7.6503	C44H84NO7P	15	PC(18:1(11Z)/P-18:1(11Z))	7	Lipids: Glycerophospholipids	KEGG_HMDB	C00157	1.00	1.02	1.29	1.14	1.42	1	0.955436	0.574094	0.664324	0.565256
771.5772102	5.8094	C43H82NO8P	24	[PE (18:0/20:2)] 1-octadecanoyl-2-(11Z,14Z-eicosadienoyl)-sn-glycero-3-phosphoethanolamine	7	Lipids: Glycerophospholipids	KEGG_Lipidmaps_HMDB	C00350	1.00	2.02	1.63	0.50	1.00	1	0.148647	0.465494	0.311206	0.996248
771.6138384	7.7095	C44H86NO7P	12	[PC (18:1/18:0)] 1-(1Z-octadecenyl)-2-(9Z-octadecenoyl)-sn-glycero-3-phosphocholine	7	Lipids: Glycerophospholipids	Lipidmaps_HMDB	0	1.00	0.97	1.08	0.85	1.12	1	0.945912	0.869413	0.751288	0.839541
774.5389351	7.9109	C42H79O10P	9	[PG (18:1/18:1)] 1,2-di-(9Z-octadecenoyl)-sn-glycero-3-phospho-(1'-sn-glycerol)	7	Lipids: Glycerophospholipids	Lipidmaps	0	1.00	0.74	1.07	0.55	1.48	1	0.468637	0.867148	0.244466	0.649225
781.5620179	7.688	C44H80NO8P	39	[PC (16:0/20:4)] 1-hexadecanoyl-2-(5Z,8Z,11Z,14Z-eicosatetraenoyl)-sn-glycero-3-phosphocholine	5	Lipids: Glycerophospholipids	KEGG_Lipidmaps_HMDB	C00157	1.00	0.97	1.20	1.00	0.73	1	0.817366	0.220329	0.98467	0.207645
783.5772752	7.6917	C44H82NO8P	21	PC(18:2(9Z,12Z)/18:1(9Z))	5	Lipids: Glycerophospholipids	KEGG_Metacyc_HMDB	C00157	1.00	0.85	1.13	0.88	0.76	1	0.474838	0.494027	0.539758	0.532552

783.5774551	6.1351	C44H82NO8P	21	[PC (18:1/18:2)] 1-(9Z-octadecenoyl)-2-(9Z,12Z-octadecadienoyl)-sn-glycero-3-phosphocholine	5	Lipids: Glycerophospholipids	KEGG_Lipidmaps_HMDB	C00157	1.00	0.91	1.01	0.65	0.75	1	0.850849	0.988675	0.413735	0.552948
785.5928932	7.7008	C44H84NO8P	54	[PC (18:1/18:1)] 1-(9Z-octadecenoyl)-2-(9Z-octadecenoyl)-sn-glycero-3-phosphocholine	5	Lipids: Glycerophospholipids	KEGG_Metacyc_Lipidmaps_HMDB	C00157	1.00	0.96	1.14	0.85	0.73	1	0.929112	0.781592	0.732145	0.554814
785.5932399	6.1355	C44H84NO8P	54	[PC (18:0/18:2)] 1-octadecanoyl-2-(9Z,12Z-octadecadienoyl)-sn-glycero-3-phosphocholine	5	Lipids: Glycerophospholipids	KEGG_Metacyc_Lipidmaps_HMDB	C00157	1.00	1.02	1.10	0.46	0.91	1	0.979424	0.875217	0.327513	0.858334
787.5156451	5.6446	C45H74NO8P	21	PE(18:2(9Z,12Z)/22:6(4Z,7Z,10Z,13Z,16Z,19Z))	5	Lipids: Glycerophospholipids	KEGG_HMDB	C00350	1.00	1.15	0.89	0.85	1.17	1	0.712987	0.733206	0.681455	0.641059
787.5353795	7.963	C42H78NO10P	8	[PS (18:1/18:1)] 1,2-di-(9E-octadecenoyl)-sn-glycero-3-phosphoserine	7	Lipids: Glycerophospholipids	Lipidmaps	0	1.00	1.04	1.21	0.66	1.11	1	0.927984	0.608757	0.33885	0.814101
787.6076899	7.6987	C44H86NO8P	24	[PC (18:0/18:1)] 1-octadecanoyl-2-(9Z-octadecenoyl)-sn-glycero-3-phosphocholine	5	Lipids: Glycerophospholipids	KEGG_Metacyc_Lipidmaps_HMDB	C00157	1.00	0.91	0.91	0.65	0.54	1	0.869616	0.862159	0.491487	0.382077
789.5306927	5.6622	C45H76NO8P	22	PE(18:1(11Z)/22:6(4Z,7Z,10Z,13Z,16Z,19Z))	7	Lipids: Glycerophospholipids	KEGG_HMDB	C00350	1.00	1.44	1.37	0.75	1.52	1	0.568791	0.634063	0.647855	0.474564
791.5465577	6.1142	C45H78NO8P	26	[PE (18:0/22:6)] 1-octadecanoyl-2-(4Z,7Z,10Z,13Z,16Z,19Z-docosahexaenoyl)-sn-glycero-3-phosphoethanolamine	5	Lipids: Glycerophospholipids	KEGG_Lipidmaps_HMDB	C00350	1.00	1.23	1.35	0.82	0.56	1	0.586506	0.468371	0.583133	0.206393

791.5470351	5.6548	C45H78NO8P	26	[PE (18:0/22:6)] 1-octadecanoyl-2-(4Z,7Z,10Z,13Z,16Z,19Z-docosahexaenoyl)-sn-glycero-3-phosphoethanolamine	5	Lipids: Glycerophospholipids	KEGG_Lipidmaps_HMDB	C00350	1.00	1.09	0.80	0.41	1.18	1	0.88408	0.718262	0.285534	0.712298
793.5614833	7.6522	C45H80NO8P	28	PC(15:0/22:5(4Z,7Z,10Z,13Z,16Z))	5	Lipids: Glycerophospholipids	KEGG_HMDB	C00157	1.00	1.04	1.16	0.84	**0.44**	1	0.821481	0.405645	0.38095	0.036705
793.5618883	6.0982	C45H80NO8P	28	PC(15:0/22:5(7Z,10Z,13Z,16Z,19Z))	5	Lipids: Glycerophospholipids	KEGG_HMDB	C00157	1.00	1.16	0.86	0.73	0.60	1	0.750605	0.72862	0.446467	0.274447
797.5935941	7.6783	C45H84NO8P	17	PE(18:1(11Z)/22:2(13Z,16Z))	5	Lipids: Glycerophospholipids	KEGG_HMDB	C00350	1.00	0.90	1.20	0.80	1.17	1	0.711596	0.524229	0.468711	0.848996
797.6297207	7.6643	C46H88NO7P	10	PC(20:1(11Z)/P-18:1(11Z))	5	Lipids: Glycerophospholipids	KEGG_HMDB	C00157	1.00	1.33	1.60	1.15	1.82	1	0.602643	0.505019	0.742061	0.533525
799.6104246	6.1802	C45H86NO8P	15	[PE (20:0/20:2)] 1-eicosanoyl-2-(11Z,14Z-eicosadienoyl)-sn-glycero-3-phosphoethanolamine	5	Lipids: Glycerophospholipids	KEGG_Lipidmaps_HMDB	C00350	1.00	1.11	1.20	0.31	0.95	1	0.696203	0.433156	0.12943	0.869434
801.5525226	7.7568	C43H80NO10P	1	[PG (17:0/20:4)] 1-heptadecanoyl-2-(5Z,8Z,11Z,14Z-eicosatetraenoyl)-sn-glycero-3-phospho-(1'-rac-glycerol) (ammonium salt)	7	Lipids: Glycerophospholipids	Lipidmaps	0	1.00	1.08	**1.25**	**0.62**	0.50	1	0.070697	0.027378	0.020636	0.055414
801.6245715	7.6928	C45H88NO8P	19	[PE (18:0/22:1)] 1-octadecanoyl-2-(13Z-docosenoyl)-sn-glycero-3-phosphoethanolamine	5	Lipids: Glycerophospholipids	KEGG_Lipidmaps_HMDB	C00350	1.00	1.25	0.86	0.71	0.78	1	0.657909	0.856602	0.565605	0.676703

803.5680786	6.159	C43H82NO10P	1	[GP (18:0/18:0)] 1-octadecanoyl-2-(9Z-octadecenoyl)-sn-glycero-3-phosphothreonine	5	Lipids: Glycerophospholipids	Lipidmaps	0	1.00	0.87	1.07	1.11	0.80	1	0.385174	0.615054	0.59078	0.657258
803.5684448	7.7555	C43H82NO10P	1	[GP (18:0/18:0)] 1-octadecanoyl-2-(9Z-octadecenoyl)-sn-glycero-3-phosphothreonine	7	Lipids: Glycerophospholipids	Lipidmaps	0	1.00	0.91	0.97	1.01	0.82	1	0.690276	0.877444	0.982788	0.751993
805.5621313	7.6398	C46H80NO8P	28	[PC (16:0/22:6)] 1-hexadecanoyl-2-(4Z,7Z,10Z,13Z,16Z,19Z-docosahexaenoyl)-sn-glycero-3-phosphocholine	5	Lipids: Glycerophospholipids	KEGG_Lipidmaps_HMDB	C00157	1.00	0.92	1.03	0.89	**0.50**	1	0.581613	0.868064	0.440649	0.030138
805.5621346	6.123	C46H80NO8P	28	[PC (18:1/20:5)] 1-(11Z-octadecenoyl)-2-(5Z,8Z,11Z,14Z,17Z-eicosapentaenoyl)-sn-glycero-3-phosphocholine	5	Lipids: Glycerophospholipids	KEGG_Lipidmaps_HMDB	C00157	1.00	1.05	1.11	0.71	0.51	1	0.903259	0.794 51	0.400416	0.195195
807.5771868	6.1291	C46H82NO8P	29	[PC (18:1/20:4)] 1-(9Z-octadecenoyl)-2-(5Z,8Z,11Z,14Z-eicosatetraenoyl)-sn-glycero-3-phosphocholine	5	Lipids: Glycerophospholipids	KEGG_Lipidmaps_HMDB	C00157	1.00	1.10	1.13	0.65	0.64	1	0.845765	0.812 25	0.411222	0.371823
809.5931745	7.6455	C46H84NO8P	24	[PC (18:1/20:3)] 1-(9Z-octadecenoyl)-2-(5Z,8Z,11Z-eicosatrienoyl)-sn-glycero-3-phosphocholine	5	Lipids: Glycerophospholipids	KEGG_Lipidmaps_HMDB	C00157	1.00	0.92	1.04	0.71	0.64	1	0.752437	0.900 05	0.261797	0.176487
811.6084608	7.6606	C46H86NO8P	21	PC(16:1(9Z)/22:2(13Z,16Z))	5	Lipids: Glycerophospholipids	KEGG_HMDB	C00157	1.00	0.96	1.05	0.78	0.84	1	0.911881	0.900 815	0.553565	0.723795

811.6086081	6.1621	C46H86NO8P	21	[PC (18:0/20:3)] 1-octadecanoyl-2-(5Z,8Z,11Z-eicosatrienoyl)-sn-glycero-3-phosphocholine	5	Lipids: Glycerophospholipids	KEGG_Lipidmaps_HMDB	C00157	1.00	0.66	0.74	**0.16**	0.65	1	0.362051	0.537272	0.029037	0.055887
813.6236261	6.1639	C46H88NO8P	22	[PC (20:0/18:2)] 1-eicosanoyl-2-(9Z,12Z-octadecadienoyl)-sn-glycero-3-phosphocholine	5	Lipids: Glycerophospholipids	KEGG_Lipidmaps_HMDB	C00157	1.00	1.15	1.27	0.33	1.27	1	0.851722	0.743514	0.299773	0.65675
813.6238693	7.6758	C46H88NO8P	22	[PC (18:0/20:2)] 1-octadecanoyl-2-(11Z,14Z-eicosadienoyl)-sn-glycero-3-phosphocholine	5	Lipids: Glycerophospholipids	KEGG_Lipidmaps_HMDB	C00157	1.00	0.99	1.21	0.76	1.11	1	0.988869	0.705848	0.596053	0.877891
817.5623998	6.117	C47H80NO8P	12	PE(20:2(11Z,14Z)/22:5(4Z,7Z,10Z,13Z,16Z))	5	Lipids: Glycerophospholipids	KEGG_HMDB	C00350	1.00	1.06	1.52	0.56	0.90	1	0.894429	0.405242	0.27275	0.866411
817.5629361	7.6335	C47H80NO8P	12	PE(20:1(11Z)/22:6(4Z,7Z,10Z,13Z,16Z,19Z))	5	Lipids: Glycerophospholipids	KEGG_HMDB	C00350	1.00	1.00	1.30	0.74	0.98	1	0.987809	0.228806	0.133782	0.975831
819.5777787	6.121	C47H82NO8P	15	PE(20:1(11Z)/22:5(4Z,7Z,10Z,13Z,16Z))	5	Lipids: Glycerophospholipids	KEGG_HMDB	C00350	1.00	1.13	1.32	0.65	0.76	1	0.81966	0.597713	0.39641	0.555106
819.577794	7.6296	C47H82NO8P	15	PE(20:0/22:6(4Z,7Z,10Z,13Z,16Z,19Z))	5	Lipids: Glycerophospholipids	KEGG_HMDB	C00350	1.00	1.03	1.17	0.90	0.73	1	0.894373	0.586094	0.60943	0.311394
821.5936674	6.1327	C47H84NO8P	20	PE(20:0/22:5(4Z,7Z,10Z,13Z,16Z))	5	Lipids: Glycerophospholipids	KEGG_HMDB	C00350	1.00	1.13	1.24	0.57	0.92	1	0.832256	0.702451	0.374317	0.852766

821.5937868	7.6386	C47H84NO8P	20	PE(18:4(6Z,9Z,12Z,15Z)/24:1(15Z))	5	Lipids: Glycerophospholipids	KEGG_HMDB	C00350	1.00	1.03	1.20	0.83	0.78	1	0.927436	0.521721	0.468128	0.396021
823.6089854	6.1477	C47H86NO8P	18	PE(18:3(9Z,12Z,15Z)/24:1(15Z))	5	Lipids: Glycerophospholipids	KEGG_HMDB	C00350	1.00	0.75	0.87	**0.28**	**0.67**	1	0.536765	0.787266	0.01818	0.047736
823.6091114	7.6425	C47H86NO8P	18	PE(18:3(6Z,9Z,12Z)/24:1(15Z))	5	Lipids: Glycerophospholipids	KEGG_HMDB	C00350	1.00	0.96	1.29	0.70	0.94	1	0.898371	0.604715	0.371708	0.858008
824.5567665	7.8364	C46H81O10P	4	PG(18:0/22:5(4Z,7Z,10Z,13Z,16Z))	5	Lipids: Glycerophospholipids	HMDB	0	1.00	0.98	1.18	**0.56**	0.73	1	0.923732	0.586958	0.044782	0.188144
825.6250504	7.6526	C47H88NO8P	14	PE(18:2(9Z,12Z)/24:1(15Z))	5	Lipids: Glycerophospholipids	KEGG_HMDB	C00350	1.00	1.03	1.09	0.71	0.87	1	0.950851	0.875649	0.525363	0.774593
826.5722826	8.129	C46H83O10P	1	PG(18:0/22:4(7Z,10Z,13Z,16Z))	7	Lipids: Glycerophospholipids	HMDB	0	1.00	0.92	0.94	0.57	0.63	1	0.84717	0.857894	0.265525	0.329287
829.5621996	6.1145	C48H80NO8P	23	[PC (20:4/20:4)] 1,2-di-(5Z,8Z,11Z,14Z-eicosatetraenoyl)-sn-glycero-3-phosphocholine	7	Lipids: Glycerophospholipids	KEGG_Lipidmaps_HMDB	C00157	1.00	1.22	1.45	0.75	1.23	1	0.598449	0.359911	0.335958	0.69979
829.5622726	7.6238	C48H80NO8P	23	[PC (18:2/22:6)] 1-(9Z,12Z-octadecadienoyl)-2-(4Z,7Z,10Z,13Z,16Z,19Z-docosahexaenoyl)-sn-glycero-3-phosphocholine	5	Lipids: Glycerophospholipids	KEGG_Lipidmaps_HMDB	C00157	1.00	1.04	1.27	0.96	1.23	1	0.780988	0.136654	0.786201	0.725826

831.5769 14	6.1158	C48H82NO8P	22	[PC (18:2/22:5)] 1-(9Z,12Z-octadecadienoyl)-2-(4Z,7Z,10Z,13Z,16Z-docosapentaenoyl)-sn-glycero-3-phosphocholine	5	Lipids: Glycerophospholipids	KEGG_Lipidmaps_HMDB	C00157	1.00	1.15	1.36	0.66	1.30	1	0.760635	0.520099	0.358007	0.675493
831.5772574	7.6328	C48H82NO8P	22	[PC (18:1/22:6)] 1-(11Z-octadecenoyl)-2-(4Z,7Z,10Z,13Z,16Z,19Z-docosahexaenoyl)-sn-glycero-3-phosphocholine	7	Lipids: Glycerophospholipids	KEGG_Lipidmaps_HMDB	C00157	1.00	1.05	1.27	0.93	1.44	1	0.786466	0.219671	0.631616	0.630805
833.5927117	6.131	C48H84NO8P	27	[PC (18:0/22:6)] 1-octadecanoyl-2-(4Z,7Z,10Z,13Z,16Z,19Z-docosahexaenoyl)-sn-glycero-3-phosphocholine	7	Lipids: Glycerophospholipids	KEGG_Lipidmaps_HMDB	C00157	1.00	1.21	1.23	0.53	1.01	1	0.755522	0.725611	0.341681	0.979593
833.5930546	7.6267	C48H84NO8P	27	[PC (18:1/22:5)] 1-(11Z-octadecenoyl)-2-(7Z,10Z,13Z,16Z,19Z-docosapentaenoyl)-sn-glycero-3-phosphocholine	7	Lipids: Glycerophospholipids	KEGG_Lipidmaps_HMDB	C00157	1.00	1.07	1.12	0.79	0.65	1	0.853945	0.7495	0.535889	0.345962
835.535331	7.8458	C46H78NO10P	3	[PS (18:0/22:6)] 1-octadecanoyl-2-(4Z,7Z,10Z,13Z,16Z,19Z-docosahexaenoyl)-sn-glycero-3-phosphoserine	5	Lipids: Glycerophospholipids	KEGG_Lipidmaps_HMDB	C02737	1.00	1.15	1.28	0.70	0.79	1	0.492597	0.158616	0.087624	0.260598
835.6080038	6.1301	C48H86NO8P	25	[PC (18:0/22:5)] 1-octadecanoyl-2-(7Z,10Z,13Z,16Z,19Z-docosapentaenoyl)-sn-glycero-3-phosphocholine	5	Lipids: Glycerophospholipids	KEGG_Lipidmaps_HMDB	C00157	1.00	1.09	1.13	0.43	1.02	1	0.89614	0.855093	0.312739	0.973234

835.6082683	7.6345	C48H86NO8P	25	[PC (18:0/22:5)] 1-octadecanoyl-2-(4Z,7Z,10Z,13Z,16Z-docosapentaenoyl)-sn-glycero-3-phosphocholine	5	Lipids: Glycerophospholipids	KEGG_Lipidmaps_HMDB	C00157	1.00	1.04	1.07	0.76	0.94	1	0.930741	0.888946	0.543644	0.880558
837.6239962	6.1706	C48H88NO8P	21	[PC (20:0/20:4)] 1-eicosanoyl-2-(5Z,8Z,11Z,14Z-eicosatetraenoyl)-sn-glycero-3-phosphocholine	5	Lipids: Glycerophospholipids	KEGG_Lipidmaps_HMDB	C00157	1.00	1.14	1.25	0.30	1.07	1	0.858029	0.767441	0.302187	0.907407
837.6240239	7.6491	C48H88NO8P	21	[PC (18:0/22:4)] 1-octadecanoyl-2-(7Z,10Z,13Z,16Z-docosatetraenoyl)-sn-glycero-3-phosphocholine	5	Lipids: Glycerophospholipids	KEGG_Lipidmaps_HMDB	C00157	1.00	1.10	1.13	0.68	0.60	1	0.838631	0.829396	0.476108	0.424405
877.5621317	6.0949	C52H80NO8P	3	[PC (22:6/22:6)] 1,2-di-(4Z,7Z,10Z,13Z,16Z,19Z-docosahexaenoyl)-sn-glycero-3-phosphocholine	5	Lipids: Glycerophospholipids	KEGG_Lipidmaps_HMDB	C00157	1.00	1.20	1.27	0.70	2.77	1	0.732186	0.620688	0.516455	0.535142
881.6132153	6.1885	C49H88NO10P	1	[PG (21:0/22:6)] 1-heneicosanoyl-2-(4Z,7Z,10Z,13Z,16Z,19Z-docosahexenoyl)-sn-glycero-3-phospho-(1'-rac-glycerol) (ammonium salt)	5	Lipids: Glycerophospholipids	Lipidmaps	0	1.00	1.04	1.16	0.72	1.52	1	0.931054	0.67544	0.502549	0.149317
883.6087013	6.1218	C52H86NO8P	4	PC(22:4(7Z,10Z,13Z,16Z)/22:5(4Z,7Z,10Z,13Z,16Z))	5	Lipids: Glycerophospholipids	KEGG_HMDB	C00157	1.00	1.14	1.36	0.59	1.32	1	0.829798	0.629346	0.396243	0.760524
108.0940069	5.2049	C16H24	1	[PR] (+)-3-longipinen-5-one	7	Lipids: Prenols	Lipidmaps	0	1.00	1.23	1.06	0.93	1.21	1	0.566798	0.873482	0.841704	0.511761

196.1463336	5.239	C12H20O2	29	(1S,2R,4S)-(-)-Bornyl acetate	7	Lipids: Prenols	KEGG_Lipidmaps	C09837	1.00	0.87	0.67	0.60	0.58	1	0.630136	0.269884	0.211474	0.194959
273.2667452	6.1337	C16H35NO2	1	Hexadecasphinganine	5	Lipids: Sphingolipids	KEGG_Lipidmaps	C13915	1.00	1.04	1.07	1.01	1.42	1	0.849402	0.720756	0.958164	0.602833
285.3031582	6.0915	C18H39NO	1	[SP] 1-deoxy-sphinganine	5	Lipids: Sphingolipids	Lipidmaps	0	1.00	0.98	1.74	1.48	**2.94**	1	0.964108	0.208829	0.31999	0.041406
327.3137025	5.2169	C20H41NO2	1	N,N-Dimethylsphing-4-enine	5	Lipids: Sphingolipids	KEGG_Lipidmaps_HMDB	C13914	1.00	0.97	1.27	0.93	0.55	1	0.939246	0.480712	0.860795	0.276907
466.3533642	8.6946	C23H51N2O5P	1	LysoSM(d18:0)	5	Lipids: Sphingolipids	HMDB	0	1.00	0.70	0.45	0.46	0.39	1	0.374959	0.116284	0.14618	0.091024
565.542922	5.1117	C36H71NO3	6	[SP (18:0)] N-(octadecanoyl)-sphing-4-enine	7	Lipids: Sphingolipids	KEGG_Lipidmaps_HMDB	C00195	1.00	1.21	1.61	0.26	1.86	1	0.81306	0.558692	0.306779	0.454401
646.5051085	9.2729	C35H71N2O6P	1	SM(d18:1/12:0)	5	Lipids: Sphingolipids	KEGG_Lipidmaps_HMDB	C00550	1.00	0.88	1.15	0.96	0.71	1	0.638027	0.737973	0.912734	0.41166
674.5358709	6.1344	C37H75N2O6P	1	SM(d18:1/14:0)	5	Lipids: Sphingolipids	Lipidmaps_HMDB	0	1.00	0.88	1.15	1.31	1.88	1	0.737828	0.638836	0.471483	0.393834
674.5362864	9.0864	C37H75N2O6P	1	SM(d18:1/14:0)	5	Lipids: Sphingolipids	Lipidmaps_HMDB	0	1.00	1.28	1.80	1.13	1.10	1	0.604264	0.306289	0.76662	0.798047
688.551637	6.1717	C38H77N2O6P	1	[SP (18:0/14:0)] N-(octadecanoyl)-tetradecasphing-4-enine-1-phosphoethanolamine	5	Lipids: Sphingolipids	Lipidmaps	0	1.00	0.62	1.16	1.26	0.52	1	0.137811	0.300635	0.500178	0.202401
688.5519419	9.0055	C38H77N2O6P	1	[SP (18:0/14:0)] N-(octadecanoyl)-tetradecasphing-4-enine-1-phosphoethanolamine	5	Lipids: Sphingolipids	Lipidmaps	0	1.00	1.04	1.58	1.11	0.81	1	0.896115	0.193826	0.769063	0.682416
702.5673227	6.2229	C39H79N2O6P	1	[SP (16:0)] N-(hexadecanoyl)-sphing-4-enine-1-phosphocholine	7	Lipids: Sphingolipids	Lipidmaps_HMDB	0	1.00	0.64	1.15	1.10	0.74	1	0.141846	0.195523	0.78857	0.569393

702.5673348	8.9039	C39H79N2O6P	1	[SP (16:0)] N-(hexadecanoyl)-sphing-4-enine-1-phosphocholine	7	Lipids: Sphingolipids	Lipidmaps_HMDB	0	1.00	1.01	1.40	0.98	0.76	1	0.977947	0.263724	0.949142	0.593028
728.5824781	8.769	C41H81N2O6P	2	SM(d18:1/18:1(9Z))	7	Lipids: Sphingolipids	KEGG_Lipidmaps_HMDB	C00550	1.00	1.06	1.57	1.03	0.93	1	0.725195	0.075851	0.876028	0.867658
730.5979114	8.7255	C41H83N2O6P	3	SM(d18:0/18:1(9Z))	5	Lipids: Sphingolipids	KEGG_Lipidmaps_HMDB	C00550	1.00	1.15	1.36	0.78	0.83	1	0.720658	0.284709	0.467348	0.648411
732.6133871	8.5728	C41H85N2O6P	1	SM(d18:0/18:0)	7	Lipids: Sphingolipids	KEGG_Lipidmaps_HMDB	C00550	1.00	0.81	0.49	0.39	1.11	1	0.776135	0.452434	0.384256	0.922986
758.6301035	8.6152	C43H87N2O6P	1	SM(d18:1/20:0)	5	Lipids: Sphingolipids	KEGG_Lipidmaps_HMDB	C00550	1.00	1.22	1.14	0.79	0.98	1	0.782705	0.849421	0.731327	0.975048
784.6455725	8.5052	C45H89N2O6P	2	SM(d18:1/22:1(13Z))	5	Lipids: Sphingolipids	KEGG_HMDB	C00550	1.00	1.11	1.07	0.84	0.95	1	0.864394	0.919622	0.778093	0.942433
786.6616711	8.5048	C45H91N2O6P	2	SM(d18:1/22:0)	5	Lipids: Sphingolipids	KEGG_Lipidmaps_HMDB	C00550	1.00	1.08	1.03	0.57	0.83	1	0.923486	0.964724	0.529099	0.817757
798.6611029	8.4629	C46H92N2O6P	1	SM(d17:1/24:1(15Z))	5	Lipids: Sphingolipids	HMDB	0	1.00	1.17	1.13	0.79	0.89	1	0.823555	0.854677	0.723083	0.869017
812.6769741	8.4274	C47H93N2O6P	1	SM(d18:1/24:1(15Z))	7	Lipids: Sphingolipids	KEGG_Lipidmaps_HMDB	C00550	1.00	1.15	1.09	0.67	0.80	1	0.849782	0.911941	0.620412	0.776907
368.3443024	5.1589	C27H44	1	[ST] (5Z,7E)-9,10-seco-5,7,10(19)-cholestatriene	7	Lipids: Sterol lipids	Lipidmaps	0	1.00	1.30	1.29	0.86	1.33	1	0.692935	0.741141	0.840797	0.673698
384.3392208	5.1879	C27H44O	28	[ST (2:0)] 5alpha-cholesta-8,24-dien-3beta-ol	6	Lipids: Sterol lipids	KEGG_Metacyc_Lipidmaps_HMDB	C05437	1.00	0.94	0.92	1.29	0.82	1	0.916389	0.885031	0.662696	0.736544
390.2768445	5.0525	C24H38O4	58	[ST hydrox] 3alpha,12alpha-Dihydroxy-5beta-chol-6-en-24-oic Acid	7	Lipids: Sterol lipids	KEGG_Lipidmaps	C11637	1.00	1.09	1.45	1.03	0.65	1	0.826918	0.334062	0.917248	0.48535

404.2923391	5.0479	C25H40O4	7	[ST (3:0)] (5Z,7E)-(1S,3R)-21-nor-20-oxa-9,10-seco-5,7,10(19)-cholestatriene-1,3,25-triol	5	Lipids: Sterol lipids	Lipidmaps	0	1.00	1.40	1.11	1.83	2.44	1	0.696477	0.785949	0.571527	0.326636
414.3128727	5.2114	C27H42O3	28	[ST hydroxy(3:0)] (5Z,7E)-(1S,3R)-1,3-dihydroxy-9,10-seco-5,7,10(19)-cholestatrien-22-one	5	Lipids: Sterol lipids	Lipidmaps	0	1.00	1.48	1.17	1.79	0.99	1	0.403153	0.670183	0.523081	0.967955
416.3285414	5.2017	C27H44O3	46	[ST (3:0)] (5Z,7E)-(1S,3R)-9,10-seco-5,7,10(19)-cholestatriene-1,3,25-triol	8	Lipids: Sterol lipids	KEGG_Metacyc_Lipidmaps_HMDB	C01673	1.00	1.32	1.04	1.86	0.88	1	0.420647	0.915635	0.468743	0.775665
418.3079675	5.0376	C26H42O4	10	[ST (3:0)] (5Z,7E)-(1S,3R,24R)-22-oxa-9,10-seco-5,7,10(19)-cholestatriene-1,3,24-triol	7	Lipids: Sterol lipids	Lipidmaps	0	1.00	1.18	0.89	1.62	2.12	1	0.838353	0.719171	0.608504	0.373909
432.3235594	5.1841	C27H44O4	34	[ST (2:0)] (7E)-(1S,3R,6R)-6,19-epidioxy-9,10-seco-5(10),7-cholestadiene-1,3-diol	5	Lipids: Sterol lipids	Lipidmaps	0	1.00	1.41	0.75	0.54	1.81	1	0.69404	0.363143	0.143875	0.417335
448.3184682	5.6106	C27H44O5	16	[ST (3:0)] 25R-spirostan-2beta,3beta,6beta-triol	5	Lipids: Sterol lipids	Lipidmaps	0	1.00	1.15	1.48	1.03	0.83	1	0.689673	0.515652	0.927604	0.525328
455.3393228	5.4283	C29H45NO3	1	[ST oxo(3:0/3:0)] (5Z,7E)-(1S,3R)-24-oxo-25-aza-26,27-propano-9,10-seco-5,7,10(19)-cholestatriene-1,3,25-triol	5	Lipids: Sterol lipids	Lipidmaps	0	1.00	0.91	1.19	1.04	0.72	1	0.788775	0.612158	0.897366	0.485314
238.0988237	20.288	C8H18N2O4S	1	HEPES	10	Medium Component	Medium	0	1.00	1.01	0.99	1.02	0.87	1	0.902829	0.784221	0.785915	0.06212
520.0761276	15.03	C26H20N2O6S2	1	Bathocuproine disulfonic acid	8	Medium Component	Medium	0	1.00	1.11	1.37	1.07	0.75	1	0.201233	0.370336	0.629608	0.557408

191.0251479	18.657	C6H9NO4S	1	a Cysteine adduct	7	Medium Contaminant	Medium	0	1.00	0.93	1.06	0.90	0.56	1	0.409385	0.64242	0.343734	0.254755
191.0251625	17.215	C6H9NO4S	1	a Cysteine adduct	7	Medium Contaminant	Medium	0	1.00	1.03	1.09	0.98	0.45	1	0.815559	0.68175	0.89428	0.218385
191.0252322	8.2298	C6H9NO4S	1	a Cysteine adduct	5	Medium Contaminant	Medium	0	1.00	0.99	1.05	0.97	0.55	1	0.978991	0.907612	0.914612	0.226976
122.0481067	7.9146	C6H6N2O	4	Nicotinamide	8	Metabolism of Cofactors and Vitamins	KEGG_Metacyc_HMDB	C00153	1.00	1.02	1.05	1.22	0.44	1	0.928648	0.77475	0.454056	0.101924
128.0474045	5.1181	C6H8O3	9	Dihydro-4,4-dimethyl-2,3-Furandione	5	Metabolism of Cofactors and Vitamins	KEGG_Metacyc	C01125	1.00	1.12	1.29	1.67	0.74	1	0.764765	0.395916	0.281939	0.438285
141.9757141	17.503	C2H6O3S2	1	2-Mercaptoethanesulfonate	6	Metabolism of Cofactors and Vitamins	KEGG_Metacyc_HMDB	C03576	1.00	1.03	0.90	0.89	**0.26**	1	0.918274	0.770687	0.728327	
155.0346523	19.867	C3H10NO4P	3	D-1-Aminopropan-2-ol O-phosphate	8	Metabolism of Cofactors and Vitamins	KEGG_Metacyc	C04122	1.00	0.94	1.22	0.74	**0.31**	1	0.796825	0.537879	0.063328	0.005312
167.0580877	10.085	C8H9NO3	9	Isopyridoxal	6	Metabolism of Cofactors and Vitamins	KEGG_Metacyc_HMDB	C06051	1.00	1.03	1.23	1.19	0.65	1	0.904062	0.502629	0.448113	0.408786
168.0897983	19.306	C8H12N2O2	3	Pyridoxamine	8	Metabolism of Cofactors and	KEGG_Metacyc_HMDB	C00534	1.00	1.22	1.12	1.58	0.58	1	0.546171	0.779018	0.19903	0.086558

						Vitamins												
183.0529467	8.2383	C8H9NO4	6	4-Pyridoxate	6	Metabolism of Cofactors and Vitamins	KEGG_Metacyc_HMDB	C00847	1.00	0.91	0.91	0.97	0.74	1	0.821682	0.833544	0.945528	0.505886
195.0756327	8.8578	C7H9N5O2	1	2-Amino-4-hydroxy-6-hydroxymethyl-7,8-dihydropteridine	6	Metabolism of Cofactors and Vitamins	KEGG_Metacyc	C01300	1.00	0.83	1.45	1.55	0.43	1	0.543407	0.135992	0.255557	0.117631
223.0067154	17.543	C6H10NO4PS	1	4-Methyl-5-(2-phosphoethyl)-thiazole	6	Metabolism of Cofactors and Vitamins	KEGG_Metacyc	C04327	1.00	1.19	1.08	1.15	2.48	1	0.095276	0.33129	0.239635	0.499061
254.0900681	13.948	C11H14N2O5	4	N-Ribosylnicotinamide	8	Metabolism of Cofactors and Vitamins	KEGG_Metacyc_HMDB	C03150	1.00	0.83	1.40	1.48	0.76	1	0.56669	0.216125	0.376407	0.629551
264.1042247	19.872	C12H17N4OS	1	Thiamin	10	Metabolism of Cofactors and Vitamins	medium_KEGG_Metacyc_HMDB	C00378	1.00	1.02	0.77	0.69	0.33	1	0.939972	0.355604	0.225473	0.052958
264.1045454	19.741	C12H17N4OS	1	Thiamin	8	Metabolism of Cofactors and Vitamins	medium_KEGG_Metacyc_HMDB	C00378	1.00	1.05	1.04	1.17	0.49	1	0.671857	0.752099	0.437424	0.154013
376.1381031	7.9681	C17H20N4O6	2	Riboflavin	10	Metabolism of Cofactors and Vitamins	KEGG_Metacyc_HMDB	C00255	1.00	0.97	0.89	1.07	0.44	1	0.787119	0.334485	0.722221	0.081276

441.1404546	10.303	C19H19N7O6	1	Folate	8	Metabolism of Cofactors and Vitamins	KEGG_HMDB	C00504	1.00	1.06	1.02	1.19	0.40	1	0.756492	0.917456	0.455498	0.070667
471.1501292	10.398	C20H21N7O7	1	10-Formyldihydrofolate	7	Metabolism of Cofactors and Vitamins	KEGG_Metacyc_HMDB	C03204	1.00	1.17	1.59	1.21	0.82	1	0.331709	0.42111	0.108646	0.542921
74.00013966	10.109	C2H2O3	1	Glyoxylate	8	Nucleotide Metabolism	KEGG_Metacyc_HMDB	C00048	1.00	1.23	1.14	1.43	0.65	1	0.597592	0.761252	0.301234	0.221135
84.03224442	14.814	C3H4N2O	1	Imidazolone	6	Nucleotide Metabolism	KEGG_Metacyc_HMDB	C06195	1.00	0.98	0.89	0.95	0.77	1	0.909689	0.365445	0.707191	0.089864
84.03224778	15.488	C3H4N2O	1	Imidazolone	6	Nucleotide Metabolism	KEGG_Metacyc_HMDB	C06195	1.00	1.01	0.95	0.96	0.97	1	0.929718	0.582367	0.673313	0.762087
84.03252349	10.364	C3H4N2O	1	Imidazolone	6	Nucleotide Metabolism	KEGG_Metacyc_HMDB	C06195	1.00	**0.89**	0.91	0.83	0.77	1	0.009737	0.425973	0.187615	0.175467
89.04763509	15.561	C3H7NO2	9	beta-Alanine	8	Nucleotide Metabolism	KEGG_Metacyc_HMDB	C00099	1.00	0.99	1.15	0.80	**0.53**	1	0.946506	0.422342	0.130722	0.012696
89.04763627	13.278	C3H7NO2	9	beta-Alanine	6	Nucleotide Metabolism	KEGG_Metacyc_HMDB	C00099	1.00	1.00	0.94	1.00	0.46	1	0.990476	0.567288	0.994248	0.115733
112.0273028	9.5126	C4H4N2O2	1	Uracil	8	Nucleotide Metabolism	KEGG_Metacyc_HMDB	C00106	1.00	0.99	1.08	1.04	0.49	1	0.959799	0.758996	0.877773	0.052427

126.0430264	7.5968	C5H6N2O2	2	Thymine	10	Nucleotide Metabolism	KEGG_Metacyc_HMDB	C00178	1.00	0.94	0.89	1.23	0.49	1	0.913696	0.739752	0.540945	0.20206
133.0484678	16.347	C3H7N3O3	2	Ureidoglycine	6	Nucleotide Metabolism	KEGG_Metacyc	C02091	1.00	1.08	0.95	0.86	0.56	1	0.748898	0.830887	0.560623	0.143243
135.0544148	10.921	C5H5N5	1	Adenine	8	Nucleotide Metabolism	KEGG_Metacyc_HMDB	C00603	1.00	1.15	1.26	**1.32**	0.75	1	0.201988	0.055837	0.028125	0.443164
151.0493461	12.467	C5H5N5O	3	Guanine	10	Nucleotide Metabolism	KEGG_Metacyc_HMDB	C00242	1.00	3.65	3.63	1.67	0.72	1	0.156519	0.23342	0.25849	0.244605
152.0334286	9.1594	C5H4N4O2	3	Xanthine	10	Nucleotide Metabolism	KEGG_Metacyc_HMDB	C00385	1.00	1.18	1.05	1.06	0.41	1	0.723683	0.920256	0.90606	0.253857
158.0437032	13.701	C4H6N4O3	3	Allantoin	8	Nucleotide Metabolism	KEGG_Metacyc_HMDB	C01551	1.00	1.01	0.94	1.07	0.43	1	0.947249	0.641236	0.674335	0.07791
168.0280669	12.476	C5H4N4O3	1	Urate	8	Nucleotide Metabolism	KEGG_Metacyc_HMDB	C00366	1.00	1.00	0.93	1.01	0.73	1	0.981907	0.633505	0.908092	0.115301
176.0542085	16.34	C4H8N4O4	1	Allantoate	8	Nucleotide Metabolism	KEGG_Metacyc_HMDB	C00499	1.00	1.06	0.88	0.89	0.52	1	0.858066	0.72538	0.751456	0.240152
228.0744783	8.0275	C9H12N2O5	3	Deoxyuridine	10	Nucleotide Metabolism	KEGG_Metacyc_HMDB	C00526	1.00	1.93	1.15	**1.49**	0.86	1	0.05971	0.444596	0.011423	0.386807

242.0903659	7.6084	C10H14N2O5	1	Thymidine	8	Nucleotide Metabolism	KEGG_Metacyc_HMDB	C00214	1.00	0.97	0.79	1.11	0.75	1	0.960158	0.48061	0.79881	0.420142
244.0692849	9.5356	C9H12N2O6	2	Uridine	10	Nucleotide Metabolism	KEGG_Metacyc_HMDB	C00299	1.00	0.94	0.77	0.94	0.45	1	0.838292	0.36917	0.795959	0.106599
244.0693086	11.953	C9H12N2O6	2	Pseudouridine	6	Nucleotide Metabolism	KEGG_Metacyc_HMDB	C02067	1.00	1.04	0.98	0.91	**0.37**	1	0.800699	0.944425	0.591022	0.037046
267.0968371	10.276	C10H13N5O4	3	Adenosine	10	Nucleotide Metabolism	KEGG_Metacyc_HMDB	C00212	1.00	0.96	1.35	1.40	0.79	1	0.838499	0.740477	0.152291	0.626877
283.0916259	12.724	C10H13N5O5	5	Guanosine	8	Nucleotide Metabolism	KEGG_Metacyc_HMDB	C00387	1.00	1.00	1.97	1.45	1.22	1	0.993849	0.116211	0.195186	0.758137
284.0755655	9.6882	C10H12N4O6	1	Xanthosine	6	Nucleotide Metabolism	KEGG_Metacyc_HMDB	C01762	1.00	0.97	0.84	0.72	0.24	1	0.931883	0.572347	0.340523	0.079248
323.0515791	20.827	C9H14N3O8P	3	CMP	10	Nucleotide Metabolism	KEGG_Metacyc_HMDB	C00055	1.00	1.38	1.69	1.72	0.82	1	0.27132	0.22164	0.094714	0.677653
324.0355752	23.234	C9H13N2O9P	4	Pseudouridine 5'-phosphate	8	Nucleotide Metabolism	KEGG_Metacyc_HMDB	C01168	1.00	0.88	0.60	0.70	**0.16**	1	0.753767	0.180125	0.354885	0.042953
347.0630043	20.288	C10H14N5O7P	7	3'-AMP	8	Nucleotide Metabolism	KEGG_Metacyc_HMDB	C01367	1.00	0.82	0.82	0.73	**0.35**	1	0.407726	0.416337	0.187281	0.017907

363.0578831	25.012	C10H14N5O8P	5	GMP	10	Nucleotide Metabolism	KEGG_Metacyc_HMDB	C00144	1.00	1.10	1.24	0.88	0.31	1	0.679213	0.370148	0.618016	0.060402
402.0227375	19.706	C10H16N2O11P2	1	dTDP	6	Nucleotide Metabolism	KEGG_Metacyc_HMDB	C00363	1.00	1.14	**1.30**	1.13	1.00	1	0.120858	0.029557	0.563848	0.991509
404.0031602	17.849	C9H14N2O12P2	1	UDP	6	Nucleotide Metabolism	KEGG_Metacyc_HMDB	C00015	1.00	1.02	1.03	0.87	0.42	1	0.912439	0.86115	0.319899	0.056278
276.0956701	16.315	C10H16N2O7	2	GammaGlutamylglutamic acid	7	Peptide	KEGG_Metacyc_HMDB	C05282	1.00	1.04	1.20	0.66	0.98	1	0.89452	0.572819	0.213971	0.981992
186.100346	11.225	C8H14N2O3	1	Ala-Pro	5	Peptide(di-)	Peptides	0	1.00	1.51	1.41	0.87	0.55	1	0.195806	0.22672	0.582916	0.179423
202.1316852	11.347	C9H18N2O3	3	Ile-Ala	5	Peptide(di-)	Peptides	0	1.00	0.99	1.03	1.01	0.67	1	0.97122	0.942436	0.982884	0.314791
202.1317357	8.309	C9H18N2O3	3	Leu-Ala	7	Peptide(di-)	Peptides	0	1.00	1.07	**1.40**	1.29	0.93	1	0.739399	0.041519	0.289409	0.758664
208.051709	21.835	C6H12N2O4S	2	Cys-Ser	7	Peptide(di-)	Peptides	0	1.00	0.88	1.39	1.13	2.93	1	0.664835	0.295673	0.637626	0.395558
212.1160167	11.235	C10H16N2O3	2	Pro-Pro	7	Peptide(di-)	Peptides_HMDB	0	1.00	1.86	1.38	1.06	0.79	1	0.200238	0.296376	0.819623	0.596443
214.1316781	10.941	C10H18N2O3	2	Val-Pro	7	Peptide(di-)	Peptides	0	1.00	0.81	0.79	1.31	0.72	1	0.622226	0.541553	0.41831	0.499951
218.1266012	12.972	C9H18N2O4	5	Leu-Ser	7	Peptide(di-)	Peptides	0	1.00	0.88	1.13	0.90	0.49	1	0.150255	0.634427	0.59811	0.140056
228.147309	10.737	C11H20N2O3	3	Leu-Pro	5	Peptide(di-)	Peptides_HMDB	0	1.00	1.13	0.93	1.19	0.46	1	0.658527	0.764848	0.578327	0.069948

228.1475003	8.9237	C11H20N2O3	3	Ile-Pro	7	Peptide(di-)	Peptides	0	1.00	1.35	1.46	1.09	0.89	1	0.206021	0.177638	0.681509	0.747674
230.0901547	14.105	C9H14N2O5	1	Aspartyl-L-proline	7	Peptide(di-)	Peptides_HMDB	0	1.00	2.04	1.34	1.16	0.81	1	0.135636	0.47513	0.61186	0.606077
230.1630213	8.052	C11H22N2O3	2	Leu-Val	7	Peptide(di-)	Peptides	0	1.00	0.94	1.28	1.65	0.59	1	0.861937	0.550159	0.184328	0.202293
244.1787291	6.3314	C12H24N2O3	4	Leucyl-leucine	5	Peptide(di-)	KEGG_Metacyc_Peptides	C11332	1.00	0.80	1.17	1.16	1.56	1	0.512275	0.511263	0.706544	0.11043
246.1215074	11.949	C10H18N2O5	6	Glu-Val	5	Peptide(di-)	Peptides	0	1.00	1.10	1.12	0.96	**0.62**	1	0.32516	0.51144	0.653679	0.038891
260.1371167	10.527	C11H20N2O5	4	Glu-Leu	5	Peptide(di-)	Peptides	0	1.00	1.16	1.07	0.92	**0.59**	1	0.23226	0.817528	0.66023	0.032559
270.0950724	17.616	C10H14N4O5	2	Asp-His	7	Peptide(di-)	Peptides	0	1.00	1.04	1.38	1.62	0.88	1	0.895747	0.206214	0.055693	0.873669
214.0926562	21.477	C17H28N6O5S	4	Ala-Met-Ala-His	7	Peptide(tetra-)	Peptides	0	1.00	0.06	1.32	1.42	2.36	1	0.411675	0.844701	0.758745	0.404109
229.0712954	23.152	C17H26N6O5S2	1	Cys-Cys-Pro-His	7	Peptide(tetra-)	Peptides	0	1.00	0.65	1.25	0.99	0.95	1	0.349158	0.599034	0.978835	0.871682
250.0701552	8.1196	C20H28N4O7S2	1	Glu-Phe-Cys-Cys	7	Peptide(tetra-)	Peptides	0	1.00	1.13	0.82	0.90	**0.25**	1	0.74095	0.375116	0.575893	0.028123
250.0903648	15.836	C18H28N8O7S	1	Asn-Cys-Gln-His	7	Peptide(tetra-)	Peptides	0	1.00	1.03	1.16	0.88	**0.17**	1	0.767617	0.415247	0.286677	0.0116
260.1269204	19.884	C18H36N10O6S	1	Arg-Cys-Ser-Arg	7	Peptide(tetra-)	Peptides	0	1.00	0.98	0.94	0.77	0.65	1	0.945294	0.846993	0.495764	0.330074
412.1722046	20.718	C16H24N6O7	3	Ala-Ala-Asp-His	5	Peptide(tetra-)	Peptides	0	1.00	0.98	1.26	0.91	0.34	1	0.958184	0.556834	0.858185	0.205614

416.1645637	17.576	C15H24N6O8	1	His-Ser-Ser-Ser	5	Peptide(tetra-)	Peptides	0	1.00	1.29	1.21	1.95	**1.10**	1	0.39724	0.569481	0.102599	
431.2140681	20.934	C16H29N7O7	4	Ala-Ala-Asp-Arg	7	Peptide(tetra-)	Peptides	0	1.00	0.37	0.71	0.65	0.31	1	0.322501	0.615613	0.583266	0.291003
433.1940868	20.682	C15H27N7O8	1	Arg-Asp-Gly-Ser	5	Peptide(tetra-)	Peptides	0	1.00	**0.53**	0.91	0.79	**0.73**	1	0.024581	0.698834	0.300406	
450.1940981	9.8897	C21H30N4O5S	2	Met-Phe-Gly-Pro	7	Peptide(tetra-)	Peptides	0	1.00	0.98	1.01	0.87	1.07	1	0.871353	0.927917	0.439903	0.886045
482.171155	17.528	C18H26N8O6S	1	Cys-Ser-His-His	5	Peptide(tetra-)	Peptides	0	1.00	1.23	1.00	0.92	**0.32**	1	0.481325	0.997519	0.773922	0.005338
532.1979363	8.2497	C25H32N4O7S	2	Cys-Phe-Thr-Tyr	5	Peptide(tetra-)	Peptides	0	1.00	0.83	0.93	1.54	0.56	1	0.844049	0.927774	0.469488	0.583155
568.2426471	19.696	C23H36N8O7S	1	Arg-Cys-Gln-Tyr	5	Peptide(tetra-)	Peptides	0	1.00	1.83	**4.31**	4.03	1.11	1	0.190531	0.017326	0.107975	0.890422
579.1994675	8.4244	C25H33N5O9S	1	Glu-Met-Trp-Asp	7	Peptide(tetra-)	Peptides	0	1.00	1.31	0.92	1.09	0.32	1	0.490708	0.406286	0.678569	0.13474
301.1636552	11.822	C13H23N3O5	2	Val-Pro-Ser	7	Peptide(tri-)	Peptides	0	1.00	1.14	1.13	0.44	0.78	1	0.670645	0.730175	0.135728	0.793149
309.1686631	10.947	C15H23N3O4	2	Pro-Pro-Pro	5	Peptide(tri-)	Peptides	0	1.00	1.55	1.54	0.98	**0.44**	1	0.166334	0.217411	0.916058	0.006307
331.21055	8.1428	C15H29N3O5	5	Leu-Leu-Ser	7	Peptide(tri-)	Peptides	0	1.00	0.95	1.43	**2.27**	1.24	1	0.947634	0.441204	0.012118	0.827874
341.1351734	20.71	C13H19N5O6	2	Ala-Asp-His	5	Peptide(tri-)	Peptides	0	1.00	0.82	0.96	0.91	0.40	1	0.506913	0.890469	0.772964	0.101887
350.1259654	20.303	C12H22N4O6S	5	Met-Asn-Ser	5	Peptide(tri-)	Peptides	0	1.00	0.89	0.91	0.76	0.79	1	0.20167	0.27506	0.078293	0.062278

405.1380914	16.14	C15H23N3O10	1	Glu-Glu-Glu	5	Peptide(tri-)	Peptides	0	1.00	1.00	1.11	0.86	**0.35**	1	0.99719	0.508482	0.413357	0.023866
446.1908701	19.748	C20H26N6O6	6	Gln-Tyr-His	5	Peptide(tri-)	Peptides	0	1.00	1.19	1.17	1.42	0.86	1	0.50857	0.577956	0.234049	0.730676
450.1570597	8.7105	C20H26N4O6S	1	Met-Trp-Asp	7	Peptide(tri-)	Peptides	0	1.00	1.05	1.09	1.07	1.08	1	0.882027	0.72776	0.814741	0.88755
464.1732053	9.873	C21H28N4O6S	1	Glu-Met-Trp	7	Peptide(tri-)	Peptides	0	1.00	0.80	0.97	0.60	0.73	1	0.512993	0.926736	0.215366	0.434902
96.02111235	14.818	C5H4O2	3	Protoanemonin	1	Xenobiotics Biodegradation and Metabolism	KEGG_Metacyc	C07090	1.00	1.02	1.28	0.85	0.63	1	0.937177	0.491071	0.585869	0.230959
131.0947143	10.536	C6H13NO2	11	6-Aminohexanoate	5.5	Xenobiotics Biodegradation and Metabolism	KEGG_Metacyc_Lipidmaps_HMDB	C02378	1.00	1.05	1.24	1.03	0.61	1	0.568875	0.470451	0.799172	0.282599
137.0476939	5.8826	C7H7NO2	13	Anthranilate	5.5	Xenobiotics Biodegradation and Metabolism	KEGG_Metacyc_HMDB	C00108	1.00	0.98	1.04	0.80	**2.61**	1	0.971538	0.946001	0.65587	0.038904
166.026316	7.4258	C8H6O4	7	Phthalate	5.5	Xenobiotics Biodegradation and Metabolism	KEGG_Metacyc_HMDB	C01606	1.00	1.97	0.83	3.28	0.32	1	0.490442	0.811112	0.389394	0.323253
166.0264344	10.599	C8H6O4	7	Terephthalate	4.5	Xenobiotics Biodegrad	KEGG_Metacyc_HMDB	C06337	1.00	1.33	1.07	2.86	1.85	1	0.111079	0.599994	0.441845	0.389476

						ation and Metabolism												
182.0867405	19.708	C6H12F2N2O2	1	Eflornithine	9	Xenobiotics Drugs etc	KEGG_Metacyc	C07997	1.00	1.26	**1.98**	**2.05**	1.04	1	0.284484	0.033984	0.038533	0.883377

Appendix 8-3. The eflornithine toxicity metabolome.

8.4 Arginase sequence alignment

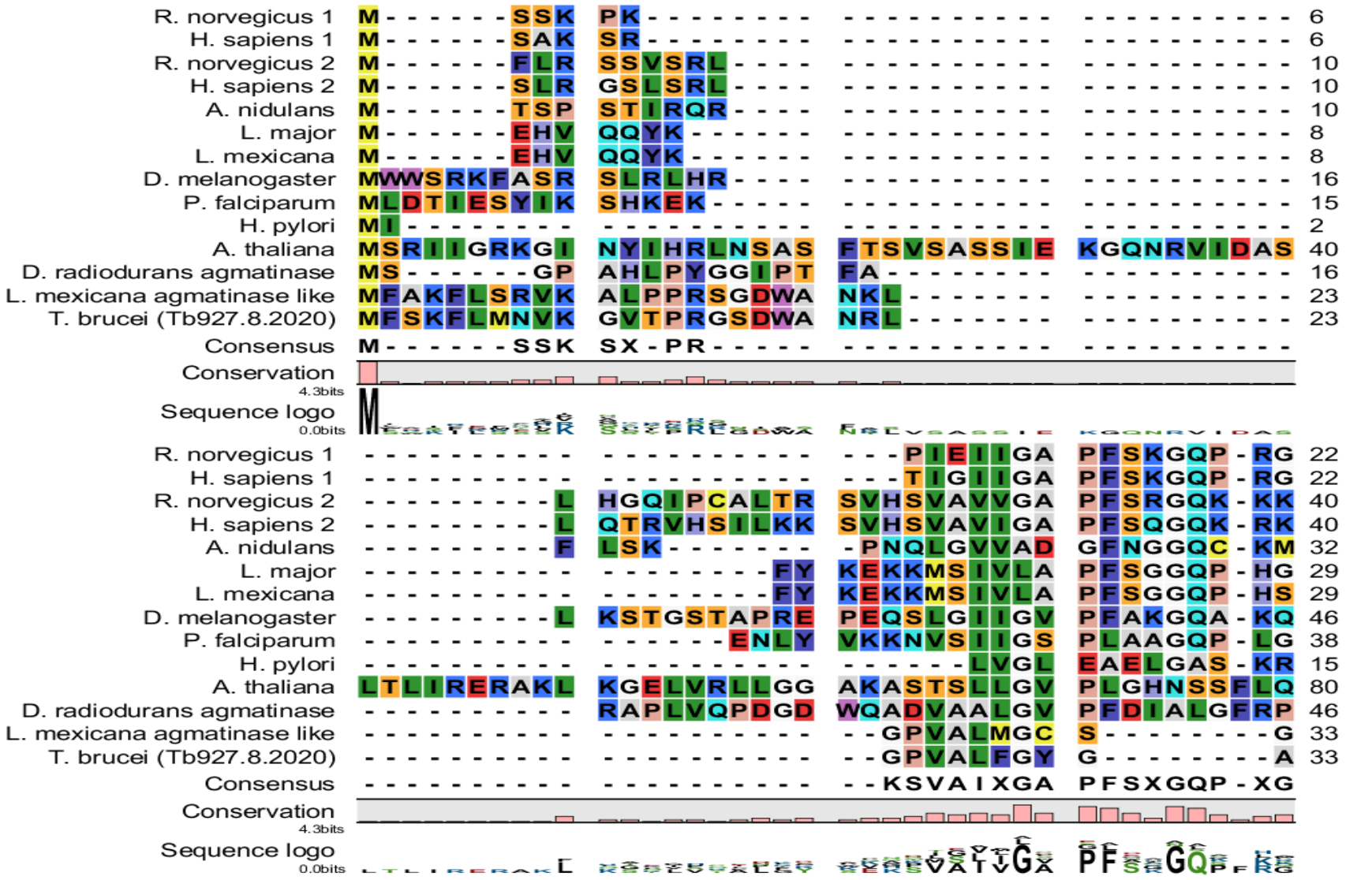
R. norvegicus 1
H. sapiens 1
R. norvegicus 2
H. sapiens 2
A. nidulans
L. major
L. mexicana
D. melanogaster
P. falciparum
H. pylori
A. thaliana
D. radiodurans agmatinase
L. mexicana agmatinase like
T. brucei (Tb927.8.2020)
Consensus
Conservation
4.3bits
Sequence logo
0.0bits

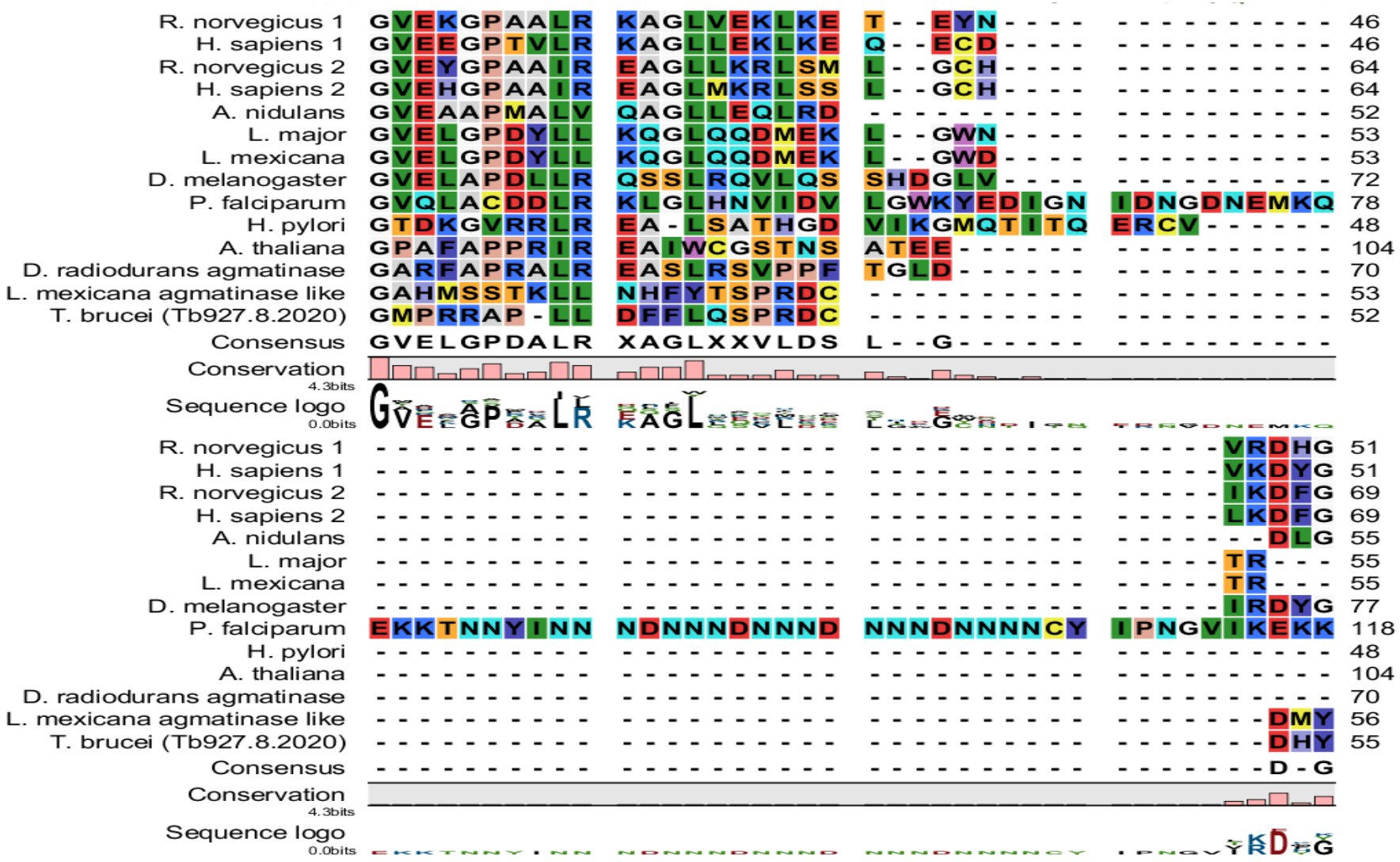
R. norvegicus 1 GVEKGPAALR KAGLVEKLKE T--EYN---------- 46
H. sapiens 1 GVEEGPTVLR KAGLLEKLKE Q--ECD---------- 46
R. norvegicus 2 GVEYGPAAIR EAGLLKRLSM L--GCH---------- 64
H. sapiens 2 GVEHGPAAIR EAGLMKRLSS L--GCH---------- 64
A. nidulans GVEAAPMALV QAGLLEQLRD ---------- ---------- 52
L. major GVELGPDYLL KQGLQQDMEK L--GWN---------- 53
L. mexicana GVELGPDYLL KQGLQQDMEK L--GWD---------- 53
D. melanogaster GVELAPDLLR QSSLRQVLQS SHDGLV---------- 72
P. falciparum GVQLACDDLR KLGLHNVIDV LGWKYEDIGN IDNGDNEMKQ 78
H. pylori GTDKGVRRLR EA-LSATHGD VIKGMQTITQ ERCV---------- 48
A. thaliana GPAFAPPRIR EAIWCGSTNS ATEE---------- 104
D. radiodurans agmatinase GARFAPRALR EASLRSVPPF TGLD---------- 70
L. mexicana agmatinase like GAHMSSTKLL NHFYTSPRDC ---------- ---------- 53
T. brucei (Tb927.8.2020) GMPRRAP-LL DFFLQSPRDC ---------- ---------- 52
Consensus GVELGPDALR XAGLXXVLDS L--G---------- ----------
Conservation
4.3bits
Sequence logo
0.0bits
R. norvegicus 1 ---------- ---------- ---------- -----VRDHG 51
H. sapiens 1 ---------- ---------- ---------- -----VKDYG 51
R. norvegicus 2 ---------- ---------- ---------- -----IKDFG 69
H. sapiens 2 ---------- ---------- ---------- -----LKDFG 69
A. nidulans ---------- ---------- ---------- -------DLG 55
L. major ---------- ---------- ---------- -----TR--- 55
L. mexicana ---------- ---------- ---------- -----TR--- 55
D. melanogaster ---------- ---------- ---------- -----IRDYG 77
P. falciparum EKKTNNYINN NDNNNDNNND NNNDNNNNCY IPNGVIKEKK 118
H. pylori ---------- ---------- ---------- ---------- 48
A. thaliana ---------- ---------- ---------- ---------- 104
D. radiodurans agmatinase ---------- ---------- ---------- ---------- 70
L. mexicana agmatinase like ---------- ---------- ---------- -------DMY 56
T. brucei (Tb927.8.2020) ---------- ---------- ---------- -------DHY 55
Consensus ---------- ---------- ---------- -------D-G
Conservation
4.3bits
Sequence logo
0.0bits

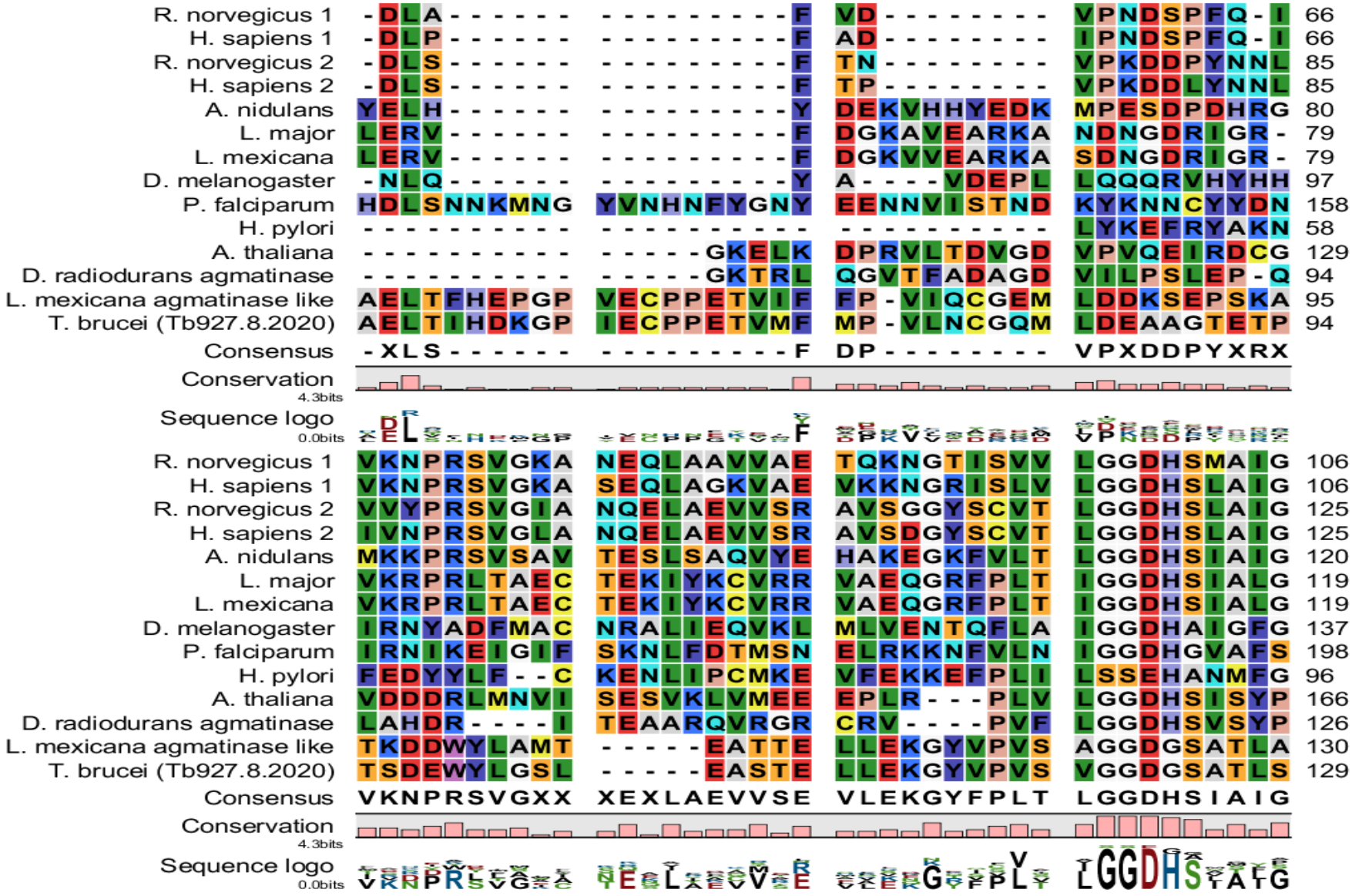
R. norvegicus 1 -DLA-------F VD--------- VPNDSPFQ-I 66
H. sapiens 1 -DLP-------F AD--------- IPNDSPFQ-I 66
R. norvegicus 2 -DLS-------F TN--------- VPKDDPYNNL 85
H. sapiens 2 -DLS-------F TP--------- VPKDDLYNNL 85
A. nidulans YELH-------Y DEKVHHYEDK MPESDPDHRG 80
L. major LERV-------F DGKAVEARKA NDNGDRIGR- 79
L. mexicana LERV-------F DGKVVEARKA SDNGDRIGR- 79
D. melanogaster -NLQ-------Y A----VDEPL LQQQRVHYHH 97
P. falciparum HDLSNNKMNG YVNHNFYGNY EENNVISTND KYKNNCYYDN 158
H. pylori ---------- ---------- ---------- LYKEFRYAKN 58
A. thaliana ---------- -----GKELK DPRVLTDVGD VPVQEIRDCG 129
D. radiodurans agmatinase ---------- -----GKTRL QGVTFADAGD VILPSLEP-Q 94
L. mexicana agmatinase like AELTFHEPGP VECPPETVIF FP-VIQCGEM LDDKSEPSKA 95
T. brucei (Tb927.8.2020) AELTIHDKGP IECPPETVMF MP-VLNCGQM LDEAAGTETP 94
Consensus -XLS-------F DP--------- VPXDDPYXRX
Conservation
4.3bits
Sequence logo
0.0bits
R. norvegicus 1 VKNPRSVGKA NEQLAAVVAE TQKNGTISVV LGGDHSMAIG 106
H. sapiens 1 VKNPRSVGKA SEQLAGKVAE VKKNGRISLV LGGDHSLAIG 106
R. norvegicus 2 VVYPRSVGIA NQELAEVVSR AVSGGYSCVT LGGDHSLAIG 125
H. sapiens 2 IVNPRSVGLA NQELAEVVSR AVSDGYSCVT LGGDHSLAIG 125
A. nidulans MKKPRSVSAV TESLSAQVYE HAKEGKFVLT LGGDHSIAIG 120
L. major VKRPRLTAEC TEKIYKCVRR VAEQGRFPLT IGGDHSIALG 119
L. mexicana VKRPRLTAEC TEKIYKCVRR VAEQGRFPLT IGGDHSIALG 119
D. melanogaster IRNYADFMAC NRALIEQVKL MLVENTQFLA IGGDHAIGFG 137
P. falciparum IRNIKEIGIF SKNLFDTMSN ELRKKNFVLN IGGDHGVAFS 198
H. pylori FEDYYLF--C KENLIPCMKE VFEKKEFPLI LSSEHANMFG 96
A. thaliana VDDDRLMNVI SESVKLVMEE EPLR---PLV LGGDHSISYP 166
D. radiodurans agmatinase LAHDR----I TEAARQVRGR CRV----PVF LGGDHSVSYP 126
L. mexicana agmatinase like TKDDWYLAMT -----EATTE LLEKGYVPVS AGGDGSATLA 130
T. brucei (Tb927.8.2020) TSDEWYLGSL -----EASTE LLEKGYVPVS VGGDGSATLS 129
Consensus VKNPRSVGXX XEXLAEVVSE VLEKGYFPLT LGGDHSIAIG
Conservation
4.3bits
Sequence logo
0.0bits

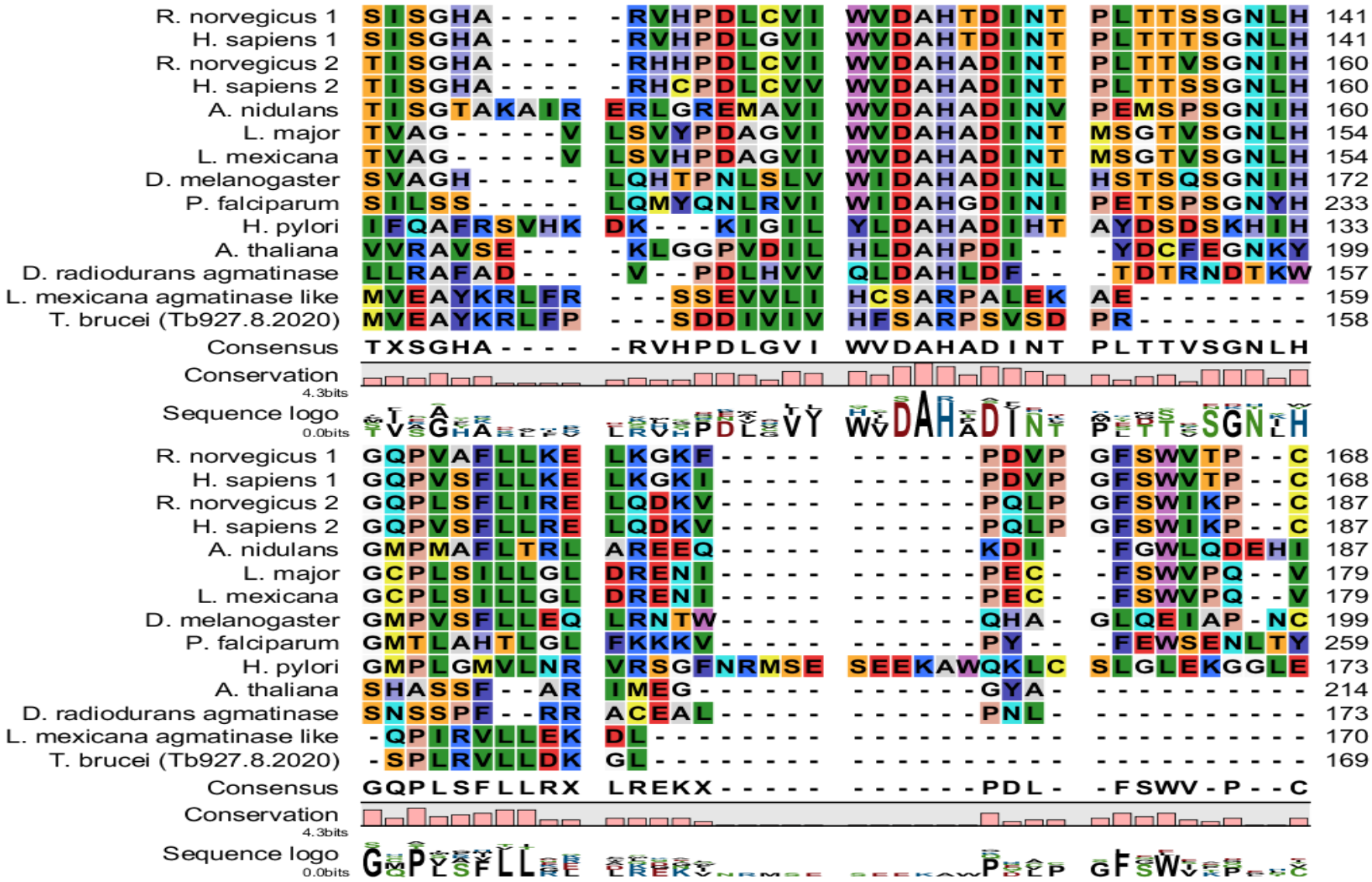
R. norvegicus 1 SISGHA----- -RVHPDLCVI WVDAHTDINT PLTTSSGNLH 141
H. sapiens 1 SISGHA----- -RVHPDLGVI WVDAHTDINT PLTTTSGNLH 141
R. norvegicus 2 TISGHA----- -RHHPDLCVI WVDAHADINT PLTTVSGNIH 160
H. sapiens 2 TISGHA----- -RHCPDLCVV WVDAHADINT PLTTSSGNLH 160
A. nidulans TISGTAKAIR ERLGREMAVI WVDAHADINV PEMSPSGNIH 160
L. major TVAG-----V LSVYPDAGVI WVDAHADINT MSGTVSGNLH 154
L. mexicana TVAG-----V LSVHPDAGVI WVDAHADINT MSGTVSGNLH 154
D. melanogaster SVAGH----- LQHTPNLSLV WIDAHADINL HSTSQSGNIH 172
P. falciparum SILSS----- LQMYQNLRVI WIDAHGDINI PETSPSGNYH 233
H. pylori IFQAFRSVHK DK---KIGIL YLDAHADIHT AYDSDSKHIH 133
A. thaliana VVRAVSE---- -KLGGPVDIL HLDAHPDI-- -YDCFEGNKY 199
D. radiodurans agmatinase LLRAFAD---- -V--PDLHVV QLDAHLDF-- -TDTRNDTKW 157
L. mexicana agmatinase like MVEAYKRLFR ---SSEVVLI HCSARPALEK AE--------- 159
T. brucei (Tb927.8.2020) MVEAYKRLFP ---SDDIVIV HFSARPSVSD PR--------- 158
Consensus TXSGHA----- -RVHPDLGVI WVDAHADINT PLTTVSGNLH
Conservation
4.3bits
Sequence logo
0.0bits
R. norvegicus 1 GQPVAFLLKE LKGKF------ -------PDVP GFSWVTP--C 168
H. sapiens 1 GQPVSFLLKE LKGKI------ -------PDVP GFSWVTP--C 168
R. norvegicus 2 GQPLSFLIRE LQDKV------ -------PQLP GFSWIKP--C 187
H. sapiens 2 GQPVSFLLRE LQDKV------ -------PQLP GFSWIKP--C 187
A. nidulans GMPMAFLTRL AREEQ------ -------KDI- -FGWLQDEHI 187
L. major GCPLSILLGL DRENI------ -------PEC- -FSWVPQ--V 179
L. mexicana GCPLSILLGL DRENI------ -------PEC- -FSWVPQ--V 179
D. melanogaster GMPVSFLLEQ LRNTW------ -------QHA- GLQEIAP-NC 199
P. falciparum GMTLAHTLGL FKKKV------ -------PY-- -FEWSENLTY 259
H. pylori GMPLGMVLNR VRSGFNRMSE SEEKAWQKLC SLGLEKGGLE 173
A. thaliana SHASSF--AR IMEG------ -------GYA- ---------- 214
D. radiodurans agmatinase SNSSPF--RR ACEAL------ -------PNL- ---------- 173
L. mexicana agmatinase like -QPIRVLLEK DL-------- ---------- ---------- 170
T. brucei (Tb927.8.2020) -SPLRVLLDK GL-------- ---------- ---------- 169
Consensus GQPLSFLLRX LREKX------ -------PDL- -FSWV-P--C
Conservation
4.3bits
Sequence logo
0.0bits

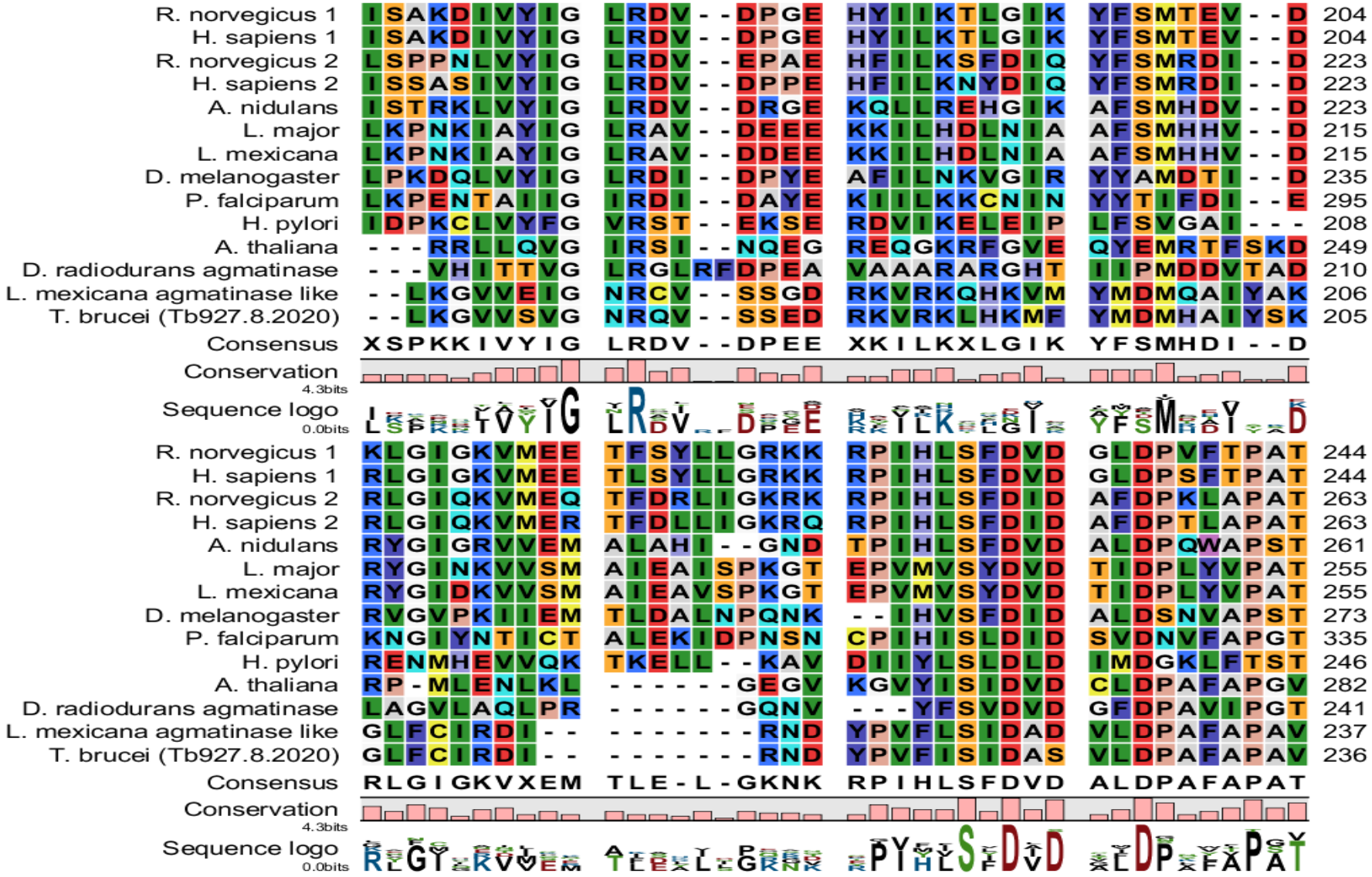
R. norvegicus 1 204
H. sapiens 1 204
R. norvegicus 2 223
H. sapiens 2 223
A. nidulans 223
L. major 215
L. mexicana 215
D. melanogaster 235
P. falciparum 295
H. pylori 208
A. thaliana 249
D. radiodurans agmatinase 210
L. mexicana agmatinase like 206
T. brucei (Tb927.8.2020) 205
Consensus XSPKKIVYIG LRDV--DPEE XKILKXLGIK YFSMHDI--D
Conservation
4.3bits
Sequence logo
0.0bits
R. norvegicus 1 244
H. sapiens 1 244
R. norvegicus 2 263
H. sapiens 2 263
A. nidulans 261
L. major 255
L. mexicana 255
D. melanogaster 273
P. falciparum 335
H. pylori 246
A. thaliana 282
D. radiodurans agmatinase 241
L. mexicana agmatinase like 237
T. brucei (Tb927.8.2020) 236
Consensus RLGIGKVXEM TLE-L-GKNK RPIHLSFDVD ALDPAFAPAT
Conservation
4.3bits
Sequence logo
0.0bits

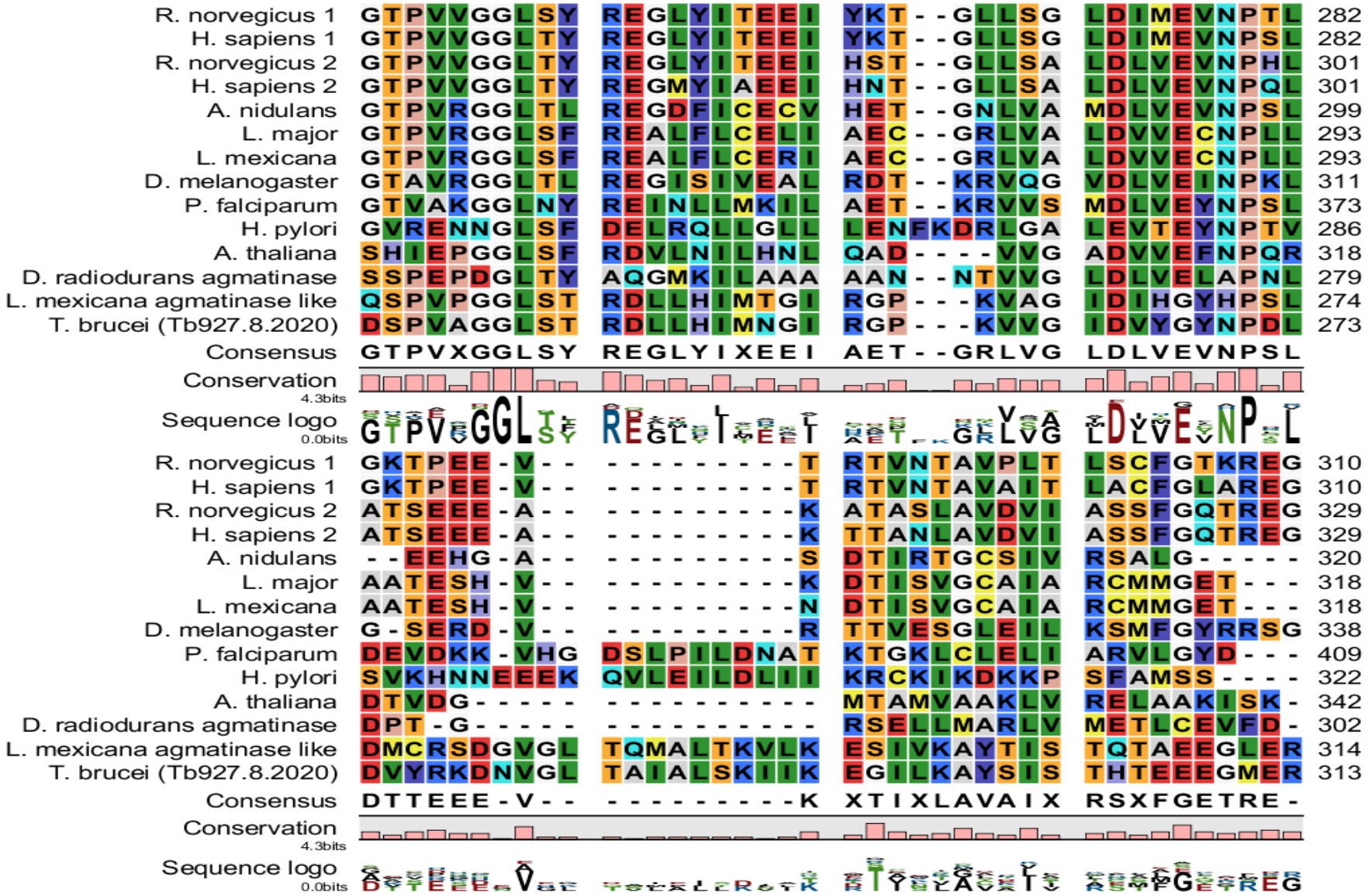
R. norvegicus 1 GTPVVGGLSY REGLYITEEI YKT--GLLSG LDIMEVNPTL 282
H. sapiens 1 GTPVVGGLTY REGLYITEEI YKT--GLLSG LDIMEVNPSL 282
R. norvegicus 2 GTPVVGGLTY REGLYITEEI HST--GLLSA LDLVEVNPHL 301
H. sapiens 2 GTPVVGGLTY REGMYIAEEI HNT--GLLSA LDLVEVNPQL 301
A. nidulans GTPVRGGLTL REGDFICECV HET--GNLVA MDLVEVNPSL 299
L. major GTPVRGGLSF REALFLCELI AEC--GRLVA LDVVECNPLL 293
L. mexicana GTPVRGGLSF REALFLCERI AEC--GRLVA LDVVECNPLL 293
D. melanogaster GTAVRGGLTL REGISIVEAL RDT--KRVQG VDLVEINPKL 311
P. falciparum GTVAKGGLNY REINLLMKIL AET--KRVVS MDLVEYNPSL 373
H. pylori GVRENNGLSF DELRQLLGLL LENFKDRLGA LEVTEYNPTV 286
A. thaliana SHIEPGGLSF RDVLNILHNL QAD----VVG ADVVEFNPQR 318
D. radiodurans agmatinase SSPEPDGLTY AQGMKILAAA AAN--NTVVG LDLVELAPNL 279
L. mexicana agmatinase like QSPVPGGLST RDLLHIMTGI RGP---KVAG IDIHGYHPSL 274
T. brucei (Tb927.8.2020) DSPVAGGLST RDLLHIMNGI RGP---KVVG IDVYGYNPDL 273
Consensus GTPVXGGLSY REGLYIXEEI AET--GRLVG LDLVEVNPSL
Conservation
4.3bits
Sequence logo
0.0bits
R. norvegicus 1 GKTPEE-V-- ----------T RTVNTAVPLT LSCFGTKREG 310
H. sapiens 1 GKTPEE-V-- ----------T RTVNTAVAIT LACFGLAREG 310
R. norvegicus 2 ATSEEE-A-- ----------K ATASLAVDVI ASSFGQTREG 329
H. sapiens 2 ATSEEE-A-- ----------K TTANLAVDVI ASSFGQTREG 329
A. nidulans --EEHG-A-- ----------S DTIRTGCSIV RSALG----- 320
L. major AATESH-V-- ----------K DTISVGCAIA RCMMGET--- 318
L. mexicana AATESH-V-- ----------N DTISVGCAIA RCMMGET--- 318
D. melanogaster G-SERD-V-- ----------R TTVESGLEIL KSMFGYRRSG 338
P. falciparum DEVDKK-VHG DSLPILDNAT KTGKLCLELI ARVLGYD--- 409
H. pylori SVKHNNEEEK QVLEILDLII KRCKIKDKKP SFAMSS---- 322
A. thaliana DTVDG----- ---------- MTAMVAAKLV RELAAKISK- 342
D. radiodurans agmatinase DPT-G----- ---------- RSELLMARLV METLCEVFD- 302
L. mexicana agmatinase like DMCRSDGVGL TQMALTKVLK ESIVKAYTIS TQTAEEGLER 314
T. brucei (Tb927.8.2020) DVYRKDNVGL TAIALSKIIK EGILKAYSIS THTEEEGMER 313
Consensus DTTEEE-V-- ----------K XTIXLAVAIX RSXFGETRE-
Conservation
4.3bits
Sequence logo
0.0bits

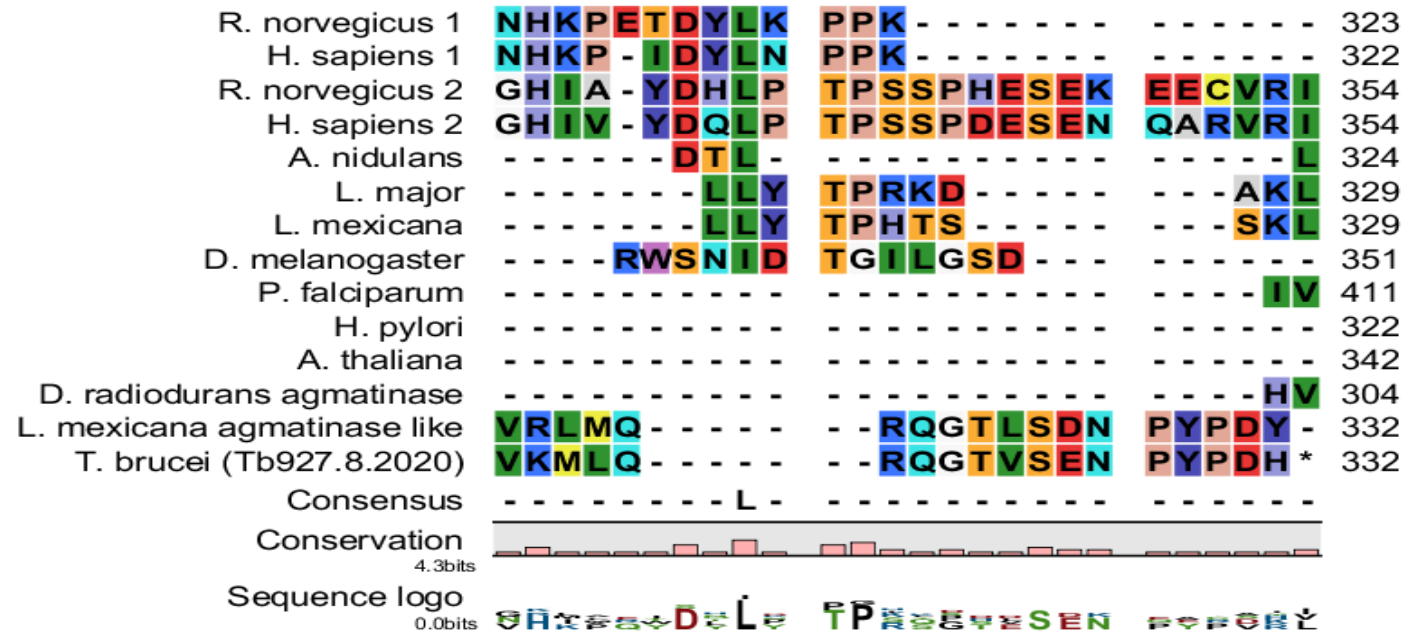

Appendix 8-4. Arginase sequence alignment.